# JGRG24

## The 24th Workshop on General Relativity and Gravitation in Japan

**10 (Mon) — 14 (Fri) November 2014**

**KIPMU, University of Tokyo**

**Chiba, Japan**

# Oral presentations: Day 3

# Contents

# Programme: Day 3
## Wednesday 12 November 2014

Morning 1 [Chair: Takeshi Chiba]

9:30 Raffaele Flaminio (NAOJ, KAGRA) [Invited]
"Status and Prospect of Gravitational Waves detectors" [JGRG24(2014)111201]

10:15 Kazunari Eda (RESCEU)
"Multiple output configuration for a torsion-bar gravitational wave antenna" [JGRG24(2014)111202]

10:30 Hirotaka Yoshino (KEK)
"How to probe string axiverse with gravitational wave observations" [JGRG24(2014)111203]

10:45-11:00 coffee break

Morning 2 [Chair: Yasusada Nambu]

11:00 Teruaki Suyama (RESCEU, Tokyo)
"Black hole perturbation in modified gravity" [JGRG24(2014)111204]

11:15 Ryotaku Suzuki (Osaka City)
"Derivation of higher dimensional black holes in the large D limit" [JGRG24(2014)111205]

11:30 Takahisa Igata (Kansai Gakuin)
"Integrability of Particle System around a Ring Source as the Newtonian Limit of a Black Ring" [JGRG24(2014)111206]

11:45 Kazufumi Takahashi (RESCEU)
"Cosmological evolution of the chameleon field in the presence of a compact object" [JGRG24(2014)111207]

12:00 Ayumu Terukina (Hiroshima)
"Observational constraint on a generalized Galileon gravity model from the gas and shear profiles of a cluster of galaxies" [JGRG24(2014)111208]

12:15 Atsuhisa Ota (TITech)
"CMB $\mu$ distortion from primordial gravitational waves" [JGRG24(2014)111209]

12:30 - 14:00 lunch & poster view

Afternoon 1 [Chair: Kunihito Ioka]

14:00 Shigeru Yoshida (Chiba, IceCube) [Invited]
"Probing the origin of UHECRs with neutrinos" [JGRG24(2014)111210]

14:45 Kenta Kiuchi (YITP, Kyoto)
"The simulation of magnetized binary neutron star mergers on K"
[JGRG24(2014)111211]

15:00 Kentaro Takami (Goethe)
"Constraining the equation of state of neutron stars from binary mergers"
[JGRG24(2014)111212]

15:15 Motoyuki Saijo (Waseda)
"Fragmentation Effects in Rotating Relativistic Supermassive Stars"
[JGRG24(2014)111213]

15:30-16:00 coffee break & poster view

Afternoon 2 [Chair: Yasufumi Kojima]

16:00 Marcus Werner (Kavli IPMU)
"New views of gravitational magnification" [JGRG24(2014)111214]

16:15 Takao Kitamura (Hirosaki)
"Gravitational lensing in Tangherlini space-time" [JGRG24(2014)111215]

16:30 Kei Yamada (Hirosaki)
"Linear Stability of the Post-Newtonian Tri-angular Solution to the General Relativistic Three-Body Problem" [JGRG24(2014)111216]

16:45 Nami Uchikata (CENTRA)
"Slowly rotating gravastars with a thin shell" [JGRG24(2014)111217]

17:00 Naoki Tsukamoto (Fudan)
"Particle Collision in Wormhole Space-times" [JGRG24(2014)111218]

17:15 Takafumi Kokubu (Rikkyo)
"Negative tension branes as stable thin shell wormholes" [JGRG24(2014)111219]

17:30 - 18:00 poster view

18:30- banquet

# “Status and Prospect of Gravitational Waves detectors”

Raffaele Flaminio [Invited]

[JGRG24(2014)111201]

KAGRA NAOJ National Astronomical Observatory of Japan

# Status and perspectives of gravitational wave detectors

Raffaele Flaminio
National Astronomical Observatory of Japan



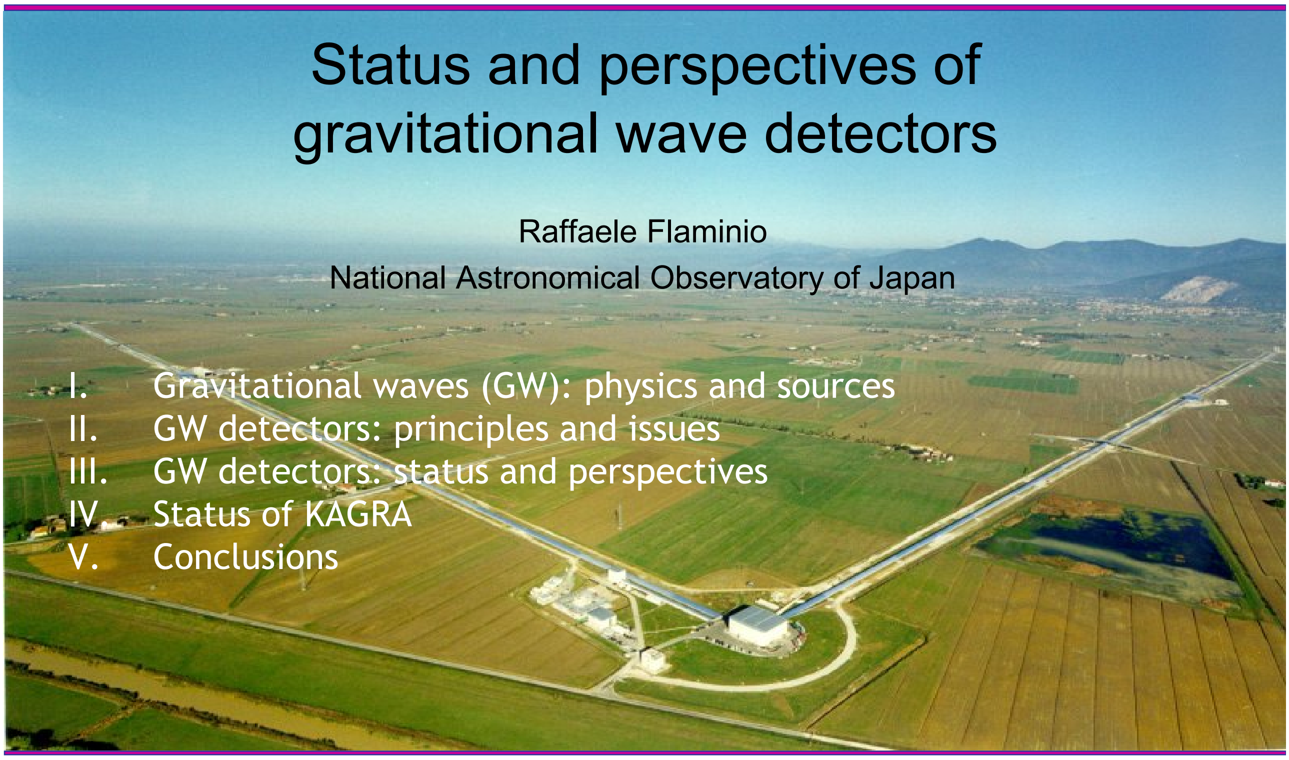



KAGRA NAOJ National Astronomical Observatory of Japan

# I. Gravitational waves: physics and sources

# Gravitational waves

- Einstein equations: space-time is a stretchable medium
  - Gravitational waves

- Weak fields approximation
  - $g_{\mu\nu} = \eta_{\mu\nu} + h_{\mu\nu}$ with $h_{\mu\nu} << 1$
  - $\Box\, h_{\mu\nu} = -\frac{16\,\pi\,G}{c^4}\left[T_{\mu\nu} - \frac{1}{2}\eta_{\mu\nu}T_{\lambda\lambda}\right]$

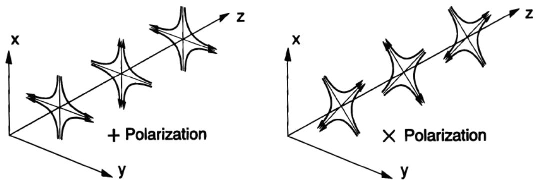


- Properties of gravitational waves
  - Speed of light
  - Two polarizations: spin 2 waves

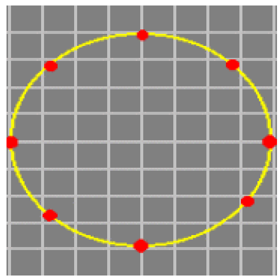

- Effect of gravitational waves
  - Change of distance among free-falling bodies
  - $\delta L = h\,L$ with L the distance between the bodies



# Generation of gravitational waves

- Solution of Einstein equations in the weak field approximation
  - Quadrupole emission
  - Energy emitted in GW: $\frac{dE}{dt} = \frac{1}{5}\frac{G}{c^5}\dddot{I}_{ij}\,\dddot{I}_{ij}$

- Back of the envelope calculation
  - System of size R, mass M, changing over a time scale T

$$\frac{dE}{dt} \approx \frac{1}{5}\frac{G}{c^5}\frac{M^2R^4}{T^6} \approx L_0\left(\frac{R_{Sch}}{R}\right)^2\left(\frac{v}{c}\right)^6$$

  - with $R_{Sch}$ = Schwartchild radius, v = R/T typical speed and $L_0 = 3.6\ 10^{52}$ J/s
  - **Large energy emission from compact and relativistic sources**

- Astrophysical sources

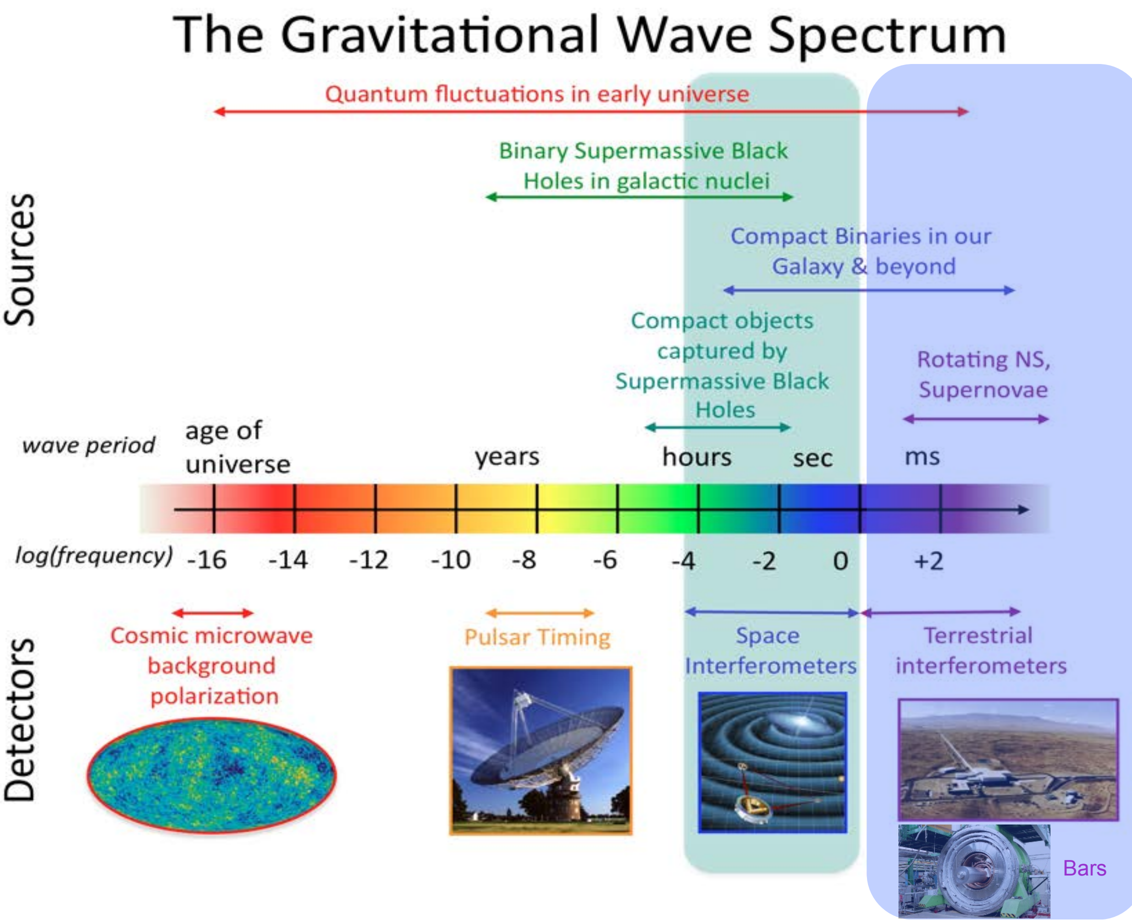


KAGRA

# Coalescing binaries

NAOJ National Astronomical Observatory of Japan

- Coalescences of compact binaries
  - ◆ Composed of neutron stars or black holes
  - ◆ Inspiral phase predicted by general relativity (a lot of tests to be done)
  - ◆ Merger unknown
  - ◆ Ring down predictable (a lot to learn)

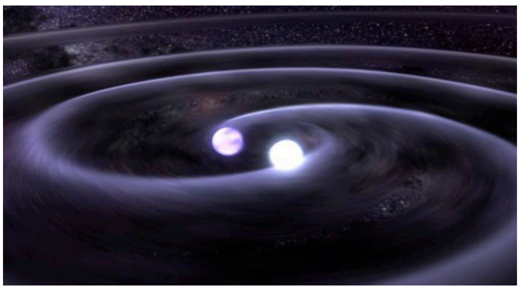

- Strong scientific potential
  - ◆ Standard candles
    - » Source distance can be found out of the waveform
  - ◆ Test of general relativity
    - » Accurate measurements of inspiral waveform can test gravity in the strong field regime
  - ◆ Nuclear physics
    - » Waveform before coalescence sensitive to the star equation of state

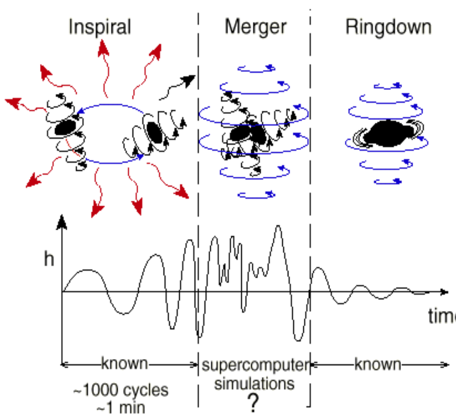

# Gravitational waves exist !

## ● Binary pulsar 1913+16 (Hulse and Taylor)

- ◆ Binary formed by two neutron stars (one being a radio pulsar)
- ◆ Orbital period (~ 8h) is decreasing due to energy loss via GW emission
- ◆ Excellent agreement with general relativity
- ◆ Physics Noble Prize in 1993
- ◆ Coalescence in 300 Myr

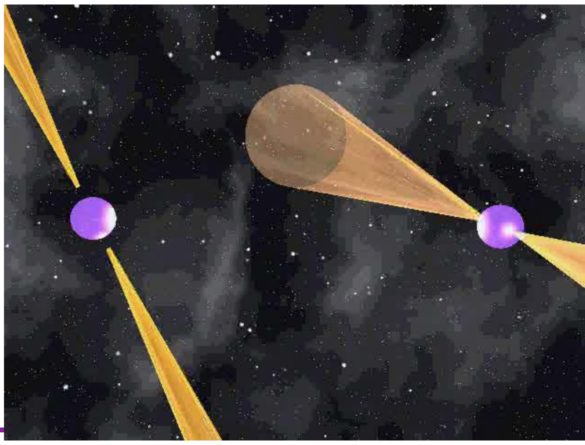

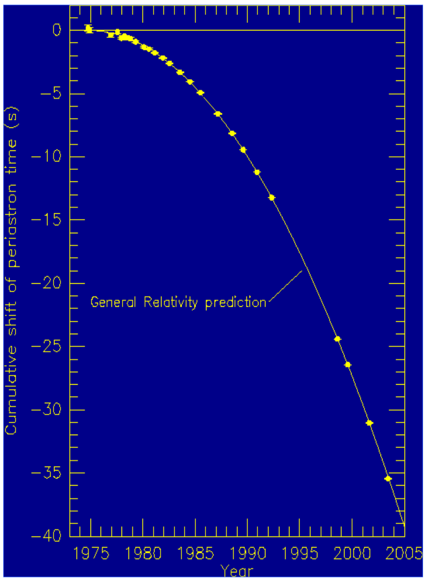




# Binary neutron stars

## ● Observed compact binaries:

- ◆ Only NS-NS observed so far
  - » About 10 binary neutron stars detected in the galaxy from pulsar detection

| | J0737–3039 | J1518+4904 | B1534+12 | J1756–2251 | J1811–1736 |
|---|---|---|---|---|---|
| $P$ [ms] | 22.7/2770 | 40.9 | 37.9 | 28.5 | 104.2 |
| $P_b$ [d] | 0.102 | 8.6 | 0.4 | 0.32 | 18.8 |
| $e$ | 0.088 | 0.25 | 0.27 | 0.18 | 0.83 |
| $\log_{10}(\tau_c/[\mathrm{yr}])$ | 8.3/7.7 | 10.3 | 8.4 | 8.6 | 9.0 |
| $\log_{10}(\tau_g/[\mathrm{yr}])$ | 7.9 | 12.4 | 9.4 | 10.2 | 13.0 |
| Masses measured? | Yes | No | Yes | Yes | Yes |

| | B1820–11 | J1829+2456 | J1906+0746 | B1913+16 | B2127+11C |
|---|---|---|---|---|---|
| $P$ [ms] | 279.8 | 41.0 | 144.1 | 59.0 | 30.5 |
| $P_b$ [d] | 357.8 | 1.18 | 0.17 | 0.3 | 0.3 |
| $e$ | 0.79 | 0.14 | 0.085 | 0.62 | 0.68 |
| $\log_{10}(\tau_c/[\mathrm{yr}])$ | 6.5 | 10.1 | 5.1 | 8.0 | 8.0 |
| $\log_{10}(\tau_g/[\mathrm{yr}])$ | 15.8 | 10.8 | 8.5 | 8.5 | 8.3 |
| Masses measured? | No | No | Yes | Yes | Yes |

Credit: Lorimer 2008

# Coalescing binaries

## Expected rates of coalescing binaries

**Table 2.** Compact binary coalescence rates per Milky Way Equivalent Galaxy per Myr.

| Source | $R_{low}$ | $R_{re}$ | $R_{high}$ | $R_{max}$ |
|---|---|---|---|---|
| NS–NS ($MWEG^{-1}$ $Myr^{-1}$) | 1 [1][a] | 100 [1][b] | 1000 [1][c] | 4000 [16][d] |
| NS–BH ($MWEG^{-1}$ $Myr^{-1}$) | 0.05 [18][e] | 3 [18][f] | 100 [18][g] | |
| BH–BH ($MWEG^{-1}$ $Myr^{-1}$) | 0.01 [14][h] | 0.4 [14][i] | 30 [14][j] | |
| IMRI into IMBH ($GC^{-1}$ $Gyr^{-1}$) | | | 3 [19][k] | 20 [19][l] |
| IMBH-IMBH ($GC^{-1}$ $Gyr^{-1}$) | | | 0.007 [20][m] | 0.07 [20][n] |

**Table 4.** Compact binary coalescence rates per $Mpc^3$ per Myr[a].

| Source | $R_{low}$ | $R_{re}$ | $R_{high}$ | $R_{max}$ |
|---|---|---|---|---|
| NS–NS ($Mpc^{-3}$ $Myr^{-1}$) | 0.01 [1] | 1 [1] | 10 [1] | 50 [16] |
| NS–BH ($Mpc^{-3}$ $Myr^{-1}$) | $6 \times 10^{-4}$ [18] | 0.03 [18] | 1 [18] | |
| BH–BH ($Mpc^{-3}$ $Myr^{-1}$) | $1 \times 10^{-4}$ [14] | 0.005 [14] | 0.3 [14] | |



Credit: Abadie et al. 2010



# GW burst sources

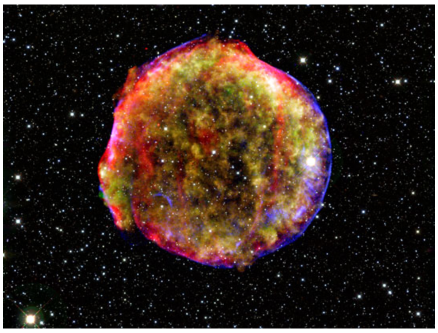

## Type II Supernovae

- Star core collapse
- Rate: from 0.01 to 0.1 per year in a Milky-way like galaxy
- $h = 1.5\ 10^{-21} \left(\frac{E}{10^{-7} M_O}\right)^{\frac{1}{2}} \left(\frac{1\ ms}{T}\right)^{\frac{1}{2}} \left(\frac{1\ kHz}{f}\right) \left(\frac{10\ kpc}{d}\right)$

  with T = duration of collapse and f frequency of GW
- Amount of energy E converted into GW uncertain
  Simulations suggest ($10^{-11}$ $M_o$ – $10^{-7}$ $M_o$)

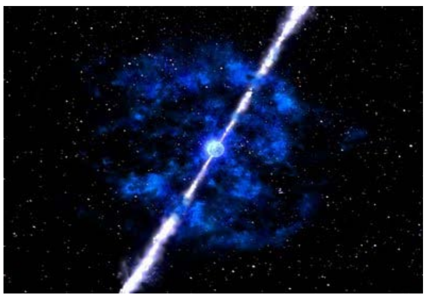

## Gamma ray-bursts

- Hypernovae
- Coalescence of neutron stars and black- holes

## Pulsar glitches and magnetar flares

## Relativistic instabilities of neutron stars

KAGRA

# Rotating neutron stars

NAOJ National Astronomical Observatory of Japan

- Neutron stars
  - Very compact stars, $M \sim 1.4\ M_0$ with $R \sim 10$km
  - Observed as sources of radio pulses (‘pulsars’)
    - » About 2000 pulsars detected in the galaxy
    - » Rotation frequency f: from 1 Hz to about 1 KHz
  - About $10^9$ neutron stars expected in the galaxy

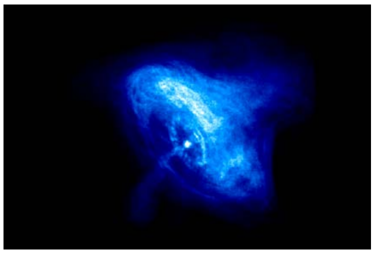

- Gravitational wave emission if stars not axis-symmetric
  - Deformation due to elastic stress or magnetic field
  - Deformation due to accreting matter
  - Free precession around rotation axis
  - ..

- Gravitational wave amplitude
  - $h = \frac{4\pi^2 G}{d\,c^4}\,\epsilon\, I_{zz}\, f^2$ with $\epsilon = \frac{I_{yy} - I_{xx}}{I_{zz}}$ ; $h = 10^{-27}\left(\frac{f}{10\ Hz}\right)^2\left(\frac{I_{zz}}{10^{38} kg \cdot m^2}\right)\left(\frac{10\ kpc}{d}\right)\left(\frac{\epsilon}{10^{-6}}\right)$
  - $\varepsilon$ can be anywhere in the range $10^{-12}$ to $10^{-3}$
  - $\varepsilon = 10^{-5}$ is a mountain of 10 cm on the neutron star!



KAGRA

# GW stochastic background

NAOJ National Astronomical Observatory of Japan

- Primordial gravitational waves
  - Produced during the early life of the Universe
  - Amplitude described by $\Omega_{GW}(f) = \frac{d\rho_{GW}}{\rho_c\, d(\ln(f))}$ with $\rho_c$ the universe critical density
  - Amplitude very dependent on model
    - » Inflation, Pre Big bang model, Cosmic strings, Electroweak transitions,
  - Detection can give unique information on the early Universe and its evolution
- Confusion background for cosmological sources
  - Superposition of many different type of sources

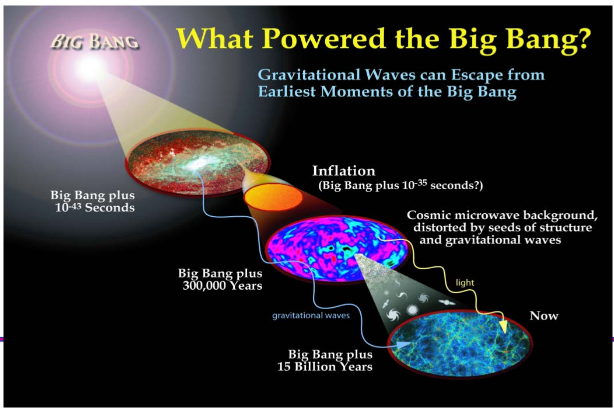


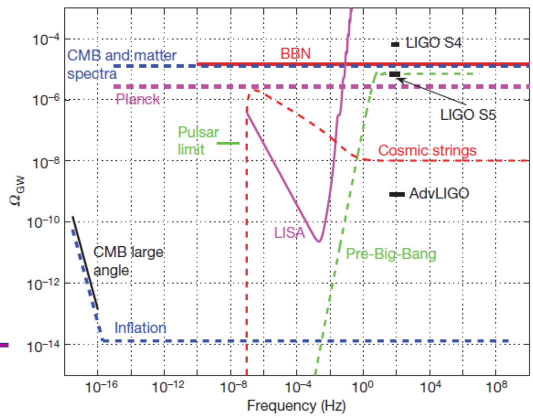

# Scientific motivations

- First direct detection of gravitational waves

- Study of the gravitational force
  - ◆ GW can be generated by pure space-time (black-hole)
  - ◆ GW can reveal the dynamic of strongly curved space-time

- New window to observe the universe
  - ◆ GW are produced by coherent relativistic motion of large masses
  - ◆ GW travel unperturbed trough opaque matter
  - ◆ GW dominate the dynamics of interesting astrophysical events



# III. Gravitational wave detectors (ground-based)

## Long baseline laser interferometers

- Michelson interferometer is the ideal tool
  - ◆ Measure light phase shift at the interferometer output
- Free falling masses
  - ◆ All mirrors suspended to pendulums
  - ◆ Free masses above the pendulum resonance
- Expected signals
  - ◆ $h=10^{-22}$, L=3 km
  - ◆ dL = 3 $10^{-19}$ m
- GW detection
  - ◆ Measure tiny light phase shifts
  - ◆ Measure tiny displacements

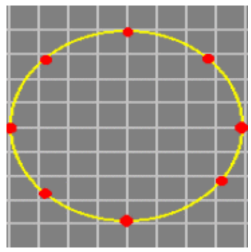

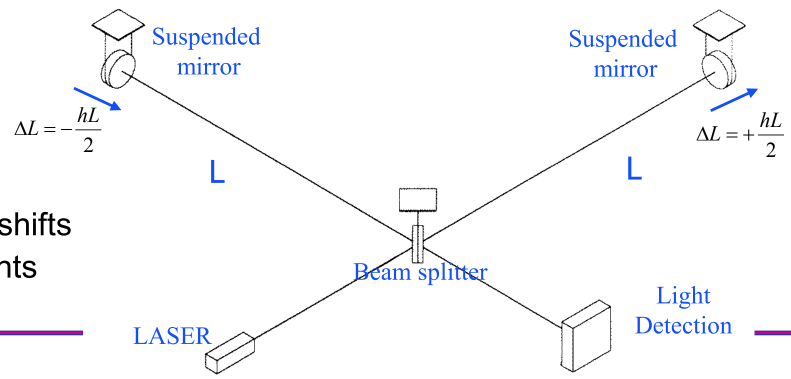




## Phase noise

- GW → Phase shift $d\phi = \frac{4\pi}{\lambda} hL$
- Phase noise $d\phi = \frac{1}{\sqrt{N}}$ with N the flux of photons injected into the interferometer
- Shot noise limit $h > \frac{\lambda}{4\pi L}\sqrt{\frac{2h\nu}{P}}$ with $P$ the laser power and $h\nu$ the photon energy
  - ◆ h ~ $10^{-23}$ requires L~100 km and P~1 kW
- Use of Fabry-Perot cavities
  - ◆ Increase effective length L
- Use of light power recycling
  - ◆ Increase power P arriving on the beam splitter

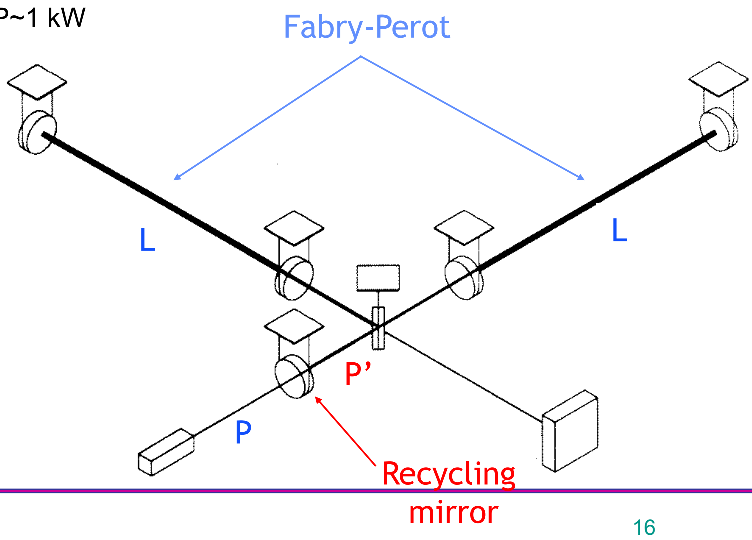

KAGRA

# Radiation pressure noise

NAOJ National Astronomical Observatory of Japan

- Can we increase the laser power further?
  - Radiation pressure noise
- Radiation pressure noise
  - Noise increases with $\sqrt{P}$
  - The Heisenberg uncertainty principle
  - A macroscopic instrument limited by quantum noise

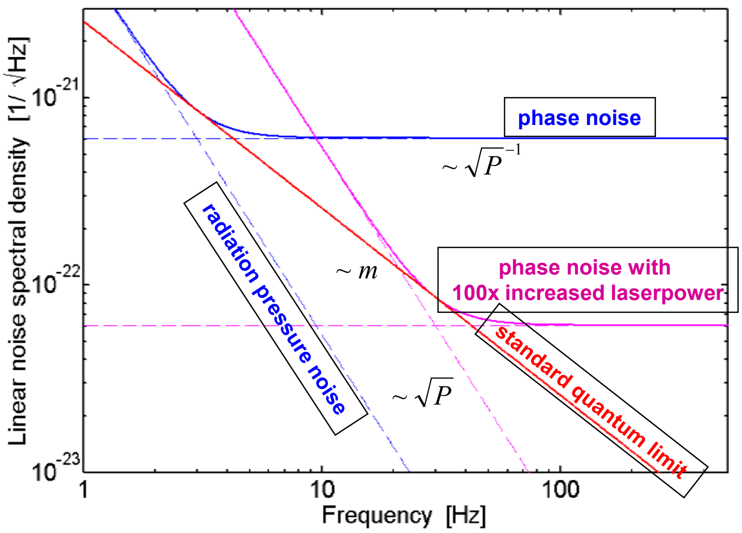


- Ways out?
  - Brute force: Larger mirrors,
  - Non classical states of light: light squeezing



KAGRA

# Squeezing

NAOJ National Astronomical Observatory of Japan

- Or inject phase squeezed vacuum from the output port
- Squeezed vacuum
  - Increase radiation pressure noise
  - Decrease phase noise
  - Equivalent to more power
  - Limit:
    - » amount of squeezing
    - » i.e. optical losses

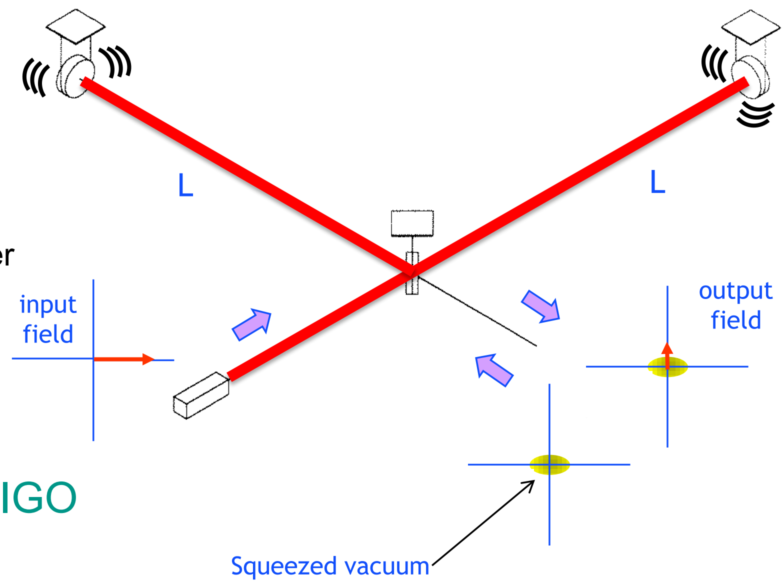


- Tested at GEO and LIGO

KAGRA

# Squeezing

- Inject frequency dependent squeezed vacuum from the output port
  - Phase squeezing at high frequency
  - Amplitude squeezing at low frequency
  - Decrease both phase noise and radiation pressure noise

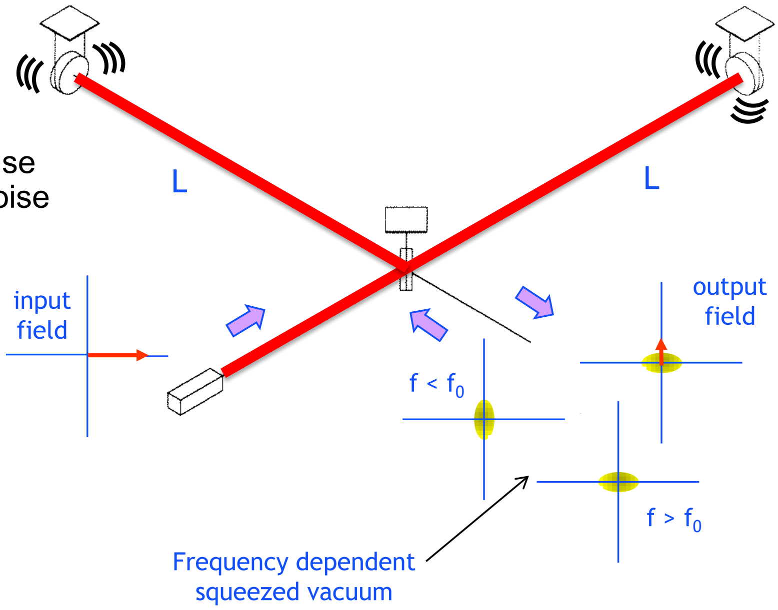


- How?
  - Filtering cavity
  - Limitation:
    - » Cavity optical losses
  - Something that could be tested at TAMA



KAGRA

# Mirror thermal noise

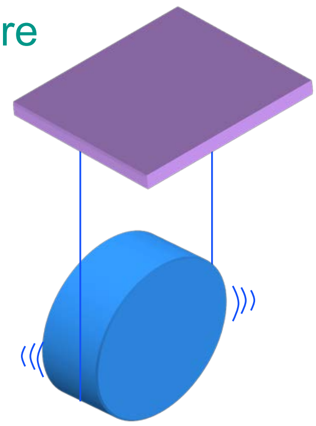

- Mirrors position fluctuations due to temperature
- Fluctuation-dissipation theorem
  - The larger the dissipation the larger the fluctuation
  - E.g. Johnson noise in a resistor
  - Also valid for mechanics
  - The larger the mechanical internal friction the larger the position fluctuation
- Mirror thermal noise
  - Due to mirror internal dissipation/friction
    - » Friction in mirror substrate
    - » Friction in mirror coating
  - Solutions
    - » Increase beam size
    - » Find coatings and substrates with lower internal friction
      - – **Crystalline coatings**
    - » Decrease the temperature

# Suspension thermal noise

- Suspension thermal noise
  - Due to internal dissipation/friction in the suspension wires
  - Main causes
    - » Friction in the suspension wires material
    - » Friction in the contact between the wires and the mirror
  - Main solutions
    - » Better wires
    - » Monolithic suspension (all in silica)
    - » Decrease the temperature

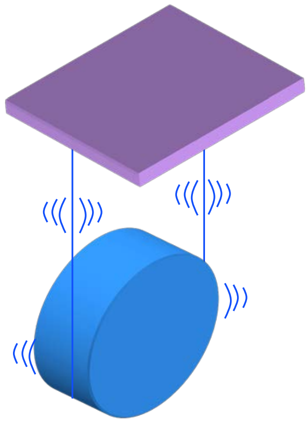

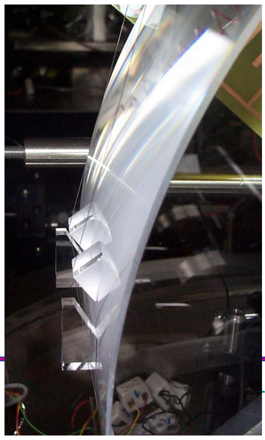

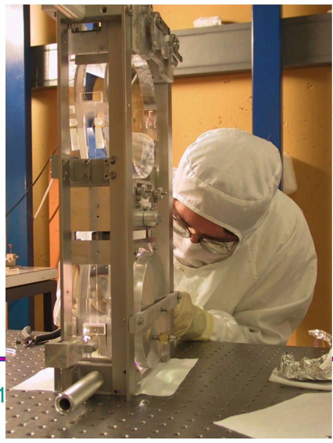

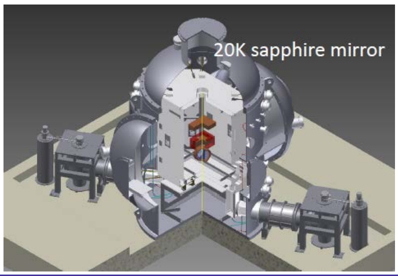




# Seismic noise

- We are in Japan . do I need to explain seismic noise?
  - Natural ground vibrations much larger than GW signals
    - » Even underground
  - Main solutions
    - » Advanced seismic isolation systems (low frequency cut-off)

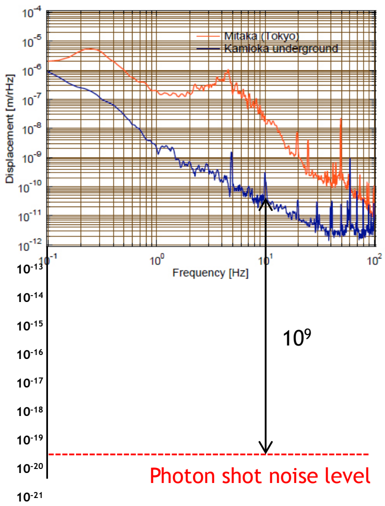


~10 m

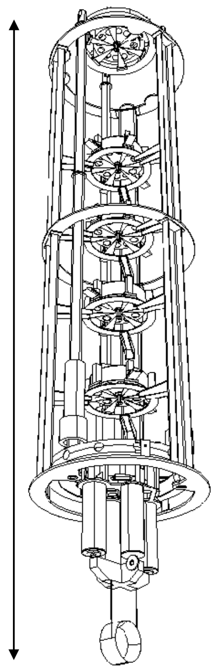

# Gravity gradient noise

- Local gravity variation due to masses motion around the mirror.
  - ◆ Originated from seismic noise (or air masses motion)
  - ◆ Main solutions:
    - » Go underground
    - » Measure seismic noise precisely and subtract from ITF signal

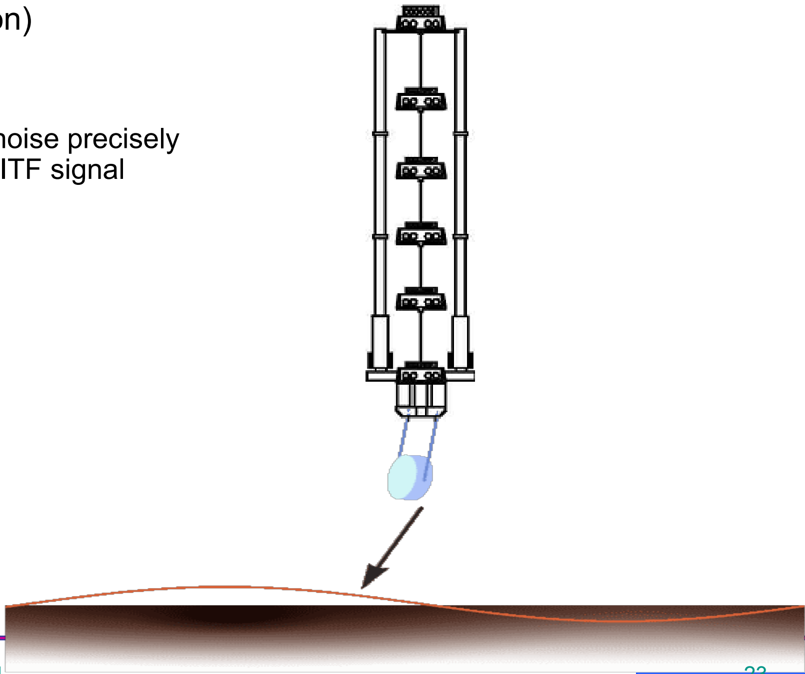



Figure: M.Lorenzini

# Environmental noise

- Acoustic noise and air index of refraction fluctuations
  - ◆ Placed all interferometer in high vacuum
- Diffused light noise
  - ◆ Low scattering optics
  - ◆ Baffles and beam dampers

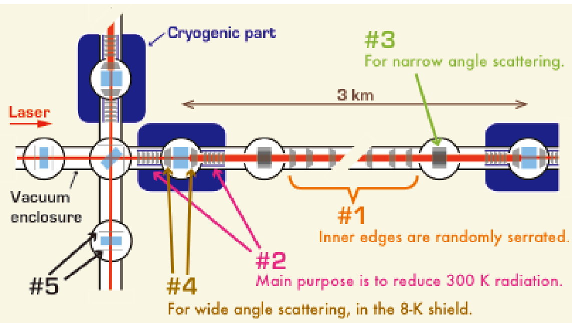



# Example of interferometer sensitivity

- Advanced Virgo

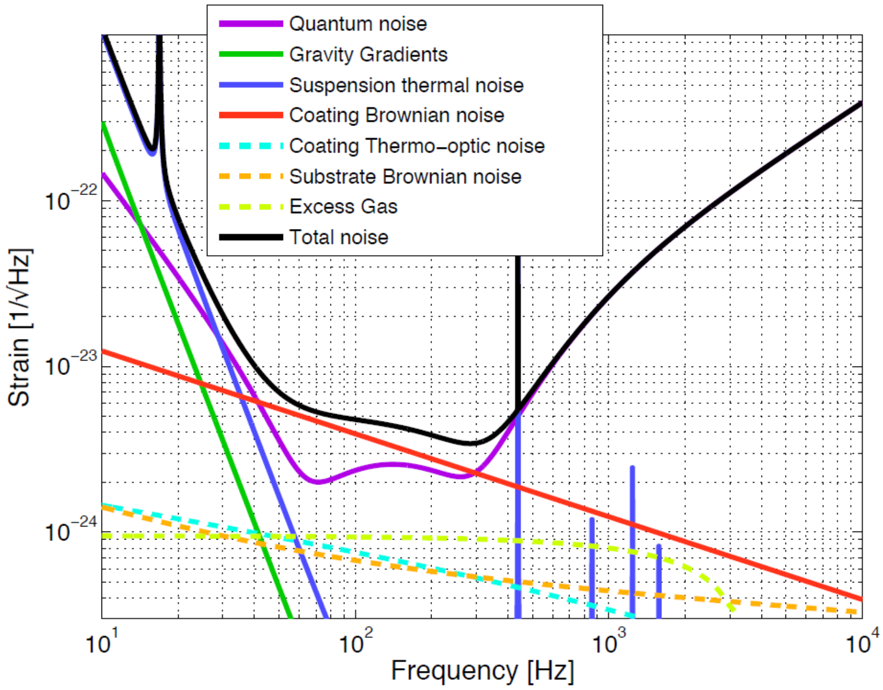




# IV. Ground-based gravitational wave detectors: status and perspectives

# Laser interferometer GW detectors

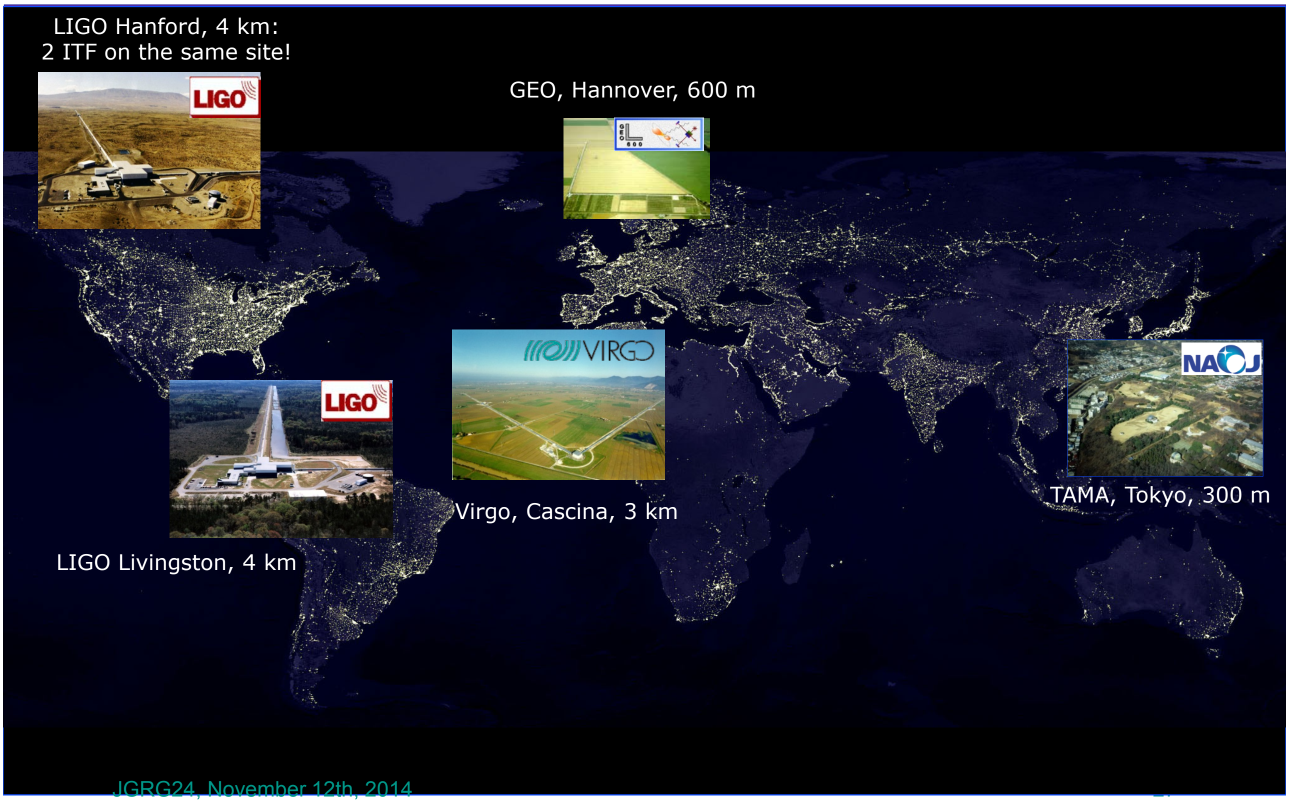




# A global network

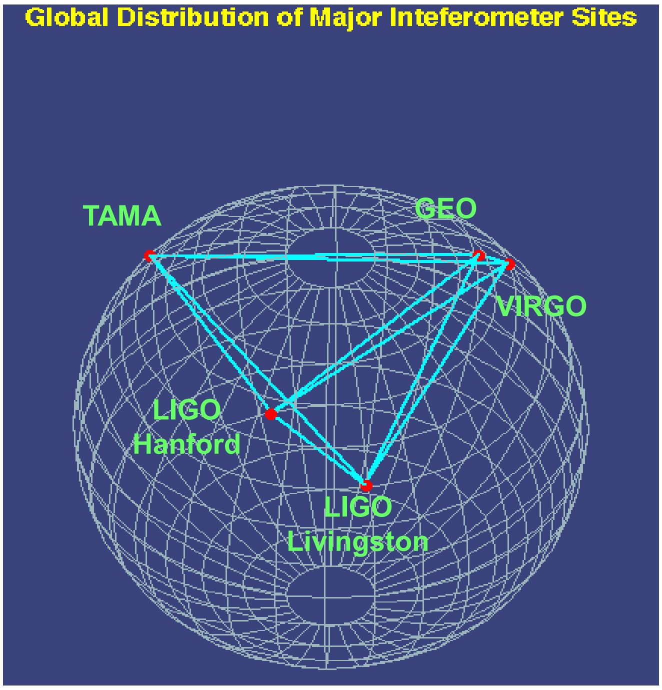


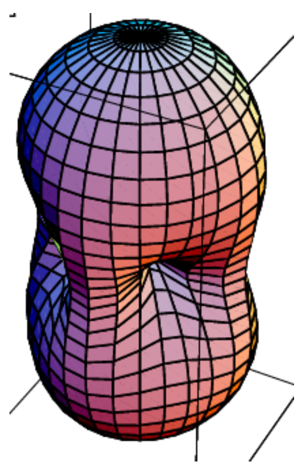

KAGRA

# The LIGO-Virgo network

NAOJ National Astronomical Observatory of Japan

- Virgo and LIGO run jointly between 2007 and 2010
- Both were at the design sensitivity
- Full data sharing and joint data analysis
- No detection
- Upper limits placed on many type of sources

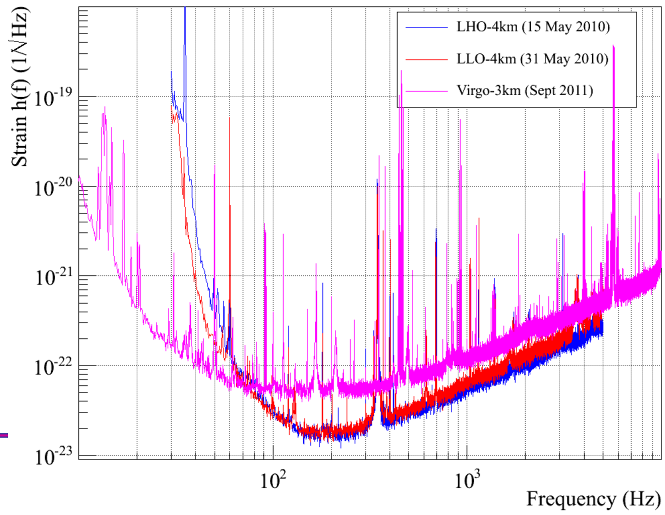




KAGRA

# The LIGO-Virgo network results

NAOJ National Astronomical Observatory of Japan

LSC-PP - publications

https://www.lsc-group.phys.uwm.edu/ppcomm/Papers.html

| | | | | | |
|---|---|---|---|---|---|
| | Phys Rev D **80** (2009) 062002 | arXiv:0904.4718 | - | - | *First LIGO search for gravitational wave bursts from cosmic (super)strings* |
| | Phys Rev D **80** (2009) 102002 | arXiv:0904.4910 | - | - | *Search for High Frequency Gravitational Wave Bursts in the First Calendar Year of LIGO's Fifth Science* |
| | Astrophys. J. **701** (2009) L68-L74 | arXiv:0905.0005 | - | - | *Stacked Search for Gravitational Waves from the 2006 SGR 1900+14 Storm* |
| | Phys Rev D **80** (2009) 102001 | arXiv:0905.0020 | - | - | *Search for gravitational-wave bursts in the first year of the fifth LIGO science run* |
| | Phys. Rev. D **80** (2009) 062001 | arXiv:0905.1654 | - | - | *Search for gravitational wave ringdowns from perturbed black holes in LIGO S4 data* |
| nderson | Phys. Rev. D **80** (2009) 042003 | arXiv:0905.1705 | - | - | *Einstein@Home search for periodic gravitational waves in early S5 LIGO data* |
| | Phys. Rev. D **80** (2009) 047101 | arXiv:0905.3710 | - | - | *Search for Gravitational Waves from Low Mass Compact Binary Coalescence in 186 Days of LIGO's fift* |
| | New J. Phys. **11** (2009) 073032 | - | - | - | *Observation of a kilogram-scale oscillator near its quantum ground state* |
| rgo | Nature **460** (2009) 990 | arXiv:0910:5772 | - | - | *An upper limit on the stochastic gravitational-wave background of cosmological origin* |
| rgo | Astrophys. J. **715** (2010) 1438 | arXiv:0908.3824 | - | - | *Search for gravitational-wave bursts associated with gamma-ray bursts using data from LIGO Science F* |
| rgo | Astrophys. J. **713** (2010) 671 | arXiv:0909.3583 | - | - | *Searches for gravitational waves from known pulsars with S5 LIGO data* |
| rgo | Astrophys. J. **715** (2010) 1453 | arXiv:1001.0165 | - | - | *Search for gravitational-wave inspiral signals associated with short Gamma-Ray Bursts during LIGO's fi* |
| rgo | Phys. Rev. D **81** (2010) 102001 | arXiv:1002.1036 | - | - | *All-sky search for gravitational-wave bursts in the first joint LIGO-GEO-Virgo run* |
| rgo | Class. Quantum Grav. 27 (2010) 173001 | arXiv:1003.2480 | - | - | *Predictions for the Rates of Compact Binary Coalescences Observable by Ground-based Gravitational-* |
| rgo | non-journal companion to papers 50,52 | arXiv:1003.2481 | - | - | *Sensitivity to Gravitational Waves from Compact Binary Coalescences Achieved during LIGO's Fifth and* |
| rgo | Phys. Rev. D **82** (2010) 102001 | arXiv:1005.4655 | - | - | *Search for Gravitational Waves from Compact Binary Coalescence in LIGO and Virgo Data from S5 and* |
| | Astrophys. J. **722** (2010) 1504 | arXiv:1006.2535 | - | - | *First search for gravitational waves from the youngest known neutron star* |
| | Nucl. Instrum. Meth. A**624** (2010) 223 | arXiv:1007.3973 | - | - | *Calibration of the LIGO Gravitational Wave Detectors in the Fifth Science Run* |
| | Phys. Rev. D**83** (2011) 042001 | arXiv:1011.1357 | - | - | *A search for gravitational waves associated with the August 2006 timing glitch of the Vela pulsar* |
| rgo, external | Astrophys. J. **734** (2011) L35 | arXiv:1011.4079 | - | - | *Search for Gravitational Wave Bursts from Six Magnetars* |
| rgo | Phys. Rev. D**83** (2011) 122005 | arXiv:1102.3781 | - | - | *Search for gravitational waves from binary black hole inspiral, merger and ringdown* |
| rgo | Astrophys. J. **737** (2011) 93 | arXiv:1104.2712 | - | - | *Beating the spin-down limit on gravitational wave emission from the Vela pulsar* |
| | Nature Physics **7** (2011) 962 | - | - | Science summary | *A gravitational wave observatory operating beyond the quantum shot-noise limit* |
| rgo | Phys. Rev. Lett. **107** (2011) 271102 | arXiv:1109.1809 | - | Science summary | *Directional limits on persistent gravitational waves using LIGO S5 science data* |
| rgo | Astron Astrophys **539** (2012) A124 | arXiv:1109.3498 | - | Science summary | *Implementation and testing of the first prompt search for gravitational wave transients with electromagne* |
| rgo | Phys. Rev. D**85** (2012) 022001 | arXiv:1110.0208 | - | - | *All-sky search for periodic gravitational waves in the full S5 LIGO data* |
| rgo | Phys. Rev D**85** (2012) 082002 | arXiv:1111.7314 | P1100034 | Science summary | *Search for Gravitational Waves from Low Mass Compact Binary Coalescence in LIGO's Sixth Science F* |
| rgo | non-journal companion to paper 63 | arXiv:1203.2674 | T1100338 | Science summary | *Sensitivity Achieved by the LIGO and Virgo Gravitational Wave Detectors during LIGO's Sixth and Virgo* |
| rgo | Astron Astrophys **541** (2012) A155 | arXiv:1112.6005 | P1100065 | Science summary | *First Low-Latency LIGO+Virgo Search for Binary Inspirals and their Electromagnetic Counterparts* |
| rgo | Phys. Rev. D **85** (2012) 122001 | arXiv:1112.5004 | P1000128 | Science Summary | *Upper limits on a stochastic gravitational-wave background using LIGO and Virgo interferometers at 600* |
| | Astrophys. J. **755** (2012) 2 | arXiv:1201.4413 | P1000097 | Science summary | *Implications for the Origin of GRB 051103 from LIGO Observations* |

# Highlights of LIGO-Virgo results

- Cosmological background

nature Vol 460 | 20 August 2009 | doi:10.1038/nature08278

LETTERS

**An upper limit on the stochastic gravitational-wave background of cosmological origin**

The LIGO Scientific Collaboration* & The Virgo Collaboration*

- Pulsars emission
  - ◆ Pulsar slow down limit beaten in several cases
  - ◆ "Pulsar mountains" < 1 mm in some cases

THE ASTROPHYSICAL JOURNAL, 737:93 (16pp), 2011 August 20 doi:10.1088/0004-637X/737/2/93


BEATING THE SPIN-DOWN LIMIT ON GRAVITATIONAL WAVE EMISSION FROM THE VELA PULSAR

- Coalescing binaries rates

PHYSICAL REVIEW D 87, 022002 (2013)

**Search for gravitational waves from binary black hole inspiral, merger, and ringdown in LIGO-Virgo data from 2009–2010**

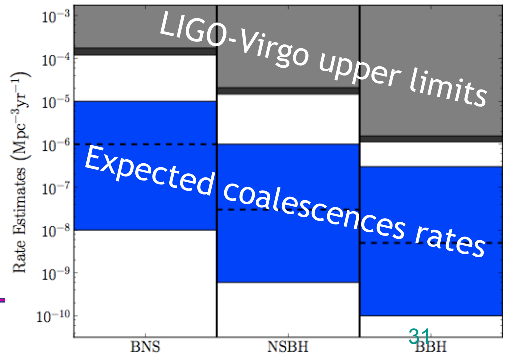




# Toward Advanced Detectors

- Goal:
  - ◆ increase sensitivity x10
  - ◆ Increase number of sources x1000
- Advanced detectors
  - ◆ US: Advanced LIGO (NSF)
  - ◆ Europe: Advanced Virgo (CNRS/INFN/NIKHEF)
  - ◆ Japan: KAGRA (MEXT)

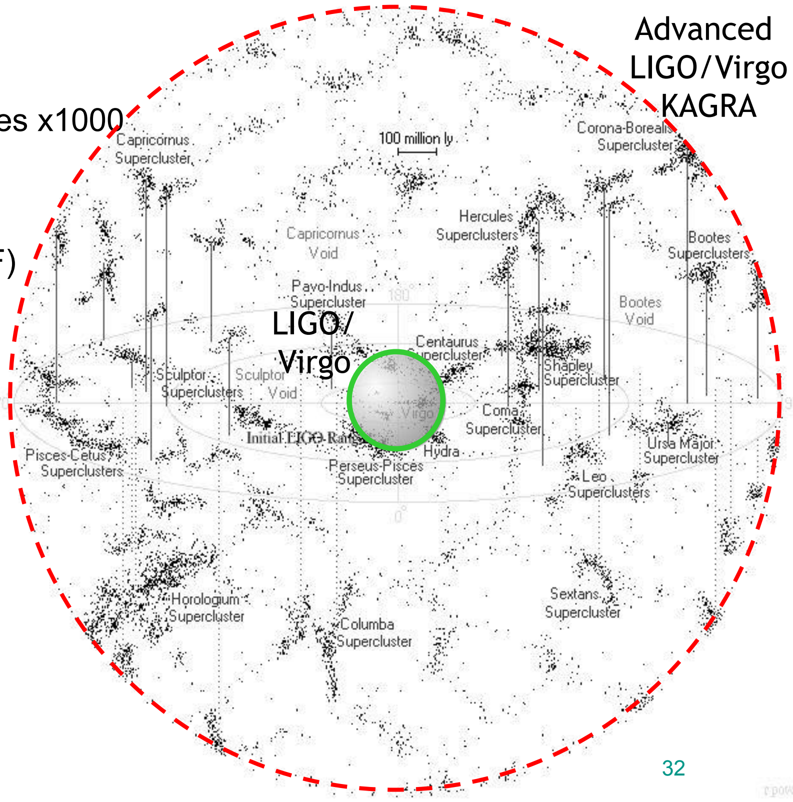

# From LIGO/Virgo to AdvLIGO/Virgo

- Major upgrades
  - Monolithic fused silica suspensions (better thermal noise)
  - Larger and better mirrors (→ 40 kg, sub-nm quality)
  - Higher laser power (→ 200 W)
  - Use of signal recycling (for quantum noise)
  - Advanced seismic isolations (for LIGO)

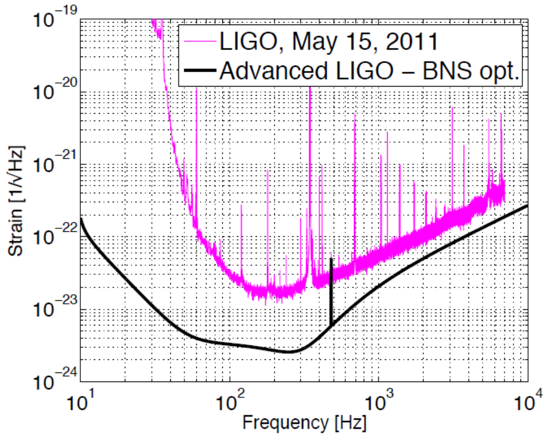


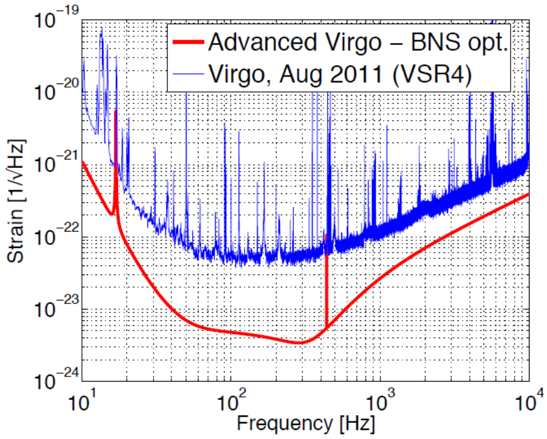




# Advanced LIGO

- Upgrade of LIGO
  - Funded by NSF with contributions from Germany, UK and Australia
  - Same infrastructure
  - New interferometer

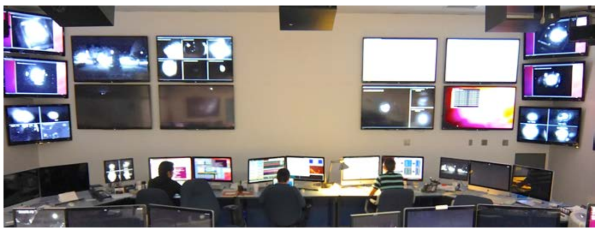

- Status
  - Project near to completion (94%)
  - Installation completed
  - First "interferometer locking" at Livingston achieved!
    - » **Sensitivity already better than Initial LIGO**
  - Commissioning on-going at Hanford
  - Third interferometer components to be shipped to India
    - » INDIGO
- First observation run in 2015

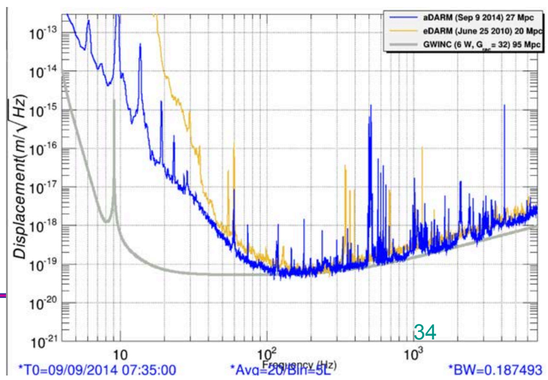

# Advanced Virgo

- Upgrade of Virgo
  - Collaboration including teams from Italy, France, the Netherlands, Poland and Hungary
  - Same infrastructure (and seismic isolation)
  - New interferometer
- Status
  - Project 70% completed
  - Installation ongoing
  - Commissioning: end of 2015
  - First science run in 2016

# Advanced LIGO/Virgo plans

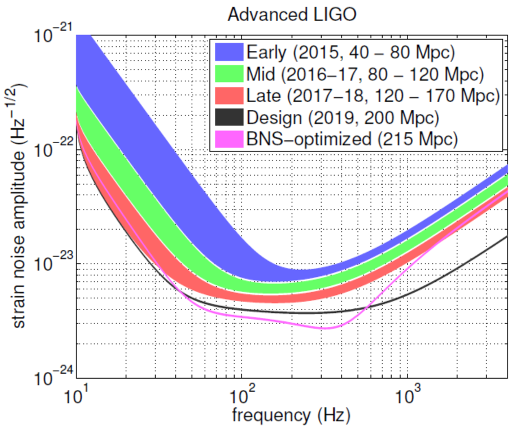


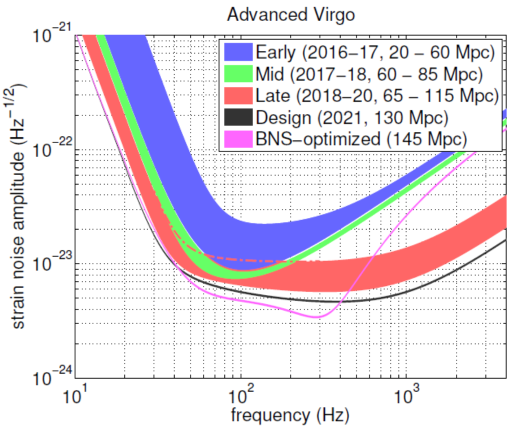


| Epoch | Estimated Run Duration | $E_{GW} = 10^{-2} M_{\odot} c^2$ Burst Range (Mpc) LIGO | Virgo | BNS Range (Mpc) LIGO | Virgo | Number of BNS Detections | % BNS Localized within 5 deg$^2$ | 20 deg$^2$ |
|---|---|---|---|---|---|---|---|---|
| 2015 | 3 months | 40 – 60 | – | 40 – 80 | – | 0.0004 – 3 | – | – |
| 2016–17 | 6 months | 60 – 75 | 20 – 40 | 80 – 120 | 20 – 60 | 0.006 – 20 | 2 | 5 – 12 |
| 2017–18 | 9 months | 75 – 90 | 40 – 50 | 120 – 170 | 60 – 85 | 0.04 – 100 | 1 – 2 | 10 – 12 |
| 2019+ | (per year) | 105 | 40 – 80 | 200 | 65 – 130 | 0.2 – 200 | 3 – 8 | 8 – 28 |
| 2022+ (India) | (per year) | 105 | 80 | 200 | 130 | 0.4 – 400 | 17 | 48 |

# The forthcoming advanced network

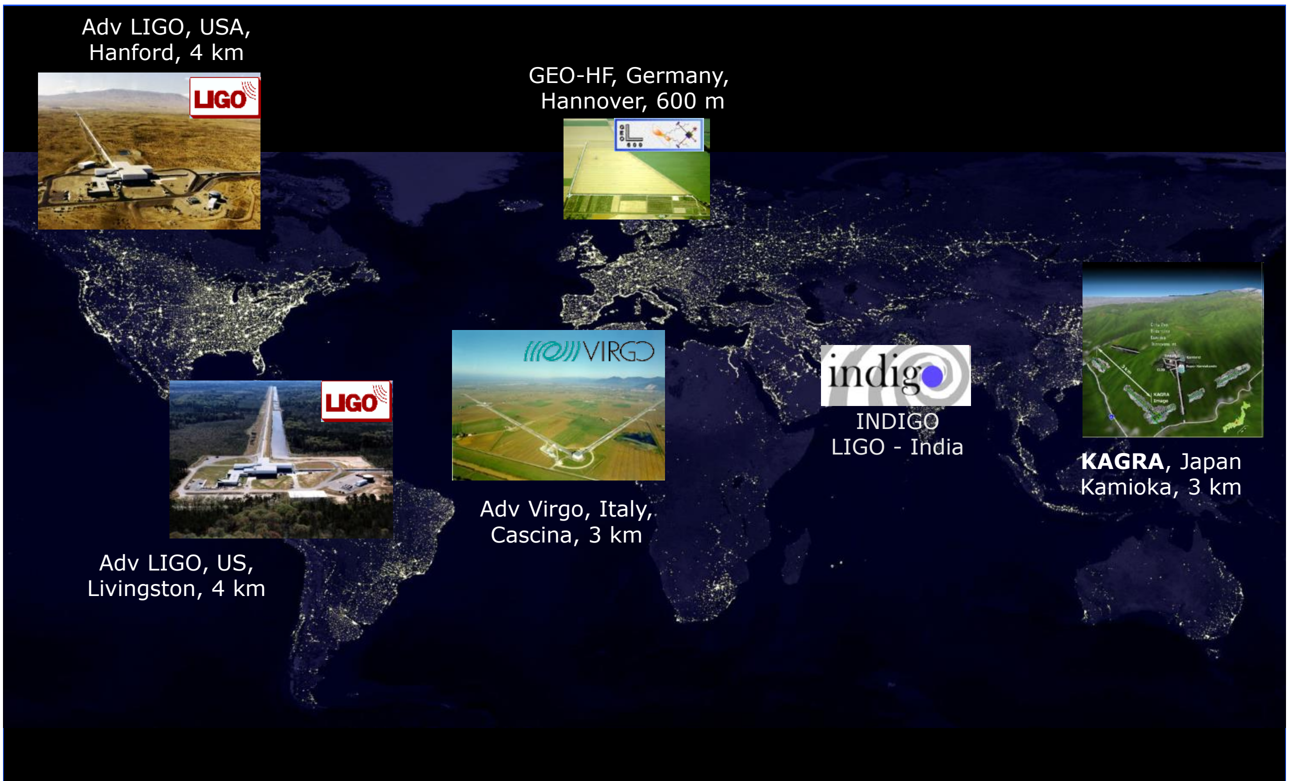




# The forthcoming advanced network


KAGRA-M1201313-v1
LIGO-M1200326-v1
VIR-0371A-12

**Memorandum of Understanding**

**between**

**KAGRA, LIGO and Virgo Scientific Collaborations**

**A. Purpose of the agreement:**

The purpose of this Memorandum of Understanding (MOU) is to establish a collaborative relationship between the signatories who are seeking to discover gravitational waves and pursue the new field of gravitational wave astronomy. The main scientific motivation is that the maximum return from gravitational wave observations is through simultaneous joint measurements by several instruments.

This MOU provides for joint work between the scientific collaborations of KAGRA, LIGO and Virgo. We enter into this agreement in order to lay the groundwork for decades of world-wide collaboration. When sensitive detectors are in operation, we intend to carry out the search for gravitational waves in a spirit of teamwork.

Details and extensions to this MOU will be provided in Attachments agreed by the parties.

**B. Parties to the agreement:**

1. KAGRA

KAGRA, previously called LCGT (Large-scale Cryogenic Gravitational-wave Telescope), is a 3-km laser interferometric gravitational wave antenna built at Kamioka underground site in Japan. One of its characteristic features is to be a cryogenic interferometer; the test-mass mirrors that form 3-km Fabry-Perot arm cavities are cooled down to cryogenic temperature of around 20K, so as to reduce the effect of thermal noises. Stable environment of the underground site and

# V. Status of KAGRA



# The KAGRA project

- Financed by MEXT
- Currently under construction near Kamioka, Gifu

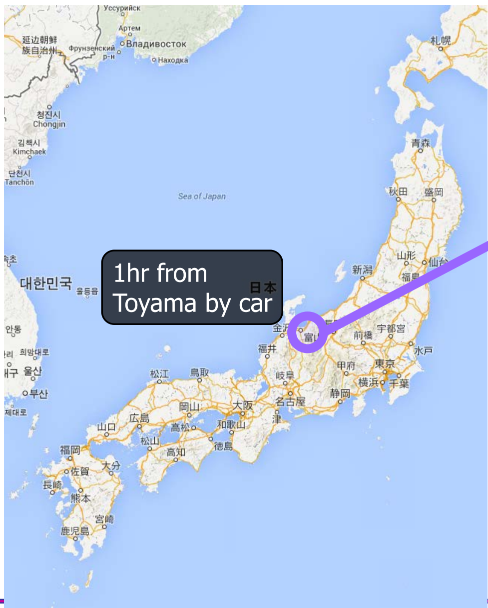


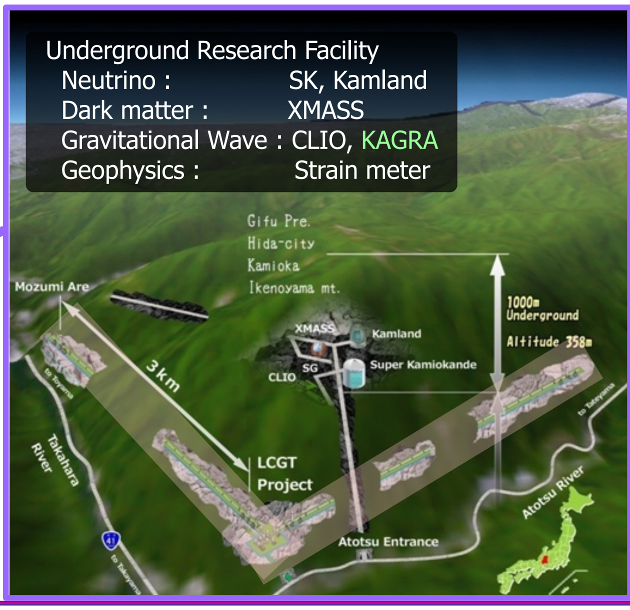

# The KAGRA project

- KAGRA project
  - 3 km long laser interferometer
  - Located underground (Kamioka mine)
    - » Less seismic and gravity noise
    - » Environmental noise reduction
  - Two floors cavern to host longer vibration isolation
  - Use of cryogenic sapphire mirrors
    - » Thermal noise reduction

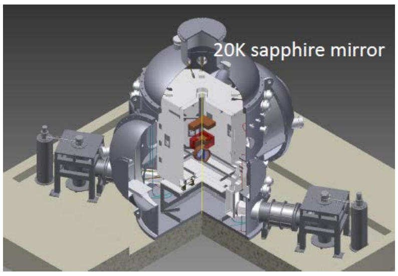


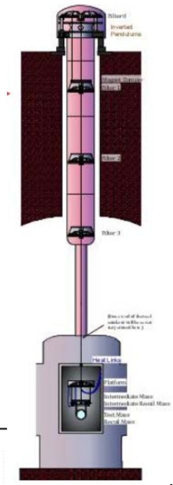


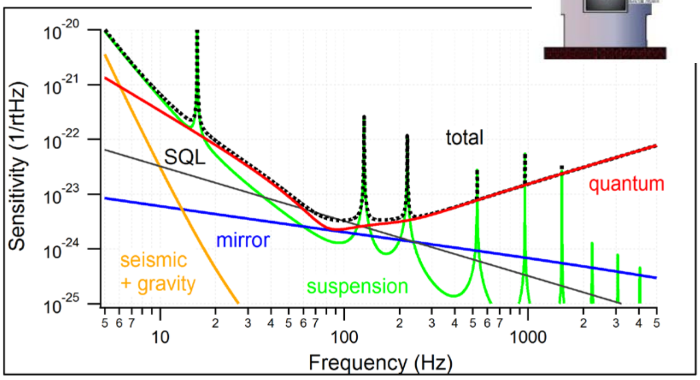


# Status of KAGRA

- Tunnels and Facility
  - Excavation completed in March 2014
  - Facility completion in progress

KAGRA

# Status of KAGRA

National Astronomical Observatory of Japan

- Vacuum tube and cryostats
  - All components delivered
  - Installation started
  - Completion by March

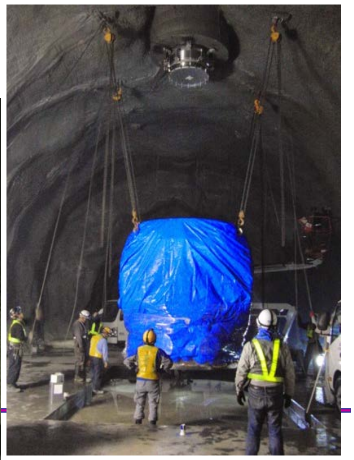



KAGRA

# Status of KAGRA

National Astronomical Observatory of Japan

- Vacuum chambers
  - Being delivered, installation started
- Interferometer components
  - In preparation, very first installation starting

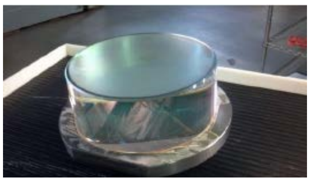

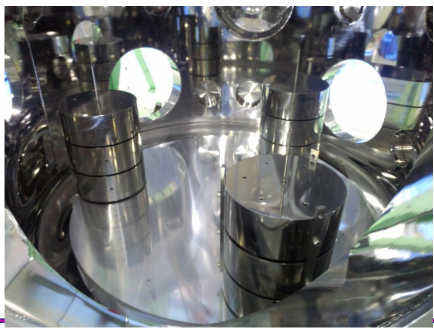

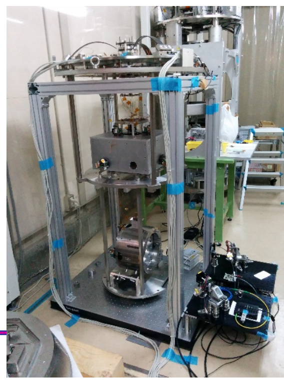

KAGRA · NAOJ National Astronomical Observatory of Japan

# KAGRA overall plan

**·iKAGRA** (2010.10 – 2015.12)
3-km FPM interferometer
- Baseline 3km room temp.
- Operation of total system with simplified IFO and VIS.

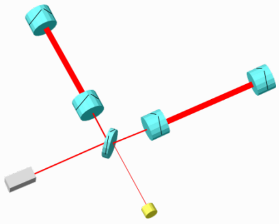

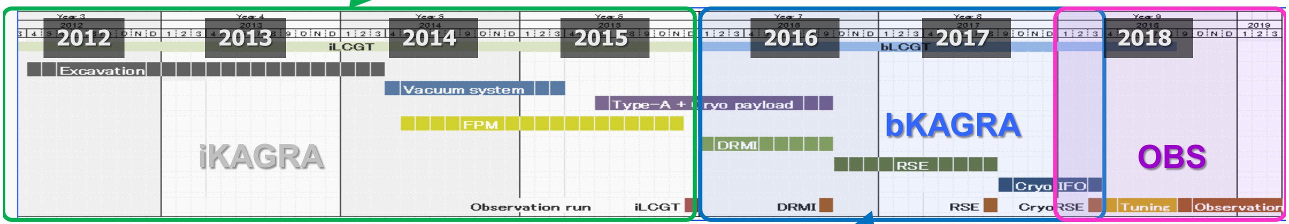


**·bKAGRA** (2016.1 – 2018.3)
Operation with full config.
- Final IFO+VIS configuration
- Cryogenic operation.

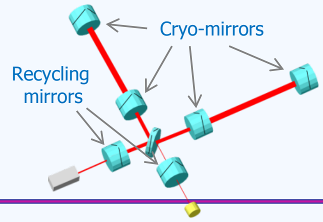




KAGRA · NAOJ National Astronomical Observatory of Japan

# bKAGRA

- The cryogenic challenge
  - ◆ A lot of power in the interferometer
    - » 400 kW of laser power stored in the arm cavities
  - ◆ About 1 W to be extracted from the mirror to keep it at 20 K
    - » **Absorption in the sapphire** substrate is critical
    - » Need to use thick sapphire fibers for the mirror suspension
    - » Compromise on suspension compliance and pendulum thermal noise
  - ◆ Detector duty cycle: cooling time
  - ◆ R&D ongoing, more needed

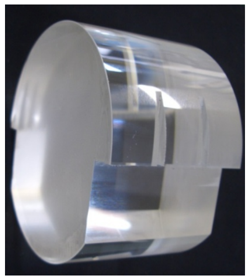

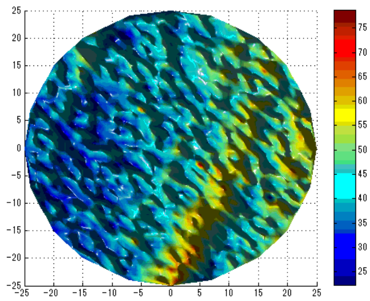

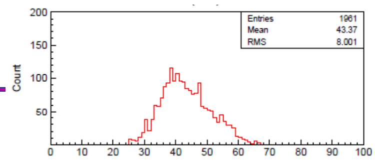

# KAGRA design sensitivity

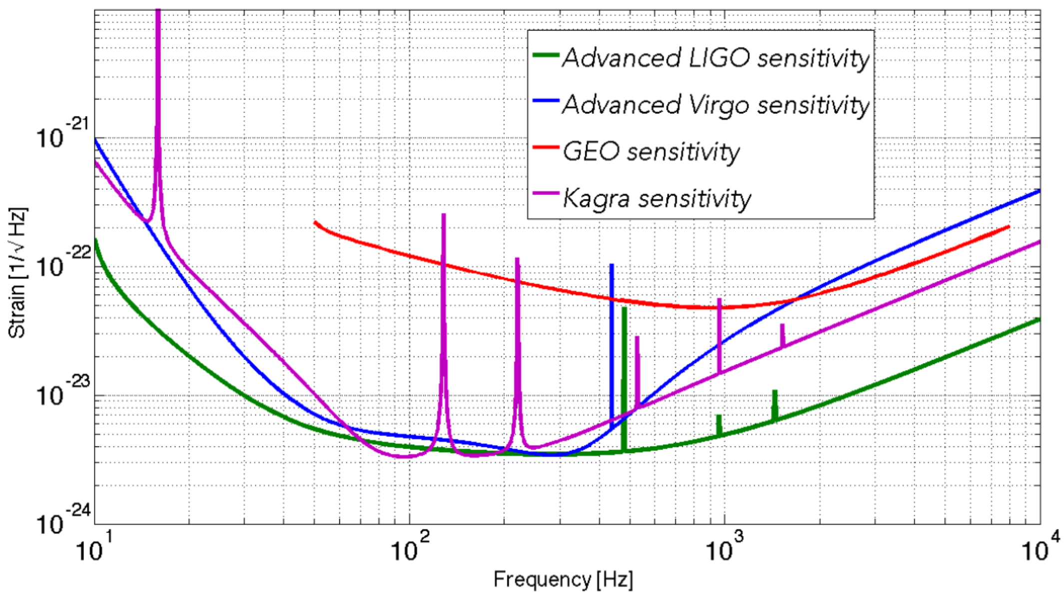


**Figure 3.** Design sensitivities of the advanced detector network.



# Summary and outlook

- Advanced LIGO is going to start operation next year
- Advanced Virgo will follow shortly afterwards
- KAGRA will join in 2018 increasing considerably the overall network capabilities

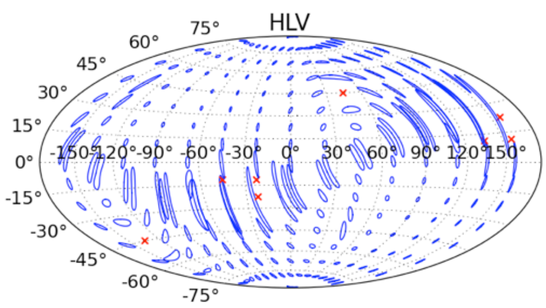


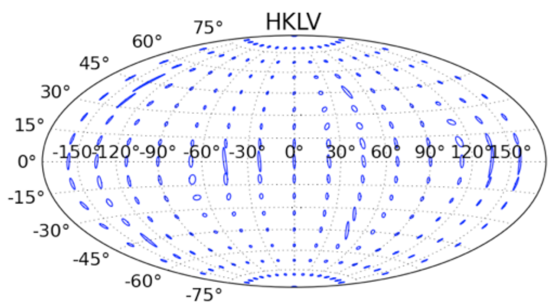


- With this global network NS-NS coalescences within 300 Mpc and BH-BH coalescences within 1 Gpc will be detectable
- Several tens of events/year expected within these distances

# EM follow up

- EM observations triggered by GW candidate events
  - Infrastructure tested with LIGO-Virgo
  - 11 EM partners (optical, x-ray and radio observatories) in 2009-2010
  - 14 GW “alerts”, 9 followed-up by at least 1 partner
  - New collaborations established for Adv LIGO - Adv Virgo
  - KAGRA will be part of it

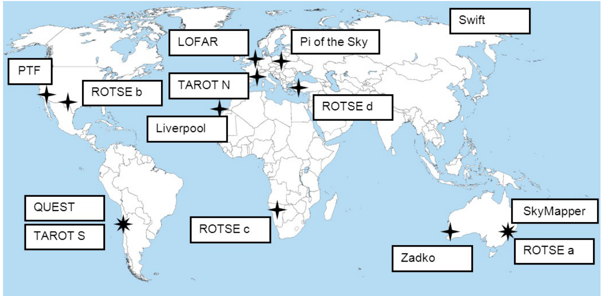


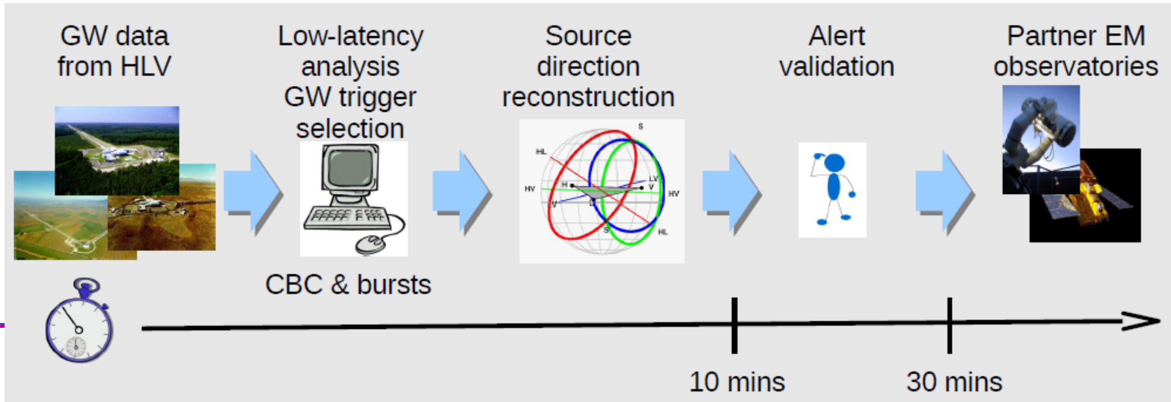


# Beyond advanced detectors

- Proposal for a new European infrastructure devoted to GW astronomy: Einstein Telescope
  - Design study financed by the EU. Released in 2011
  - Goal: x10 better sensitivity compared to advanced detectors
- Keywords:
  - Underground
  - 10 km triangle
  - Cryogenic

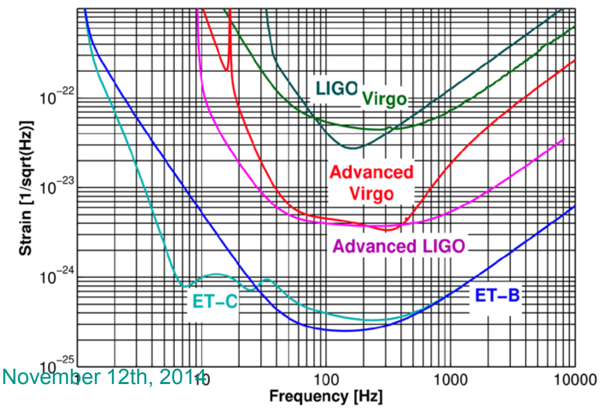


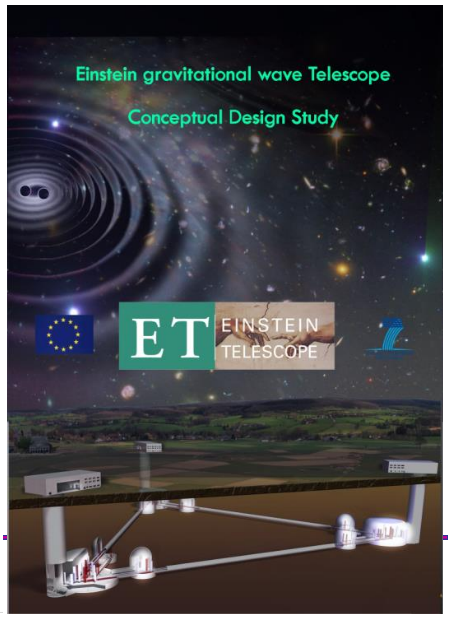

KAGRA

# eLISA

NAOJ National Astronomical Observatory of Japan

- evolving Laser Interferometer Space Antenna
  - Michelson interferometer
    - L = 1 million km
  - 3 S/C in heliocentric orbit
  - 10-30 degrees behind the earth
  - Plane inclined by 60 degrees
- Sensitive to low frequencies
  - $10^{-3}$ – $10^{-1}$ Hz
- Complementary to ground-based detectors
- Selected as L3 mission by ESA
  - Launch planned in 2034

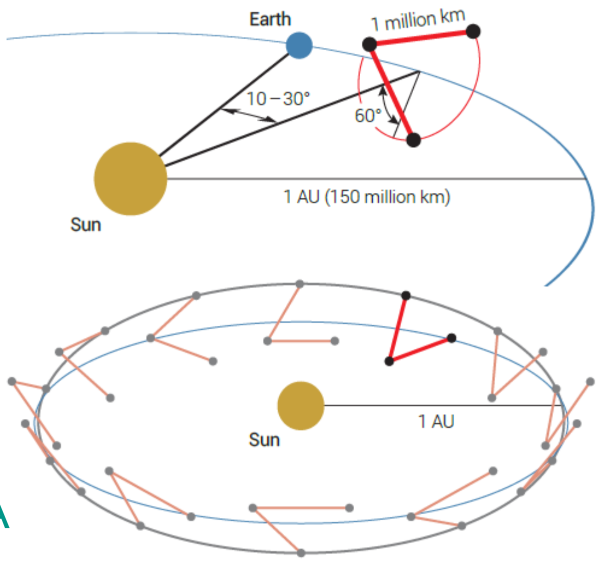




KAGRA

# eLISA

NAOJ National Astronomical Observatory of Japan

- Massive black hole binary inspiral and merger
  - Dynamical behavior of space-time
  - Growth of massive black holes
  - Absolute distances
- Ultra compact binaries
  - Extreme degenerate stars (mainly WD, NS, BH, )
- Extreme mass ratio inspirals
  - Test Kerr black hole solution of GR
  - Galaxy nuclei
- Cosmological backgrounds

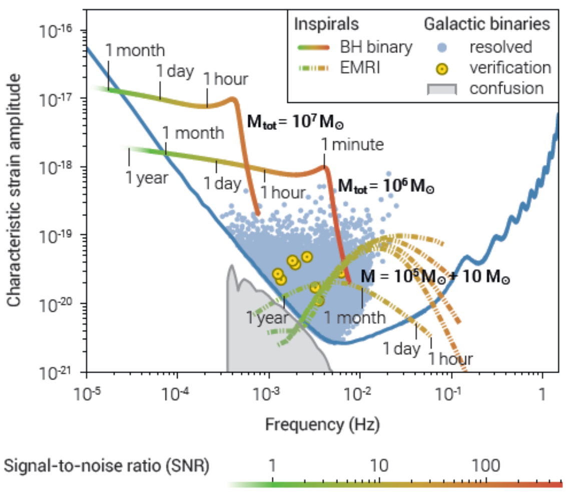

# “Multiple output configuration for a torsion-bar gravitational wave antenna”

Kazunari Eda

[JGRG24(2014)111202]

# Multiple output configuration for a torsion-bar gravitational-wave antenna

e-Print: arXiv:1406.7059
PhysRevD.90.064039

Kazunari Eda

The University of Tokyo, RESCEU

(RESearch Center for the Early Universe)

Collaborators:
A.Shoda, Y.Itoh & M.Ando

2014/11/12
JGRG24@IPMU

1

# Motivation

- One of the most important information in GW observations is the location of the source on the sky.
- The accuracy of angular positions will be the crucial step in identifying sources and opening them for study by EM observations.
- A single GW detector cannot locate the source position for short-duration GW signals.

Schutz, arXiv:gr-qc/0111095

✓ We propose a new antenna configuration for a TOrsion-Bar GW Antenna (TOBA) to improve the angular resolution.

✓ We investigate its angular resolution.

2

# What is a TOBA ?

■ **TOrsion-bar Antenna (TOBA)** (Ando et al. Phys. Rev. Lett. 105, 161101)

- ✓ GW antenna for low-frequency on the ground
- ✓ formed by two bar-shaped orthogonal test masses
- ✓ sensitive to low-frequency ( f=0.1-1 Hz ) even on ground thanks to its resonant frequency $f_{res}$ < 1mHz.

| Main Targets ⇨ | • Compact binary coalescence<br>• Stochastic GW background |
|---|---|

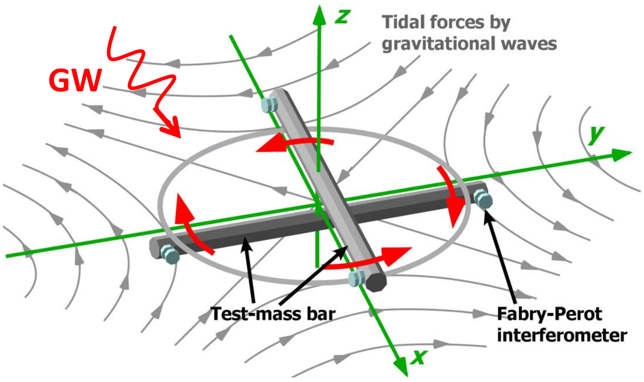


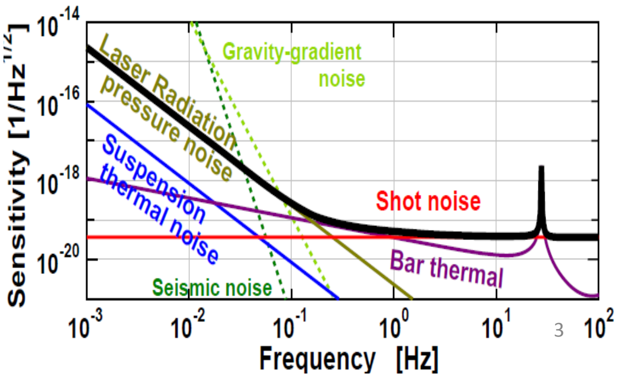


# New antenna configuration

■ **Multiple-output configuration**

- ✓ Previously, only the rotation on the xy plane has been considered.

⇩

- ✓ We incorporate the additional outputs by measuring the rotation of the bars on the yz and xz planes

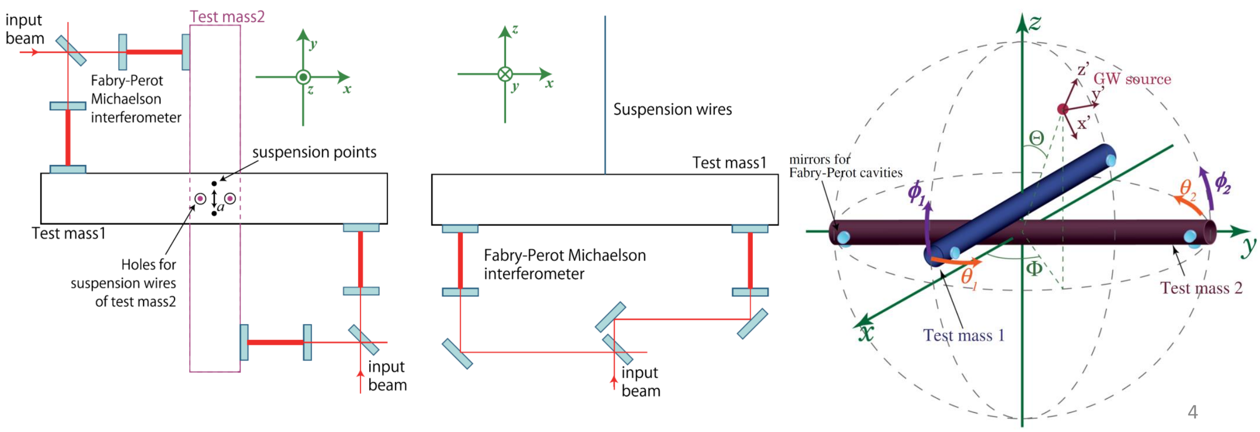

# Parameters of a TOBA

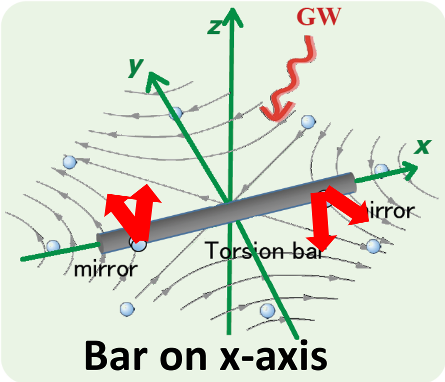


**Equation of motion**

$$I\ddot{\theta}(t) + \gamma_\theta \dot{\theta}(t) + \kappa_\theta \theta(t) = \frac{1}{4}\ddot{h}_{jk} q_\theta^{jk}$$

$$I\ddot{\phi}(t) + \gamma_\phi \dot{\phi}(t) + \kappa_\phi \phi(t) = \frac{1}{4}\ddot{h}_{jk} q_\phi^{jk}$$

**κ : Spring constant, γ : dissipation coefficient**

| | | |
|---|---|---|
| Test mass | Material | Aluminum |
| | Length of the bar | 10 [m] |
| | Diameter of the bar | 0.6 [m] |
| | Mass ($m$) | 7400 [kg] |
| | Moment of inertia ($I$) | $6.4 \times 10^4$ [N m s$^2$] |
| | Loss angle | $10^{-7}$ |
| Suspension | Distance between the two suspension points ($a$) | 5 [cm] |
| | Length of the suspension wires ($l$) | 3 [m] |
| | Dissipation coefficient ($\gamma_\theta$) | $1.0 \times 10^{-7}$ |
| Fabry-Perot laser interferometric sensor | Wave length | 1064 [nm] |
| | Power | 10 [W] |
| | Finesse | 100 |

# Antenna response

## ■ Antenna pattern functions $F_+$ and $F_\times$

**GW waveform** $h_{ij}$

⇩ **+ Geometrical information** ← ✓ Antenna configuration ✓ Antenna direction ✓ Antenna location

**GW signal** $h(t) = F_+(t)\, h_+(t) + F_\times(t)\, h_\times(t)$

## ■ Antenna pattern power $P \equiv \sqrt{\sum_k F_{+,k}^2 + F_{\times,k}^2}$

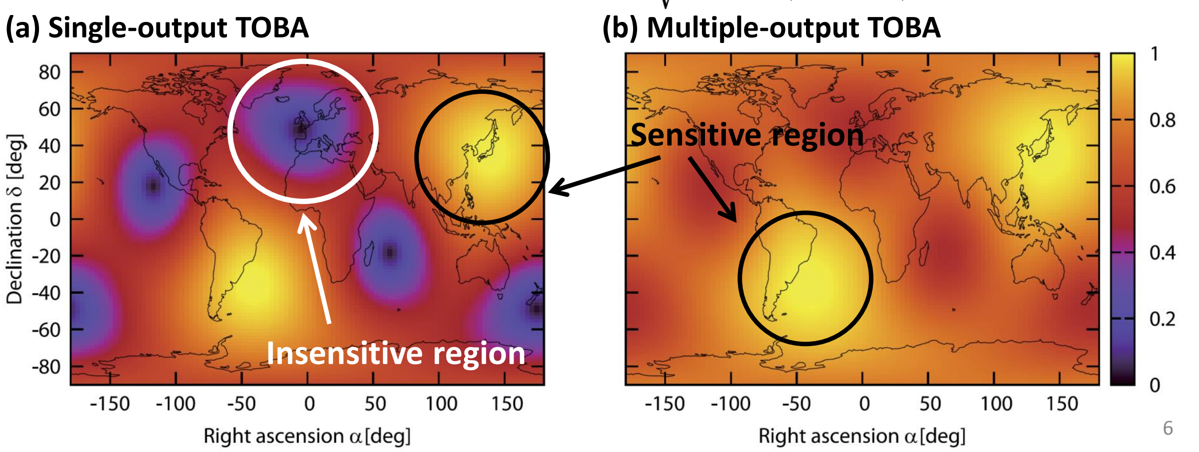

# Monochromatic source

- **GW waveforms**

$$h_+(t) = A_+ \cos(2\pi f_0 t)$$
$$h_\times(t) = A_\times \sin(2\pi f_0 t)$$

✓ **Newtonian circular binary**

$$A_+ = \frac{1}{r}\frac{4G\mu\omega_s R^2}{c^4}\frac{1+\cos^2\iota}{2}$$
$$A_\times = \frac{1}{r}\frac{4G\mu\omega_s R^2}{c^4}\cos\iota$$

- **GW signals of the N-th output**

$$h_N(t) = A_N(t)\cos[\Phi_N(t)]$$
$$A_N(t) = \mathcal{A}Q_N(t),$$
$$Q_N(t) = \left[\left(\frac{1+\cos^2\iota}{2}\right)^2 F_N^{+2}(t) + \cos^2\iota F_N^{\times 2}(t)\right]^{1/2}$$
$$\Phi_N(t) = 2\pi f_0 t + \varphi_0 + \varphi_{p,N}(t) + \varphi_D(t),$$
$$\varphi_{p,N}(t) = \arctan\left[-\frac{2\cos\iota}{1+\cos^2\iota}\frac{F_N^\times(t)}{F_N^+(t)}\right],$$
$$\varphi_D(t) = 2\pi f_0 \frac{\boldsymbol{n}_0\cdot\boldsymbol{r}_d(t)}{c}$$

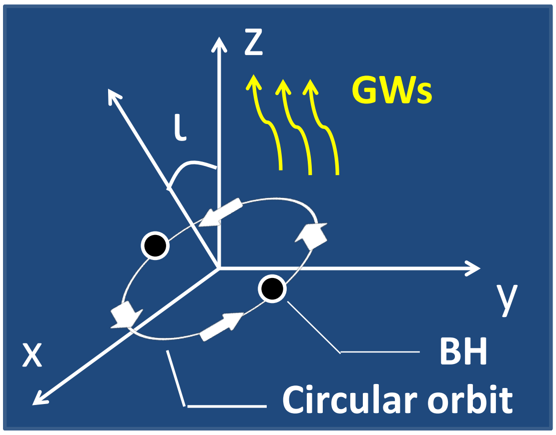




# GW phase

$$\Phi_N(t) = 2\pi f_0 t + \varphi_0 + \varphi_{p,N}(t) + \varphi_D(t)$$

**N-th output signal**

- **Polarization phase**

$$\varphi_{p,N}(t) = \arctan\left[-\frac{2\cos\iota}{1+\cos^2\iota}\frac{F_N^\times(t)}{F_N^+(t)}\right]$$

⇨ **Reflects the geometrical information on the antenna configuration**

⇨ **Significant for <u>short-duration observations</u>**

- **Doppler phase**

$$\varphi_D(t) = 2\pi f_0 \frac{\boldsymbol{n}_0\cdot\boldsymbol{r}_d(t)}{c}$$

⇨ **Induced by the relative motion between the antenna and the GW source**

⇨ **Significant for <u>long-duration observations</u>**

# Angular resolution（single antenna case)

■ Angular resolution

✓ Red line : Multiple-output TOBA

✓ Blue line : Single-output TOBA

✓ frequency 1.0 [Hz]

✓ S/N = 10

✓ α=δ=1.0 [deg]

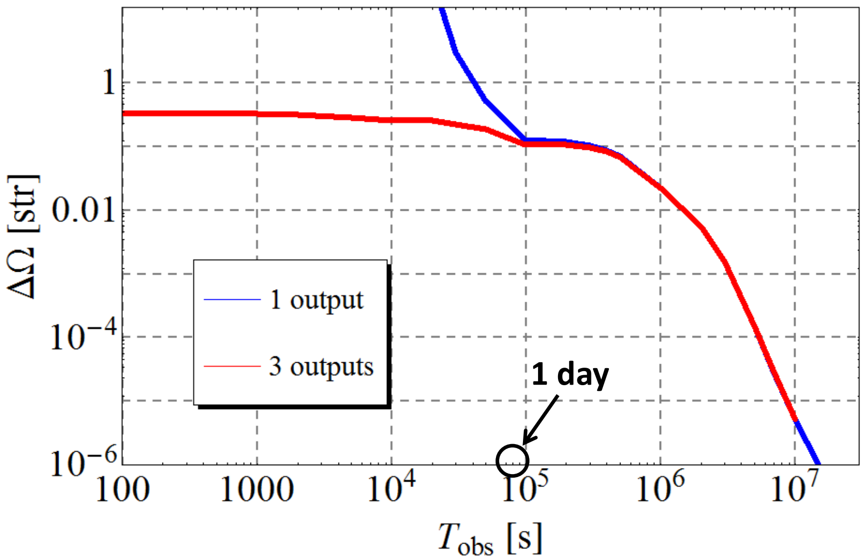




# Summary

✓ We propose multiple-output configuration for a TOBA.

✓ We investigate its angular resolution.

■ Short-duration signals ($T_{obs}$ < 1 day)

□ Inspiral GWs

□ Burst GWs

✓ Previous TOBA can't specify the direction of the GW source.

✓ The angular resolution of the TOBA we proposed is of the order of 0.1 [str] thanks to having 3 independent signals.

■ Long-duration signals ($T_{obs}$ > 1 day)

□ Continuous GWs

✓ There is no difference between previous and new configuration.

✓ The main advantage of the multiple TOBA is just the accumulation of the signal-to-noise ratio.

# “How to probe string axiverse with gravitational wave observations”

Hirotaka Yoshino

[JGRG24(2014)111203]

# *How to probe string axiverse with gravitational wave observations*

Hirotaka Yoshino
Hideo Kodama (KEK)

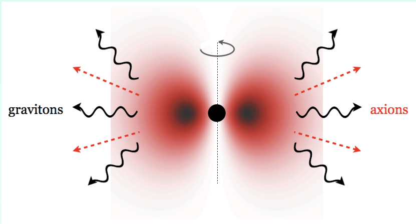


*PTP128, 153 (2012)*
*PTEP2014, 043E02 (2014)*
*arXiv:1407.2030*

JGRG24 @ IPMU (November 12th, 2014)

# CONTENTS

- Introduction *PTP128, 153 (2012) PTEP2014, 043E02 (2014)*
- Constraining string axion models from GW observations *arXiv:1407.2030*
- Summary

# Introduction

## Very interesting era of GR

Advanced LIGO

Advanced VIRGO

KAGRA

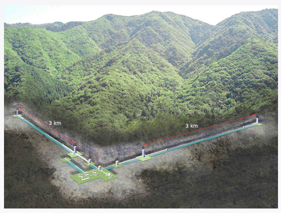

- One of the interesting possibilities is to find new physics beyond GR!

## Can we find a signal of string theory?

Arvanitaki, Dimopoulos, Dubvosky, Kaloper, March-Russel, PRD81 (2010), 123530.

⇨ *Maybe Yes,* if there are String Axions with very tiny mass

- In string theory, many moduli appear when the extra dimensions get compactified.
- Some of them (10-100) are expected to behave like scalar fields with very tiny mass, which are called string axions.

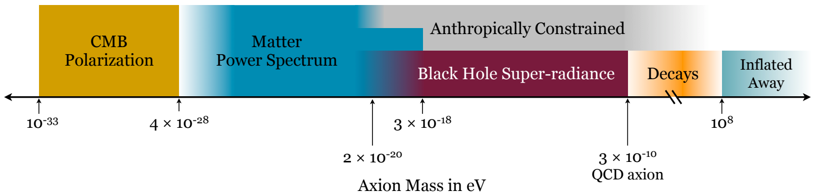


AXIVERSE SCENARIO

## Axion field around a rotating BH

- Axion field extracts BH rotation energy and forms an “axion cloud”

⇨ Gravitational Atom

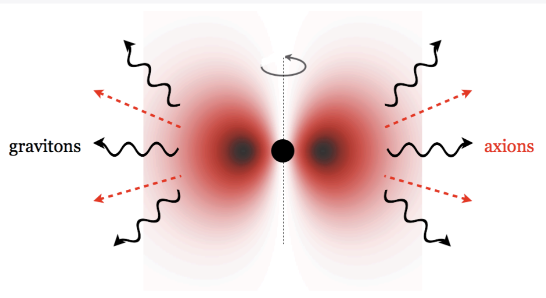


Detweiler, PRD22 (1980), 2323.

Zouros and Eardley, Ann. Phys. 118 (1979), 139.

# Kerr BH

- Metric

$$ds^2 = -\left(\frac{\Delta - a^2\sin^2\theta}{\Sigma}\right)dt^2 - \frac{2a\sin^2\theta(r^2+a^2-\Delta)}{\Sigma}dtd\phi + \left[\frac{(r^2+a^2)^2 - \Delta a^2\sin^2\theta}{\Sigma}\right]\sin^2\theta d\phi^2 + \frac{\Sigma}{\Delta}dr^2 + \Sigma d\theta^2$$

$$\Sigma = r^2 + a^2\cos^2\theta,$$
$$\Delta = r^2 + a^2 - 2Mr.$$

$$J = Ma$$

- Ergoregion

$\xi^\mu$ becomes spacelike

Energy density can be negative,

$$-T_{\mu\nu}\xi^\mu n^\nu < 0$$

Superradiant condition: $\omega < m\Omega_H$

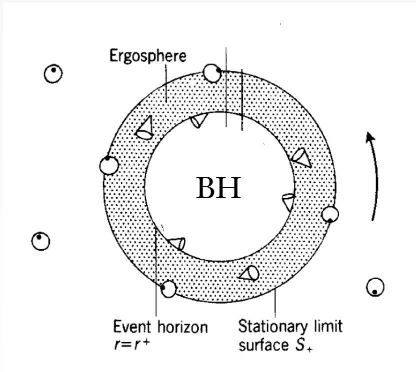


# Gravitational Atom

- Massive Klein-Gordon field $\nabla^2\Phi - \mu^2\Phi = 0$

$$\Phi = \mathrm{Re}[e^{-i\omega t}R(r)S(\theta)e^{im\phi}]$$
$$R = \frac{u}{\sqrt{r^2+a^2}}$$

$$\frac{d^2u}{dr_*^2} + [\omega^2 - V(\omega)]\,u = 0$$

$$\omega = \omega_R + i\,\boxed{\omega_I}$$ ← Unstable if positive

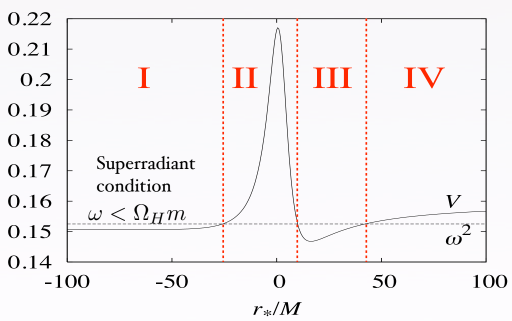


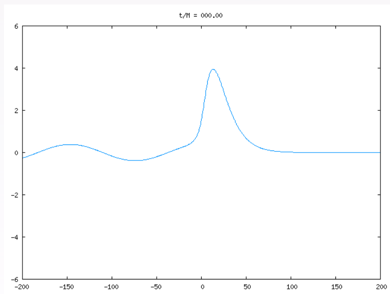

## Growth rate

- Growth rate (continued fraction method) Dolan, PRD76 (2007), 084001.

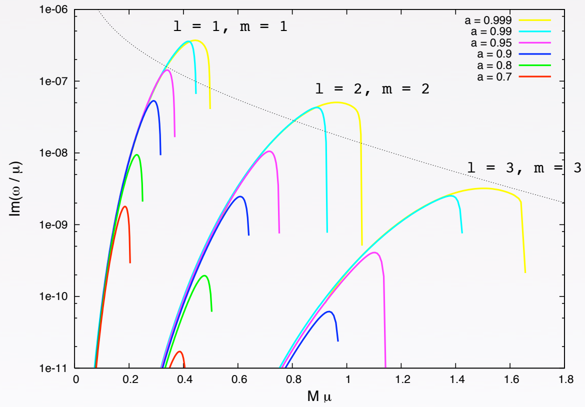


- Typical time scale:

$$M = M_\odot \qquad \begin{array}{lll} \omega_I M \sim 10^{-7} & \Rightarrow & \sim 1 \text{ min.} \\ \omega_I M \sim 10^{-12} & \Rightarrow & \sim 1 \text{ day} \end{array}$$

# Physics of G-Atom

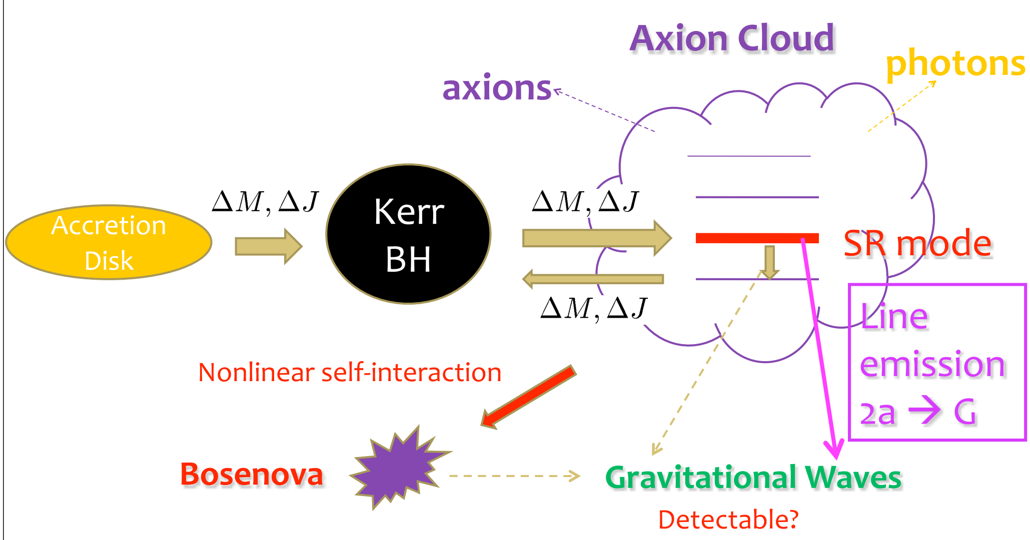

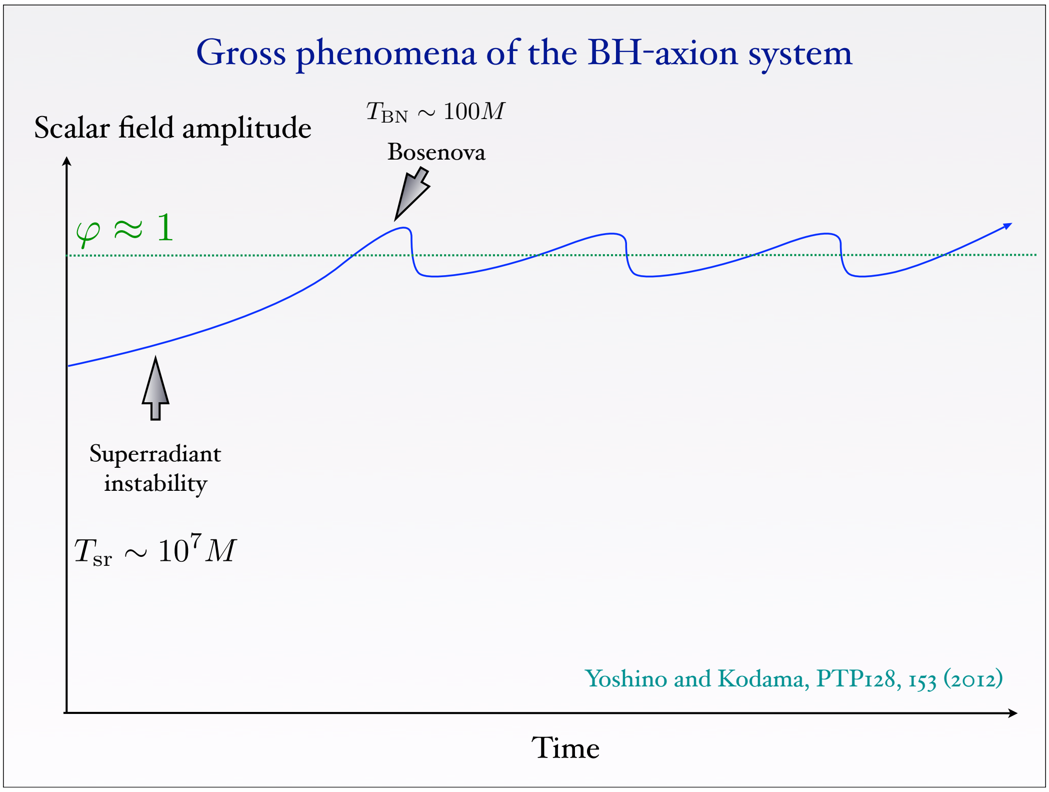
Gross phenomena of the BH-axion system
Scalar field amplitude
$T_{\rm BN} \sim 100M$
Bosenova
$\varphi \approx 1$
Superradiant instability
$T_{\rm sr} \sim 10^7 M$
Yoshino and Kodama, PTP128, 153 (2012)
Time

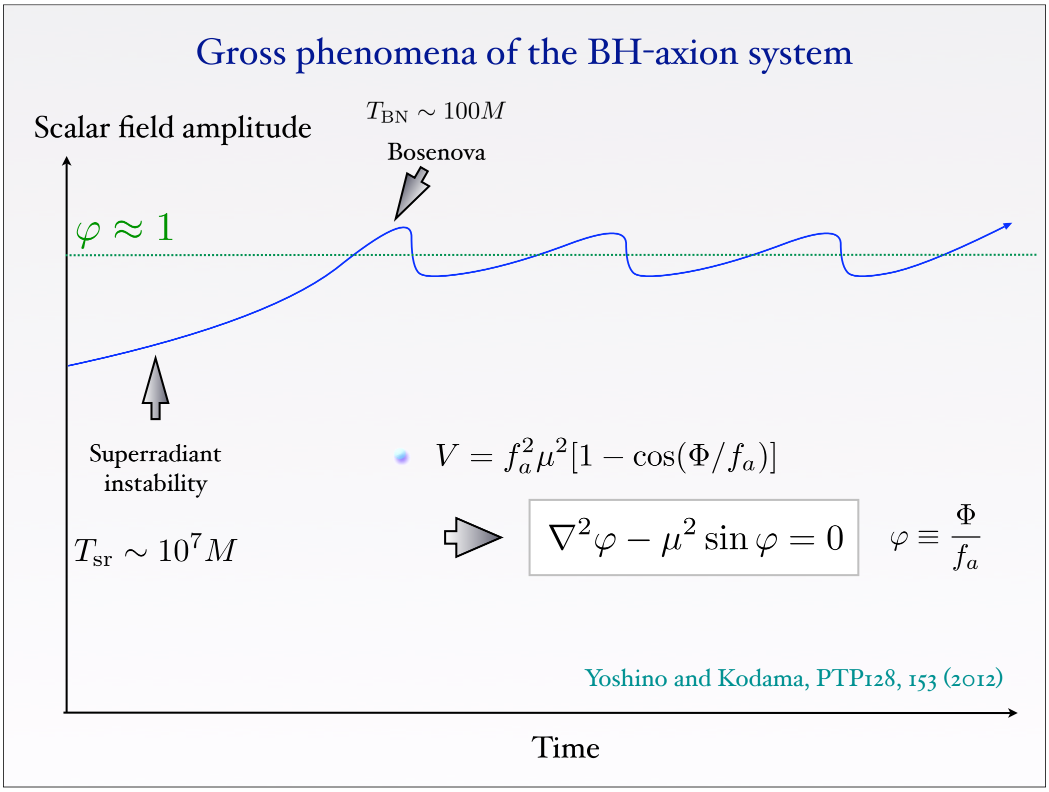
Gross phenomena of the BH-axion system
Scalar field amplitude
$T_{\rm BN} \sim 100M$
Bosenova
$\varphi \approx 1$
Superradiant instability
$T_{\rm sr} \sim 10^7 M$
$V = f_a^2 \mu^2 [1 - \cos(\Phi/f_a)]$
$\boxed{\nabla^2 \varphi - \mu^2 \sin\varphi = 0}$
$\varphi \equiv \frac{\Phi}{f_a}$
Yoshino and Kodama, PTP128, 153 (2012)
Time

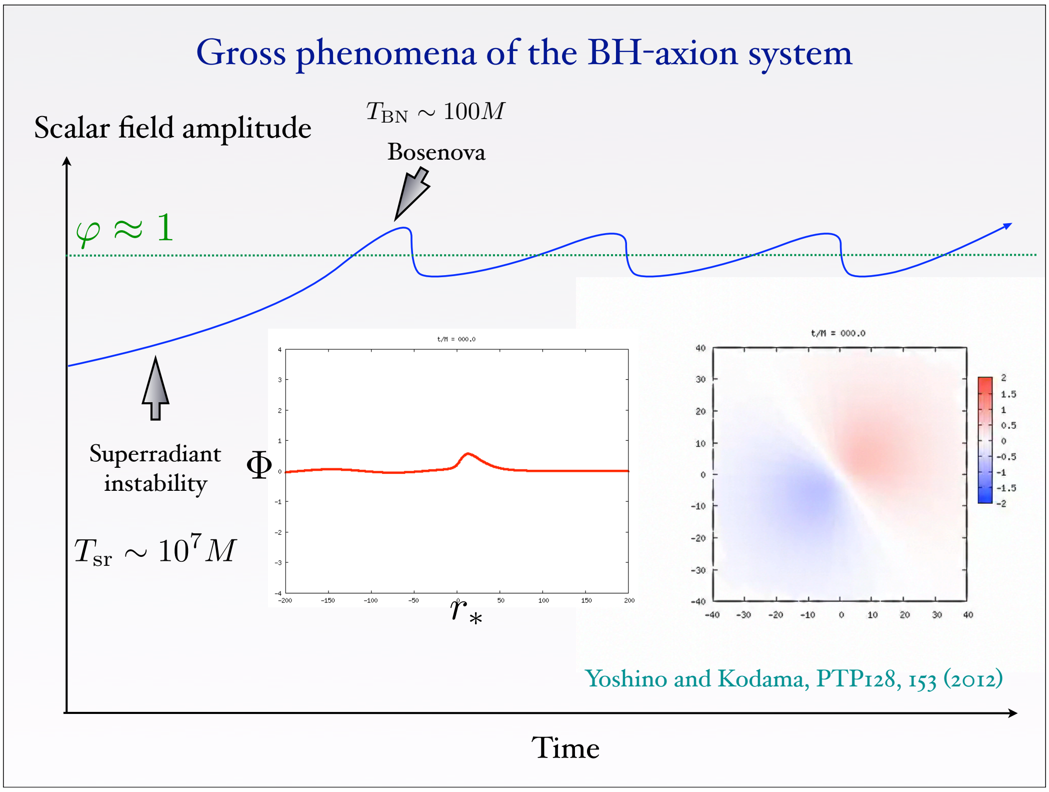
Gross phenomena of the BH-axion system
Scalar field amplitude
$T_{\rm BN} \sim 100M$
Bosenova
$\varphi \approx 1$
Superradiant instability
$T_{\rm sr} \sim 10^7 M$
$\Phi$
$r_*$
t/M = 000.0
Yoshino and Kodama, PTP128, 153 (2012)
Time

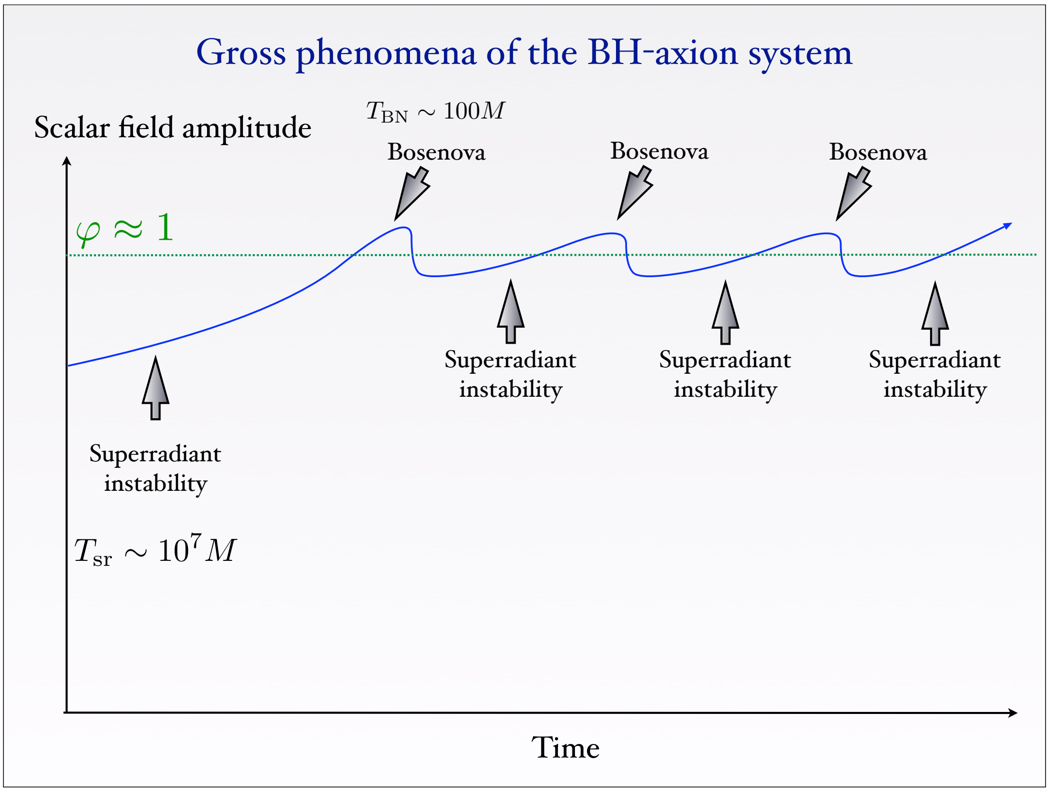
Gross phenomena of the BH-axion system
Scalar field amplitude
$T_{\rm BN} \sim 100M$
Bosenova
Bosenova
Bosenova
$\varphi \approx 1$
Superradiant instability
Superradiant instability
Superradiant instability
Superradiant instability
$T_{\rm sr} \sim 10^7 M$
Time

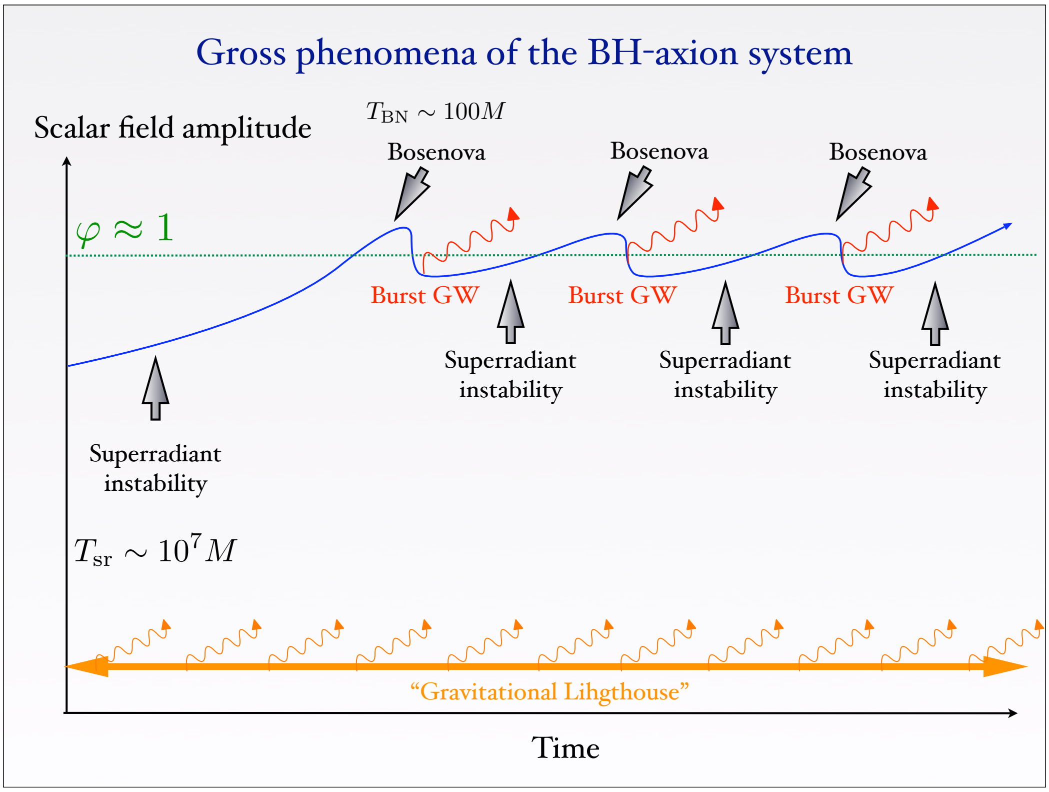
Gross phenomena of the BH-axion system
Scalar field amplitude
$T_{BN} \sim 100M$
Bosenova
Bosenova
Bosenova
$\varphi \approx 1$
Burst GW
Burst GW
Burst GW
Superradiant instability
Superradiant instability
Superradiant instability
Superradiant instability
$T_{sr} \sim 10^7 M$
"Gravitational Lihgthouse"
Time

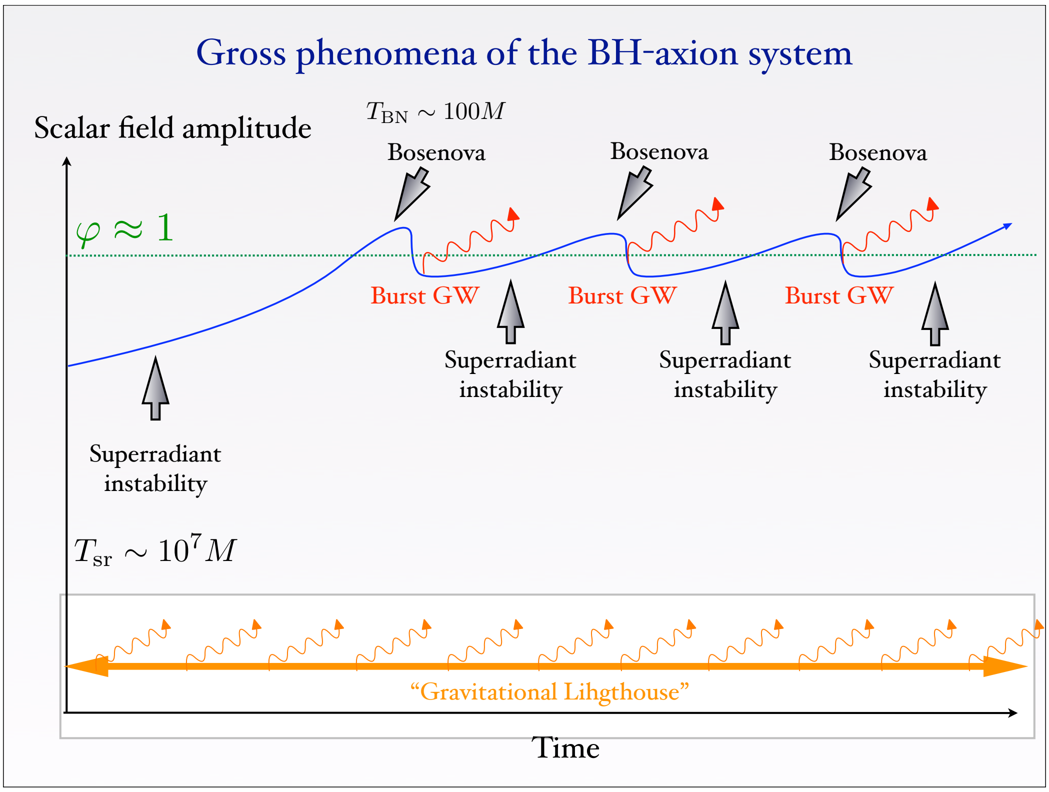
Gross phenomena of the BH-axion system
Scalar field amplitude
$T_{BN} \sim 100M$
Bosenova
Bosenova
Bosenova
$\varphi \approx 1$
Burst GW
Burst GW
Burst GW
Superradiant instability
Superradiant instability
Superradiant instability
Superradiant instability
$T_{sr} \sim 10^7 M$
"Gravitational Lihgthouse"
Time

## Continuous GW emission

- Equation *HY and Kodama, PTEP2014, 043E02 (2014)*

$$\nabla^2 h_{\mu\nu} - 2R_{\mu\ \nu}^{\ \rho\ \sigma} h_{\rho\sigma} = 16\pi G \left( T_{\mu\nu} - \frac{1}{2}\bar{g}_{\mu\nu} T^{\rho}_{\ \rho} \right) \propto e^{i(2\omega)t}$$

  - Ignore nonlinear self-interaction
  - Frequency of continuous GWs $\tilde{\omega} = 2\omega \approx 2\mu$

- In the approximation $\mu M \ll 1$
  - Amplitude of continuous GWs $h_0 \approx C \left(\frac{E_a}{M}\right) (\mu M)^6 \left(\frac{M}{d}\right)$

(for l = m = 1, n=2 axion cloud)

# Constraining string axion models from GW observation

*arXiv:1407.2030*

# LIGO’s science runs

PRD69, 082004 (2004); ...; arXiv:1311.2409 [gr-qc]

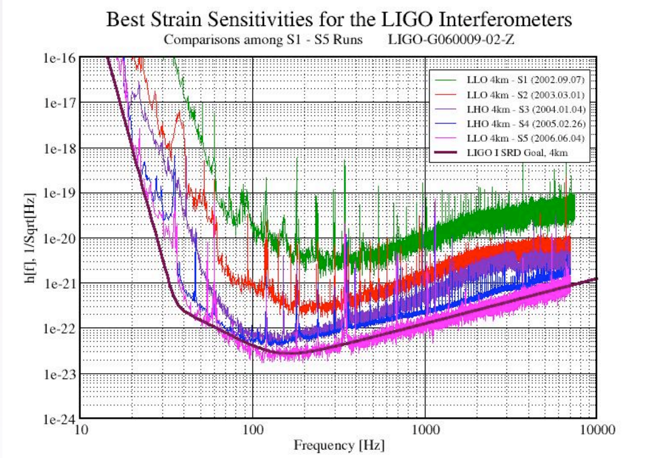


- They looked for continuous waves from distorted pulsars
- Detectable amplitude can be made smaller by increasing observation time $h_{\rm rss} \sim h\sqrt{T_{\rm obs}}$

# LIGO’s continuous wave search

PRD87, 042001 (2013)

No GWs have been detected,
upper limit on the amplitude is given.

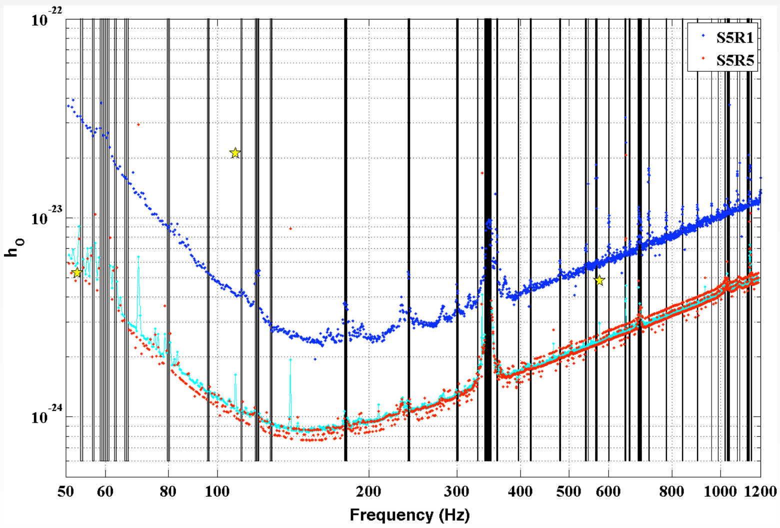

## Exploring Axiverse (1)

- Consider continuous waves from BH-axion system

$$50 \text{ Hz} \le f \le 1200 \text{ Hz}$$
$$\Leftrightarrow \quad 10^{-13} \text{ eV} \le \mu \le 2.4 \times 10^{-12} \text{ eV}$$

- If we assume $M \approx 15 M_\odot$, $\quad 0.0125 \le M\mu \le 0.3$

$\Rightarrow$ We consider axion cloud in the l = m = 1 mode
We use the approximate formula for small $M\mu$

$\Rightarrow$ The wave form is same as the distorted pulsar case

Amplitude: $$h_0 \approx \left(\frac{E_a}{M}\right)(\mu M)^6 \left(\frac{M}{d}\right)$$

## Exploring Axiverse (2)

- We adopt the axion cloud energy when the nonlinear self-interaction becomes important

$$\frac{\Phi_{\max}}{f_a} \approx \frac{1}{\sqrt{8\pi e^2}} \sqrt{\frac{E_a}{M}} \left(\frac{f_a}{M_p}\right)^{-1} (\mu M)^2 \approx 1$$

$$\Rightarrow \boxed{10^{-22} \left(\frac{f_a}{10^{16}\text{GeV}}\right)^2 \left(\frac{M}{15 M_\odot}\right)^3 \left(\frac{\mu}{10^{-12}\text{eV}}\right)^2 \left(\frac{d}{1\text{kpc}}\right)^{-1} < h_{\text{UL}}}$$

- In order to exclude the situation where gravitational backreaction is significant, we require

$$\frac{E_a}{M} < 0.05 \quad \Rightarrow \quad \boxed{\frac{f_a}{10^{16}\text{GeV}} < 0.1 \times \left(\frac{M}{15 M_\odot}\right)^2 \left(\frac{\mu}{10^{-12}\text{eV}}\right)^2}$$

## Let us consider Cygnus X-1

$M \approx 15 M_{\odot}$

$a/M \approx 0.95$

$d \approx 1.86\ \text{kpc}$

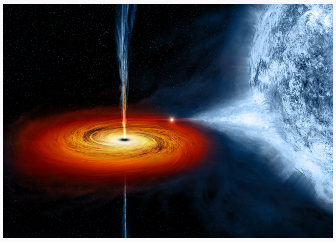

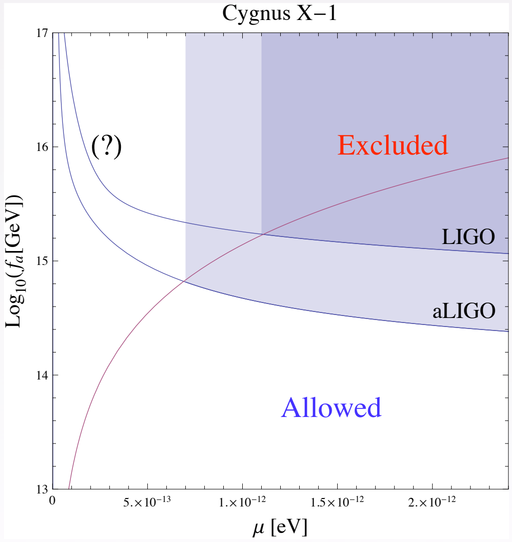


McClintock, et al., arXiv:1106.3688-3690{astro-ph}

## Remark (1)

- The result of the continuous wave search cannot be used in our case because
  - In the data analysis, isolated pulsar is assumed.
  - Cygnus X-1 is a binary system, and therefore, GW frequency fluctuates by the Doppler shift
  - The data analysis strongly depend on the assumed situation
- Targeted search for continuous GWs from the Cygnus X-1 is necessary
- Signal may be detected, or, a constraint can be obtained.

# Remark (2)

- In our analyses of GW emissions, we have ignored the nonlinear self-interaction.
- In our simulation, the nonlinear self-interaction causes radial oscillation of the axion cloud.

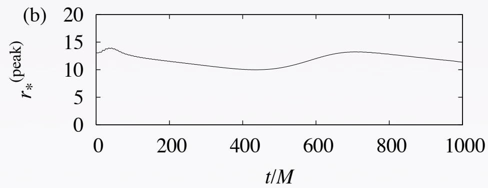


- Taking account of the Doppler shift due to axion cloud position, the GW frequency may fluctuate by about 3 %.
- These modulations can be exactly determined by using the results of our direct numerical simulations including nonlinear self-interaction.

# Summary

## Summary

- It is possible to constrain string axion models from existing LIGO observational data.
- Targeted search for continuous GWs from Cygnus X-1 is required to obtain rigorous constraint.
- Prediction of GWs including the effect of nonlinear self-interaction is necessary, and this study is now ongoing.

*Thank you!*

# “Black hole perturbation in modified gravity”

Teruaki Suyama

[JGRG24(2014)111204]

# Black hole perturbation in modified gravity


Teruaki Suyama

**Research Center for the Early Universe, University of Tokyo**

Collaborators: Tsutomu Kobayashi(Rikkyo University),
Hayato Motohashi (KICP, Chicago University)


Refs. PRD 85 (2012) 084025 and PRD 89 (2014) 084042



## Dawn of gravitational wave physics

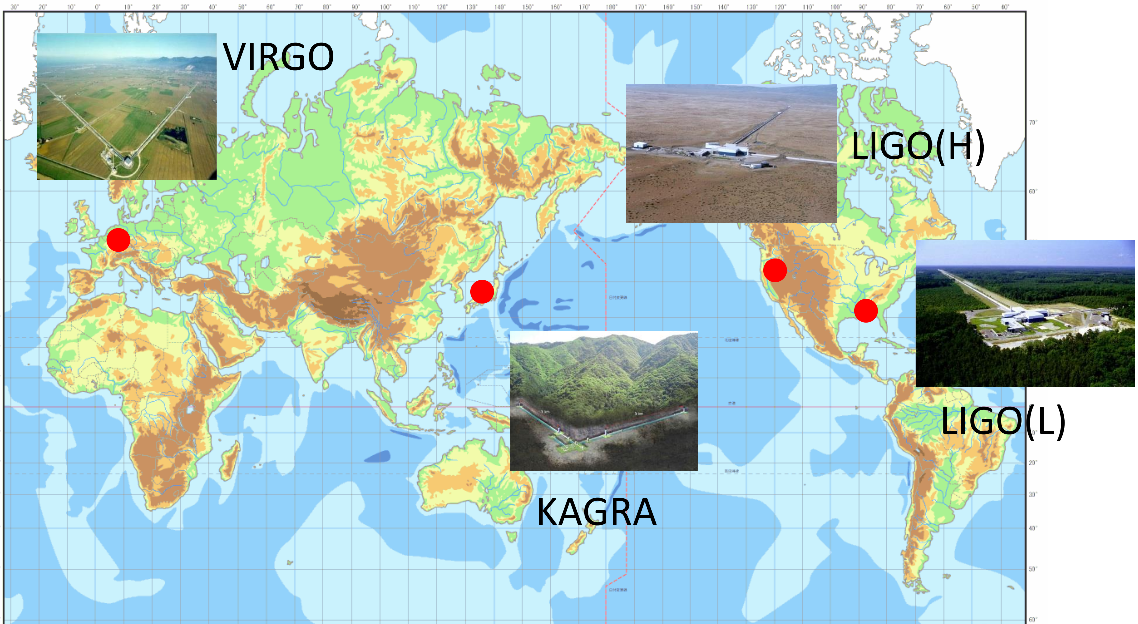


**It is expected that gravitational waves (GWs) will be detected within a few years.**

## Detection of GWs allows us to test modified gravity in strong gravity regime

Typical system

BH spacetime + linear perturbation
(involves gravitational waves)

in modified gravity

As a first step, we consider static and spherically symmetric spacetime as BH spacetime and study linear perturbation.

Derivation of the perturbation equations and see differences from GR.

Derivation of the stability conditions (which any healthy theory should satisfy). They should be known before the theory is compared with observations.



## Horndeski theory (Modified gravity theories we consider)

$$\mathcal{L} = \mathcal{L}(\phi, g_{\mu\nu})$$

Horndeski 1974

Scalar-tensor theory in which field equations are at most second order both in scalar field and metric field. (good framework to start with)

This includes a wide range of modified gravity theories such as Brans-Dicke theory, f(R) theories, Gauss-Bonnet theories, Galileon theories as special cases.

Formulation of BH perturbation in Horndeski theory (without specifying particular theory) thus provides general and versatile applicability.

**Aim is to establish BH perturbation theory.**

# Horndeski theory

$$S=\sum_{i=2}^{5}\int \mathrm{d}^4x\sqrt{-g}\mathcal{L}_i.$$

Lagrangian is specified by four arbitrary functions.

$$\mathcal{L}_2 = K(\phi, X), \qquad \mathcal{L}_3 = -G_3(\phi, X)\Box\phi,$$

$$\mathcal{L}_4 = G_4(\phi, X)R + G_{4X}[(\Box\phi)^2 - (\nabla_\mu\nabla_\nu\phi)^2],$$

$$\mathcal{L}_5 = G_5(\phi, X)G_{\mu\nu}\nabla^\mu\nabla^\nu\phi - \frac{1}{6}G_{5X}[(\Box\phi)^3 - 3\Box\phi(\nabla_\mu\nabla_\nu\phi)^2 + 2(\nabla_\mu\nabla_\nu\phi)^3], \quad X := -(\partial\phi)^2/2$$

# BH perturbation

Background solutions

$$ds^2 = -A(r)dt^2 + \frac{dr^2}{B(r)} + r^2\left(d\theta^2 + \sin^2\theta\, d\varphi^2\right)$$

$\phi = \phi(r)$ A(r), B(r) : solution of background EOMs.

Decomposition of the perturbation variables into odd and even parity part defined on the spherical coordinate (θ, ϕ).

Example

$$V_a = \partial_a S + \epsilon_{ab}\partial_b U$$

even(no ε) odd(with ε)

$$2 = 1 + 1$$

# Odd parity case

## Odd parity metric perturbations

$$
\begin{aligned}
h_{tt} &= 0, \quad h_{tr} = 0, \quad h_{rr} = 0, \\
h_{ta} &= \sum_{\ell,m} h_{0,\ell m}(t,r) E_{ab} \partial^b Y_{\ell m}(\theta,\varphi), \\
h_{ra} &= \sum_{\ell,m} h_{1,\ell m}(t,r) E_{ab} \partial^b Y_{\ell m}(\theta,\varphi), \\
h_{ab} &= \frac{1}{2} \sum_{\ell,m} h_{2,\ell m}(t,r) \left[ E_a{}^c \nabla_c \nabla_b Y_{\ell m}(\theta,\varphi) + E_b{}^c \nabla_c \nabla_a Y_{\ell m}(\theta,\varphi) \right]
\end{aligned}
$$

Scalar field does not acquire odd parity perturbation.

7

# Even parity case

$$
\begin{aligned}
h_{tt} &= A(r) \sum_{\ell,m} H_{0,\ell m}(t,r) Y_{\ell m}(\theta,\varphi), \\
h_{tr} &= \sum_{\ell,m} H_{1,\ell m}(t,r) Y_{\ell m}(\theta,\varphi), \\
h_{rr} &= \frac{1}{B(r)} \sum_{\ell,m} H_{2,\ell m}(t,r) Y_{\ell m}(\theta,\varphi), \\
h_{ta} &= \sum_{\ell,m} \beta_{\ell m}(t,r) \partial_a Y_{\ell m}(\theta,\varphi), \\
h_{ra} &= \sum_{\ell,m} \alpha_{\ell m}(t,r) \partial_a Y_{\ell m}(\theta,\varphi), \\
h_{ab} &= \sum K_{\ell m}(t,r) g_{ab} Y_{\ell m}(\theta,\varphi) + \sum G_{\ell m}(t,r) \nabla_a \nabla_b Y_{\ell m}(\theta,\varphi) .
\end{aligned}
$$

$$
\phi(t,r,\theta,\varphi) = \phi(r) + \sum_{\ell,m} \delta\phi_{\ell m}(t,r) Y_{\ell m}(\theta,\varphi),
$$

Not only metric but also scalar field are perturbed.

8

Metric perturbations are decomposed into odd and even parts.

10(total) = 3(odd) + 7(even)

As for the scalar field, we have

1(total) = 0(odd) + 1(even)

**Advantage of this decomposition**

Linear perturbations for even and odd are decoupled. Thus we can solve them separately, which makes the analysis easier.



# Basic procedure

Perturbed variables (either odd-modes or even modes and particular multipole)

Action second order in perturbation

Identification of dynamical variables

Derivation of Schrodinger type master equations

Determination of perturbation behavior (stability, sound speed, etc.)

**Methodology is simple!**

# Case of GR

Perturbation of Schwarzshild spacetime

Regge-Wheeler-Zerilli formalism



## Computation is cumbersome even in GR.

Regge

Wheeler

able example of Wheeler's role with students. In 1955, when Wheeler had just published his geon paper and was beginning to struggle with the issue of the final state, he met Regge at the first Rochester Conference on High Energy Physics. Regge, an Italian graduate student, was introduced to Wheeler as "mathematically brilliant," so Wheeler suggested he work out the theory of weak perturbations of a Schwarzschild singularity. Wheeler, knowing roughly how the calculation should go, wrote a draft of a paper titled "On the Stability of the Schwarzschild Singularity" with the equations left blank and invited Regge to calculate the details and fill in the equations. Remarkably, it all worked out more or less as planned, and their paper has become a classic.[13] A few

(Misner, Thorne&Zurek, Physics today, 2009)

PHYSICAL REVIEW VOLUME 108, NUMBER 4 NOVEMBER 15, 1957

**Stability of a Schwarzschild Singularity**

TULLIO REGGE, *Istituto di Fisica della Università di Torino, Torino, Italy*

AND

JOHN A. WHEELER, *Palmer Physical Laboratory, Princeton University, Princeton, New Jersey*

(Received July 15, 1957)

Odd type perturbation equations were successfully compactified into a single master equation (Regge-Wheeler equation).

$$d^2Q/dr^{*2}+k_{\mathrm{eff}}{}^2(r)Q=0.$$

$$k_{\mathrm{eff}}{}^2=k^2-L(L+1)e^{\nu}/r^2+6m^*e^{\nu}/r^3,$$

Represents propagation of gravitational wave.

13

Even type perturbation equations, due to complex structure of perturbation equations, were not successfully compactified into a single master equation.

> There remains the discussion for the even waves. Here we have to examine the system (27b,c,d) supplemented by the condition (28). Unfortunately, owing to the complication of the equations involved, we were not able to establish a convenient "effective potential" picture. However, as far as stability is concerned there
>
> (Regge&Wheeler, 1959)

VOLUME 24, NUMBER 13 PHYSICAL REVIEW LETTERS 30 MARCH 1970

EFFECTIVE POTENTIAL FOR EVEN-PARITY REGGE-WHEELER GRAVITATIONAL PERTURBATION EQUATIONS*

Frank J. Zerilli
Physics Department, University of North Carolina, Chapel Hill, North Carolina 27514
(Received 29 January 1970)

A master equation for the even-parity perturbations was successfully derived.

$$d^2\hat{K}_{LM}/dr^{*2} + [\omega^2 - V_L(r)]\hat{K}_{LM} = 0.$$

Regge-Wheeler eq. (1957)

Zerilli eq. (1970)

13 years gap!!



## BH perturbation in the Horndeski theory

Master equation of odd-parity perturbation in 2012

Master equations of even-parity perturbation in 2014

We have shortened 13 years gap to 2 years gap!!

As expected, master equations take forms of the Schrodinger equation.

<u>One big difference from GR</u>

Since we have scalar field in addition to the metric, we obtain coupled equations for two dynamical variables (GW and scalar wave).

# Table

| | Odd-parity | Even-parity |
|---|---|---|
| DOF | 1 (only GW) | 2 (GW and scalar wave) |
| No-ghost | $\mathcal{G} > 0$ | $\mathcal{F} > 0 \quad 2\mathcal{P}_1 - \mathcal{F} > 0$ |
| Propagation speeds | $c_r^2 = \dfrac{\mathcal{G}}{\mathcal{F}}, \quad c_\theta^2 = \dfrac{\mathcal{G}}{\mathcal{H}}$ | $c_{s1}^2 = \dfrac{\mathcal{G}}{\mathcal{F}}$ <br> $c_{s2}^2 = \dfrac{2r^2\Gamma\mathcal{H}\Xi\phi'^2 - \mathcal{G}\Xi^2\phi'^2 - 4r^4\Sigma\mathcal{H}^2/B}{(2r\mathcal{H}+\Xi\phi')^2(2\mathcal{P}_1 - \mathcal{F})}$ |
| No-gradient instability | $\mathcal{F} > 0 \quad \mathcal{H} > 0$ | $2r^2\Gamma\mathcal{H}\Xi\phi'^2 - \mathcal{G}\Xi^2\phi'^2 - \dfrac{4r^4}{B}\Sigma\mathcal{H}^2 > 0$ |

$$\mathcal{F} := 2\left(G_4 + \frac{1}{2}B\phi' X' G_{5X} - XG_{5\phi}\right) \qquad \mathcal{H} := 2\left[G_4 - 2XG_{4X} + X\left(\frac{B\phi'}{r}G_{5X} + G_{5\phi}\right)\right]$$

$$\mathcal{G} := 2\left[G_4 - 2XG_{4X} + X\left(\frac{A'}{2A}B\phi' G_{5X} + G_{5\phi}\right)\right]$$

17

$$\mathcal{P}_1 := \frac{B(2r\mathcal{H}+\Xi\phi')}{2Ar^2\mathcal{H}^2}\left[\frac{Ar^4\mathcal{H}^4}{(2r\mathcal{H}+\Xi\phi')^2 B}\right]'$$

$$\Xi := 2r^2\left[-XG_{3X} + \frac{2B\phi'}{r}\{G_{4XY} - (XG_{5\phi})_X\} + G_{4\phi Y} - \frac{1}{r^2}XG_{5X} + \frac{B}{r^2}(XG_{5X})_Y\right]$$

$$\Gamma := \Gamma_1 + \frac{A'}{A}\Gamma_2$$

$$\Gamma_1 := 4\left[-XG_{3X} + G_{4\phi Y} + \frac{B\phi'}{r}\{G_{4XY} - (XG_{5\phi})_X\}\right]$$

$$\Gamma_2 := 2B\phi'\left[G_{4XY} - (XG_{5\phi})_X - \frac{B\phi'}{2rX}(XG_{5X})_Y\right]$$

## Summary

BH perturbation in the Horndeski framework was formulated
(Both for odd parity and even parity perturbations).

Healthy conditions such as no-ghost condition are obtained.

Master equations are derived.

This formulation can be applied to a wide range of modified gravity theories such as f(R), Galileon gravity, kinetic braiding gravity, etc.

Dynamical degrees of freedom: 1 for odd parity and 2 for even parity.

Gravitational odd and even parity perturbations propagate at the same speed. But the scalar wave propagates at different speed in general. They are independent of the multipole L.



# appendix

# Odd parity case

(T.Kobayashi, H.Motohashi and TS, 2012)

Odd parity perturbations

$$h_{tt}=0,\quad h_{tr}=0,\quad h_{rr}=0,$$
$$h_{ta}=\sum_{\ell,m}\underline{h_{0,\ell m}(t,r)}E_{ab}\partial^b Y_{\ell m}(\theta,\varphi),$$
$$h_{ra}=\sum_{\ell,m}\underline{h_{1,\ell m}(t,r)}E_{ab}\partial^b Y_{\ell m}(\theta,\varphi),$$

Gauge fixing

$$h_{ab}=\frac{1}{2}\sum_{\ell,m}\cancel{h_{2,\ell m}(t,r)}\left[E_a{}^c\nabla_c\nabla_b Y_{\ell m}(\theta,\varphi)+E_b{}^c\nabla_c\nabla_a Y_{\ell m}(\theta,\varphi)\right]$$

Scalar field does not acquire odd parity perturbation.



Computation of the 2nd order action shows that one field is an auxiliary field. (1 dynamical degree of freedom)

Final 2nd order Lagrangian

$$\frac{2\ell+1}{2\pi}\mathcal{L}^{(2)}=\frac{\ell(\ell+1)}{2(\ell-1)(\ell+2)}\left[\frac{\mathcal{F}}{AB\mathcal{G}}\dot{Q}^2-Q'^2-\frac{\ell(\ell+1)\mathcal{F}}{r^2B\mathcal{H}}Q^2-V(r)Q^2\right]$$

$$V(r)=-\frac{1}{16}\left[4\frac{A'}{A}\left(\frac{\mathcal{F}'}{\mathcal{F}}+\frac{\mathcal{H}'}{\mathcal{H}}+\frac{3}{r}\right)+3\frac{B'^2}{B^2}+4\left(\frac{B'}{B}\frac{\mathcal{F}'}{\mathcal{F}}+\frac{B'}{rB}-\frac{B''}{B}+\frac{10\mathcal{F}}{Br^2\mathcal{H}}\right)\right.$$
$$\left.-4\left(3\frac{\mathcal{F}'^2}{\mathcal{F}^2}-\frac{2\mathcal{F}''}{\mathcal{F}}+\frac{4\mathcal{F}'}{r\mathcal{F}}+\frac{2\mathcal{H}'}{r\mathcal{H}}+\frac{10}{r^2}\right)\right].$$

Once Q is solved, h0 and h1 are uniquely determined.

Master equation

$$\boxed{\frac{\mathcal{F}}{AB\mathcal{G}}\ddot{Q} - Q'' + \frac{\ell(\ell+1)\mathcal{F}}{r^2 B\mathcal{H}}Q + V(r)Q = 0.}$$

$$\mathcal{F} := 2\left(G_4 + \frac{1}{2}B\phi' X' G_{5X} - XG_{5\phi}\right),$$

$$\mathcal{G} := 2\left[G_4 - 2XG_{4X} + X\left(\frac{A'}{2A}B\phi' G_{5X} + G_{5\phi}\right)\right],$$

$$\mathcal{H} := 2\left[G_4 - 2XG_{4X} + X\left(\frac{B\phi'}{r}G_{5X} + G_{5\phi}\right)\right]$$

These quantities are uniquely determined once modified gravity Langrangian and background solutions are provided.



Propagation speed

$$c_r^2 = \frac{\mathcal{G}}{\mathcal{F}}, \qquad c_\theta^2 = \frac{\mathcal{G}}{\mathcal{H}},$$

radial angular

They are generally different from the velocity of light.
(but do not depend on multipole L)

Stability conditions

$\mathcal{G} > 0.$ No-ghost condition

$\mathcal{F} > 0 \quad \mathcal{H} > 0.$

## Dipole perturbation (L=1)

This mode is exceptional in the sense that no dynamical field appears.

$$\dot{h}_0' - \frac{2}{r}\dot{h}_0 = 0,$$
$$a_3 h_0'' + a_3' h_0' - \frac{2(ra_3)'}{r^2} h_0 = 0,$$

$$h_0 = \frac{3Jr^2}{4\pi}\int^r \frac{d\tilde{r}}{\tilde{r}^4\mathcal{H}}\sqrt{\frac{A}{B}}$$

This represents a slowly rotating BH. (In GR, this coincides with a Kerr metric expanded to first order in the angular momentum.)



## Even parity case

(Kobayashi, Motohashi and TS, 2014)

$$h_{tt} = A(r)\sum_{\ell,m} H_{0,\ell m}(t,r)Y_{\ell m}(\theta,\varphi),$$
$$h_{tr} = \sum_{\ell,m} H_{1,\ell m}(t,r)Y_{\ell m}(\theta,\varphi),$$
$$h_{rr} = \frac{1}{B(r)}\sum_{\ell,m} H_{2,\ell m}(t,r)Y_{\ell m}(\theta,\varphi),$$

Gauge fixing

$$h_{ta} = \sum_{\ell,m} \cancel{\beta_{\ell m}(t,r)}\partial_a Y_{\ell m}(\theta,\varphi),$$
$$h_{ra} = \sum_{\ell,m} \alpha_{\ell m}(t,r)\partial_a Y_{\ell m}(\theta,\varphi),$$

Gauge fixing

$$h_{ab} = \sum \cancel{K_{\ell m}(t,r)}g_{ab}Y_{\ell m}(\theta,\varphi) + \sum \cancel{G_{\ell m}(t,r)}\nabla_a\nabla_b Y_{\ell m}(\theta,\varphi)\,.$$
$$\phi(t,r,\theta,\varphi) = \phi(r) + \sum_{\ell,m}\delta\phi_{\ell m}(t,r)Y_{\ell m}(\theta,\varphi),$$

Not only metric but also scalar field are perturbed.

## 2nd order Lagrangian

After some manipulations, we end up with two dynamical fields.

$$\frac{2\ell+1}{2\pi}\mathcal{L} = \frac{1}{2}\mathcal{K}_{ij}\dot{v}^i\dot{v}^j - \frac{1}{2}\mathcal{G}_{ij}v^{i\prime}v^{j\prime} - Q_{ij}v^i v^{j\prime} - \frac{1}{2}\mathcal{M}_{ij}v^i v^j,$$

K,G,Q and M are background dependent 2 × 2 matrices.

Variations yield a closed set of wave equations.

Explicit confirmation of

- 2 dynamical degrees of freedom (one gravitational wave and one scalar wave).
- second order field equations which is a characteristic of the Horndeski theory.



This is a generalization of the Zerilli equation.

Master equation in GR

$$d^2\hat{K}_{LM}/dr^{*2} + [\omega^2 - V_L(r)]\hat{K}_{LM} = 0.$$

$$V_L(r) = \left(\frac{1-2m}{r}\right)\frac{2\lambda^2(\lambda+1)r^3 + 6\lambda^2 m r^2 + 18\lambda m^2 r + 18m^3}{r^3(\lambda r + 3m)^2}$$

$$\lambda = \tfrac{1}{2}(L-1)(L+2)$$

In the Horndeski case, we have two dynamical variables (scalar and gravitational wave).

In the GR limit, degrees of freedom is reduced and we go back to the Zerilli equation.

## No-ghost conditions

$$\mathcal{K}_{11} = \frac{8\sqrt{AB}(2r\mathcal{H}+\Xi\phi')^2}{\ell(\ell+1)A^2\mathcal{H}^2}\frac{\ell(\ell+1)\mathcal{P}_1-\mathcal{F}}{(2r\mathcal{H}\ell(\ell+1)+\mathcal{P}_2)^2} > 0$$

$$\det(\mathcal{K}) = \frac{2(\ell-1)(\ell+2)(2r\mathcal{H}+\Xi\phi')^2\mathcal{F}(2\mathcal{P}_1-\mathcal{F})}{3\ell(\ell+1)A^2\mathcal{H}^2\phi'^2(2r\mathcal{H}\ell(\ell+1)+\mathcal{P}_2)^2} > 0$$

$$\mathcal{P}_1 = \frac{B(2r\mathcal{H}+\Xi\phi')}{2Ar^2\mathcal{H}^2}\left(\frac{Ar^4\mathcal{H}^4}{(2r\mathcal{H}+\Xi\phi')^2B}\right)'$$

$$\mathcal{P}_2 = -B\left(2-\frac{rA'}{A}\right)(2r\mathcal{H}+\Xi\phi').$$

As a result, we obtain a concise formula.

$$\boxed{2\mathcal{P}_1-\mathcal{F}>0}$$

This imposes further restriction on the modified gravity theory.



## Propagation speeds

$$c_1^2 = \frac{\mathcal{G}}{\mathcal{F}}, \quad \text{(gravitational wave)}$$

$$c_2^2 = \frac{2r^2\Gamma\mathcal{H}\Xi\phi'^2 - \mathcal{G}\Xi^2\phi'^2 - \frac{4r^4}{B}\Sigma\mathcal{H}^2}{(2r\mathcal{H}+\Xi\phi')^2(2\mathcal{P}_1-\mathcal{F})} \quad \text{(scalar wave)}$$

These should be positive as well.

Interestingly, $c_1^2$ coincides with the one of the odd parity perturbation. Odd parity and even parity gravitational waves propagate at the same speed (but not necessarily equal to c).

If odd and even parity gravitational waves turn out to propagate with different speeds, all the theories in the Horndeski class is excluded!!

Propagation speed of the scalar wave is generally different from that of the gravitational waves.

## Monopole perturbation (L=0)

In GR, such perturbation does not exist. But in Horndeski theory, it does. (existence of the scalar wave)

$$\mathcal{L} = \frac{1}{2}\mathcal{K}\delta\dot{\phi}^2 - \frac{1}{2}\mathcal{G}\delta\phi'^2 - \frac{1}{2}\mathcal{M}\delta\phi^2$$

$$\mathcal{K} = \frac{2}{\sqrt{AB}\phi'^2}\left(2\mathcal{P}_1 - \mathcal{F}\right),$$

$$c_s^2 = \frac{2r^2\Gamma\mathcal{H}\Xi\phi'^2 - \mathcal{G}\Xi^2\phi'^2 - \frac{4r^4}{B}\Sigma\mathcal{H}^2}{\left(2r\mathcal{H} + \Xi\phi'\right)^2(2\mathcal{P}_1 - \mathcal{F})}$$

The same no-ghost condition as that for higher multipoles.

The same propagation speed as that for higher multipoles.



## Dipole perturbation (L=1)

In GR, such perturbation does not exist. But in Horndeski theory, it does.

The same no-ghost condition as that for higher multipoles.

The same propagation speed as that for higher multipoles.

This is a generalization of the Regge-Wheeler equation.

Master equation in GR

$$d^2Q/dr^{*2} + k_{\mathrm{eff}}{}^2(r)Q = 0.$$

$$k_{\mathrm{eff}}{}^2 = k^2 - L(L+1)e^{\nu}/r^2 + 6m^* e^{\nu}/r^3,$$

$$ds^2 = -e^{\nu}dT^2 + e^{\lambda}dr^2 + r^2(d\theta^2 + \sin^2\theta d\varphi^2);$$

Our master equation reduces to the Regge-Wheeler equation in the GR limit.



Bocharova-Bronnikov-Melnikov-Bekenstein solution

$$S = \frac{M_{\mathrm{Pl}}^2}{2}\int d^4x\,\sqrt{-g}R - \int d^4x\,\sqrt{-g}\left(\frac{1}{2}\partial^{\mu}\phi\partial_{\mu}\phi + \frac{R}{12}\phi^2\right)$$

$$f(\phi) = \frac{M_{\mathrm{Pl}}^2}{2} - \frac{\phi^2}{12}$$

BBMB solution

$$ds^2 = -\left(1 - \frac{M}{r}\right)^2 \mathrm{d}t^2 + \frac{\mathrm{d}r^2}{(1 - M/r)^2} + r^2\mathrm{d}\Omega^2$$

$$\phi = \pm\frac{\sqrt{6}M_{\mathrm{Pl}}M}{r - M},$$

Horizon at r=M

$$\mathcal{F} = \mathcal{G} = \mathcal{H} = \frac{M_{\mathrm{Pl}}^2 r(r - 2M)}{(r - M)^2}$$

Unstable for r< 2M

Therefore, BBMB solution is unstable.

## Derivative coupling to the Einstein tensor

$$S = \int d^4x \sqrt{-g}\,[\zeta R - \eta \partial^\mu \phi \partial_\mu \phi + \beta G^{\mu\nu} \partial_\mu \phi \partial_\nu \phi - 2\Lambda]$$

$$K = 2(\eta X - \Lambda), \quad G_3 = 0, \quad G_4 = \zeta, \quad G_5 = -\beta\phi$$

### Background solution

Babichev&Charmousis(2013)

$$\begin{aligned}
A &= 1 - \frac{\mu}{r} + \frac{\eta}{3\beta}\frac{2\zeta\eta - \lambda}{2\zeta\eta + \lambda} r^2 + \frac{\lambda^2}{4\zeta^2\eta^2 - \lambda^2}\frac{\arctan(r\sqrt{\eta/\beta})}{r\sqrt{\eta/\beta}} \\
B &= \frac{(\beta + \eta r^2)A}{\beta (rA)'}, \\
\phi'^2 &= -\frac{r\lambda (r^2 A^2)'}{2(\beta + \eta r^2)^2 A^2},
\end{aligned}$$

35

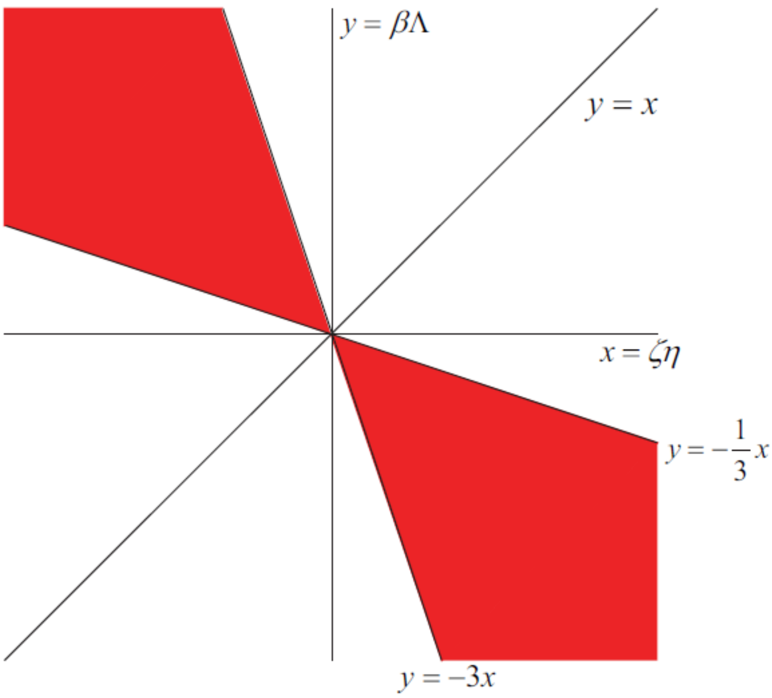


Stable regions are colored red.

36

# “Derivation of higher dimensional black holes in the large D limit”

Ryotaku Suzuki

[JGRG24(2014)111205]

# Derivation of higher dimensional black holes in the large D limit

**Ryotaku Suzuki (Osaka City U.)**

based on recent works in collaboration with
Roberto Emparan, Takahiro Tanaka,
Kentaro Tanabe, Tetsuya Shiromizu

JGRG24, 10-14 November 2014, IPMU, Japan

# Motivation

In Higher Dimension, BH of various topology is possible, but the phase of BHs are still unclear.
In D>5, no general technique for solving Einstein Eq.

► **We need help of Approximations in higher dimension**

**Blackfold approach** Emparan et.al. (2007)

Applied to BHs with **large hierarchy** in horizon scale*s*
Ex) Black ring, saturn, di-ring ***in thin ring limit***, etc.

**Large D limit** Emparan, **RS**, Tanabe (2013)
not quantitatively good for low D
but applied to more general configurations

# Large D limit

### Vacuum Einstein equation

$$S = \int dx^{D} R$$

Take $D \to \infty$ as if D is a continuous parameter

$\longrightarrow$ Variables = ( D=∞ )+( 1/D correction) +…
Leading

Einstein eq. is expanded by 1/D
, then solved order by order

# Gravity in Large D limit

**New Hierarchy**

Gravity
$\Phi \sim \left(\frac{r_0}{r}\right)^{D-3}$
exponentially suppressed
$\ll 1/D^k$

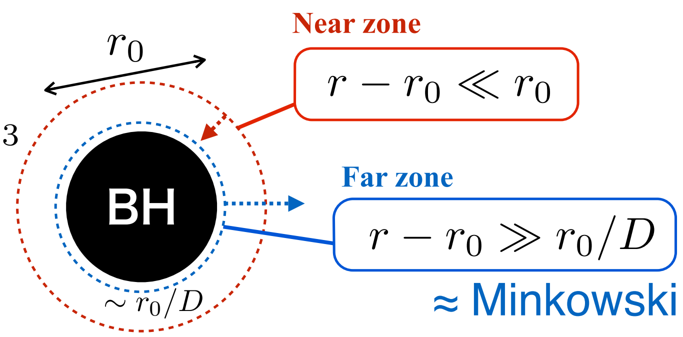


Overlap zone $r_0/D \ll r - r_0 \ll r_0$
$\rightarrow$ Matching Near and Far Sols.

**Simplification of Einstein Eq.**

ex) PDE→ODE,
decoupling of variables

# Large D limit for BH perturbations

We have shown **BH perturbations** are well described by analytically in the large D limit. Followings are studied

- Gregory-Laflamme instability — Asnin et.al.(2007), Emparan, RS, Tanabe (2013)
- QNMs of BH (AdS/rotating/brane) — Emparan, RS, Tanabe (2014)
- Inst. of MPBH (bar/axissym. modes)

etc...

→ **How about beyond linear analysis ?**



# Outline

1. ***Einstein Equation in the large D limit***
2. ***Example: Non-Uniform black string***
3. ***Summary***

# Outline

1. ***Einstein Equation in the large D limit***
2. *Example: Non-Uniform black string*
3. *Summary*

## Hierarchy at Large D limit

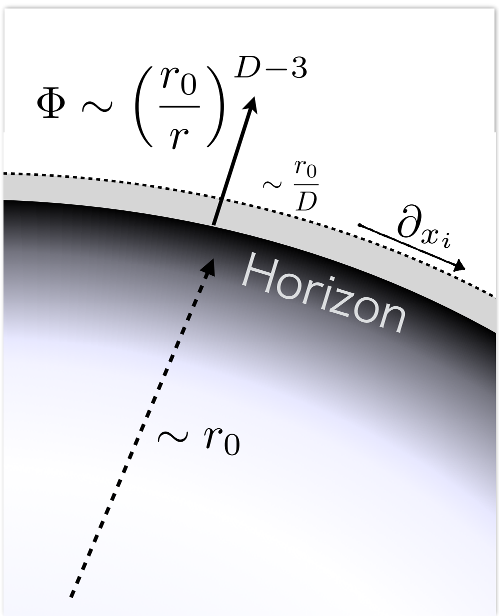


**Near coordinate**

$$\mathsf{R} = \left(\frac{r}{r_0}\right)^{D-3} \Rightarrow r \simeq r_0 + \frac{r_0}{D}\ln \mathsf{R}$$

Gravity is localized near H

$$r - r_0 < r_0/D$$

**Decoupling of Equations**

If $\quad \partial_r \sim D\partial_{\mathsf{R}} \gg \partial_{x_i}$

Einstein Eq $\rightarrow$ ODE(R)+PDE(x)

# Setup

## d+1 decomposition

$$ds^2 = N^2(\rho, x)d\rho^2 + g_{\mu\nu}(\rho, x)dx^\mu dx^\nu$$

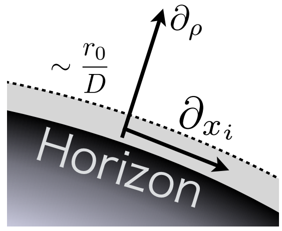


## Assumptions

$$N \simeq \frac{N_0(x)}{D} \qquad : \quad r \sim r_0 + \frac{\rho}{D}$$

ex) $\rho = \ln \mathrm{R}$

$$\mathcal{R}_0(x)e^{\frac{\phi(\rho,x)}{D}}d\Omega^2_{D-p} \in g_{\mu\nu}dx^\mu dx^\nu$$

D-p sphere



# Large D limit of Einstein Eq

## Trace of Evolution Equation

curvature of Sph.

$$\boxed{\frac{1}{N}\partial_\rho K = K^2} \underbrace{- R + \frac{1}{N}\nabla^2 N}_{\simeq -\frac{D^2}{\mathcal{R}_0^2} + \mathcal{O}(D)}$$

$\sim \mathcal{O}(D^2)$

$$\Rightarrow \quad K = -\frac{1}{\mathcal{R}_0}\coth\frac{N_0}{\mathcal{R}_0}(\rho - C(x))$$

Integral const.

$\rho = C(x)$: Horizon

## Other components

$$\boxed{\frac{1}{N}\partial_\rho K^\mu{}_\nu = KK^\mu{}_\nu} \underbrace{- R^\mu{}_\nu + \frac{1}{N}\nabla^\mu\nabla_\nu N}_{\sim \mathcal{O}(D)}$$

$\sim \mathcal{O}(D^2)$

Evolution Eq. is reduced to ODE in radial coordinate

Constraint Eq. detemines. for Integral constants $: C(x)$

Subleading Eqs. becomes linear perturbations

# Outline

1. *Einstein Equation in the large D limit*
2. ***Example: Non-Uniform black string***
3. *Summary*

# Non Uniform Black String

$n = D - 4 \quad \Longrightarrow$ expansion by 1/n

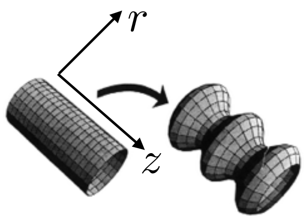


**Ansatz ( Conformal coordinate)**

$$ds^2 = -A dt^2 + B\left(dr^2 + dz^2/n\right) + r^2 C d\Omega_{n+1}^2$$

$$r \to \mathsf{R} = \left(\frac{r}{r_0}\right)^{D-4}$$

**Leading order**

$$ds^2 = -\underbrace{\left(\frac{\mathsf{R} - M_0(z)}{\mathsf{R} + M_0(z)}\right)^2}_{\text{horizon}} dt^2 + \left(\frac{\mathsf{R}}{\mathsf{R} + M_0(z)}\right)^{\frac{4(M_0(z)M_0''(z) - M_0'(z)^2)}{nM_0(z)^2}} (dr^2 + dz^2/n) + r^2 \left(\frac{\mathsf{R} + M_0(z)}{\mathsf{R}}\right)^{4/n} d\Omega_{n+1}^2$$

**Boundary condition**

Regularity at $\mathsf{R} = M_0(z) + \mathcal{O}(n^{-1})$, a-flatness R→∞

# Deformation Equation

**Next-to-Leading order**

From the constraint eq.,

$$\boxed{M_0(z)\ln M_0(z) - M_0(z) + \frac{M_0'(z)^2}{2M_0(z)} = aM_0(z) + \underbrace{b}_{\text{integral constant}}}$$

- 'a' is a scaling : $a \to 0$ by $M_0(z) \to e^a M_0(z) \quad b \to e^a b$
- match with asymptotic monopoles gives

$$\mathcal{M}_{\mathrm{ADM}} = \frac{n\omega_{n+1}L}{4\pi G}\langle M_0\rangle \qquad \mathcal{T}_{\mathrm{ADM}} = -\frac{\omega_{n+1}}{4\pi G}b$$

➡ **- b ~ tension** $\quad L(e^{-a}b) = \frac{2}{\sqrt{n}}\int_{M_{min}}^{M_{max}}\frac{dM}{M'}$



# Potential

By rescaling

$$\varphi(z) = e^{\frac{-a}{2}}\sqrt{M(z)}, \quad \tilde{b} = e^{-a}b$$

reduced to potential problem

$$\Rightarrow \frac{1}{2}\varphi'^2 = \frac{\tilde{b}}{4} - V(\varphi), \quad \boxed{V(\varphi) = \frac{1}{4}(\varphi^2\ln\varphi^2 - \varphi^2).}$$

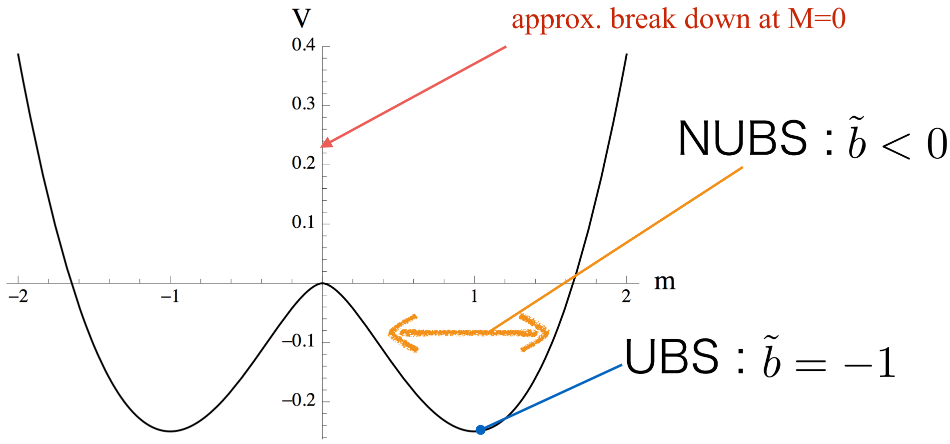

# Solutions

## Sol. for M_max to M_min

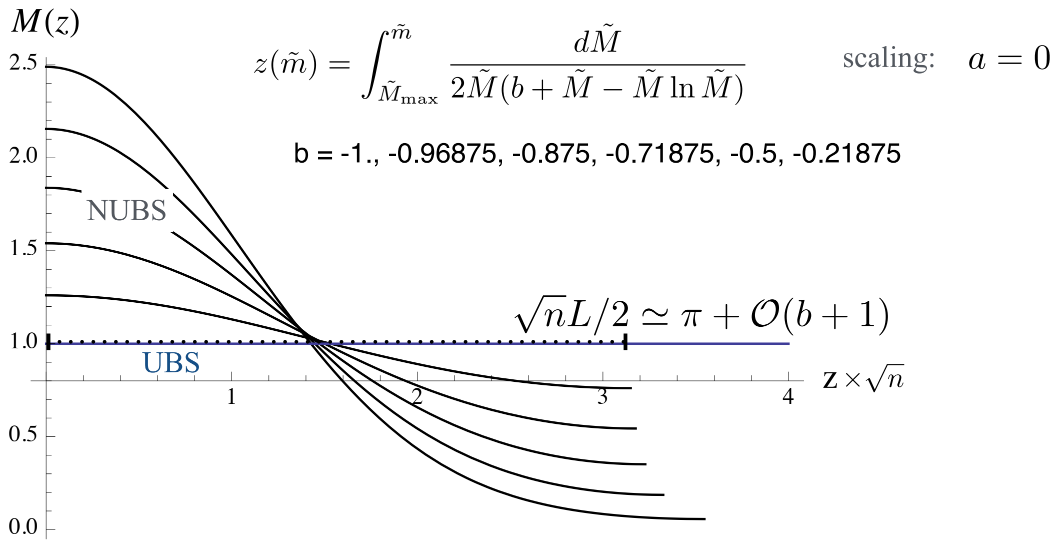




# Summary

- We show the Einstein Eq. is separated to ODE in radial and PDE in the other coordinates in the limit.
- We analysed NUBS for the simplest example
- Extension to AdS BHs and Stationary BHs are also possible (*Work in progress*)
- Time dependent case will be more interesting.

Thank you !

# “Integrability of Particle System around a Ring Source as the Newtonian Limit of a Black Ring”

Takahisa Igata

[JGRG24(2014)111206]

JGRG24@IPMU

# Integrability of Particle System around a Ring Source
## as the Newtonian Limit of a Black Ring


# Takahisa IGATA

Kwansei Gakuin University

collaborators : Hirotaka YOSHINO(KEK)・Hideki ISHIHARA (OCU)




# Abstract


In 5d black ring, particle system(geodesics) shows

**chaos**

unlike the case in 4d Kerr black hole. In this talk, however, we show that

**recovery of integrability**

of particle system in the Newtonian limit of 5d black ring.

## Introduction

— integrable system, Newtonian gravity —

- Integrable particle system :
  - ・#(COM) ≧ #(DOF)
  - ・understand qualitative properties in analytical way

- Integrable particle system in Newtonian gravity
  - ・Kepler problem

$$V \propto -\frac{M}{r}$$

  - ・Euler's three body problem

$$V \propto -\frac{M_1}{|\boldsymbol{r}-\boldsymbol{a}|}-\frac{M_2}{|\boldsymbol{r}+\boldsymbol{a}|}$$



## Introduction

— relativistic case —

- background spacetimes of integrable particle system
  - 4-dimensional Kerr BH [Carter 1968]
  - higher-dimensional Myers-Perry BH [e.g., Yasui&Houri 2011]

**Hamilton-Jacobi equation occurs the separation of variables**

non-trivial constants of motion (**Carter's constants)**

# Motivation

- general potential in Newton gravity leads chaos
- backgrounds of chaotic particle system
  - 4d and HD multi-BH [Contopoulos 1990, Hanan&Radu 2007]
  - **5d black ring** [T.I, Ishihara&Takamori 2011]

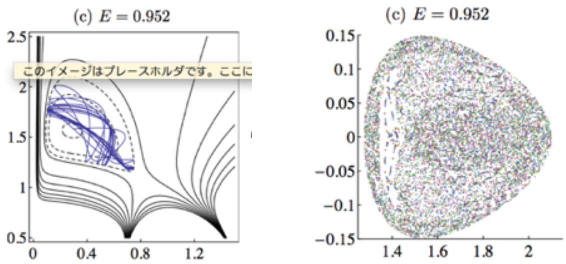






# questions

For chaotic particle system in 5d black rings,

- limit to recover integrability ?
- Is chaos whether relativistic effect or not ?

**Let's find a non-trivial constant in Newtonian limit of particle system in 5d black ring.**

# main contents

(1) 5d black ring metric

(2) Newtonian limit of geodesic equation
- prescription
- Newtonian gravitational potential

(3) Application of Hamilton-Jacobi method
- suitable coord. for separation of variables
- a separation constant

(4) conclusion






# main contents

(1) 5d black ring metric

(2) Newtonian limit of geodesic equation
- prescription
- Newtonian gravitational potential

(3) Application of Hamilton-Jacobi method
- suitable coord. for separation of variables
- a separation constant

(4) conclusion

# 5d Black Ring [Emparan&Reall 2002]

$$ds^2 = -\frac{F(y)}{F(x)}\left(dt - CR\frac{1+y}{F(y)}d\psi\right)^2 + \frac{R^2}{(x-y)^2}F(x)\left(-\frac{G(y)}{F(y)}d\psi^2 - \frac{dy^2}{G(y)} + \frac{dx^2}{G(x)} + \frac{G(x)}{F(x)}d\phi^2\right)$$

$$F(\xi) = 1+\lambda\xi, \quad G(\xi) = (1-\xi^2)(1+\nu\xi), \quad C = \sqrt{\lambda(\lambda-\nu)\frac{1+\lambda}{1-\lambda}}, \quad \lambda = \frac{2\nu}{1+\nu^2}$$

- ring radius：R
- thickness： $\nu$
- Horizon： $y = -\frac{1}{\nu}$ $\quad S^2 \times S^1$
- Killing vectors： $\partial_t,\ \partial_\phi,\ \partial_\psi$
- polar coordinates：

$$\zeta = R\frac{\sqrt{y^2-1}}{x-y}, \quad \rho = R\frac{1-x^2}{x-y}$$

$$(ds^2 = -dt^2 + d\rho^2 + \rho^2 d\phi^2 + d\zeta^2 + \zeta^2 d\psi^2)$$

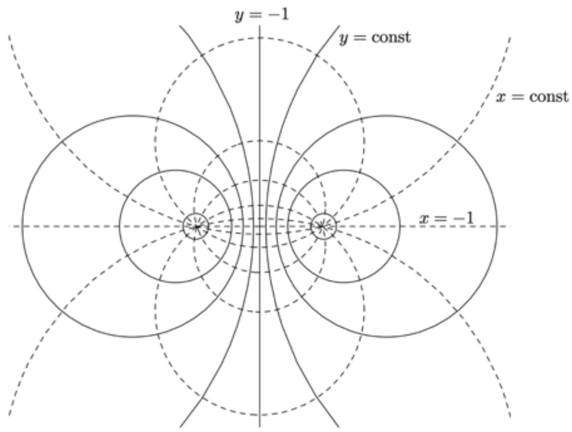


contours of constant x and constant y in ζ-ρ plane





# Newtonian limit of geodesic equation in thin black ring $\nu \ll 1$

- prescription
  - slow motion limit： $v \ll 1$
  - weak gravitational limit： $g_{\mu\nu} = \eta_{\mu\nu} + h_{\mu\nu} \quad (|h_{\mu\nu}| \ll 1)$

$$\frac{d^2x^\mu}{dt^2} - \frac{1}{2}\eta^{\mu\nu}\partial_\nu h_{00} = 0$$

- Newtonian gravitational potential：

$$\phi(\boldsymbol{r}) = -\frac{1}{2}h_{00} = -\frac{M}{2\sqrt{(\zeta+R)^2+\rho^2}\sqrt{(\zeta-R)^2+\rho^2}}$$

$$M = \frac{2\lambda R^2}{1-\nu}$$ ：ADM mass

# Newtonian gravitational sense

- homogeneous ring source

$$\sigma(\boldsymbol{r}) = \frac{M}{(2\pi)^2 \zeta\, \rho}\, \delta(\zeta - R)\, \delta(\rho)$$

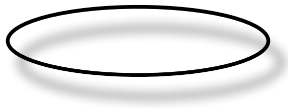

- 5d Newton's grav. eq

$$\nabla^2 \phi(\boldsymbol{r}) = S_3 G\, \sigma(\boldsymbol{r})$$

- solution:

$$\phi(\boldsymbol{r}) = -\frac{GM}{2\sqrt{(\zeta+R)^2+\rho^2}\sqrt{(\zeta-R)^2+\rho^2}}$$

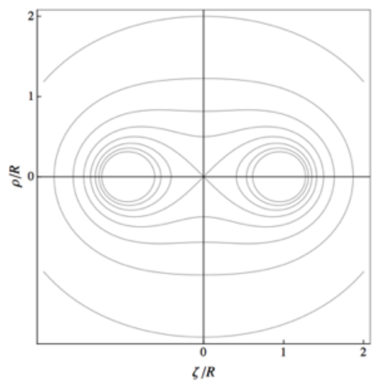


equipotential surface
(Cassini ovals)



# main contents

(1) 5d black ring metric

(2) Newtonian limit of geodesic equation
- prescription
- Newtonian gravitational potential

(3) Application of Hamilton-Jacobi method
- suitable coord. for separation of variables
- a separation constant

(4) conclusion

# Particle system around a ring source

- Hamiltonian（non-separable in ( $\zeta$ , $\rho$ ))

$$H = \frac{1}{2m}\left(p_\zeta^2 + \frac{p_\psi^2}{\zeta^2} + p_\rho^2 + \frac{p_\phi^2}{\rho^2}\right) - \frac{GMm}{2\,r_+ r_-}$$

$$r_\pm = \sqrt{(\zeta \pm R)^2 + \rho^2}$$

- **coordinate transformation**

$$\boxed{r_\pm = R\,(\xi \pm \eta)}$$

**(spheroidal coordinates)**

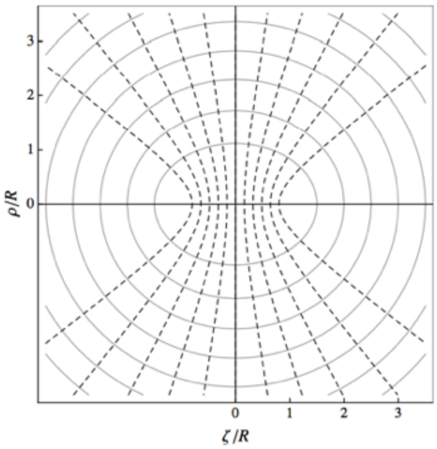






# Particle system in a ring source

- Hamiltonian (separable form)

$$H = \frac{1}{2mR^2(\xi^2-\eta^2)}\Bigg[(\xi^2-1)\,p_\xi^2 + (1-\eta^2)\,p_\eta^2 + \left(\frac{1}{\eta^2} - \frac{1}{\xi^2}\right)p_\psi^2 + \left(\frac{1}{\xi^2-1} + \frac{1}{1-\eta^2}\right)p_\phi^2\Bigg] - \frac{GMm}{2R^2(\xi^2-\eta^2)}$$

**⇒ Hamilton-Jacobi Eq. is separable**

## Carter's constant

- non-trivial separation constant

$$\boxed{C = L^2 + R^2 \left( p_\zeta^2 + \frac{p_\psi^2}{\zeta^2} \right) - \frac{GMm^2}{4} \frac{r_+^2 + r_-^2}{r_+ r_-}}$$

where

$$L^2 = (\zeta\, p_\rho - \rho\, p_\zeta)^2 + (\zeta^2 + \rho^2) \left( \frac{p_\psi^2}{\zeta^2} + \frac{p_\phi^2}{\rho^2} \right)$$

: sum of squared angular momenta

- Poisson commutable constants:

$(p_\phi, p_\psi, H, C)$ **integrable!**





## conclusion

The Newtonian limit of geodesic eq in 5d thin black ring leads to EOM of a particle in Newtonian gravitational potential of a homogeneous ring source.

- HJeq is separable in spheroidal coordinates
- Non-trivial constant of motion quadratic in p

The Newtonian limit of particle system in 5d thin black ring is the limit to recover integrability. Therefore, we can understand that the appearance of chaotic geodesic is relativistic effect.

“Cosmological evolution of the chameleon field in the presence of the compact object”

Kazufumi Takahashi

[JGRG24(2014)111207]

# Cosmological Evolution of the Chameleon Field in the Presence of the Compact Object

The University of Tokyo, RESCEU K. Takahashi, J. Yokoyama

## Introduction

# Dark Energy Problem

- What is dark energy? What is the origin of the cosmic acceleration?
  → cosmological constant, modified gravity, etc.

- $f(R)$ gravity is one of the candidates.

- In $f(R)$ gravity, the EOS parameter $w_{\mathrm{DE}}$ deviates from $-1$.

- Previous work (P. Brax et al., Phys. Rev. D 78, 104021 (2008))

$$\boxed{|(1+w_{\mathrm{DE}})\Omega_{\mathrm{DE}}| < \Phi_N} \Leftarrow \text{Really?}$$

$\Phi_N$: Newton's potential for a "thin-shell" object



# $f(R)$ Gravity

- Action

$$S = \frac{M_{\mathrm{Pl}}^2}{2}\int d^4x\sqrt{-g}f(R) + \underbrace{S_{\mathrm{m}}(g_{\mu\nu},\Psi)}$$

matter field

- Conformal transformation

$$g_{\mu\nu} \to \bar{g}_{\mu\nu} = f'(R)g_{\mu\nu}$$

$$f'(R) \equiv F(R) \equiv e^{-2\beta\phi/M_{\mathrm{Pl}}}, \quad \beta \equiv \frac{1}{\sqrt{6}}$$

$$S = \int d^4x\sqrt{-\bar{g}}\left(\frac{M_{\mathrm{Pl}}^2}{2}\bar{R} - \frac{1}{2}(\bar{\nabla}\phi)^2 - V(\phi)\right) + S_{\mathrm{m}}(e^{2\beta\phi/M_{\mathrm{Pl}}}\bar{g}_{\mu\nu},\Psi)$$

GR

scalar field

$\phi$ couples to matter

→ fifth force

$$V(\phi) = \frac{1}{16\pi G}\frac{RF-f}{F^2}$$

# Chameleon Mechanism

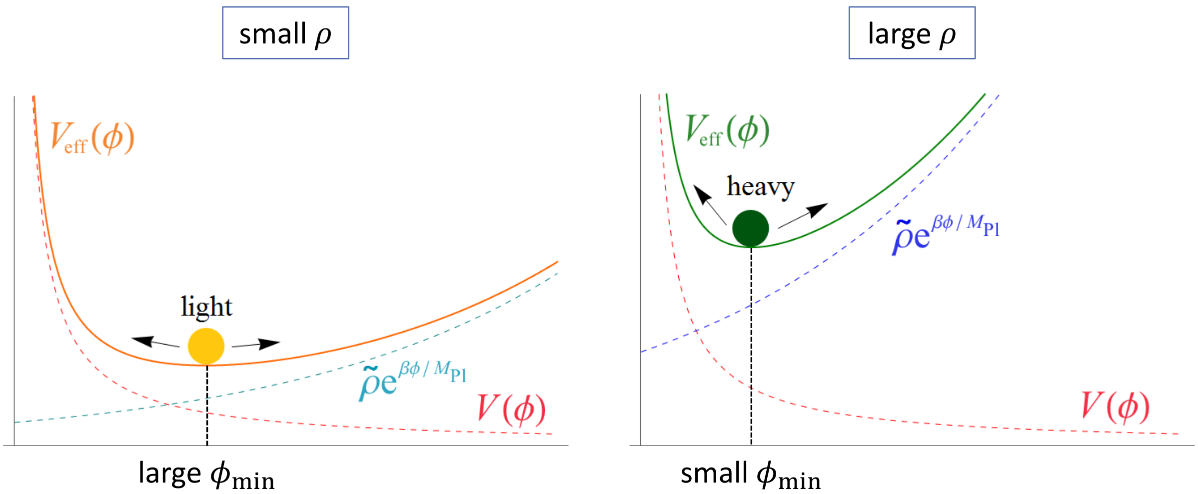


$$V_{\rm eff}(\phi) \equiv V(\phi) + \tilde{\rho}_{\rm m} e^{\beta\phi/M_{\rm Pl}}$$

$$0 = V'_{\rm eff}(\phi_{\rm min}) = V'(\phi_{\rm min}) + \frac{\beta}{M_{\rm Pl}} \tilde{\rho}_{\rm m} e^{\beta\phi_{\rm min}/M_{\rm Pl}}$$



# Thin-Shell Solution

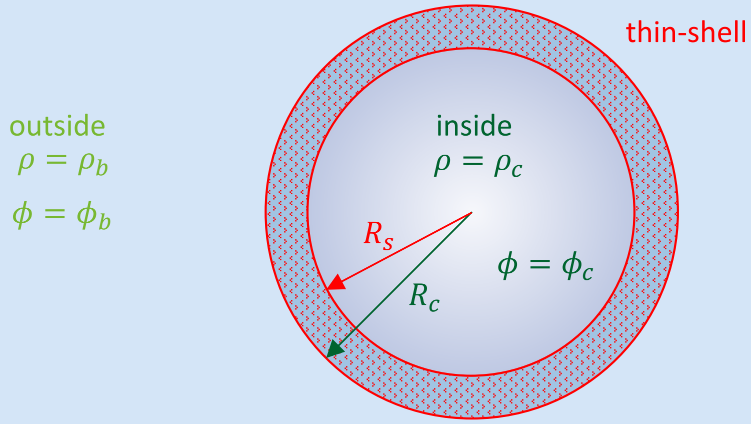


$g_{\mu\nu} = \eta_{\mu\nu}$ (Minkowski metric)

# Thin-Shell Solution

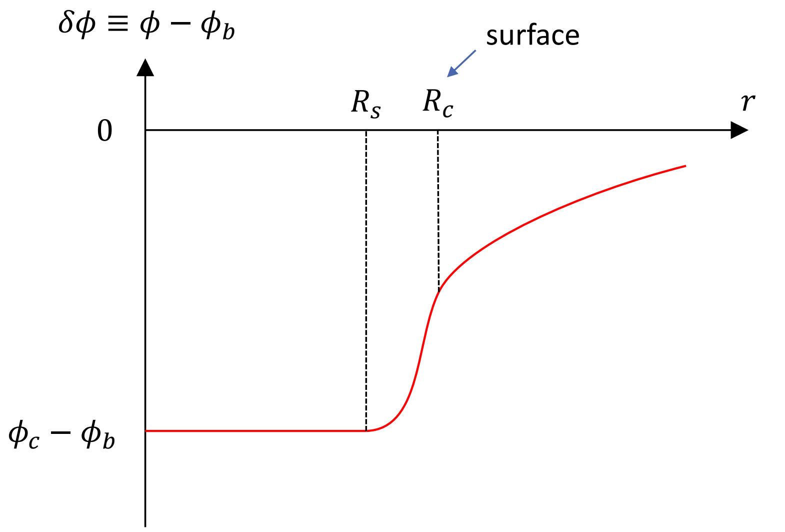


$$\epsilon_{\rm th} \equiv \frac{M_{\rm Pl}}{\beta}\frac{\phi_b - \phi_c}{R_c^2 \rho_c} \approx \frac{R_c - R_s}{R_c} : \text{thin-shell parameter}$$



# Thin-Shell Solution

## Requirements

- static
- $\phi = \phi_c$ if $r < R_s$
- $\phi \to \phi_b$ as $r \to \infty$
- smooth at $r = R_s, R_c$
- $R_c \ll m_b^{-1}$

$\delta\phi \equiv \phi - \phi_b$

$$\delta\phi = \begin{cases} \delta\phi_c & , r < R_s \\ \dfrac{\beta\rho_c}{3M_{\rm Pl}}\left(\dfrac{r^2}{2} + \dfrac{R_s^3}{r} - \dfrac{3}{2}R_s^2\right) + \delta\phi_c & , R_s < r < R_c \\ -\dfrac{\beta\rho_c}{3M_{\rm Pl}}\epsilon_{\rm th}\dfrac{R_c^3}{r}e^{-m_b(r-R_c)} & , r > R_c \end{cases}$$

$$\epsilon_{\rm th} \equiv \frac{M_{\rm Pl}}{\beta}\frac{|\delta\phi_c|}{R_c^2 \rho_c} \approx \frac{R_c - R_s}{R_c} : \text{thin-shell parameter}$$

## ➢ Fifth Force

- Fifth force (per unit mass)

$$F = \frac{\beta}{M_{\rm Pl}} \nabla \phi$$

- Outside a thin-shell object

$$F_\phi = \frac{\epsilon_{\rm th}}{3} \frac{GM_c}{r^2} (1 + m_b r) e^{-m_b (r - R_c)}$$

$$\rightarrow \quad \frac{F_\phi}{F_N} = O(\epsilon_{\rm th}) \qquad\qquad F_N \equiv \frac{GM_c}{r^2}$$

- Fifth force is small if $\epsilon_{\rm th} < 1$.

- The condition for thin-shell can be rewritten as

$$\frac{\beta}{M_{\rm Pl}} |\delta \phi_c| < \Phi_N$$

- This explains why $f(R)$ gravity can pass local tests.



# Previous Work

P. Brax et al., Phys. Rev. D 78, 104021 (2008)

## ➢ P. Brax et al.

- Friedmann eq. (background)

$$H^2 = \frac{8\pi G}{3}\left(\frac{\rho_{\rm matter}}{F} + FV(\phi_b)\right) + \frac{2\beta}{M_{\rm Pl}} H\dot{\phi}_b \equiv \frac{8\pi G}{3F_0}(\rho_{\rm matter} + \rho_{\rm DE})$$

- Conservation law

$$\dot{\rho}_{\rm DE} + 3H(1+w_{\rm DE})\rho_{\rm DE} = 0$$

$$(1+w_{\rm DE})\Omega_{\rm DE} = \frac{2\beta}{3M_{\rm Pl}}\left(\frac{\dot{\phi}_b}{H} - \frac{\ddot{\phi}_b}{H^2} + \frac{\beta}{3M_{\rm Pl}}\frac{\dot{\phi}_b^2}{H^2}\right) + \left(e^{-2\beta(\phi_0-\phi_b)/M_{\rm Pl}} - 1\right)\Omega_{\rm matter}$$

- Order of magnitude

$\Delta\phi$: change of $\phi_b$ in Hubble time

$$\boxed{|(1+w_{\rm DE})\Omega_{\rm DE}| \sim O\left(\frac{\beta}{M_{\rm Pl}}\Delta\phi\right)}$$



## ➢ P. Brax et al.

$$\boxed{|(1+w_{\rm DE})\Omega_{\rm DE}| \sim O\left(\frac{\beta}{M_{\rm Pl}}\Delta\phi\right)}$$

- $\Delta\phi$: change of $\phi_b$ fr[illegible] $t$ to $t_0$
- Chameleon mechani[illegible]n

$\phi_b$ is assumed to follow the minimum of $V_{\rm eff}(\phi)$

$$\rho_c > \rho_b(t) > \rho_b(t_0) \quad \Rightarrow \quad \phi_c < \phi_b(t) < \phi_b(t_0)$$

$$\boxed{\frac{\beta}{M_{\rm Pl}}\Delta\phi < \frac{\beta}{M_{\rm Pl}}|\delta\phi_c(t_0)|}$$

$$\delta\phi_c(t_0) \equiv \phi_c - \phi_b(t_0)$$

- Assume the fifth forc[illegible] is small ⇔ the object has thin-shell

$$\boxed{\frac{\beta}{M_{\rm Pl}}|\delta\phi_c(t_0)| < \Phi_N}$$

It is not trivial whether we can use thin-shell solution if the background is expanding

$$\boxed{|(1+w_{\rm DE})\Omega_{\rm DE}| < \Phi_N}$$

# Our Work

## Our Work

outside
$\rho = \rho_b$
$\phi = \phi_b$

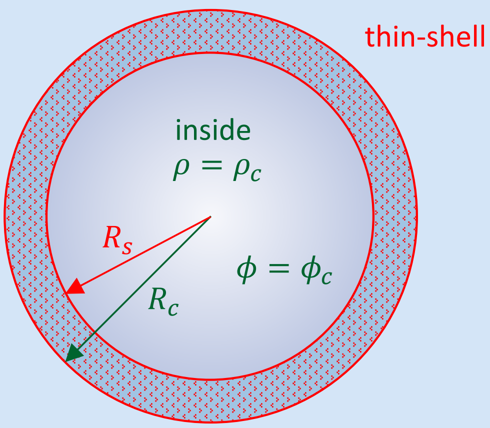


$g_{\mu\nu} = \cancel{\eta_{\mu\nu}}$ ~~(Minkowski metric)~~
FLRW metric

# Formalism

- Metric

$$g_{\mu\nu} = -(1+2\Psi)dt^2 + a^2(1+2\Phi)d\boldsymbol{x}^2$$

- Conformal transformation

$$\begin{aligned}\bar{g}_{\mu\nu} &= e^{-2\beta(\phi_b+\delta\phi)/M_{\rm Pl}} g_{\mu\nu} \\ &= -e^{-\frac{2\beta\phi_b}{M_{\rm Pl}}}(1+2\tilde{\Psi})dt^2 + e^{-\frac{2\beta\phi_b}{M_{\rm Pl}}} a^2(1+2\tilde{\Phi})d\boldsymbol{x}^2\end{aligned}$$

$$\tilde{\Phi} \equiv \Phi - \frac{\beta}{M_{\rm Pl}}\delta\phi, \qquad \tilde{\Psi} \equiv \Psi - \frac{\beta}{M_{\rm Pl}}\delta\phi$$

- Density

$$\rho = \begin{cases} \rho_c & , ar < R_c \\ \rho_b & , ar > R_c \end{cases}$$

$$\rho_b \propto a^{-3}$$



# Equations of Motion

- Einstein eq.

$$-\frac{\Delta}{a^2}\tilde{\Phi} + 3\tilde{H}\left(\dot{\tilde{\Phi}} - \tilde{H}\tilde{\Psi}\right) = 4\pi G\left[F\left(V(\phi)-V(\phi_b)\right) + \frac{\rho-\rho_b}{F} + \frac{4\beta}{M_{\rm Pl}}\frac{\rho}{F}\delta\phi - \dot{\phi}_b^2\tilde{\Psi} + \dot{\phi}_b\delta\dot{\phi}\right]$$

$$\partial_i\left(\dot{\tilde{\Phi}} - \tilde{H}\tilde{\Psi}\right) = \frac{4\pi G\rho}{F}\delta u_i$$

$$\tilde{\Phi} + \tilde{\Psi} = 0$$

$$\boxed{\tilde{H} \equiv H - \frac{\beta}{M_{\rm Pl}}\dot{\phi}_b}$$

- Klein-Gordon eq.

$$\boxed{-\delta\ddot{\phi} - 3H\delta\dot{\phi} + \frac{\Delta}{a^2}\delta\phi = F\left(V'(\phi)-V'(\phi_b)\right) + \frac{\beta}{M_{\rm Pl}}\frac{(\rho+3P)-\rho_b}{F} + \frac{16\pi G\rho}{3F}\delta\phi + \dot{\phi}_b\left(3\dot{\tilde{\Phi}} - \dot{\tilde{\Psi}}\right) + \frac{4\beta}{M_{\rm Pl}}\dot{\phi}_b^2\Psi}$$

$$\Big\downarrow \; |\Phi|, |\Psi| \ll 1$$

$$\boxed{-\delta\ddot{\phi} - 3H\delta\dot{\phi} + \frac{\Delta}{a^2}\delta\phi = V'_{\rm eff}(\phi) - V'_{\rm eff}(\phi_b)}$$

## Naïve "solution"

- Introduce time dependence to thin-shell solution:

$$\boxed{r \to ar, \phi_b \to \phi_b(t)}$$

$$\delta\phi(t) \equiv \phi - \phi_b(t)$$

$$\delta\phi(t) = \begin{cases} \delta\phi_c(t) & , ar < R_s(t) \\ \dfrac{\beta\rho_c}{3M_{\rm Pl}}\left(\dfrac{(ar)^2}{2} + \dfrac{R_s(t)^3}{ar} - \dfrac{3}{2}R_s(t)^2\right) + \delta\phi_c & , R_s(t) < ar < R_c \\ -\dfrac{\beta\rho_c}{3M_{\rm Pl}}\epsilon_{\rm th}(t)\dfrac{R_c^3}{ar}e^{-m_b(t)(ar-R_c)} & , ar > R_c \end{cases}$$

$$\epsilon_{\rm th}(t) \equiv \frac{M_{\rm Pl}}{\beta}\frac{|\delta\phi_c(t)|}{R_c^2\rho_c} \approx \frac{R_c - R_s(t)}{R_c}$$



## Is It Really a Solution?

- Outside the object

$$-\ddot{\delta\phi} - 3H\dot{\delta\phi} + \left(\frac{\Delta}{a^2} - m_b^2\right)\delta\phi = 0$$

※inside $\dfrac{\Delta}{a^2} \approx R_c^{-2} \gg H^2$

Here

$$\ddot{\delta\phi}, 3H\dot{\delta\phi} \approx H^2\delta\phi$$

$$\frac{\Delta}{a^2}\delta\phi \approx m_b^2\delta\phi$$

same order (for models in which $m_b \sim H$)

- Perturbative treatment

$$\delta\phi \equiv \delta\phi^{(0)} + \delta\phi^{(1)}$$

- Equation for $\delta\phi^{(1)}$

$$-\ddot{\delta\phi}^{(1)} - 3H\dot{\delta\phi}^{(1)} + \left(\frac{\Delta}{a^2} - m_b^2\right)\delta\phi^{(1)} = \ddot{\delta\phi}^{(0)} + 3H\dot{\delta\phi}^{(0)}$$

$$\Rightarrow \delta\phi^{(1)} \approx (Har)\frac{H}{m_b}\delta\phi^{(0)}$$

- Evaluate at $ar = m_b^{-1}$

$$\delta\phi^{(1)} \approx \left(\frac{H}{m_b}\right)^2\delta\phi^{(0)} \approx \delta\phi^{(0)}$$

## ➢ P. Brax et al. (again)

$$\boxed{|(1+w_{\mathrm{DE}})\Omega_{\mathrm{DE}}| \sim O\left(\frac{\beta}{M_{\mathrm{Pl}}}\Delta\phi\right)}$$

$\phi_b$ is assumed to follow the minimum of $V_{\mathrm{eff}}(\phi)$

- $\Delta\phi$: change of $\phi_b$ from $t$ to $t_0$
- Chameleon mechanism

$$\rho_c > \rho_b(t) > \rho_b(t_0) \quad \Rightarrow \quad \phi_c < \phi_b(t) < \phi_b(t_0)$$

$$\boxed{\frac{\beta}{M_{\mathrm{Pl}}}\Delta\phi < \frac{\beta}{M_{\mathrm{Pl}}}|\delta\phi_c(t_0)|}$$

$$\delta\phi_c(t_0) \equiv \phi_c - \phi_b(t_0)$$

- Assume the fifth force is small ~~⇔~~ the object has thin-shell

$$\cancel{\boxed{\frac{\beta}{M_{\mathrm{Pl}}}|\delta\phi_c(t_0)| < \Phi_N}}$$

It is not trivial whether we can use thin-shell solution if the background is expanding

$$\cancel{\boxed{|(1+w_{\mathrm{DE}})\Omega_{\mathrm{DE}}| < \Phi_N}}$$



## ➢ Summary

- $f(R)$ gravity can be reformulated into chameleon theory.
- If an object has thin-shell solution, then the fifth force is suppressed.

- We demonstrated that if the background spacetime is expanding, the thin-shell solution can be strongly modified outside the object.
- This modification propagates to fifth force.
- Then small thin-shell parameter no longer corresponds to small fifth force.
- The constraint on $w_{\mathrm{DE}}$ breaks down.

# “Observational constraint on a generalized Galileon gravity model from the gas and shear profiles of a cluster of galaxies”

Ayumu Terukina

[JGRG24(2014)111208]

# Observational constraint on a generalized Galileon model from the gas and shear profiles of a cluster of galaxies

Contents



JGRG24 @ Kavli IPMU 14/11/12


**Ayumu Terukina** (Hiroshima Univ.)

Collaboration with Kazuhiro Yamamoto


# Introduction

**Modified gravity**

・To explain the accelerated expansion of the Universe.

・Additional degrees of freedom.

・Recovery of the local gravity (Screening mechanism)

nonlinear scales ? linear scales

General relativity
Scalar field is screened

Modified gravity

Test of modified gravity

・Cluster of galaxies（~Mpc）

# Test of modified gravity in Cluster

- Using gas observations (AT & Yamamoto,12, AT et al,14)

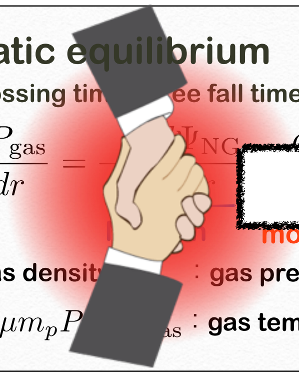

**Hydrostatic equilibrium**

(sound crossing time < free fall time)

$$\rho_{\rm gas}^{-1}\frac{dP_{\rm gas}}{dr} = -\left(\frac{d\Psi_{\rm NG}}{dr} + \frac{d\Psi_{\rm MG}}{dr}\right)$$

modification

$\rho_{\rm gas}$: gas density, $P_{\rm gas}$: gas pressure

$T_{\rm gas} = \mu m_p P_{\rm gas}/\rho_{\rm gas}$ : gas temperature

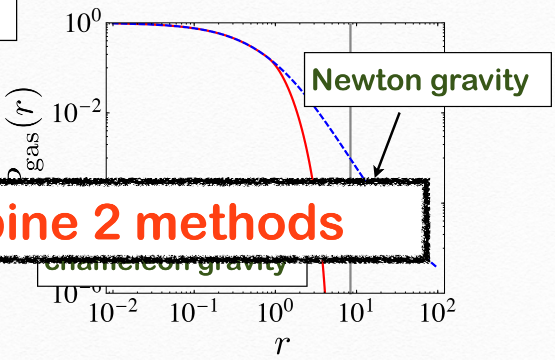


**Combine 2 methods**

- Using lensing shear observation (Narikawa & Yamamoto,12)

**Surface mass density**

$$\Sigma_S \simeq -\frac{1}{2}\int_0^{\chi_S} d\chi \triangle^{(2D)}(\Phi - \Psi)$$

lens potential

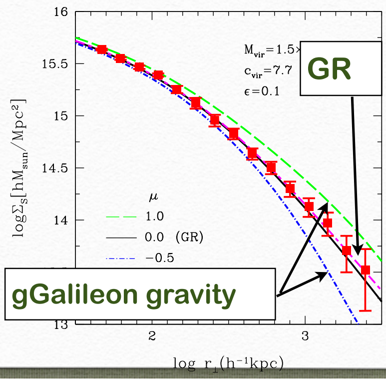


# Generalized Galileon Model

$$S = \int d^4x\sqrt{-g}\Big[G_4(\phi)R + K(\phi, X) - G_3(\phi, X)\Box\phi + \mathcal{L}_{\rm m}\Big],$$

- e.g. DGP model, original Galileon model

  ⇒ Recovery of local gravity by Vainsthein mechanism

- Spherical symmetric solution with Viainsthein

**Kimura et al. 2012**

$$\frac{d\Psi}{dr} = \frac{GM(<r)}{r^2} - \mu_{\rm G}\frac{d\tilde{Q}}{dr}$$

gravitational potential

$$\frac{d}{dr}\left(\frac{\Phi - \Psi}{2}\right) = \frac{GM(<r)}{r^2} - \mu_{\rm L}\frac{d\tilde{Q}}{dr}$$

lens potential

$$\frac{d\tilde{Q}}{dr} = \frac{r}{4}\left(1 - \sqrt{1 + \frac{8G\epsilon^2 M(<r)}{H_0^2 r^3}}\right)$$

scalar field

independent parameter

$$M(<r) = 4\pi\int_0^r dr' r'^2 \rho(r)$$

$\mu_{\rm G}, \mu_{\rm L}, \epsilon$ : functions of $K, G_3, G_4$ determined from back ground

# Vainsthein mechanism

$$\frac{d\Psi}{dr} = \frac{GM(<r)}{r^2} - \mu_G \frac{d\tilde{Q}}{dr}$$ gravitational potential

$$\frac{d}{dr}\left(\frac{\Phi-\Psi}{2}\right) = \frac{GM(<r)}{r^2} - \mu_L \frac{d\tilde{Q}}{dr}$$ lens potential

$$\frac{d\tilde{Q}}{dr} = \frac{r}{4}\left(1-\sqrt{1+\frac{8G\epsilon^2 M(<r)}{H_0^2 r^3}}\right)$$ scalar field

Vainsthein radius $r_V \equiv [8G\epsilon^2 M_{\rm vir}/H_0^2]^{1/3}$

**Newton limit**

$r \ll r_V \propto \epsilon^{2/3}$

$$\frac{d}{dr}\left(\frac{\Phi-\Psi}{2}\right) = \frac{d\Psi}{dr} \simeq \frac{GM(r)}{r^2}$$

(Vainsthein mechanism)

**Modified gravity limit**

$r \gg r_V \propto \epsilon^{2/3}$

$$\frac{d\Psi}{dr} \simeq \frac{G(1+\mu_G)M(r)}{r^2}$$

$$\frac{d}{dr}\left(\frac{\Phi-\Psi}{2}\right) \simeq \frac{G(1+\mu_L)M(r)}{r^2}$$

# Gas distribution profiles

AT et al. 2014

**Assumptions**

Hydrostatic equilibrium

$$\rho_{\rm gas}^{-1}\frac{dP_{\rm gas}}{dr} = -\frac{d\Psi}{dr}$$

Electron number density (β-model)

$$n_{\rm e}(r) = n_0\left[1+\left(\frac{r}{r_c}\right)^2\right]^{\beta}$$

Equation of state

$$P_{\rm gas} = \rho_{\rm gas} kT_{\rm gas}/\mu m_{\rm p}$$

**3D profiles**

Gas pressure

$$P_{\rm gas} = n_0 T_0 - \mu m_{\rm p}\int_0^r n_{\rm e}\frac{d\Psi}{dr}dr$$

dependence of $\mu_G$, $\epsilon$

Gas density

$$\rho_{\rm gas} = \frac{5\mu m_{\rm p}}{2+\mu} n_{\rm e}$$

Gas temperature

$$kT_{\rm gas} = \frac{\mu m_{\rm p} P_{\rm gas}}{\rho_{\rm gas}}$$

# Gas distribution observations

- X-ray temperature
- X-ray surface brightness

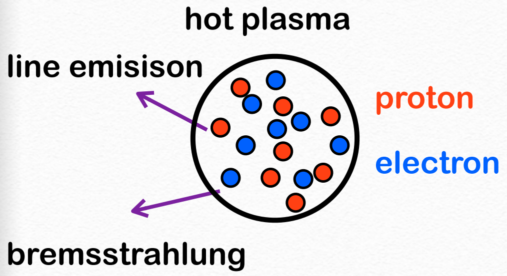


- Sunyaev-Zel'dovich effect

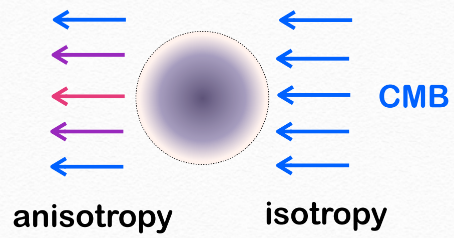


**observations**

**X-ray temperature**

$$T_X(r_\perp) = \frac{\int dz \lambda_c(r) n_e^2(r) T_{gas}(r)}{\int dz \lambda_c(r) n_e^2(r)}$$

**X-ray surface brightness**

$$S_X(r_\perp) = \int dz \lambda_c(r) n_e^2(r)$$

**SZ effect**

$$\frac{\Delta T(r_\perp)}{T_{CMB}} = -2\frac{\sigma_T}{m_e}\int dz P_e(r) = -2y(r_\perp)$$

# Lensing shear

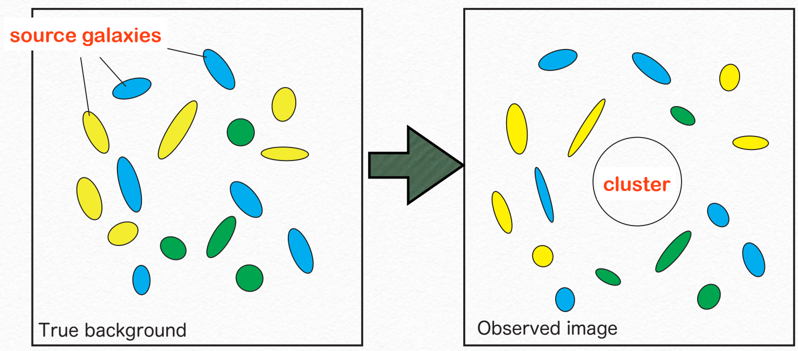


- **Convergence**

$$\kappa \simeq -\frac{1}{2}\int_0^{\chi_S} d\chi \frac{(\chi_S - \chi)\chi}{\chi_S} \triangle^{(2D)}(\Phi - \Psi)$$

- **Tangential shear**

$$\gamma_+(r_\perp) = \bar{\kappa}(< r_\perp) - \kappa(r_\perp),$$

$$\bar{\kappa}(< r_\perp) \equiv \frac{2}{r_\perp^2}\int_0^{r_\perp} dr'_\perp r'_\perp \kappa(r'_\perp).$$

- **Reduced shear (observed)**

$$g_+(r_\perp) \equiv \frac{\gamma_+(r_\perp)}{1 - \kappa(r_\perp)} = \langle \epsilon_+^{obs.} \rangle$$

dependence of $\mu_L$, $\epsilon$

# matter distribution and non-thermal pressure

- **NFW profile**

$$\rho(r) = \frac{\rho_s}{r/r_s(1+r/r_s)^2}$$

**Concentration parameter**

$$c \equiv \frac{r_{\rm vir}}{r_s},$$

**Virial mass**

$$M_{\rm vir} \equiv M(<r_{\rm vir}) = \int_0^{r_{\rm vir}} dr r^2 \rho(r)$$

- **A bias between gas obs. and lensing obs.**

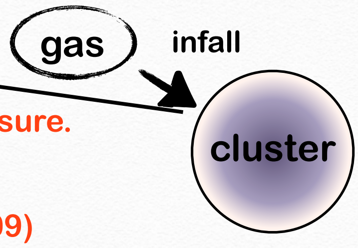


**Non-thermal effect from turbulent gas**

→ Equilibrium include the non-thermal pressure.

→ A bias in concentration between gas and lens profile is appeared. (Lau et al., 09)

$$b_c \equiv \frac{c_{\rm gas}}{c_{\rm shear}} \longleftarrow$$

**Introducing a bias as systematic effect from non-thermal effects.**

# Comparison with Coma cluster

$$\chi^2(\underbrace{M_{\rm vir}, c, b_c}_{\text{NFW}}, \underbrace{T_0, n_0, \beta, r_c}_{\text{gas}}, \underbrace{\mu'_{\rm G}, \mu'_{\rm L}, \epsilon'}_{\text{gravity model}}) = \chi^2_{\rm XT} + \chi^2_{\rm SZ} + \chi^2_{\rm SZ} + \chi^2_{\rm WL}$$

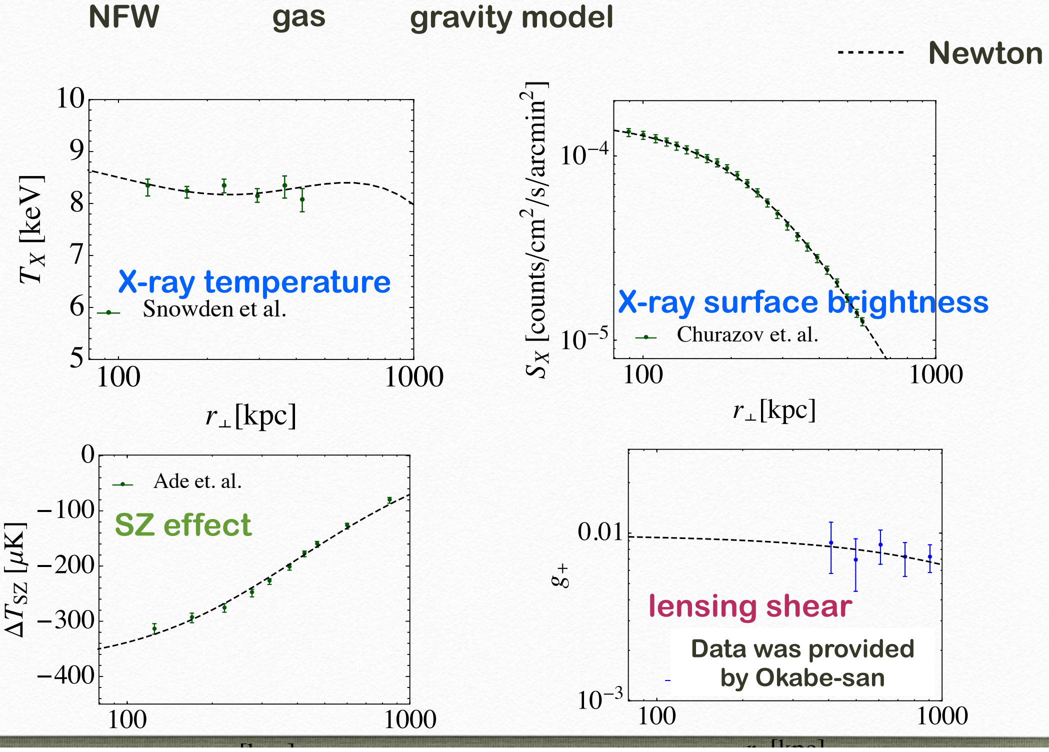

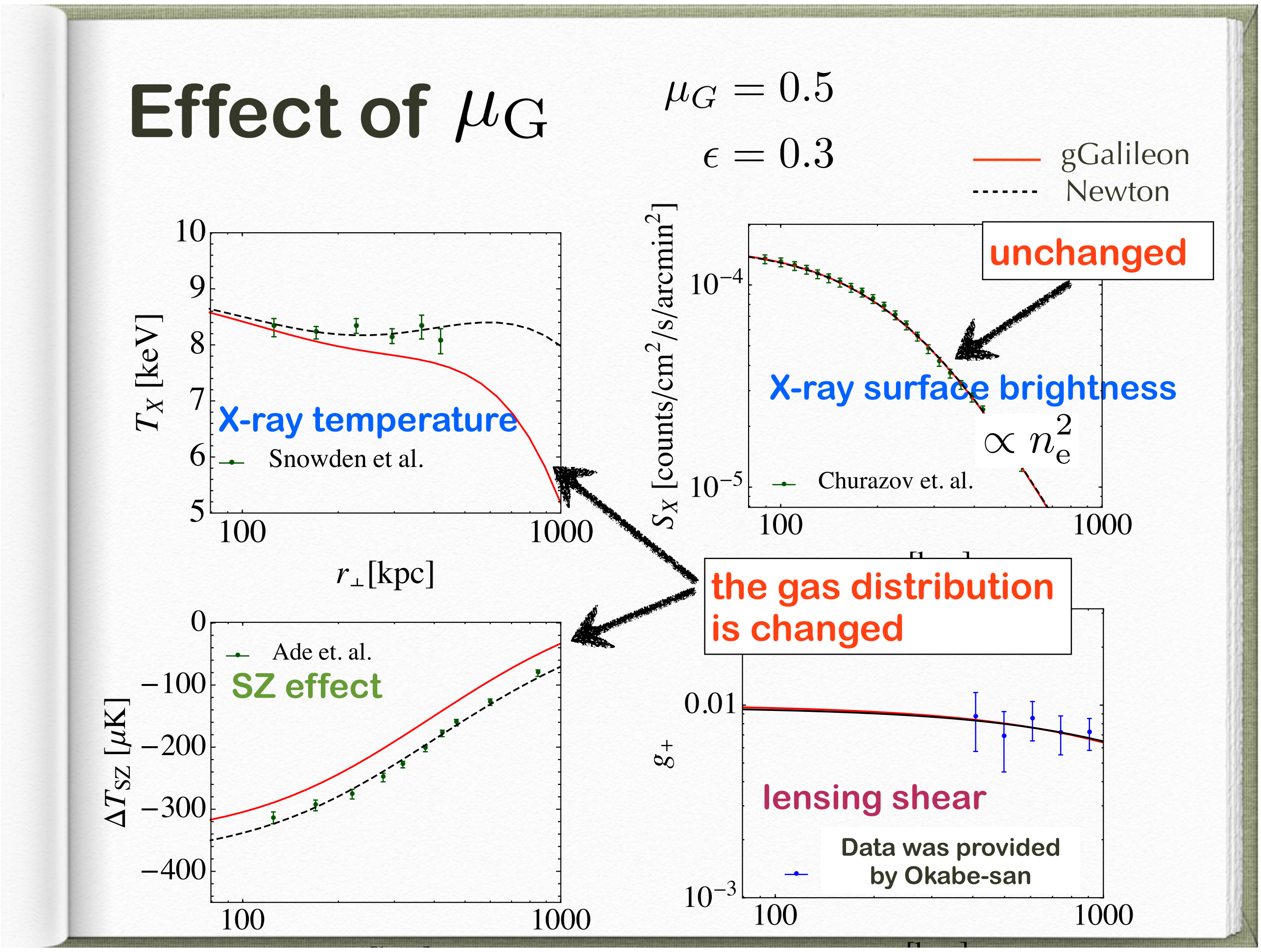
Effect of $\mu_G$
$\mu_G = 0.5$
$\epsilon = 0.3$
gGalileon
Newton
unchanged
X-ray temperature
Snowden et al.
$T_X$ [keV]
$r_\perp$[kpc]
X-ray surface brightness
$\propto n_e^2$
Churazov et. al.
$S_X$ [counts/cm$^2$/s/arcmin$^2$]
the gas distribution is changed
Ade et. al.
SZ effect
$\Delta T_{SZ}$ [$\mu$K]
$g_+$
lensing shear
Data was provided by Okabe-san

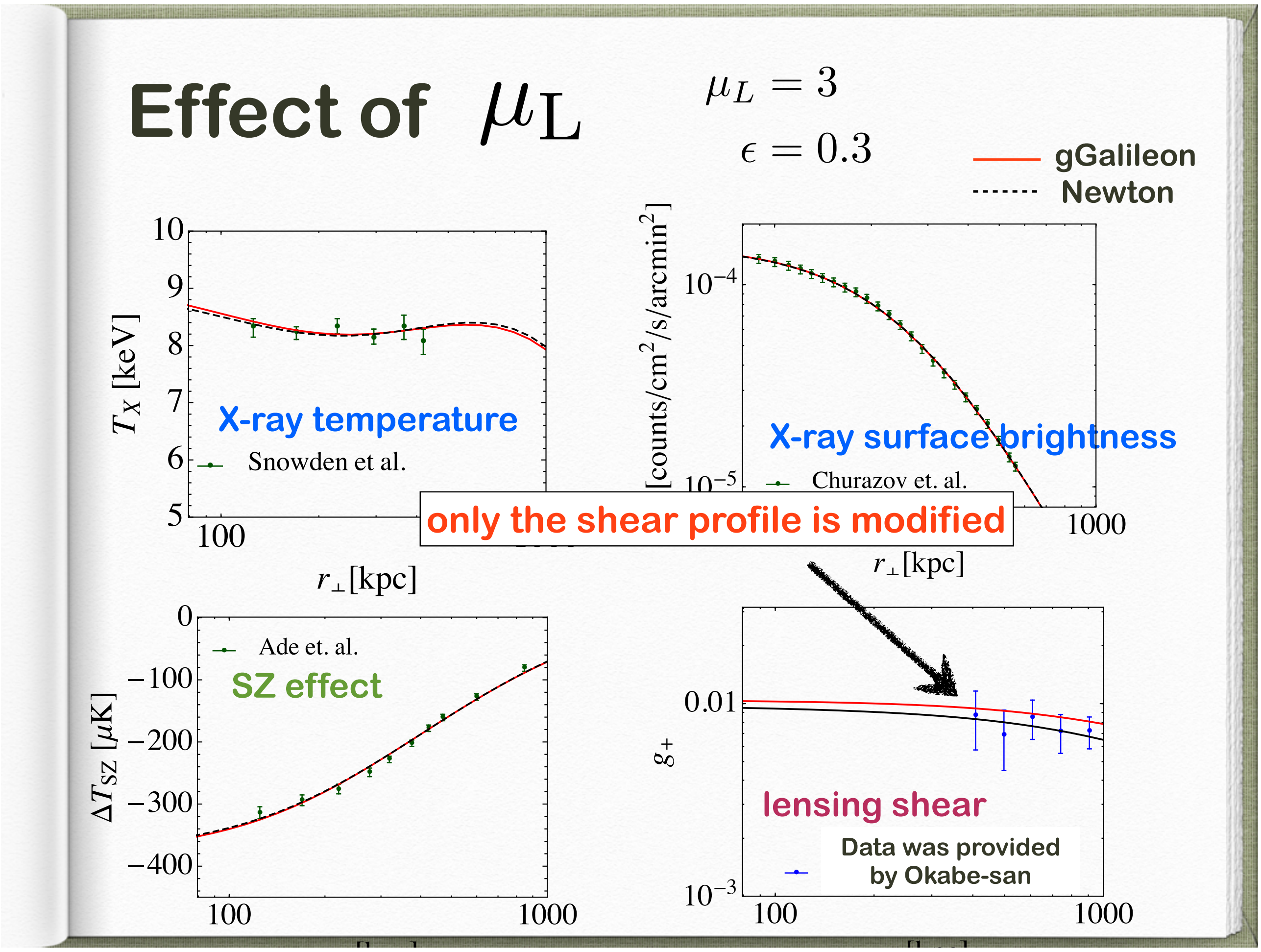
Effect of $\mu_L$
$\mu_L = 3$
$\epsilon = 0.3$
gGalileon
Newton
X-ray temperature
Snowden et al.
$T_X$ [keV]
$r_\perp$[kpc]
X-ray surface brightness
Churazov et. al.
[counts/cm$^2$/s/arcmin$^2$]
only the shear profile is modified
Ade et. al.
SZ effect
$\Delta T_{SZ}$ [$\mu$K]
$g_+$
lensing shear
Data was provided by Okabe-san

# Preliminary Result

$$\mu' = \frac{\mu}{1+|\mu|}, \quad \epsilon' = 1 - \exp(-\epsilon)$$

$$-1 < \mu' < 1, \quad 0 < \epsilon' < 1$$

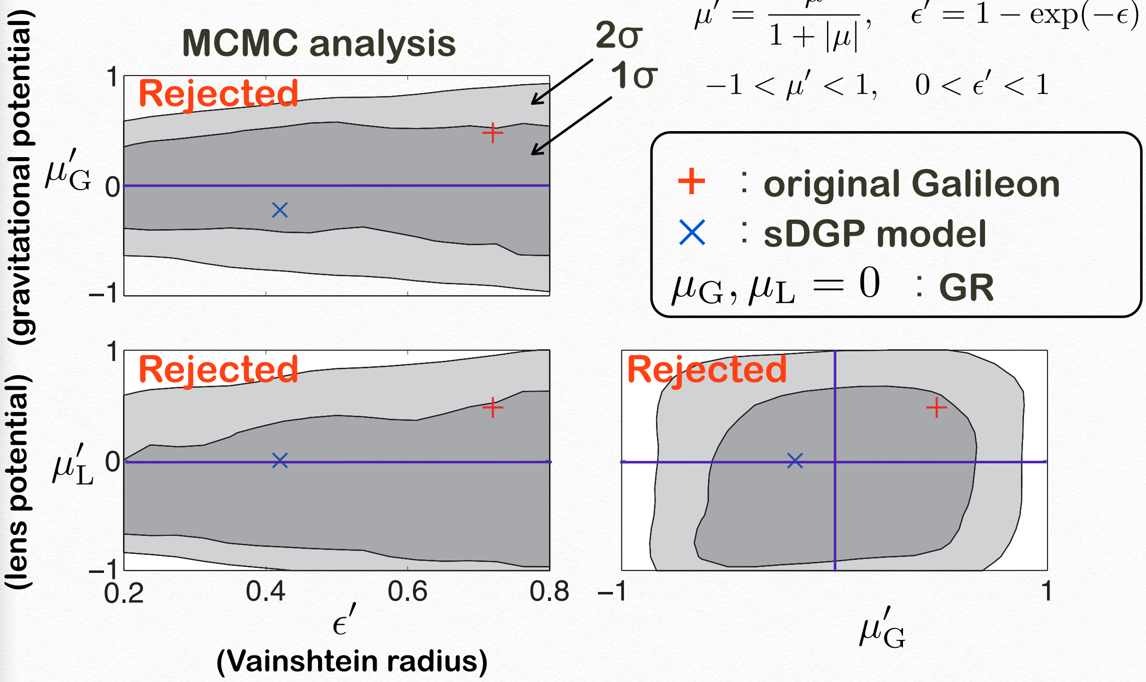


- 2 parameters are constrained at the same time.
- Original Galileon is marginal.

# Summary

- I have discussed testing gravity theory using cluster's observations of the gas and shear profiles simultaneously.
- The gas distributions depend on the gravitational potential, while the shear profile depends on the lens potential, which are complimentary to put a constraint.
- Using the observations of the gas and shear profiles of the Coma cluster, I put a constraint on the generalized Galileon model. ( $\mu_G, \mu_L, \epsilon$ )
- 2 parameters are constrained at the same time.
- The constraint on the original Galileon model is marginal.

# “CMB $\mu$ distortion from primordial gravitational waves”

Atsuhisa Ota

[JGRG24(2014)111209]

2014 Nov. 12　JGRG24@IPMU

# CMB μ distortion from primordial gravitational waves

Atsuhisa Ota

In collaboration with H. Tashiro, T. Takahashi and M. Yamaguchi

Tokyo Institute of Technology Department of Physics Cosmology group

Based on JCAP10(2014)029[arXiv:1406.0541]

## Outline

1. Introduction
2. Basics of μ distortion
3. Primordial fluctuations and the distortion
4. Results

# 1 Introduction

CMB as observables of primordial fluctuations



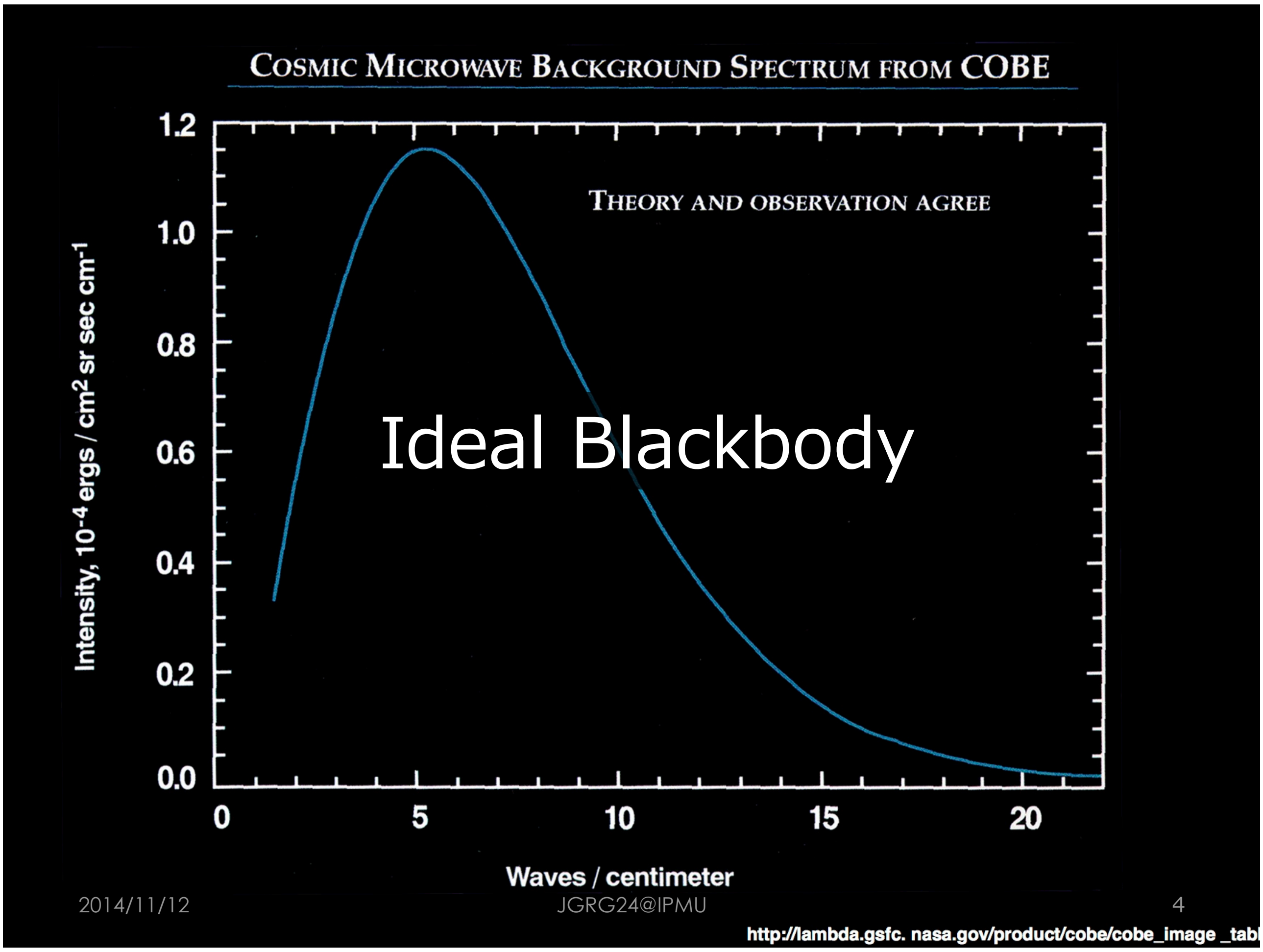

Deviations from the isotropic Planck distribution

Keys for the study of Primordial fluctuations

There are two types of approaches, let us see···

❶ Temperature anisotropy

❷ Spectrum distortion (μ type)

Chemical potential of more general Bose distribution



# 2 Basics of μ distortion

Mixing of blackbodies induce non-zero chemical potential

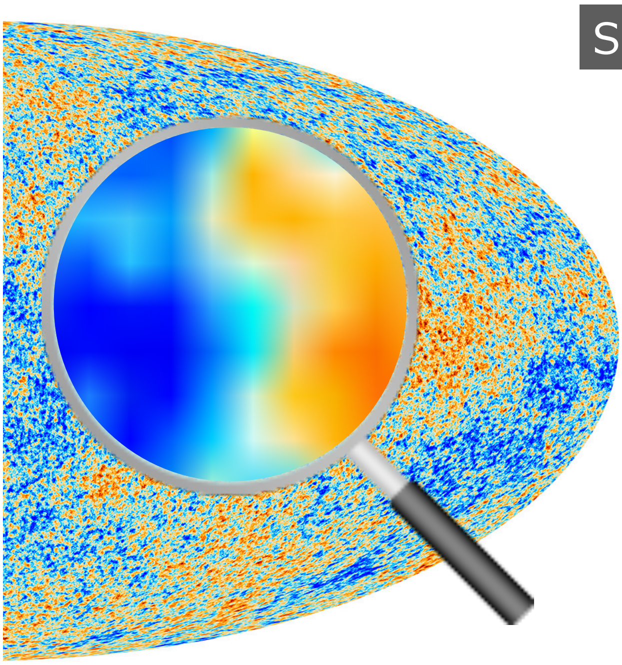

## Simplify

$T_0 - \delta T$ | $T_0 + \delta T$



## Pick up a partition!

Two Blackbodies

$T_0 - \delta T$ | $T_0 + \delta T$

Spatially inhomogeneous

Dissipation
&
Thermalizaion

Single Blackbody

$$T_{\rm new} = ?$$

Spatially homogeneous

**Energy density**

$$\rho_\gamma = \frac{1}{2}\left[\frac{\pi^2}{15}(T_0+\delta T)^4 + \frac{\pi^2}{15}(T_0-\delta T)^4\right]$$
$$\vdots$$
$$= \frac{\pi^2}{15}T_0^4\left[1+6\left(\frac{\delta T}{T_0}\right)^2+\cdots\right]$$

$$T_{\rm new} = T_0\left[1+\frac{3}{2}\left(\frac{\delta T}{T_0}\right)^2+\cdots\right]$$



**Number density**

$$n_\gamma^{\rm old} = \frac{2\zeta(3)}{\pi^2}T_0^3\left[1+3\left(\frac{\delta T}{T_0}\right)^2+\cdots\right]$$

$$n_\gamma^{\rm new} = \frac{2\zeta(3)}{\pi^2}T_0^3\left[1+\frac{9}{2}\left(\frac{\delta T}{T_0}\right)^2+\cdots\right]$$

- $\Delta n \propto \left(\frac{\delta T}{T_0}\right)^2$

Thermalization of different BB under number conservation

Chemical potential (No more Planck dist.)

Conditions for μ distortion are …

## ❶ Mixing of local Blackbodies

Track temperature evolution by Boltzmann eq.

## ❷ Thermalization

Pair annihilation, Bremss, Compton, ~~Thomson~~, …

## ❸ Number conservation

~~Pair annihilation~~, ~~Bremss~~, Compton, Thomson, …

Compton dominant era ($z \sim 10^6$, $\ell \sim 10^7$)



# 3 Primordial fluctuations and the distortions

Primordial fluctuations as sources of distortions

## μ distortion & primordial fluctuations

❶ Curvature origin (Hu '94, Chluba '12 etc.)

$$\mathcal{R}, \Theta_\gamma^S \xrightarrow[\text{Thermalization}]{\text{Dissipation (Silk damp.)}} \mu \sim 10^{-8}$$

$\mathrm{COBE}: \quad \mu < 9 \times 10^{-5}$

❷ PGW origin (Our study)

$$h \xrightarrow[\text{ISW}]{\text{Horizon entry}} \Theta_\gamma^T \xrightarrow[\text{Thermalization}]{\text{Dissipation (No Silk damp.)}} \mu \sim ?$$

$$\frac{d\Theta_\gamma^T}{d\eta} \sim -\dot{\tau}\Theta_\gamma^T$$



# 4 Results

## Constraints on r & $n_T$

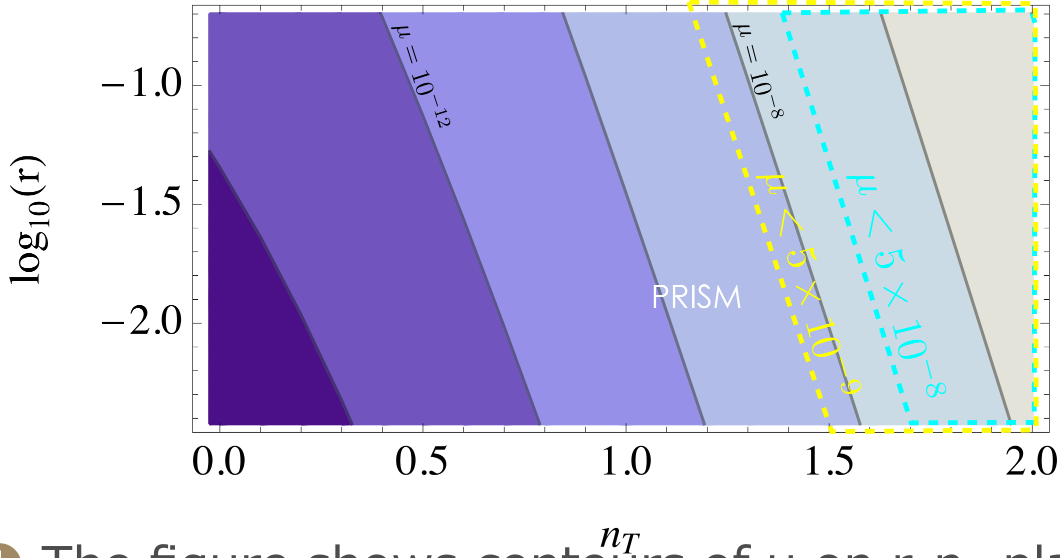


1. The figure shows contours of μ on r-$n_T$ plane
2. r=0.2 can ruled out $n_T$>1.2 by Future space mission PRISM



## Scale dependence of the μ (Tensor origin, r=0.2)

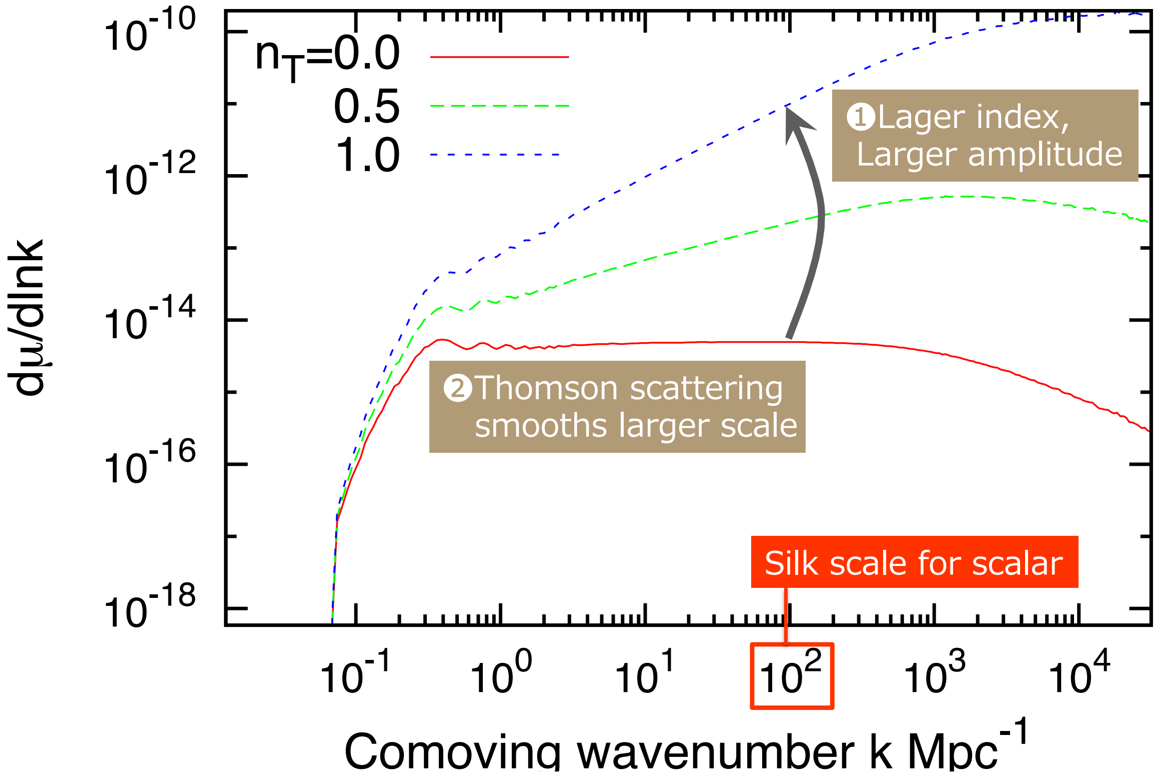

## Conclusions

1. New Generation mechanism of μ via Thomson isotropic nature for Tensor type
2. We obtain the constraints on r & $n_T$ by small scale CMB data alone
3. For r=0.2, $n_T$=0 generates $\mu \sim 10^{-14}$
4. Blue-tilted tensor can be ruled out by the Future observations

# “Probing the origin of UHECRs with neutrinos”

Shigeru Yoshida [Invited]

[JGRG24(2014)111210]


# Probing the origin of UHECRs with neutrinos

The recent results from IceCube and its outlook

Shigeru Yoshida
Department of Physics
ICEHAP, Chiba University

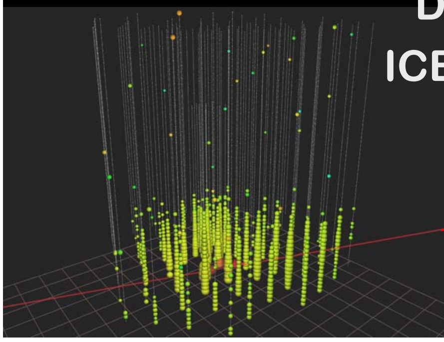

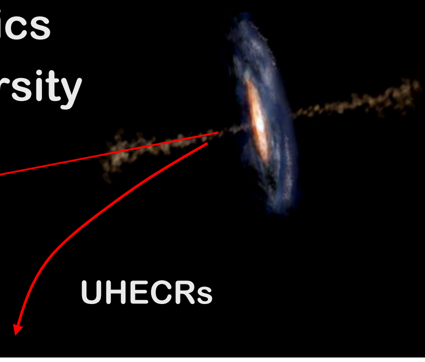


# The Neutrino Flux: overview

Solar ν ($^{8}$B)

SN relic ν

**Atmospheric ν**
The main background for astro-ν

**"On-source" astro-ν**
produced at the UHECR sources
Not established yet

**"GZK" cosmogenic ν**
produced in the CMB field
Not detected yet

MeV GeV TeV PeV EeV

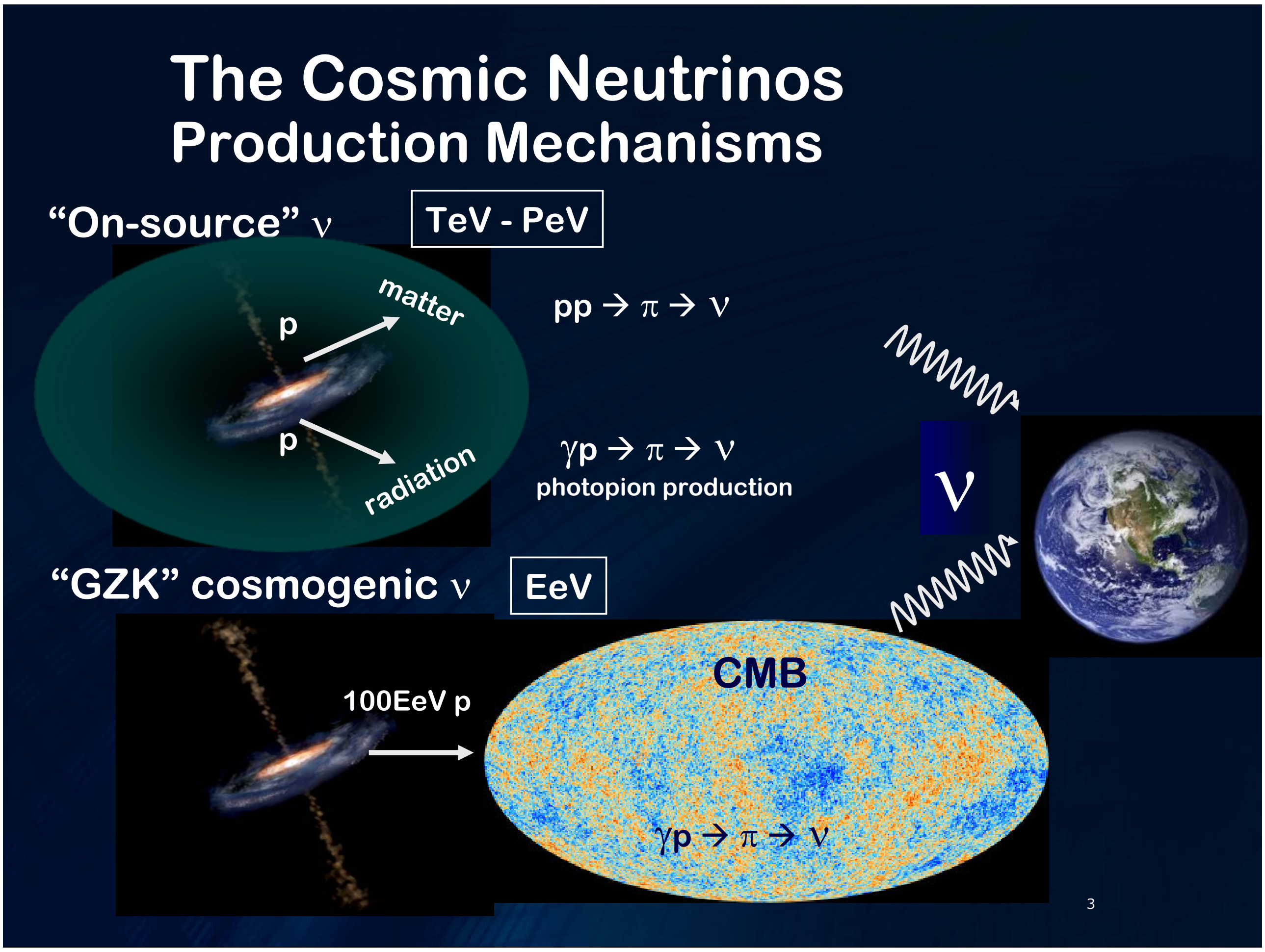
The Cosmic Neutrinos
Production Mechanisms
"On-source" ν
TeV - PeV
matter
p
p
radiation
pp → π → ν
γp → π → ν
photopion production
ν
"GZK" cosmogenic ν
EeV
100EeV p
CMB
γp → π → ν
3

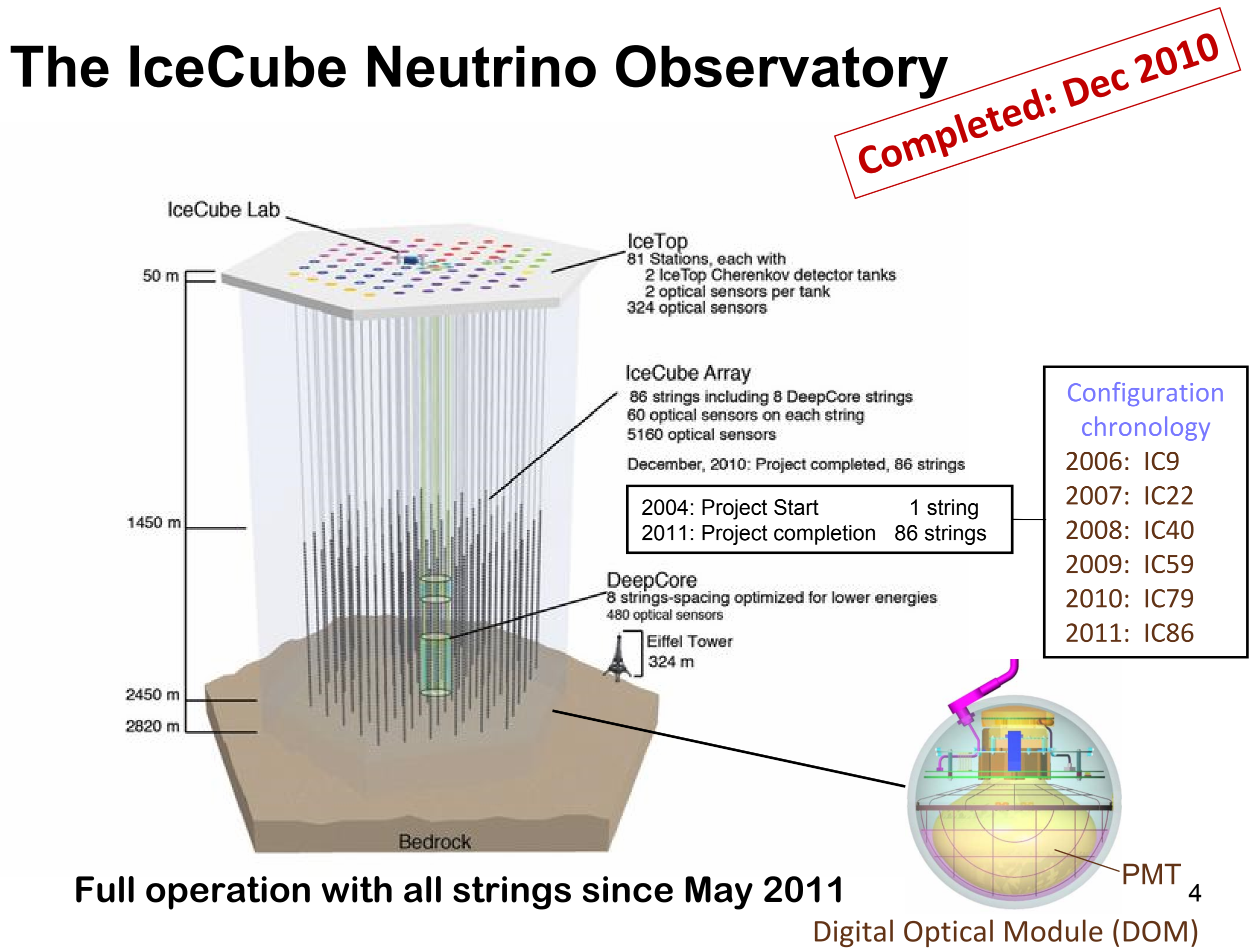
The IceCube Neutrino Observatory
Completed: Dec 2010
IceCube Lab
IceTop
81 Stations, each with
2 IceTop Cherenkov detector tanks
2 optical sensors per tank
324 optical sensors
50 m
IceCube Array
86 strings including 8 DeepCore strings
60 optical sensors on each string
5160 optical sensors
December, 2010: Project completed, 86 strings
2004: Project Start 1 string
2011: Project completion 86 strings
Configuration chronology
2006: IC9
2007: IC22
2008: IC40
2009: IC59
2010: IC79
2011: IC86
1450 m
DeepCore
8 strings-spacing optimized for lower energies
480 optical sensors
Eiffel Tower
324 m
2450 m
2820 m
Bedrock
PMT
Full operation with all strings since May 2011
4
Digital Optical Module (DOM)

# Constructions 2005-2011

Detectors shipped from Japan


Drill House

The IceCube Lab 「Beer Can」

Researchers working on deployment

ICECUBE

5

ICECUBE

# Topological signatures of IceCube events

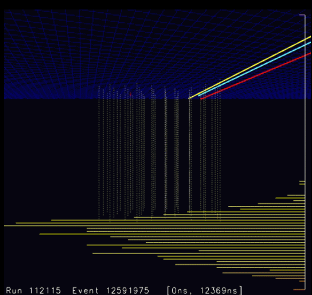


**Down-going track**

- atmospheric $\mu$
- secondary produced
  $\mu$ from $\nu_\mu$
  $\tau$ from $\nu_\tau$ @ >> PeV

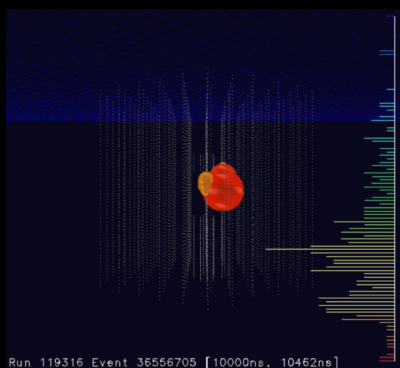


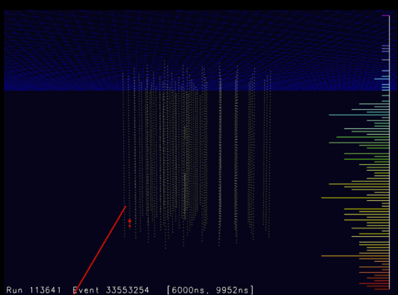


**Up-going track**

- atmospheric $\nu_\mu$

**Cascade (Shower)**

directly induced by $\nu$ inside the detector volume

- via CC from $\nu_e$
- via NC from $\nu_e$, $\nu_\mu$, $\nu_\tau$

all 3 flavor sensitive

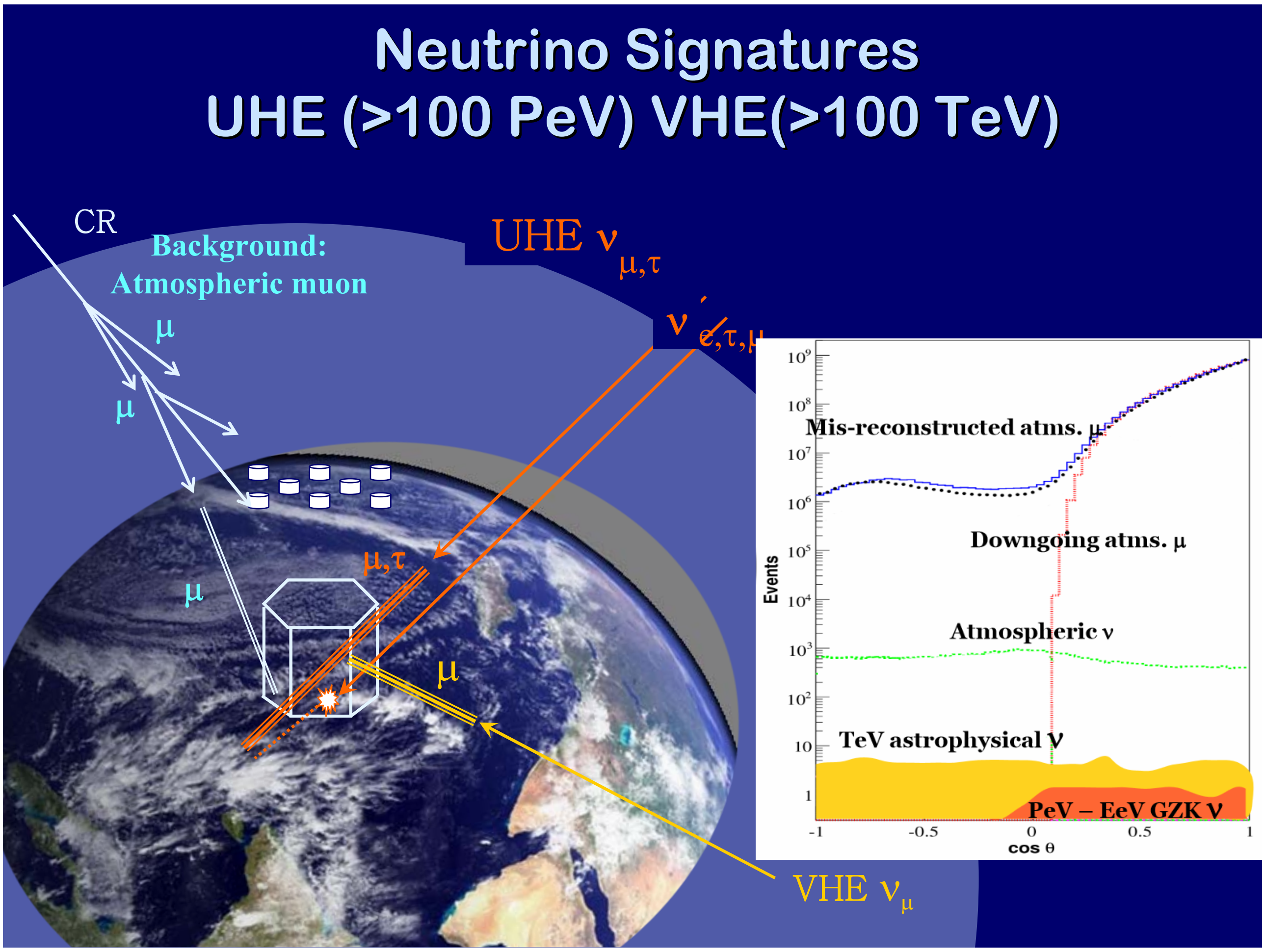


## Post Bert & Ernie

### The Discovery Analyses

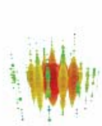

NEWSPAPER

Observation of a high-energy particle shower event from August 2011, identified as a PeV-energy neutrino. Each sphere represents a digital optical module sensor in the IceCube detector. Sphere size is a measure of the recorded number of photoelectrons. Colors represent arrival times of photons (red, early; blue, late). Selected for a Synopsis in *Physics* and an Editors' Suggestion. [M. G. Aartsen *et al.*, IceCube Collaboration, Phys. Rev. Lett. 111, 021103 (2013)]

PHYSICAL REVIEW LETTERS

*Contents*

*Articles published 6 July–12 July 2013*

VOLUME 111, NUMBER 2 — 12 July 2013



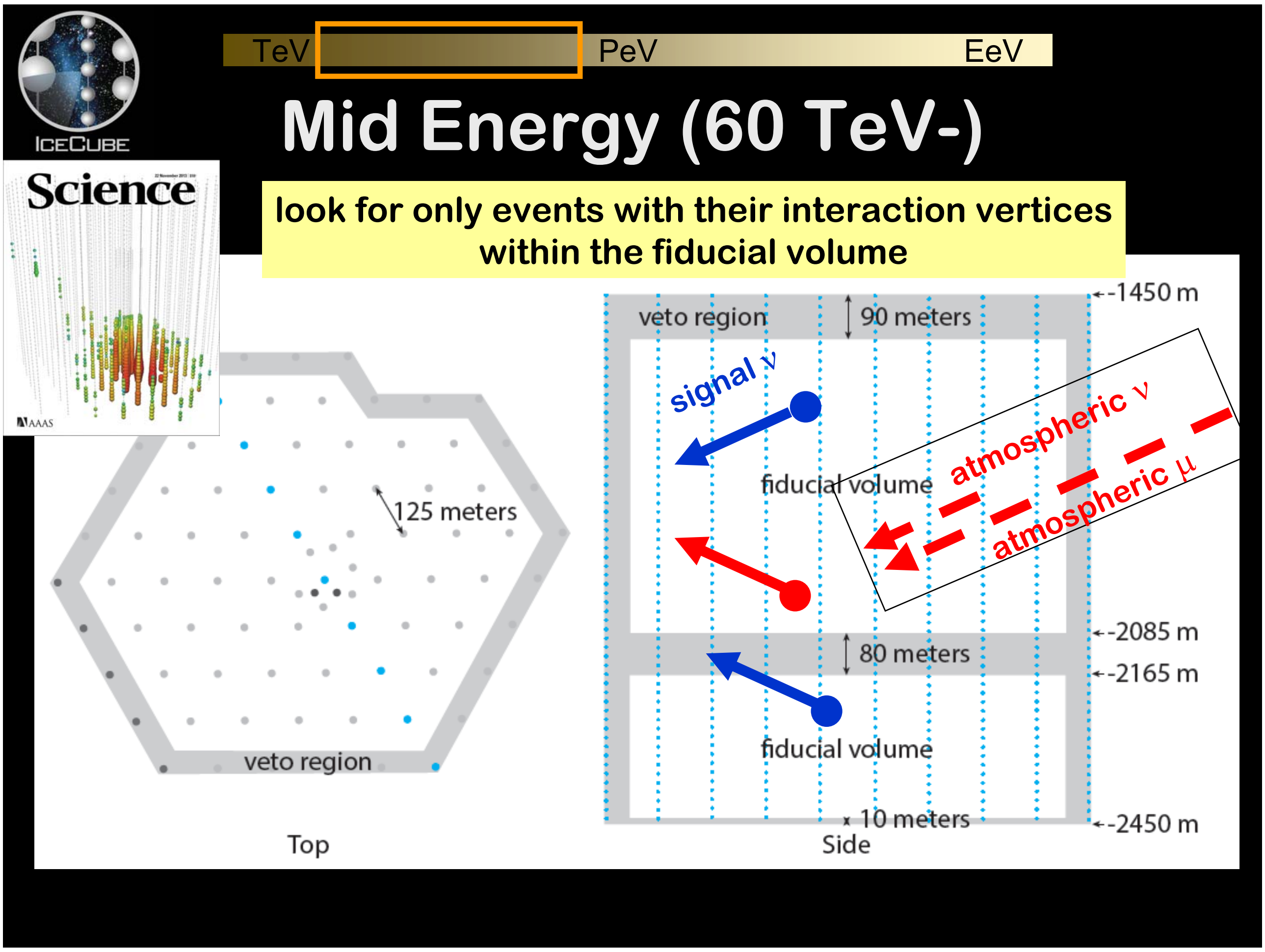
TeV
PeV
EeV
ICECUBE
Mid Energy (60 TeV-)
Science
look for only events with their interaction vertices within the fiducial volume
125 meters
veto region
Top
veto region
90 meters
-1450 m
signal ν
atmospheric ν
atmospheric μ
fiducial volume
80 meters
-2085 m
-2165 m
fiducial volume
10 meters
-2450 m
Side

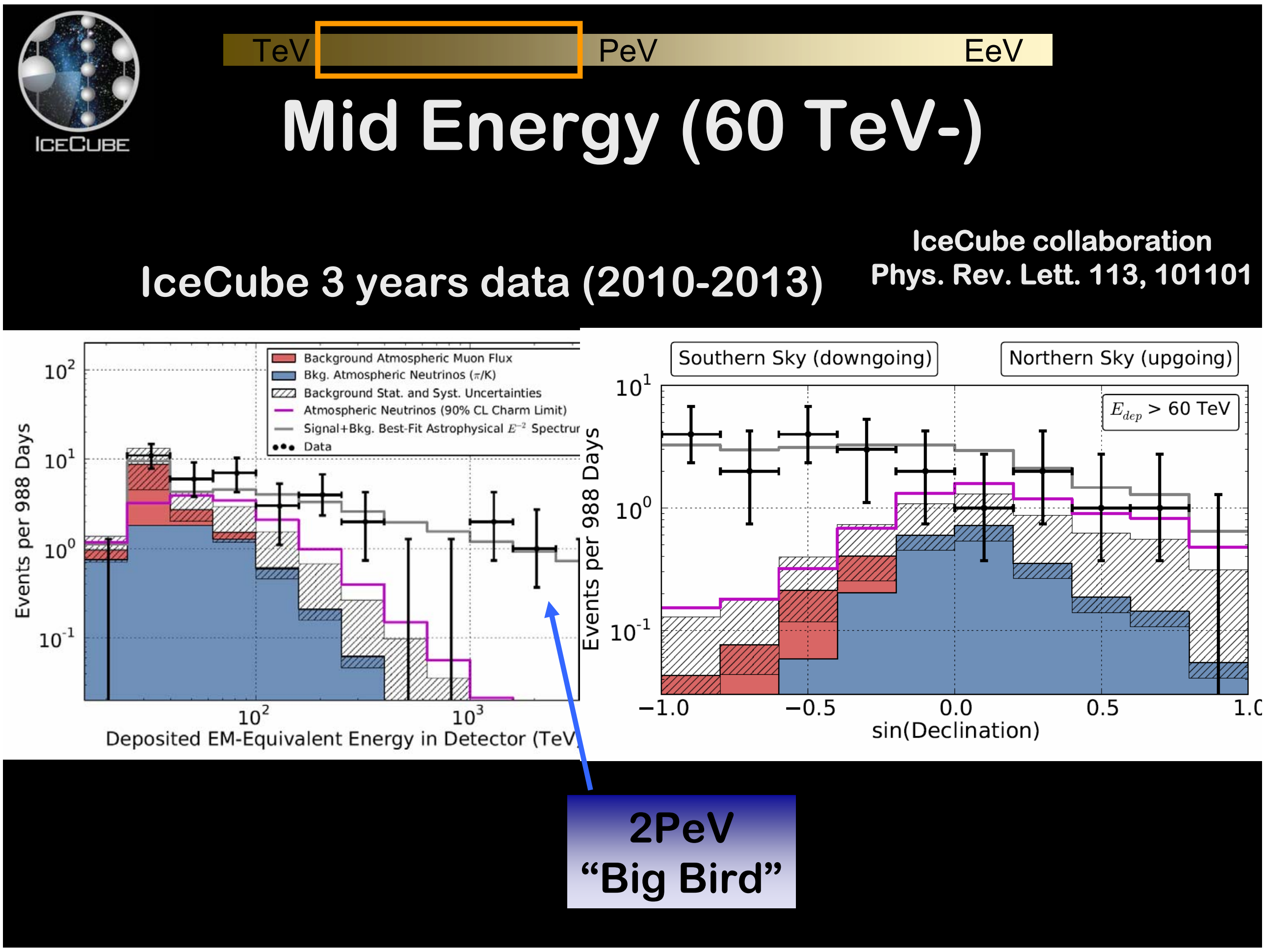
TeV
PeV
EeV
ICECUBE
Mid Energy (60 TeV-)
IceCube 3 years data (2010-2013)
IceCube collaboration
Phys. Rev. Lett. 113, 101101
Background Atmospheric Muon Flux
Bkg. Atmospheric Neutrinos (π/K)
Background Stat. and Syst. Uncertainties
Atmospheric Neutrinos (90% CL Charm Limit)
Signal+Bkg. Best-Fit Astrophysical E^-2 Spectrum
Data
Events per 988 Days
Deposited EM-Equivalent Energy in Detector (TeV)
Southern Sky (downgoing)
Northern Sky (upgoing)
E_dep > 60 TeV
Events per 988 Days
sin(Declination)
2PeV
"Big Bird"

TeV PeV EeV

# Mid Energy (60 TeV-)

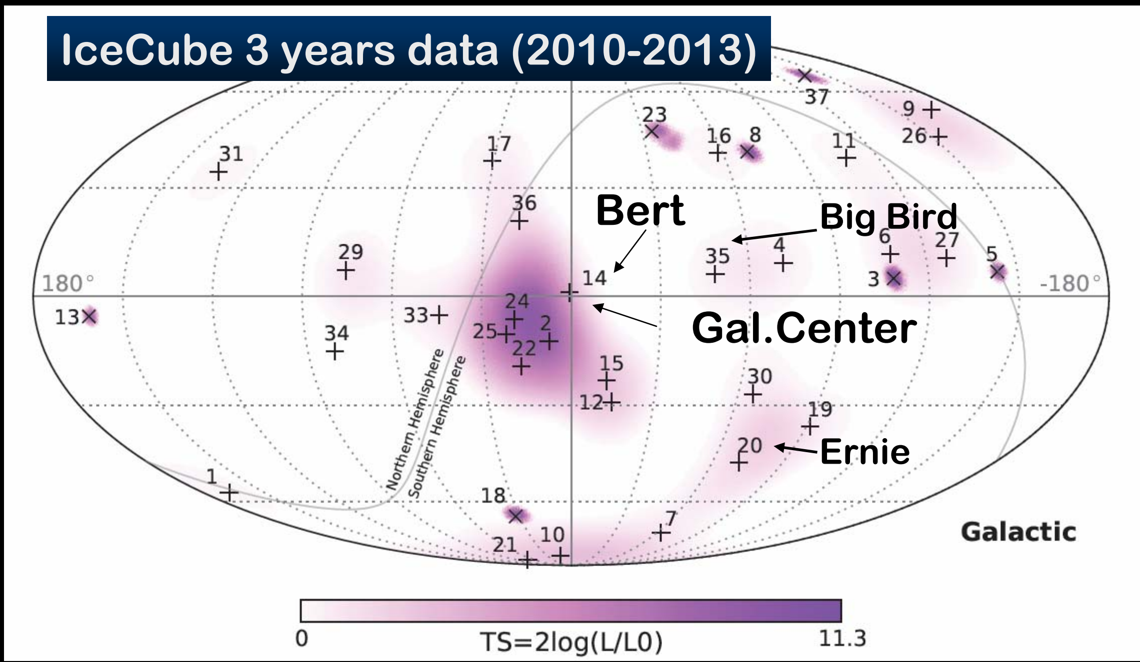


TeV PeV EeV

# Mid Energy (10 TeV-)

veto + “cascade”

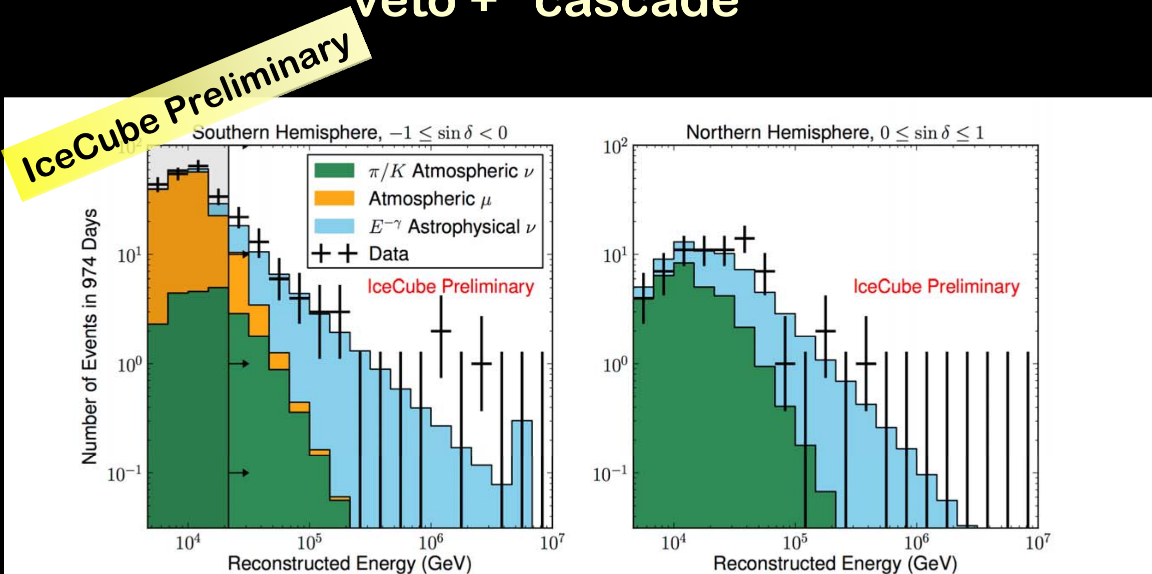

TeV PeV EeV

# LE (<10 TeV)

**Energy-dependent active veto**

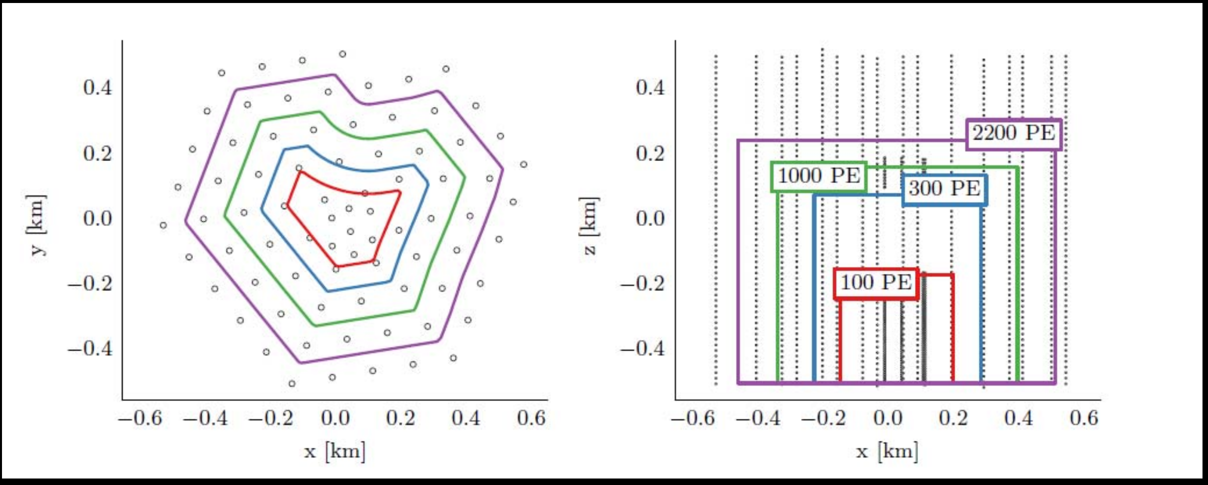


TeV PeV EeV

# LE (<10 TeV)

IceCube Preliminary

IceCube 2 years data (2010-2012)

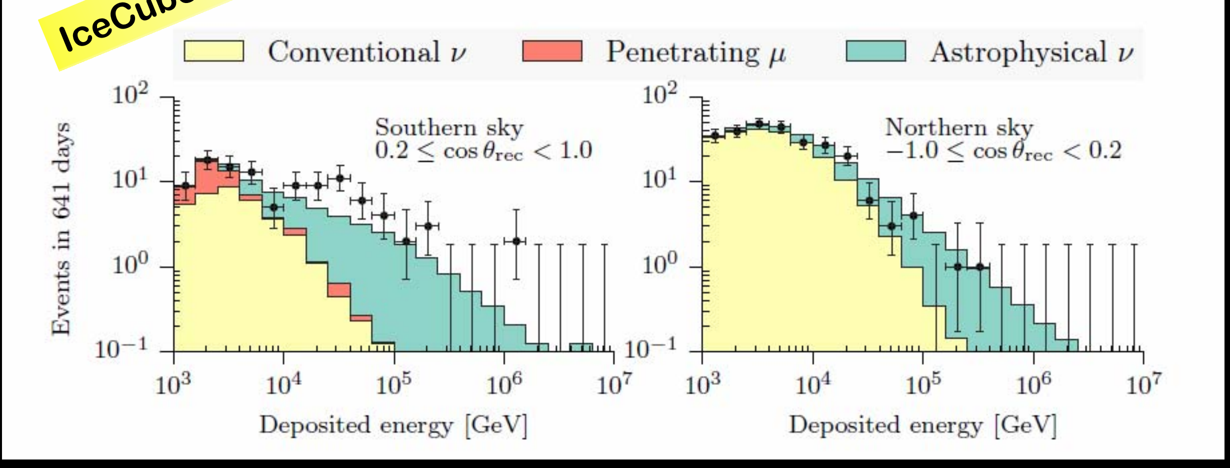

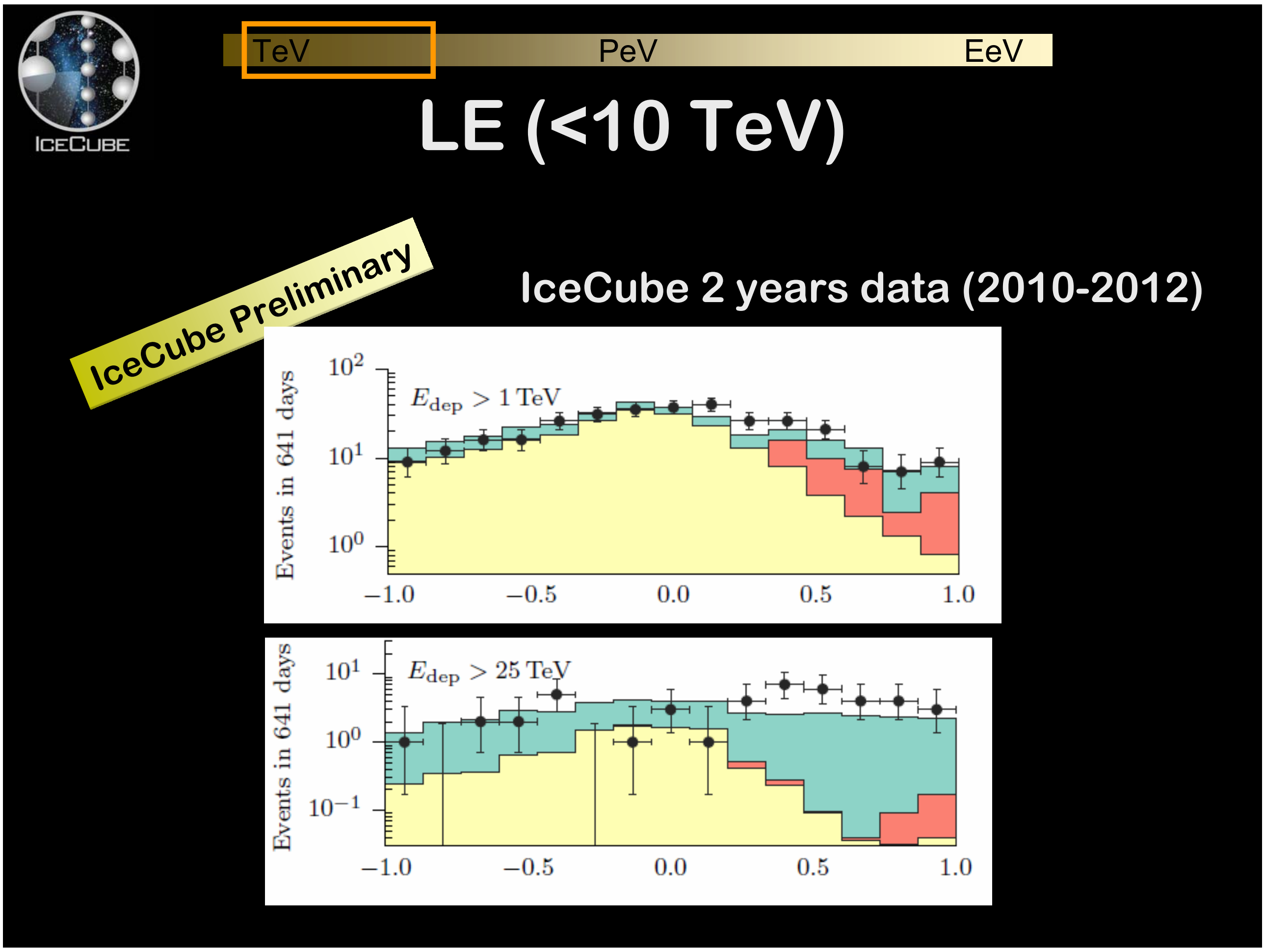
TeV
PeV
EeV
ICECUBE
LE (<10 TeV)
IceCube Preliminary
IceCube 2 years data (2010-2012)
Events in 641 days
$E_{dep} > 1$ TeV
$10^2$
$10^1$
$10^0$
−1.0
−0.5
0.0
0.5
1.0
Events in 641 days
$E_{dep} > 25$ TeV
$10^1$
$10^0$
$10^{-1}$
−1.0
−0.5
0.0
0.5
1.0

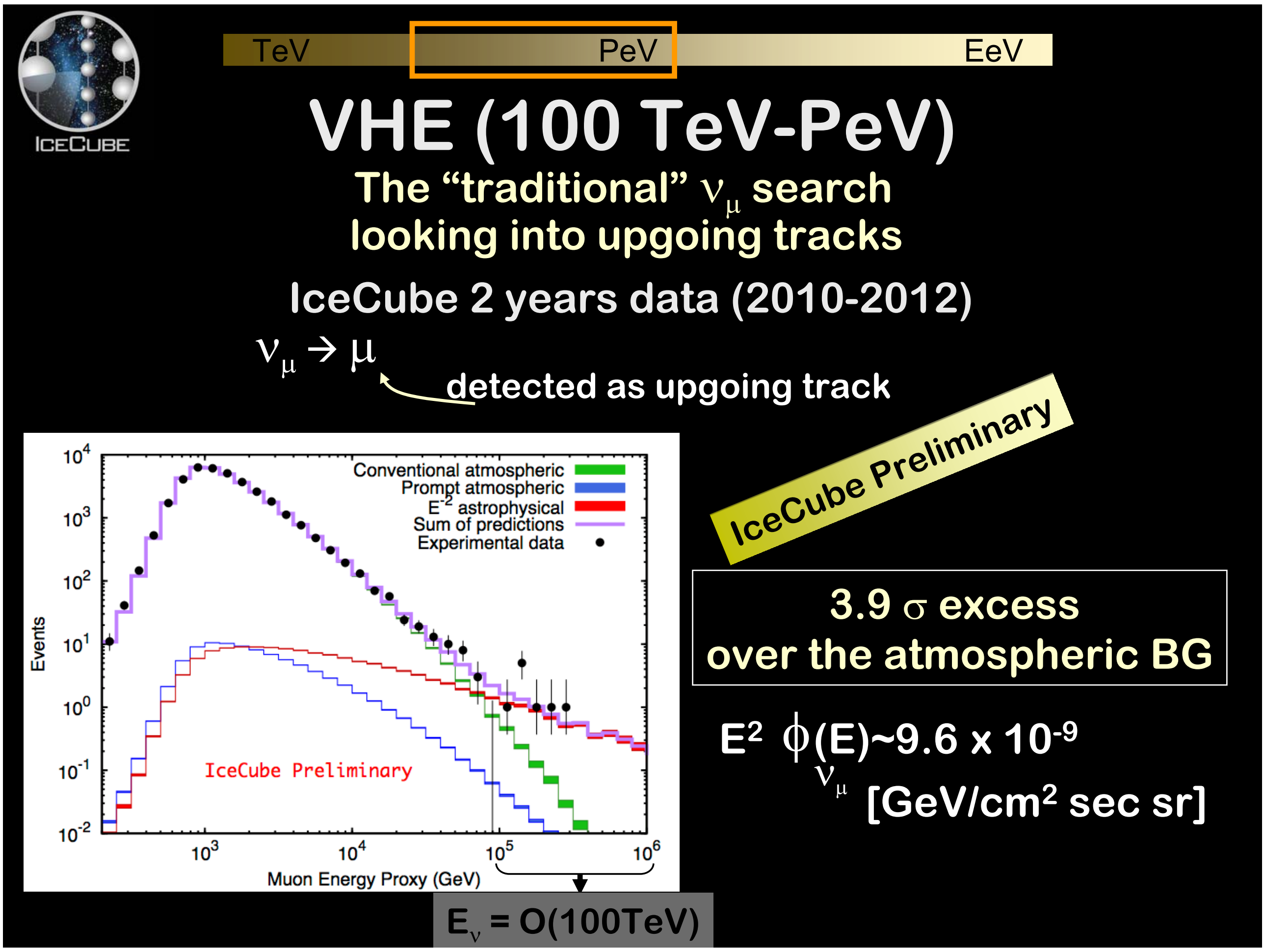
TeV
PeV
EeV
ICECUBE
VHE (100 TeV-PeV)
The "traditional" $\nu_\mu$ search
looking into upgoing tracks
IceCube 2 years data (2010-2012)
$\nu_\mu \rightarrow \mu$
detected as upgoing track
Conventional atmospheric
Prompt atmospheric
$E^{-2}$ astrophysical
Sum of predictions
Experimental data
Events
IceCube Preliminary
Muon Energy Proxy (GeV)
$E_\nu$ = O(100TeV)
IceCube Preliminary
3.9 $\sigma$ excess
over the atmospheric BG
$E^2\ \phi_{\nu_\mu}(E) \sim 9.6 \times 10^{-9}$
[GeV/cm² sec sr]

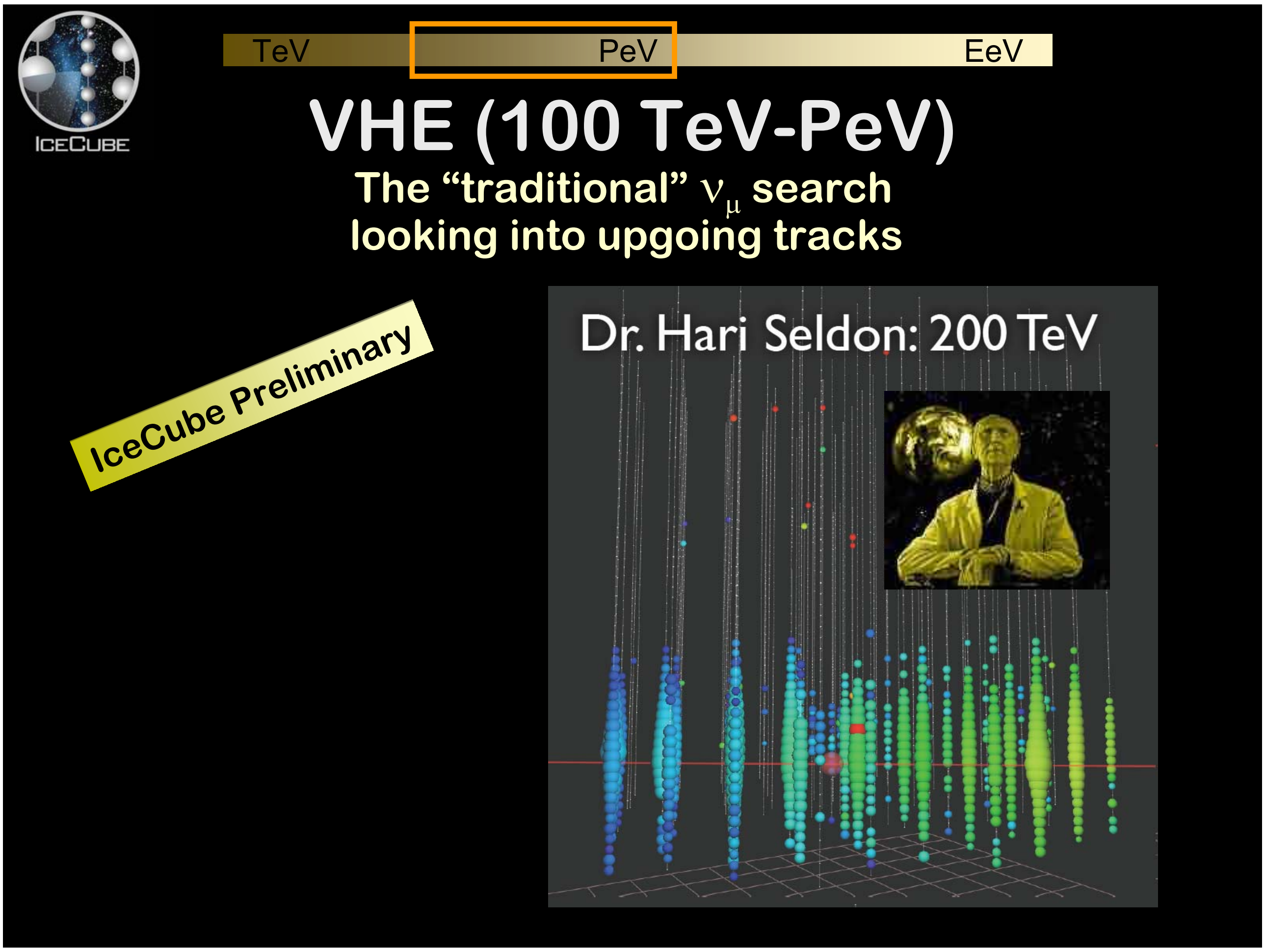
ICECUBE
TeV
PeV
EeV
VHE (100 TeV-PeV)
The "traditional" $\nu_\mu$ search
looking into upgoing tracks
IceCube Preliminary
Dr. Hari Seldon: 200 TeV

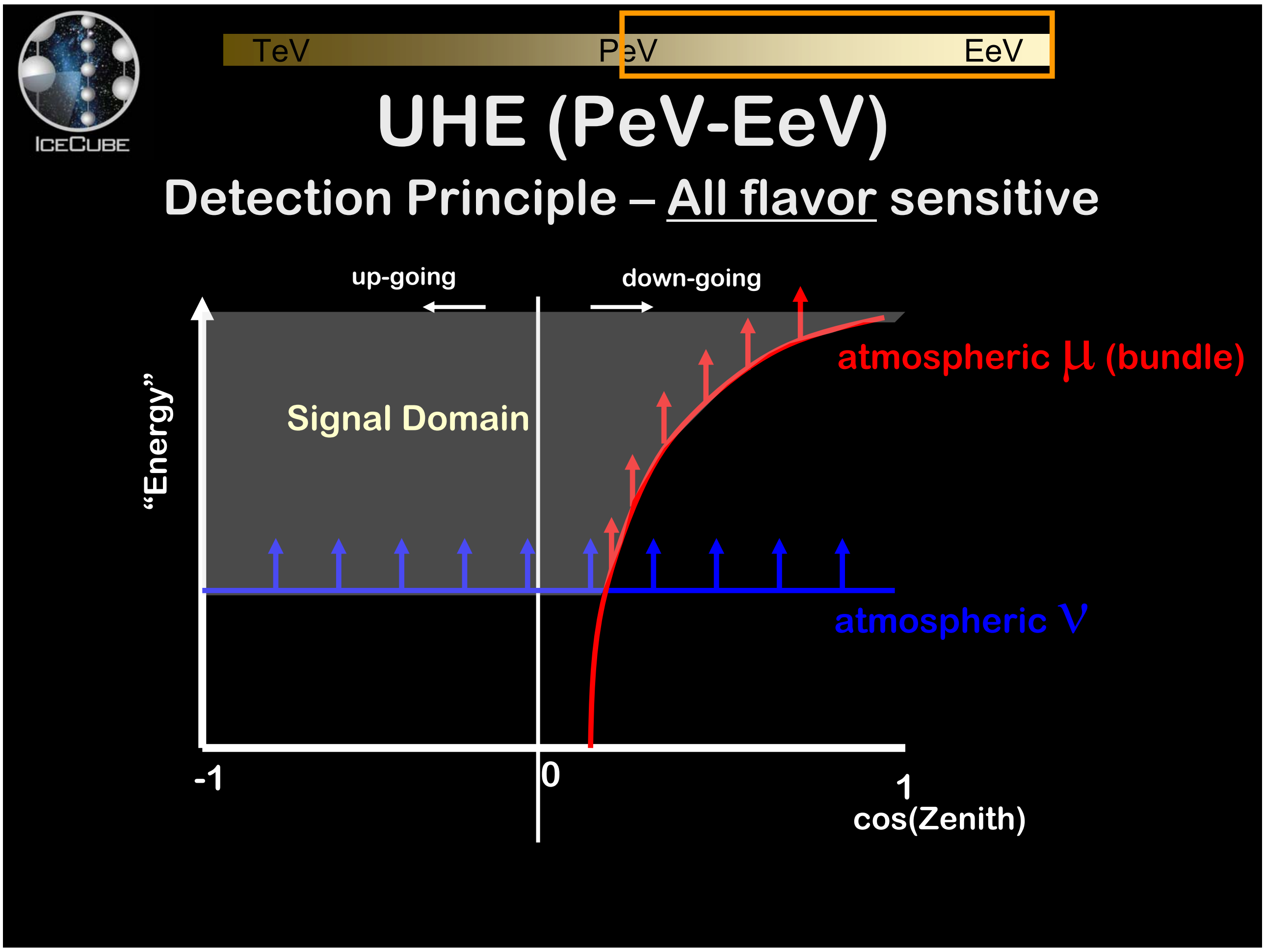
ICECUBE
TeV
PeV
EeV
UHE (PeV-EeV)
Detection Principle – All flavor sensitive
up-going
down-going
"Energy"
Signal Domain
atmospheric $\mu$ (bundle)
atmospheric $\nu$
-1
0
1
cos(Zenith)

TeV PeV EeV

# UHE (PeV-EeV)

Number of events (z-axis) per the test-sample livetime

test-sample data | atmospheric $\mu$ | atmospheric $\nu$ (conventional only) | signal GZK $\nu$

IceCube2010

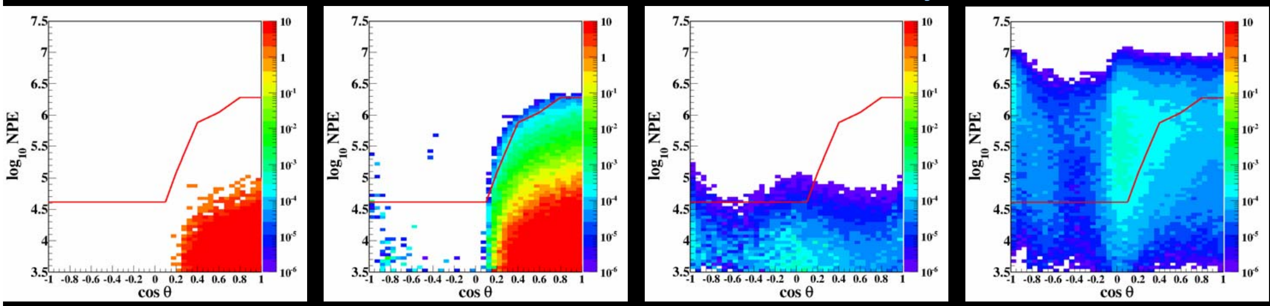

IceCube2011

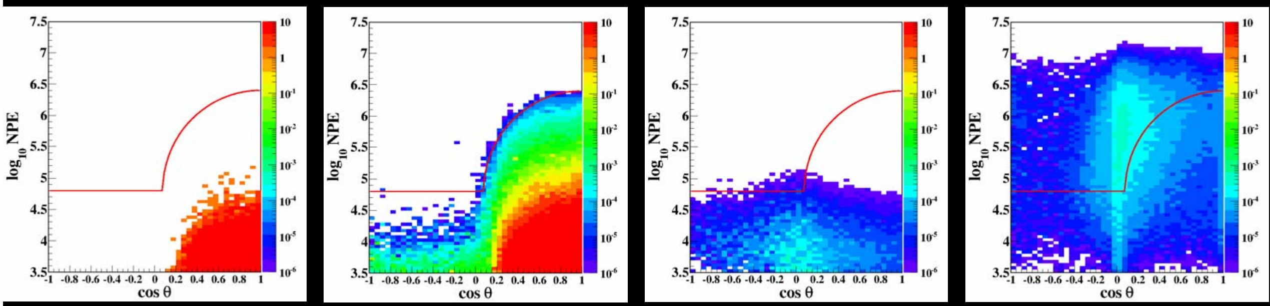

TeV PeV EeV

# UHE (PeV-EeV)

The model-independent upper limit on flux

IceCube 2 years data (2010-2012)

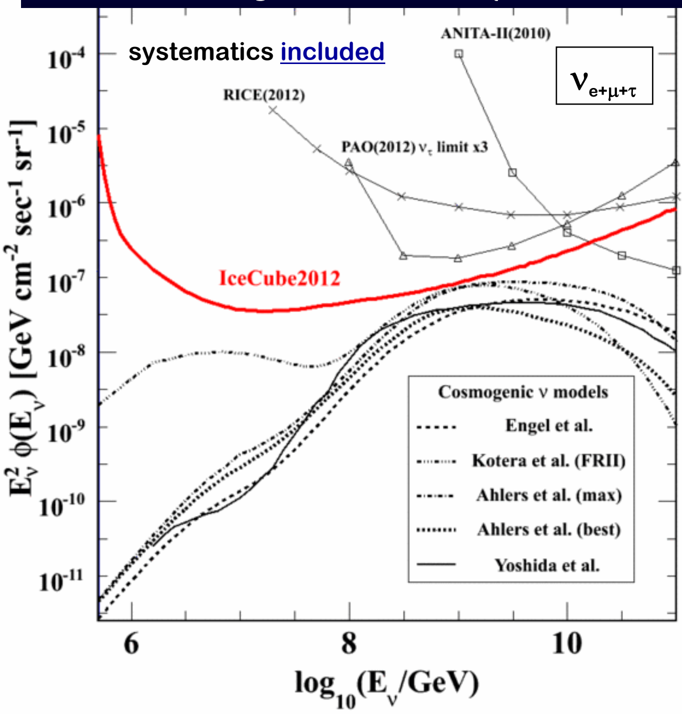


IceCube collaboration
Phys. Rev. D 88, 112008

any model adjacent to the limit is disfavored by the observation

Effective $\nu_{e+\mu+\tau}$ detection exposure

$6\times10^7$ m$^2$ days sr @ 1EeV

= 0.2 km$^2$ sr year

Note: $\phi_{CR}$(>1EeV) ~ 20/km$^2$ sr year

$\nu$ with CR comparable flux should have been detected

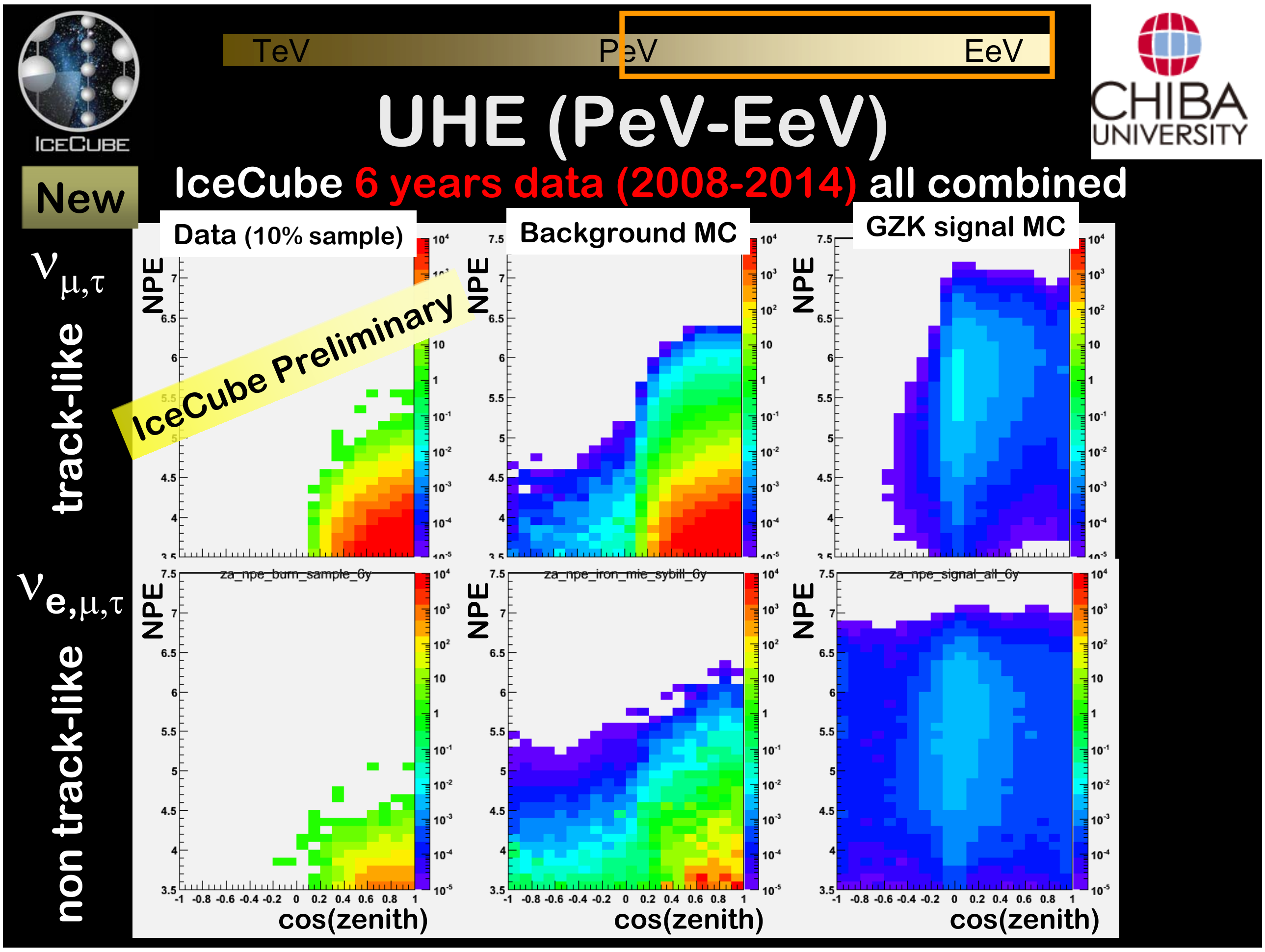
TeV
PeV
EeV
UHE (PeV-EeV)
ICECUBE
CHIBA UNIVERSITY
New
IceCube 6 years data (2008-2014) all combined
Data (10% sample)
Background MC
GZK signal MC
IceCube Preliminary
$\nu_{\mu,\tau}$
track-like
$\nu_{e,\mu,\tau}$
non track-like
NPE
za_npe_burn_sample_6y
za_npe_iron_mie_sybill_6y
za_npe_signal_all_6y
cos(zenith)

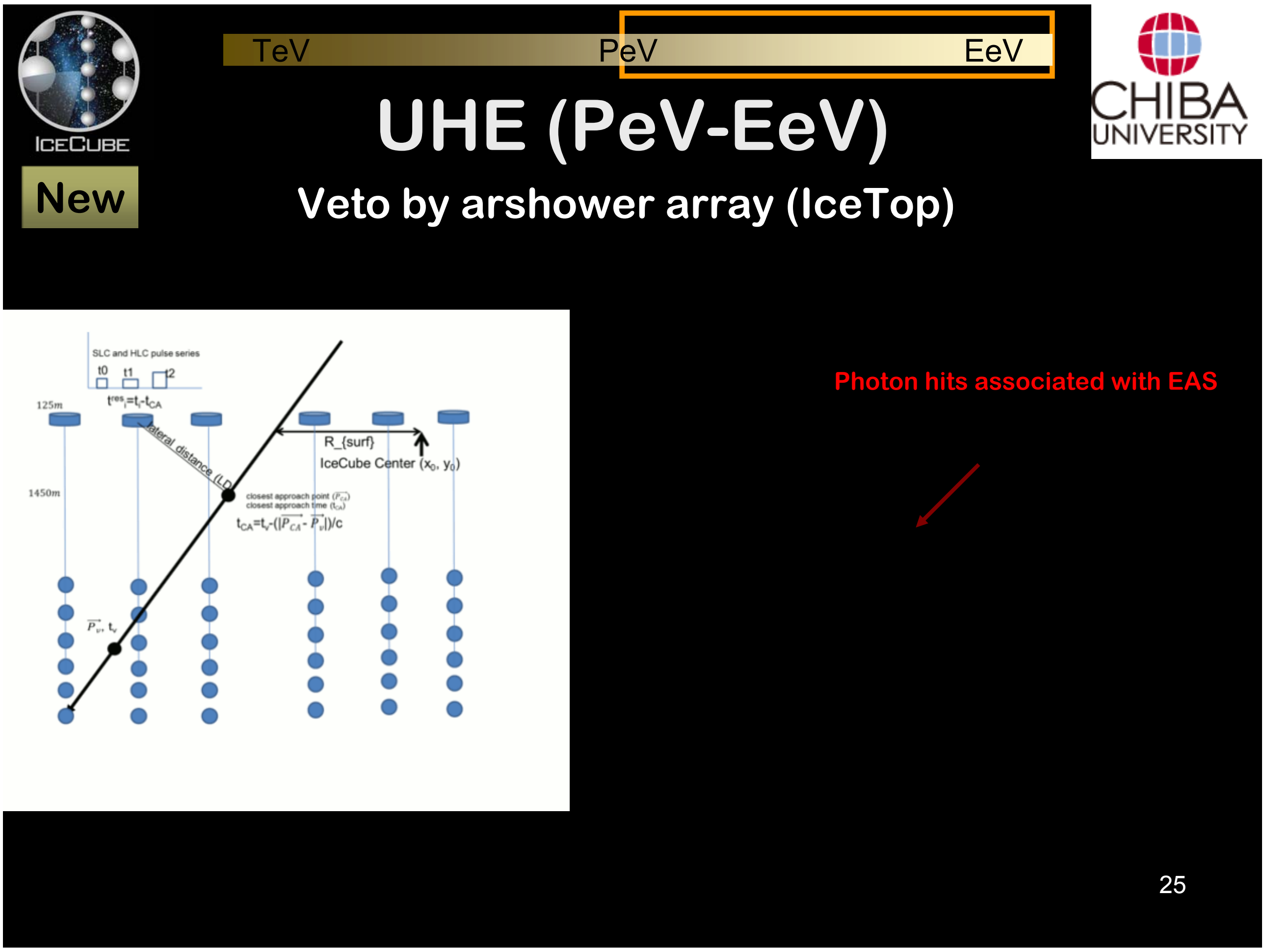
TeV
PeV
EeV
UHE (PeV-EeV)
ICECUBE
CHIBA UNIVERSITY
New
Veto by arshower array (IceTop)
SLC and HLC pulse series
t0
t1
t2
125m
1450m
lateral distance (LD)
R_{surf}
IceCube Center ($x_0$, $y_0$)
closest approach point
closest approach time
Photon hits associated with EAS
25

TeV PeV EeV

# UHE (PeV-EeV)

## IceCube 6 years data (2008-2014) all combined

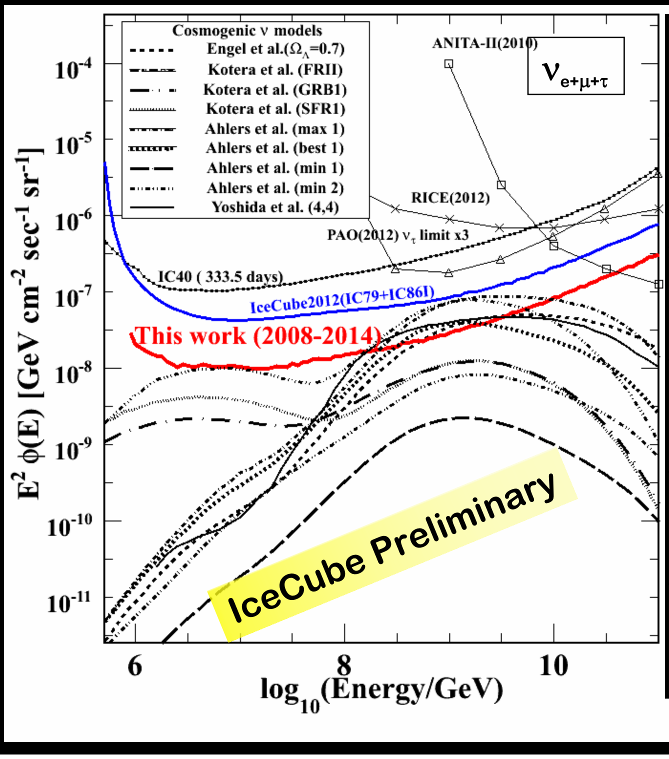


| Model | Event Rate [/(2008-20014)] |
|---|---|
| Yoshida (FR-II compat.) | 6.5 |
| Ahlers (Best fit to HiRes) | 5.0 |
| Ahlers (Minimum) | 1.1 |
| Kotera (GRB) | 3.9 |
| Kotera (STF) | 2.9 |


TeV PeV EeV

# UHE (PeV-EeV)

## IceCube 6 years data (2008-2014) all combined


IceCube Confidential

# Search Results coming soon

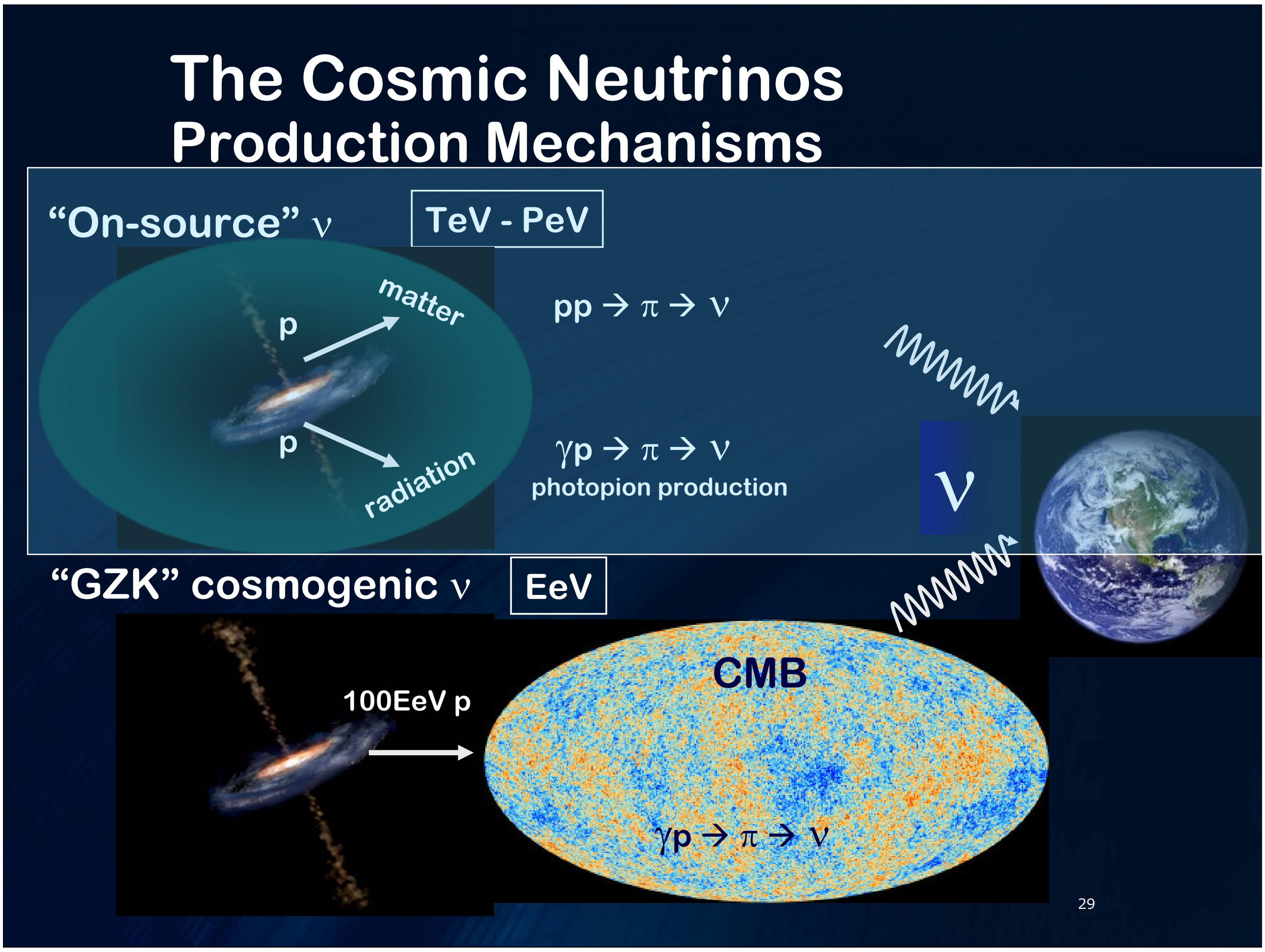
The Cosmic Neutrinos
Production Mechanisms
"On-source" ν
TeV - PeV
matter
p
p
radiation
pp → π → ν
γp → π → ν
photopion production
ν
"GZK" cosmogenic ν
EeV
100EeV p
CMB
γp → π → ν
29

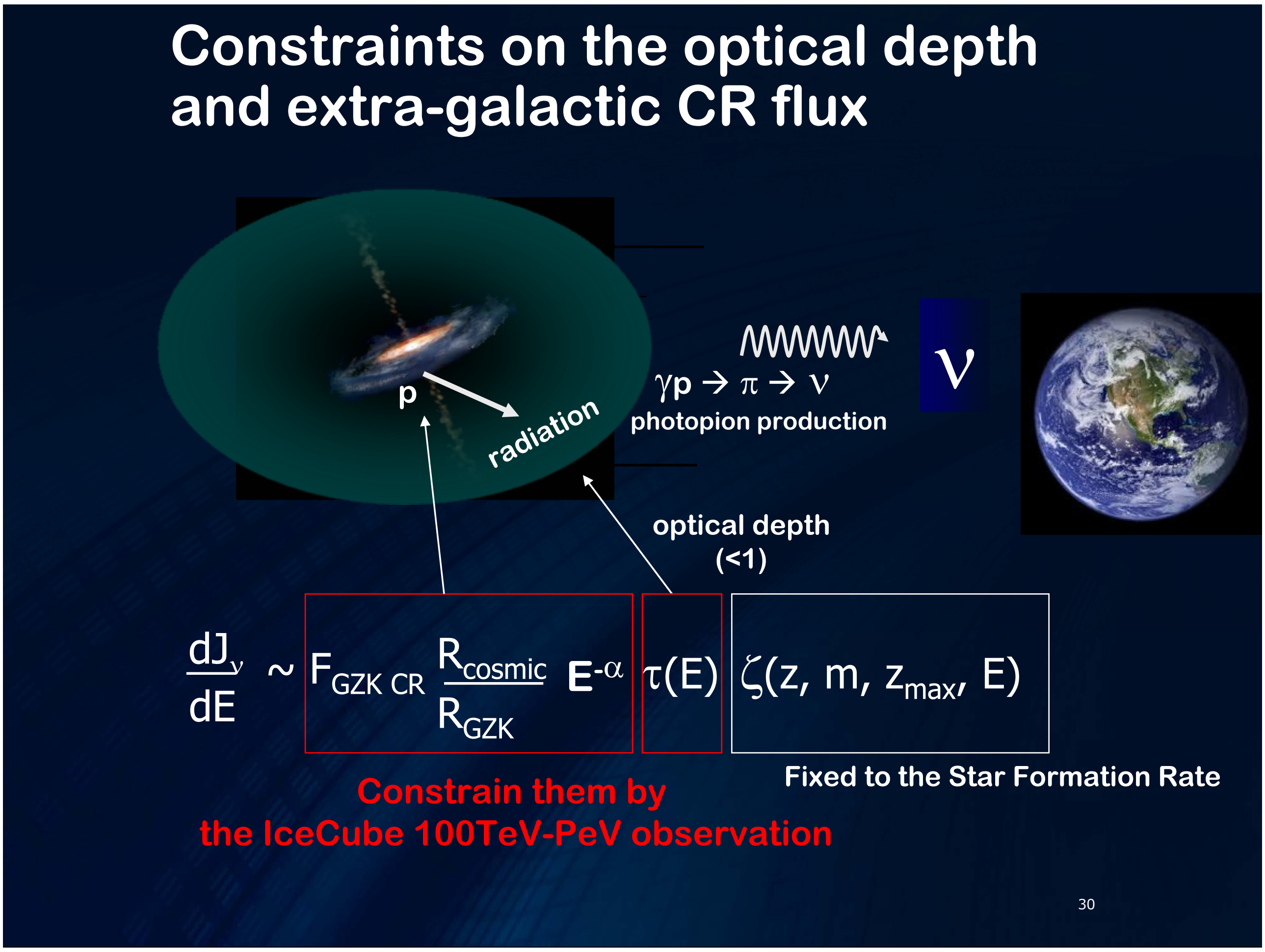
Constraints on the optical depth
and extra-galactic CR flux
p
radiation
γp → π → ν
photopion production
ν
optical depth
(<1)
$\frac{dJ_\nu}{dE} \sim F_{GZK\ CR} \frac{R_{cosmic}}{R_{GZK}} E^{-\alpha}\ \tau(E)\ \zeta(z, m, z_{max}, E)$
Fixed to the Star Formation Rate
Constrain them by
the IceCube 100TeV-PeV observation
30

# Constraints on the optical depth and extra-galactic CR flux

Yoshida, Takami
arXiv:1409.2950

extra-galactic proton flux must be > $10^{-2}$ of the all-particle CR flux @ 10 PeV

optical depth must be $\gtrsim 10^{-2}$



# Constraints on the optical depth and extra-galactic CR flux

if they are also 100EeV CR sources

strong evolution

Quasars/FR-II
GRBs (internal shock)

energetics

BL Lac/FR-I
GRBs (external shock)

# Suppose the PeV $\nu$ emitters are *also UHECR (E~100EeV) sources*

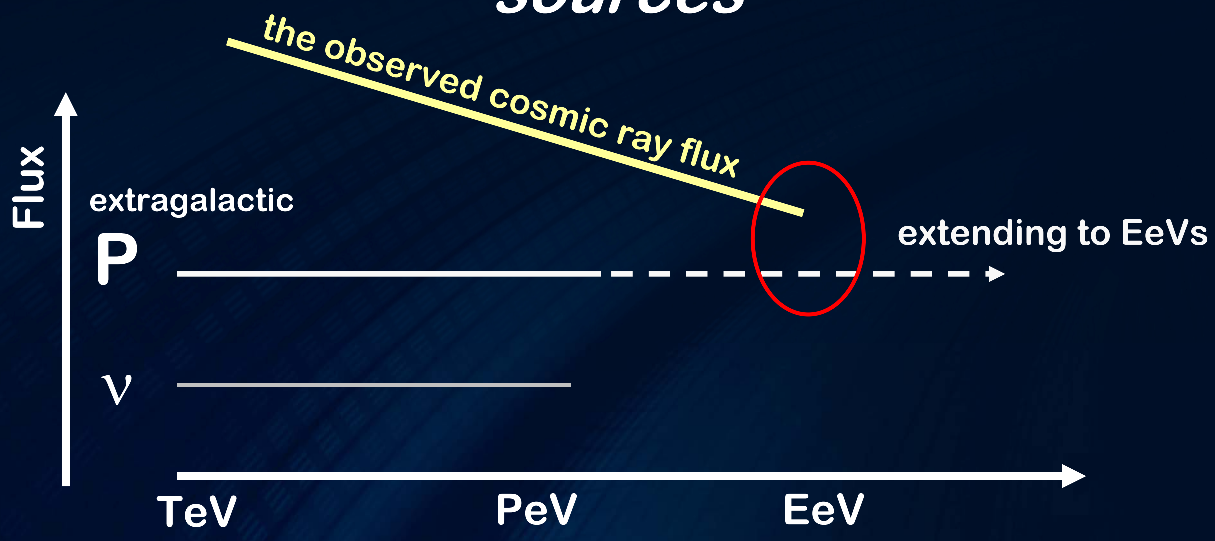




# Constraints on the optical depth and extra-galactic CR flux

- extra-galactic proton flux must ***dominate*** in the all-particle CR flux @ 1 EeV(=1000PeV)
- optical depth must be ~1

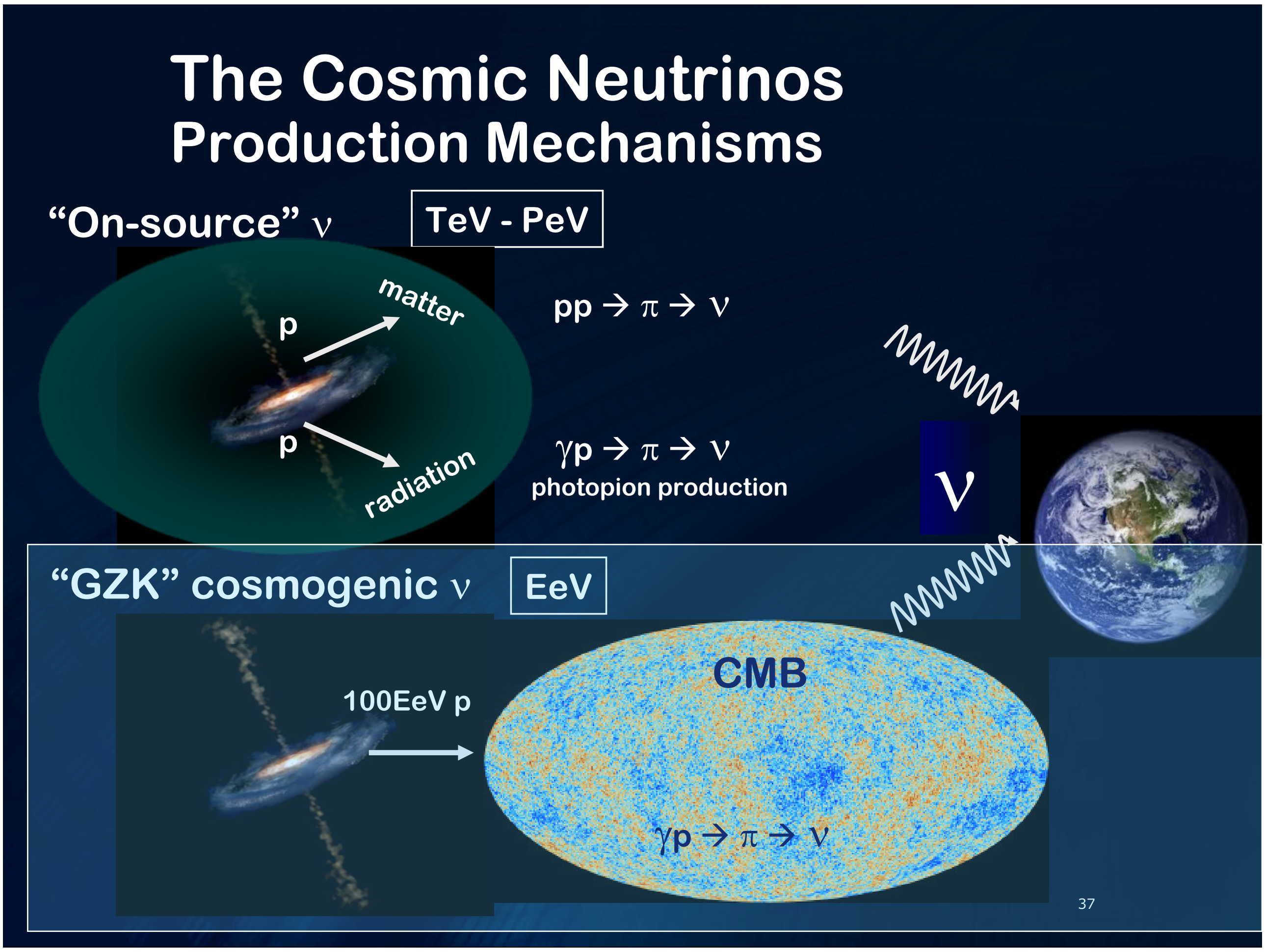
The Cosmic Neutrinos
Production Mechanisms
“On-source” ν
TeV - PeV
matter
p
p
radiation
pp → π → ν
γp → π → ν
photopion production
ν
“GZK” cosmogenic ν
EeV
100EeV p
CMB
γp → π → ν
37

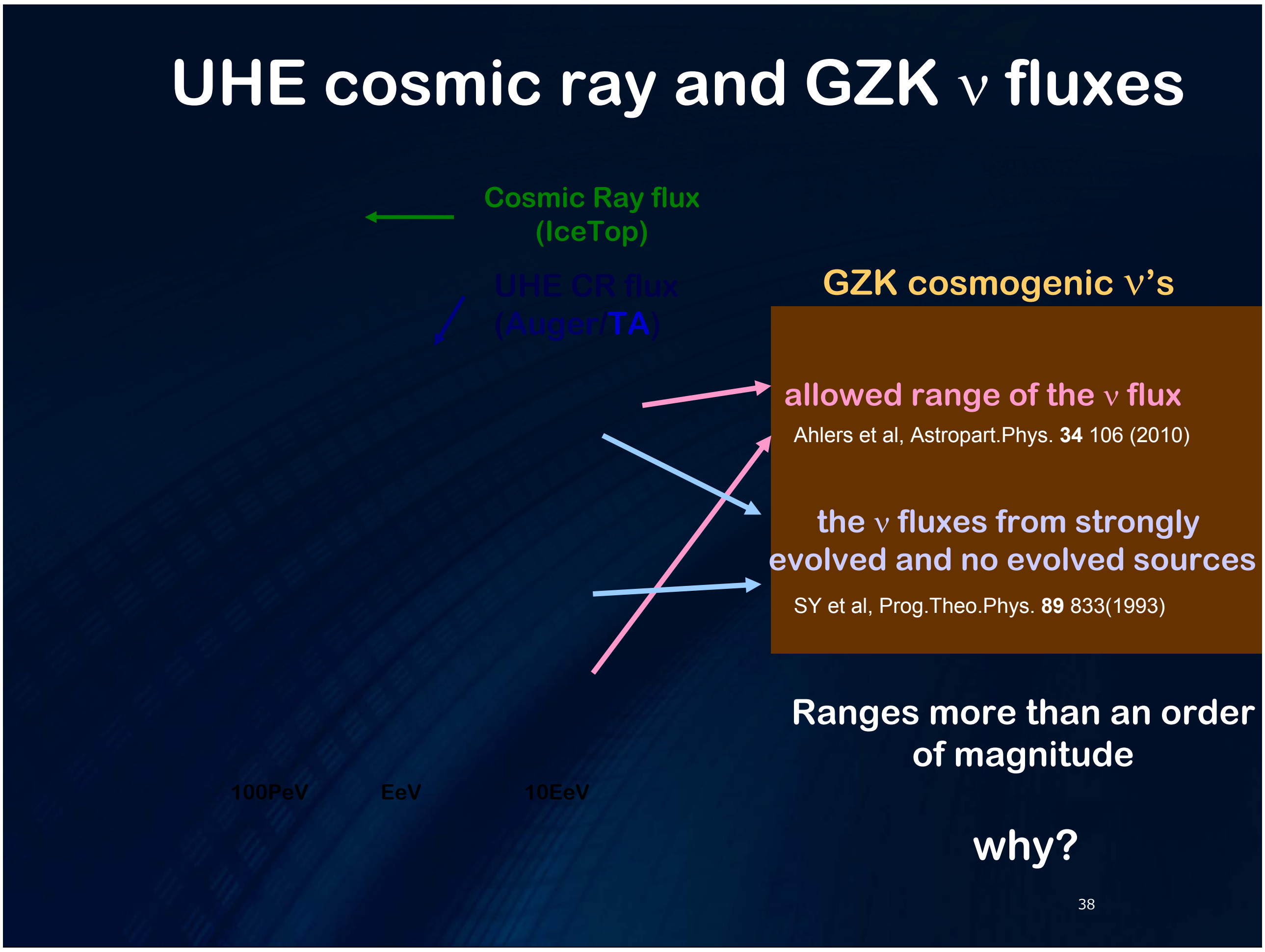
UHE cosmic ray and GZK ν fluxes
Cosmic Ray flux
(IceTop)
UHE CR flux
(Auger/TA)
GZK cosmogenic ν’s
allowed range of the ν flux
Ahlers et al, Astropart.Phys. 34 106 (2010)
the ν fluxes from strongly
evolved and no evolved sources
SY et al, Prog.Theo.Phys. 89 833(1993)
Ranges more than an order
of magnitude
why?
100PeV
EeV
10EeV
38

# Tracing *history* of the particle emissions with ν flux

color : emission rate of ultra-high energy particles

Intensity gets higher if the emission is more active in the past

because ν beams are penetrating over cosmological distances

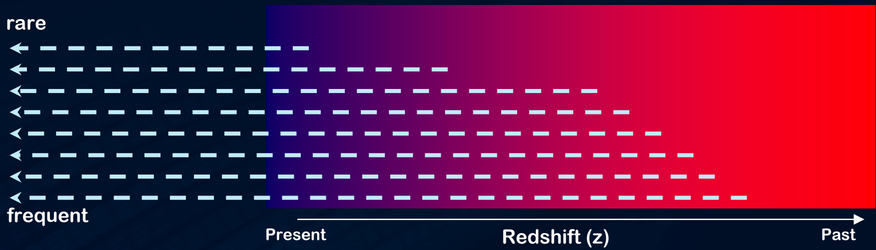


The cosmological evolution

Many indications that the past was more active.

Star formation rate→

Hopkins and Beacom, Astrophys. J. **651** 142 (2006)

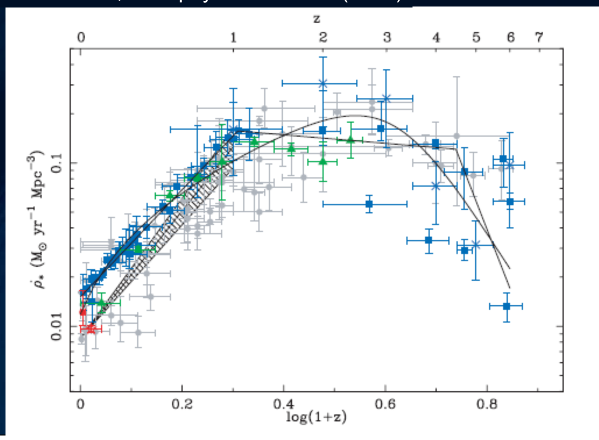


The spectral emission rate

$\rho(z) \sim (1+z)^m$

m= 0 : No evolution

# Ultra-high energy ν intensity depends on the emission rate in far-universe

Yoshida and Ishihara, PRD 85, 063002 (2012)

intensity above 1 EeV(=10^18 eV)

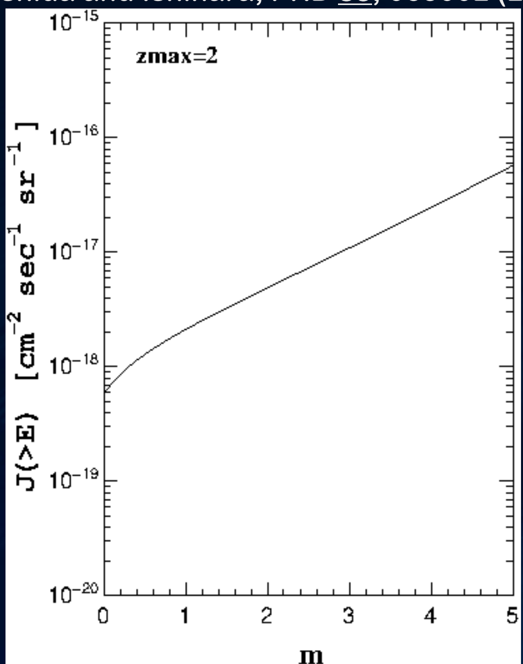


more than an order of magnitude difference

$\rho(z) \sim (1+z)^m$

“quiet” “dynamic”

particle emissions in far-universe

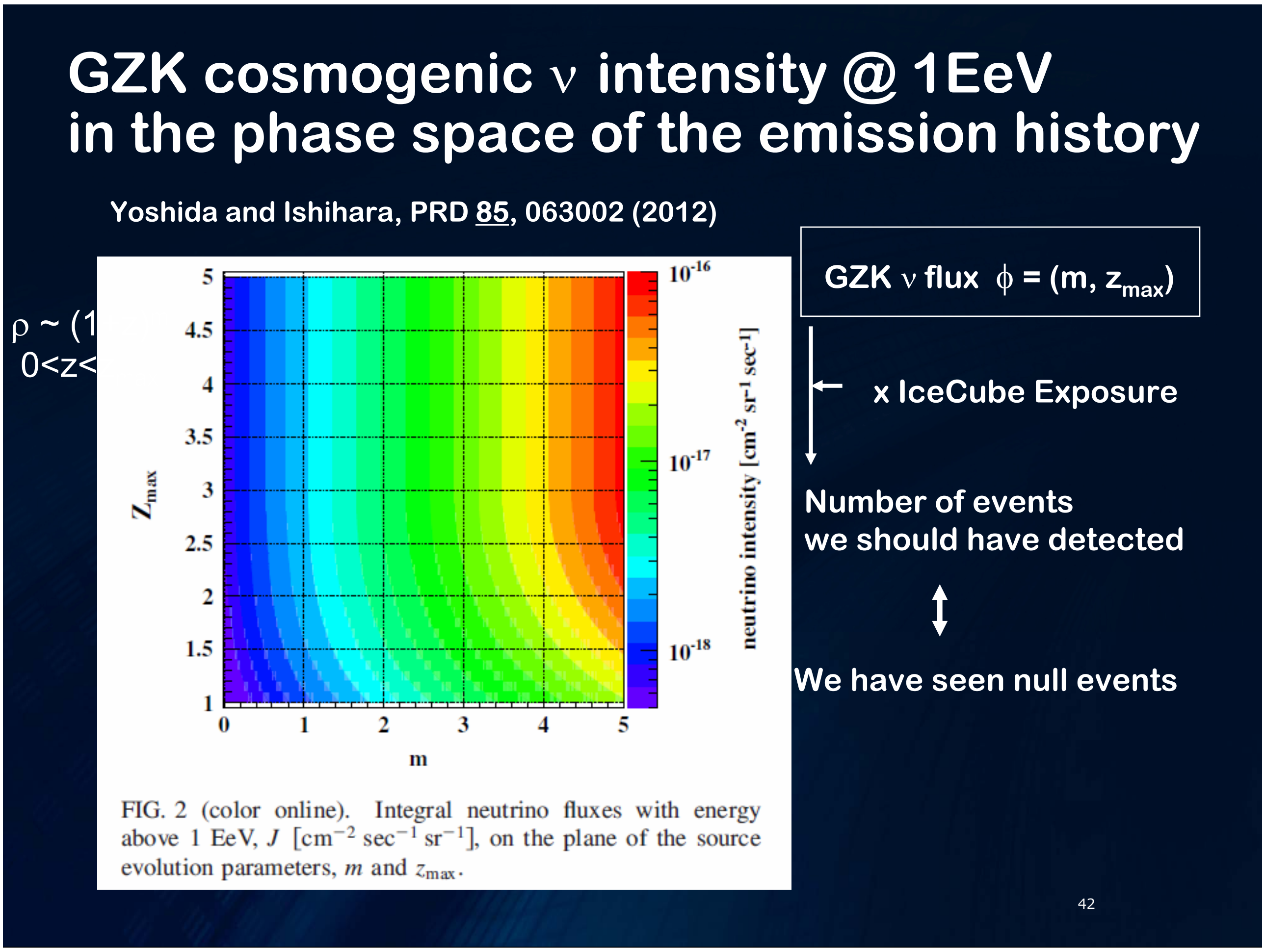
GZK cosmogenic ν intensity @ 1EeV
in the phase space of the emission history
Yoshida and Ishihara, PRD 85, 063002 (2012)
ρ ~ (1
0<z<
$Z_{max}$
m
neutrino intensity [$cm^{-2}$ $sr^{-1}$ $sec^{-1}$]
$10^{-16}$
$10^{-17}$
$10^{-18}$
FIG. 2 (color online). Integral neutrino fluxes with energy above 1 EeV, $J$ [$cm^{-2}$ $sec^{-1}$ $sr^{-1}$], on the plane of the source evolution parameters, $m$ and $z_{max}$.
GZK ν flux $\phi$ = (m, $z_{max}$)
x IceCube Exposure
Number of events
we should have detected
We have seen null events
42

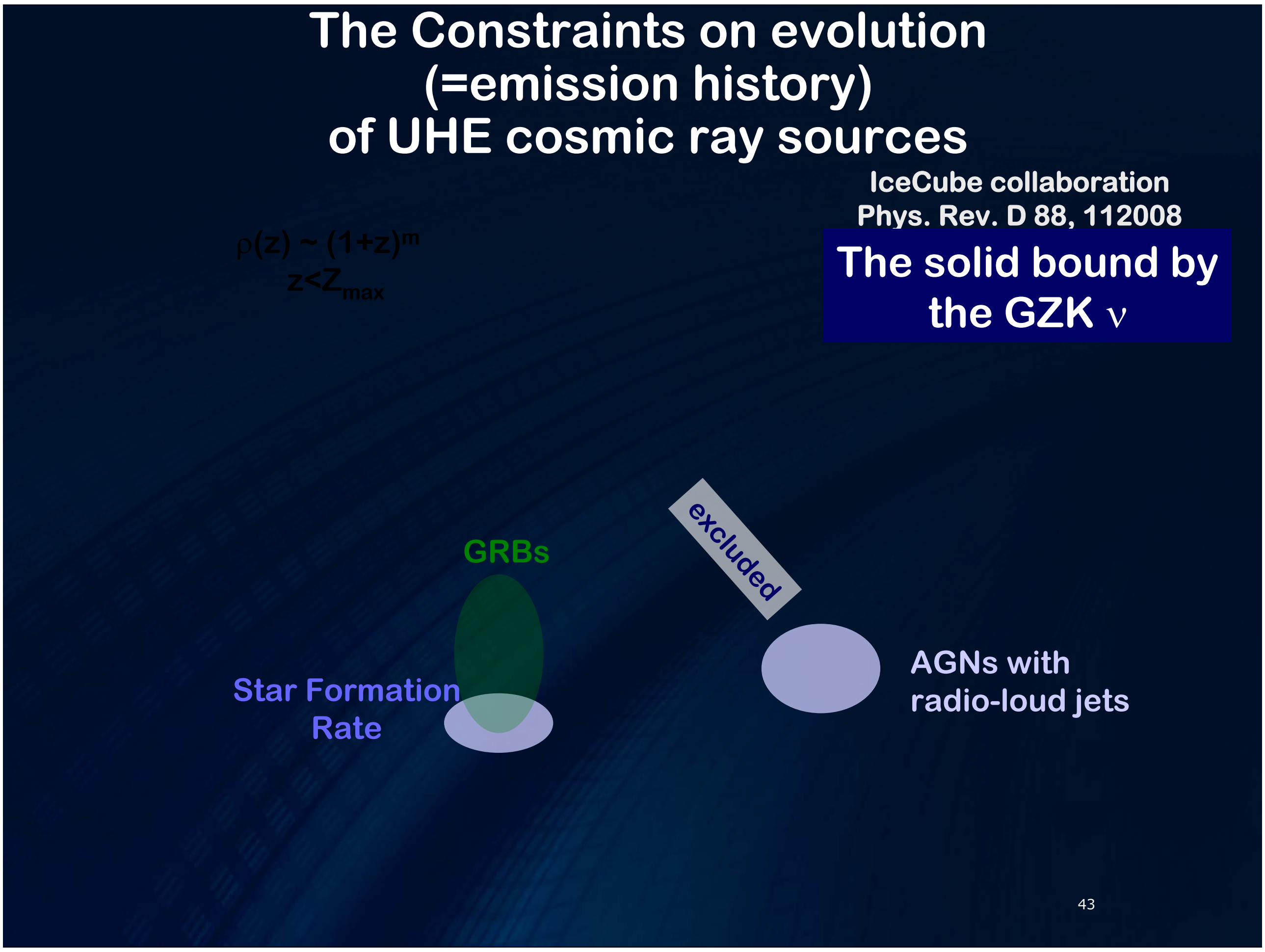
The Constraints on evolution
(=emission history)
of UHE cosmic ray sources
IceCube collaboration
Phys. Rev. D 88, 112008
The solid bound by
the GZK ν
ρ(z) ~ $(1+z)^m$
$z<Z_{max}$
excluded
GRBs
Star Formation
Rate
AGNs with
radio-loud jets
43

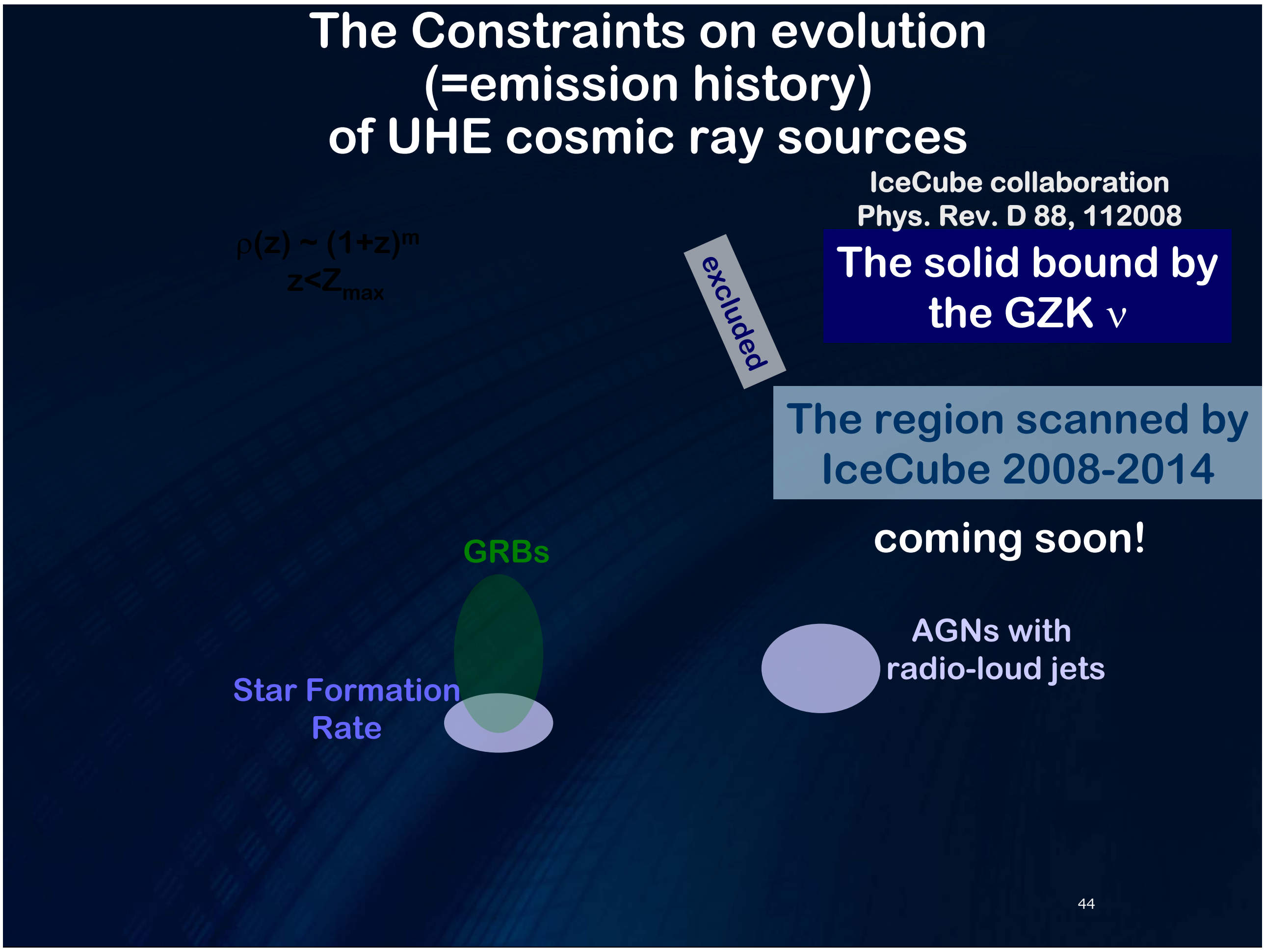
The Constraints on evolution
(=emission history)
of UHE cosmic ray sources
IceCube collaboration
Phys. Rev. D 88, 112008
$\rho(z) \sim (1+z)^m$
$z<Z_{max}$
excluded
The solid bound by the GZK $\nu$
The region scanned by IceCube 2008-2014
coming soon!
GRBs
AGNs with radio-loud jets
Star Formation Rate
44

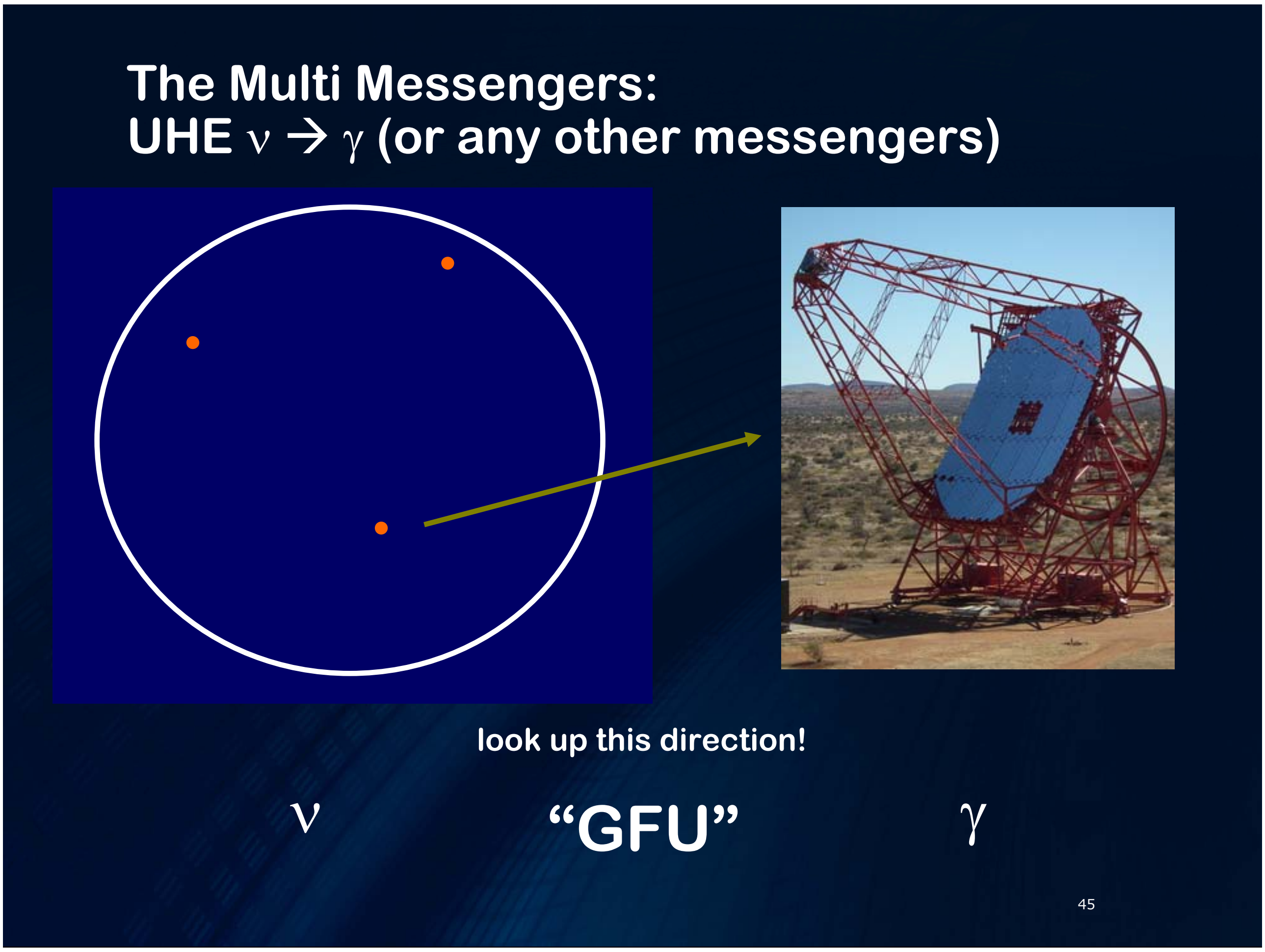
The Multi Messengers:
UHE $\nu$ → $\gamma$ (or any other messengers)
look up this direction!
$\nu$
“GFU”
$\gamma$
45

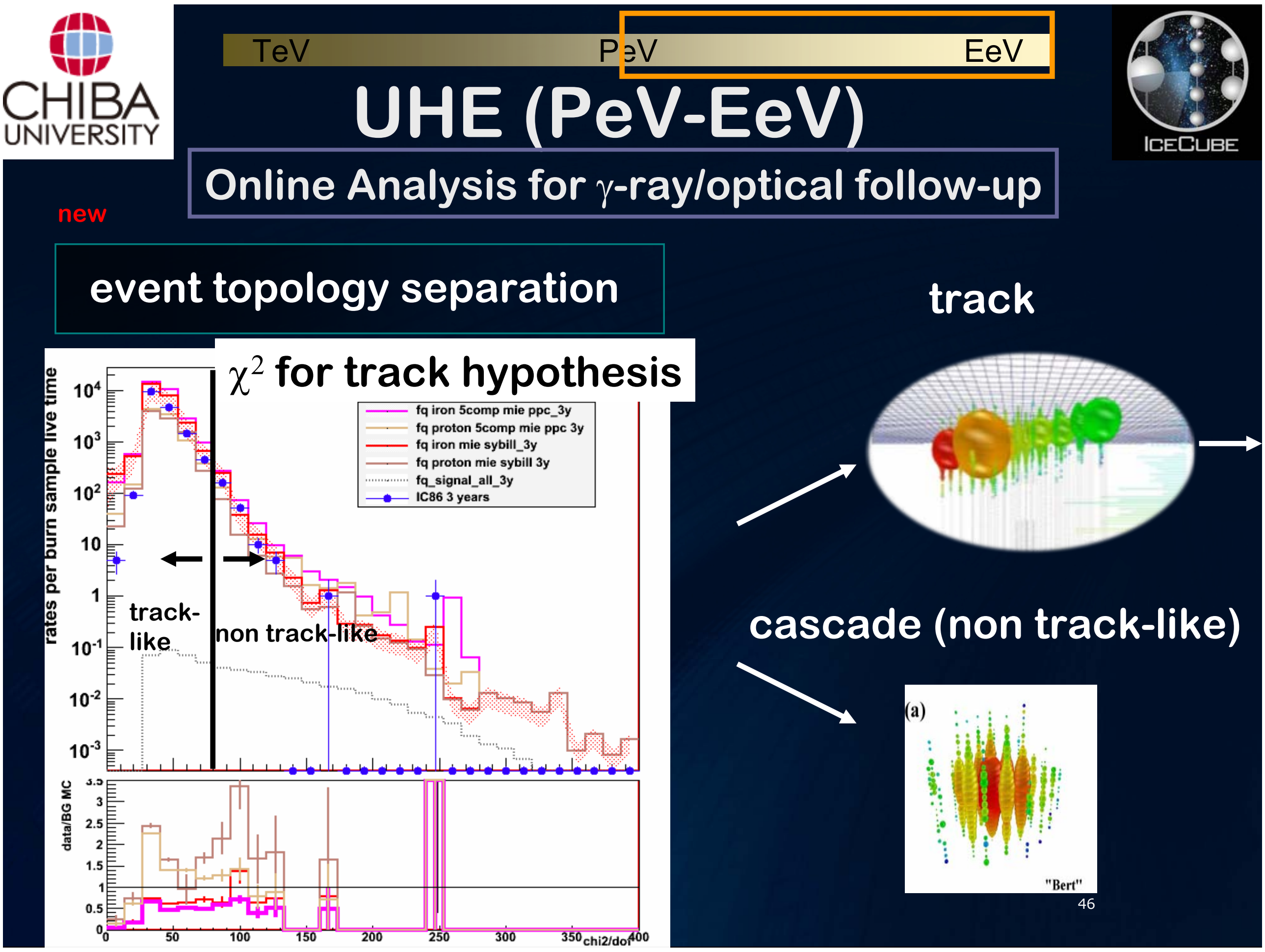
TeV
PeV
EeV
UHE (PeV-EeV)
Online Analysis for γ-ray/optical follow-up
new
event topology separation
χ² for track hypothesis
fq iron 5comp mie ppc_3y
fq proton 5comp mie ppc 3y
fq iron mie sybill_3y
fq proton mie sybill 3y
fq_signal_all_3y
IC86 3 years
rates per burn sample live time
track-like
non track-like
data/BG MC
chi2/dof
track
cascade (non track-like)
(a)
"Bert"
46

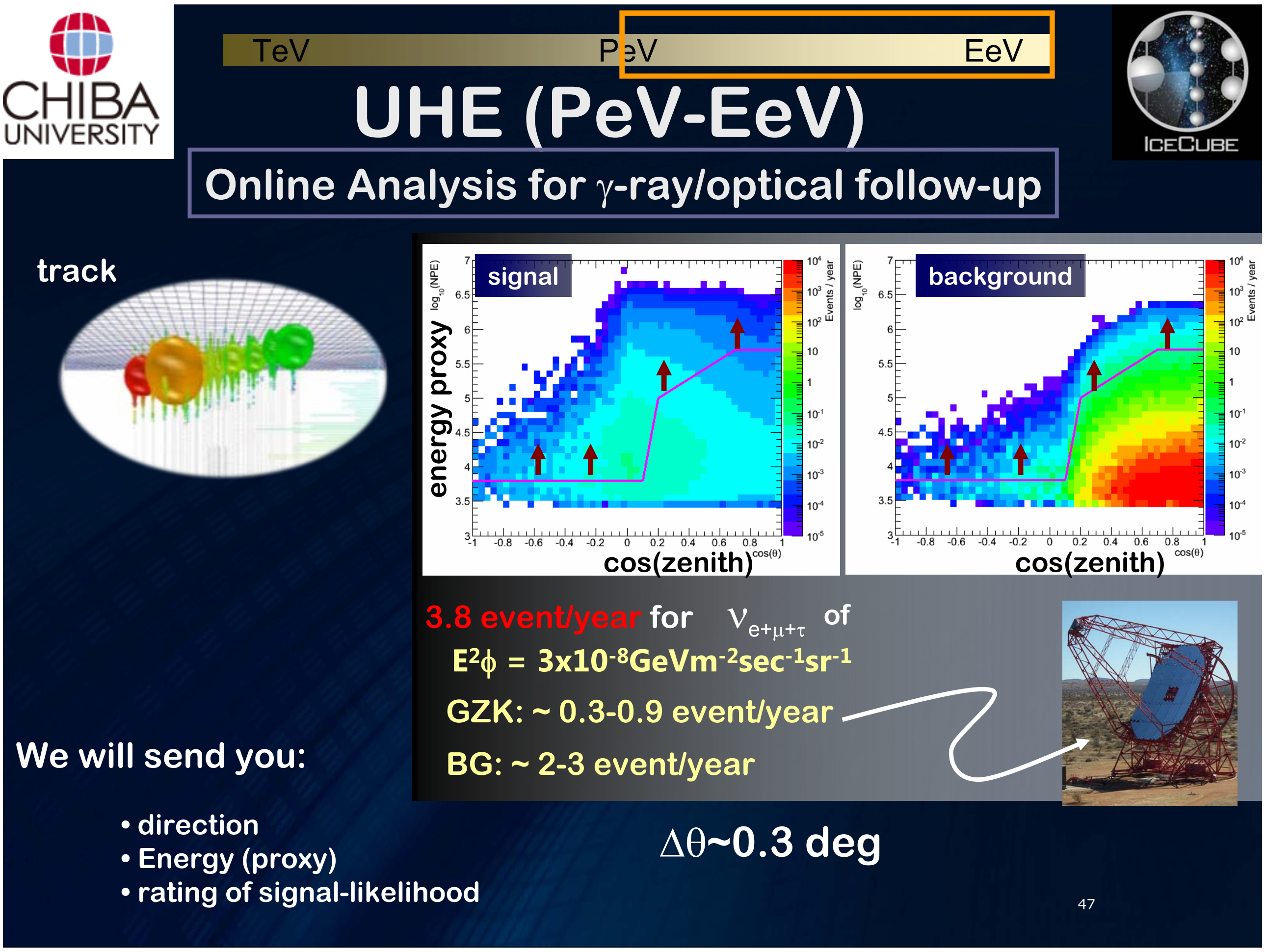
TeV
PeV
EeV
UHE (PeV-EeV)
Online Analysis for γ-ray/optical follow-up
track
signal
background
energy proxy
cos(zenith)
cos(zenith)
Events / year
3.8 event/year for ν e+μ+τ of
E²φ = 3x10⁻⁸GeVm⁻²sec⁻¹sr⁻¹
GZK: ~ 0.3-0.9 event/year
BG: ~ 2-3 event/year
We will send you:
• direction
• Energy (proxy)
• rating of signal-likelihood
Δθ~0.3 deg
47

# Next Generation: IceCube HEX

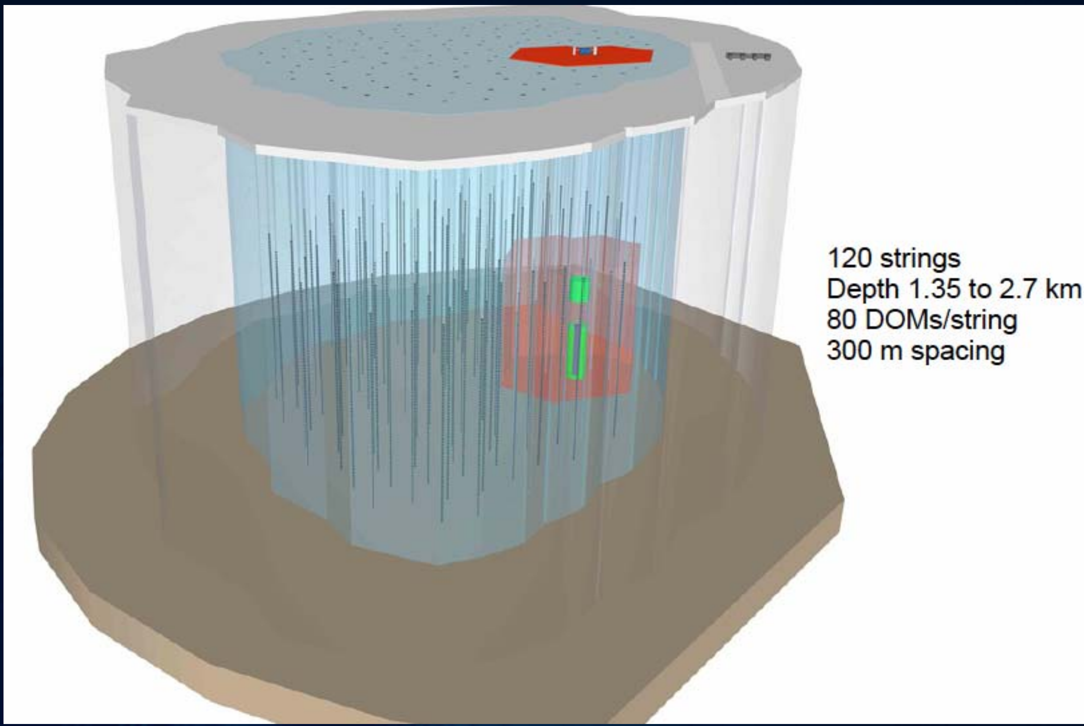




# A veto airshower array

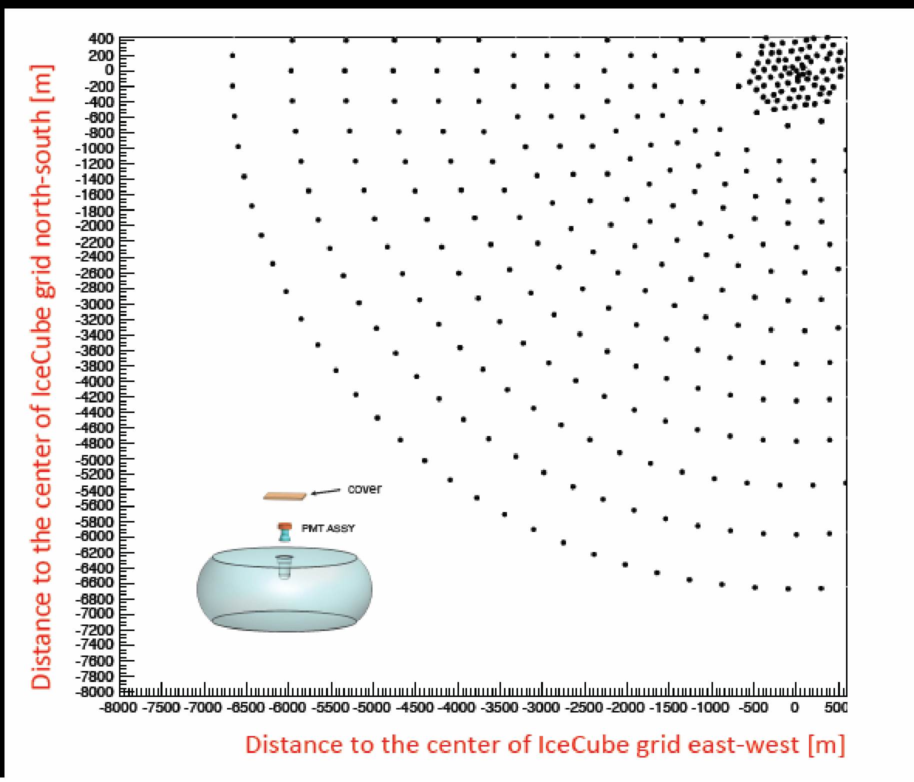

# Next Generation: IceCube HEX

## Photo-detector development

JOHANNES GUTENBERG UNIVERSITÄT MAINZ — Wavelength shifter coated tube

ERLANGEN CENTRE FOR ASTROPARTICLE PHYSICS — A la KM3Net

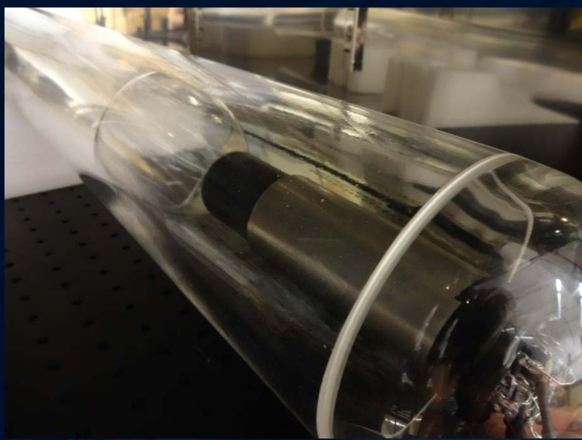

# Next Generation: IceCube HEX

## Photo-detector development

CHIBA UNIVERSITY

Two 8' Hamamatsu R5912 High-QE PMTs
- up/down symmetry: good for veto, reco etc
- two PMTs insead of one: Better saturation response

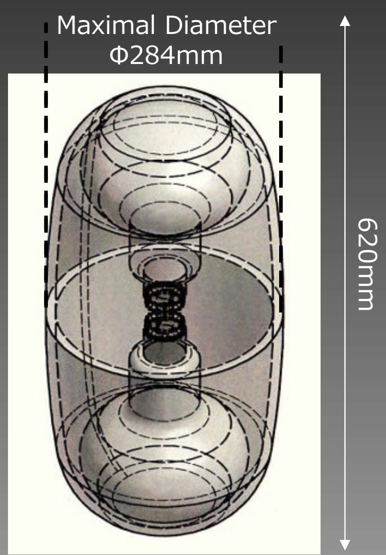


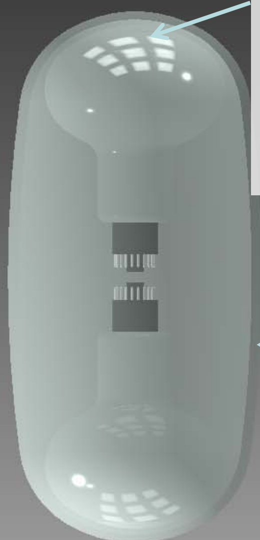

customized glass shape/curvature
- designed best match curvature to our PMT
- less thickness top/bottom part (9mm-10mm where PMT cceptance) for better light transmittance

Slightly enhanced diameter and glass thickness in the middle for a mechanical strength

# Next Generation: IceCube HEX

## Photo-detector development

8' high-QE PMT

Glass + PMT assembly

Lovely ball

Silicon gel

52

# Next Generation: ARA

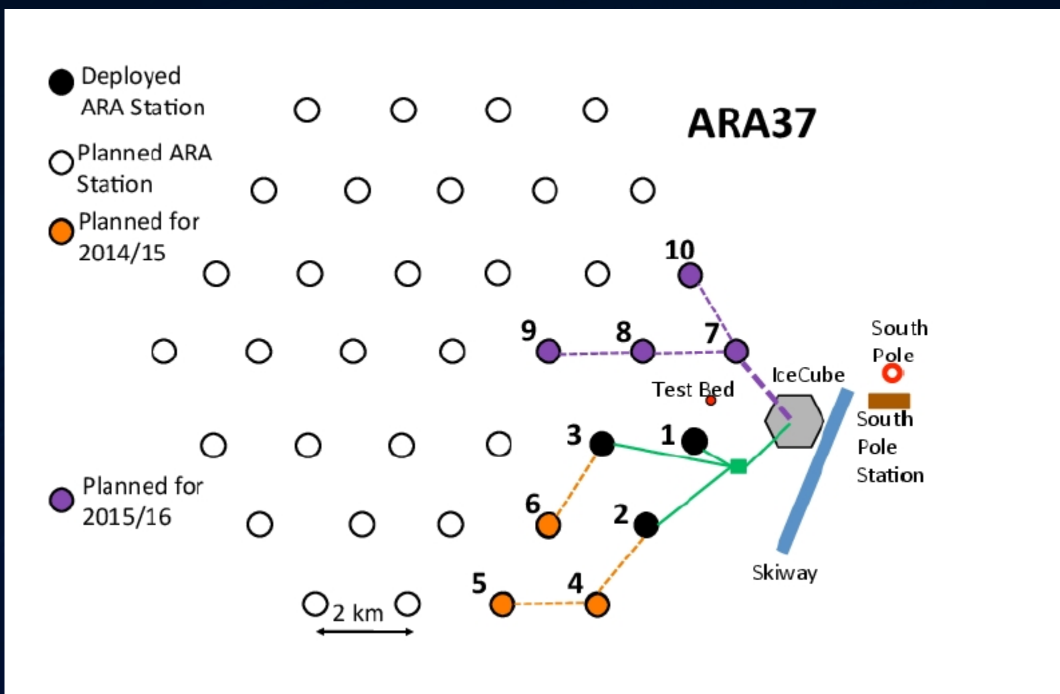


55

# Next Generation: ARA

## Antenna Assembly and calibration

chamber

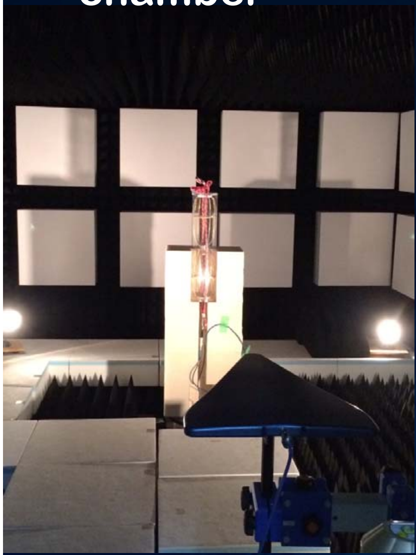

transmission coefficient

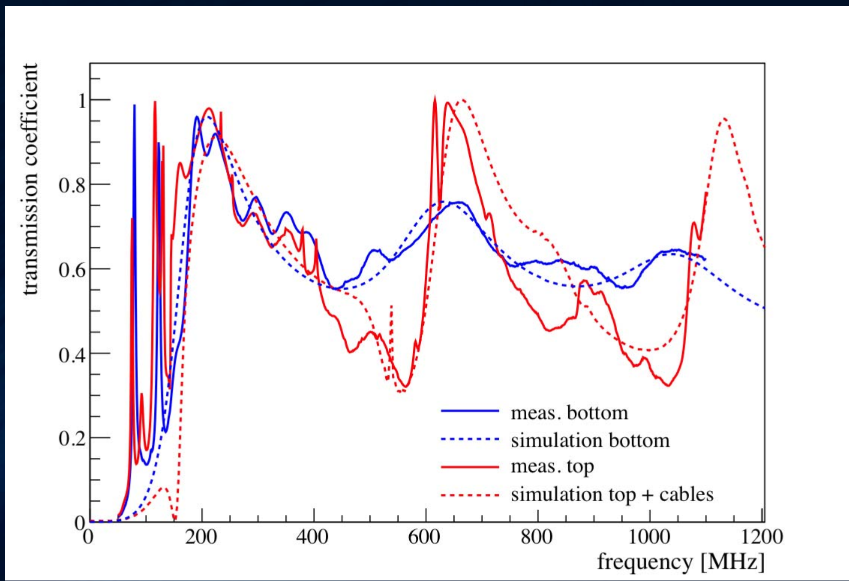




# Next Generation: ARA

## “end-to-end” calibration

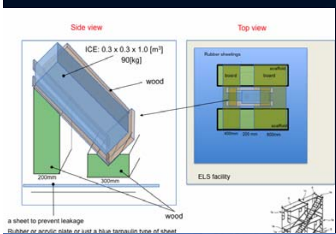


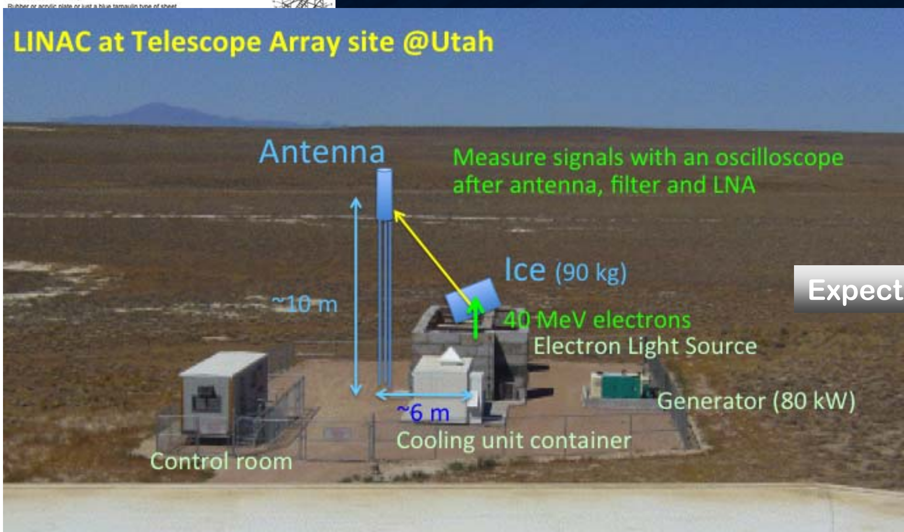


Expected signals from ice

CHIBA UNIVERSITY

# Executive Summary

## $\nu$ = THE smoking gun

# "The simulation of magnetized binary neutron star mergers on K"

Kenta Kiuchi

[JGRG24(2014)111211]

# The simulation of magnetized binary neutron star mergers on K

Kenta Kiuchi (YITP)

Ref.) PRD 90, 041502(R) (2014)
with Koutarou Kyutoku (UWM), Yuichiro Sekiguci (YITP), Masaru Shibata (YITP), Tomohide Wada (NAOJ)

YITP
YUKAWA INSTITUTE FOR THEORETICAL PHYSICS

K computer $= 10^{16}$ $= 10$ Peta

## Motivation

1. Gravitational waves = ripples of the space-time
- ▶ Verification of GR
- ▶ The EOS of neutron star matter
- ▶ The central engine of SGRB
- ▶ ~10 events / yr for KAGRA

GW detectors


2. A possible site of the r-process synthesis
A significant amount of neutron star matter could be ejected from BNS mergers ($M_{eje} \approx 10^{-4}$-$10^{-2} M_{\odot}$, Hotokezaka et al. 13)

Nuclear synthesis in the ejecta (Lattimer & Schramm 76)
⇒ Radio active decay of the r-process elements

Electromagnetic counterpart = kilonova (Li-Paczynski 98, Kulkarni 05, Metzger+10, Kasen et al. 13, Barnes-Kasen 13, Tanaka-Hotokezaka 13, Berger et al.13, Tanvir et al. 13)

Kyoto NR group approaches from two directions;

- MHD (KK et al. 14)
- Microphysics (Sekiguchi et al. 11a, 11b, 14)

Why B-fields ?

- Observed magnetic field of the pulsars is $10^{11}$-$10^{13}$ G
- The existence of the magnetar, c.f. $10^{14}$-$10^{15}$ G

$P - \dot{P}$ Diagram

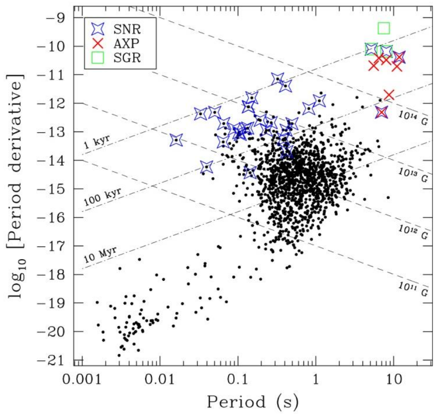


The short-wavelength mode is essential for the MHD instabilities which could activate during BNS merger.

⇒ Necessary to perform a high-resolution simulation which covers a large dynamical range of O(10)km-O(1,000)km.

# Japanese supercomputer K @ AICS

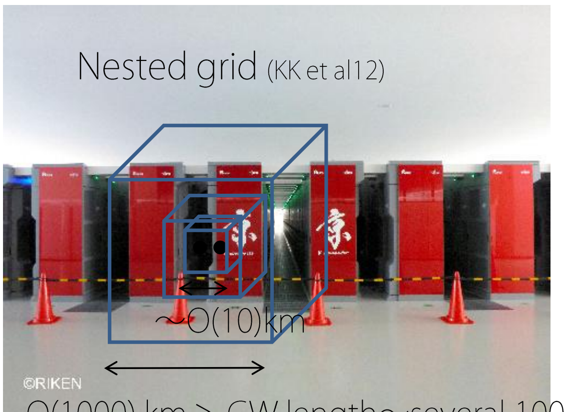


O(1000) km ≳ GW length~several 100 km

Execution performance (%) (Weak scale)

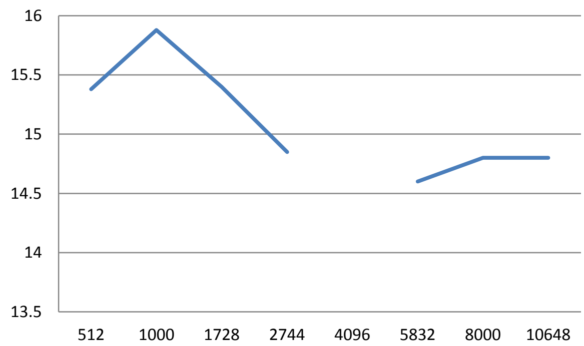


Node number (core =8×node)

- Total peak efficiency is 10.6 PFLOPS (~700K cores)
- Interpolation of B-fields on the refinement boundary is non-trivial : Flux conservation and Div B = 0 (KK et al 12, Balsara 01)
- MPI communication rule is complicated, e.g., refinement boundary
- Good scaling up to about 80k cores

## Overview of BNS mergers

(Bartos et al. 13)

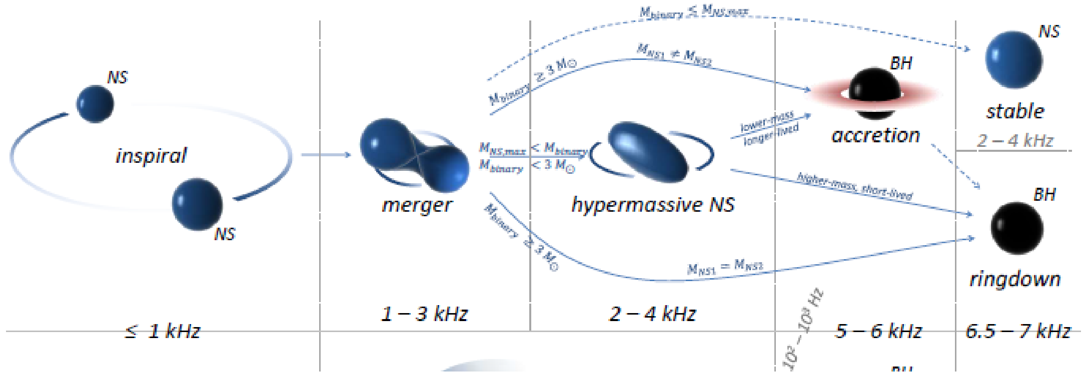


Time

▶Lower limit of the maximum mass of neutron star is about $2M_\odot$ (Antoniadis+13)

▶Observed mass of the BNSs 2.6-$2.8M_\odot$ (Lattimer & Prakash 06)
⇒ It is a "realistic" path that a BH-torus is formed via hypermassive NS (HMNS) collapse.

## Numerical Relativity simulation of magnetized BNS mergers

▶High resolution $\Delta x$=70m (16,384 cores on K)
▶Medium resolution $\Delta x$=110m (10,976 cores on K)
▶Low resolution $\Delta x$=150m (XC30, FX10 etc.)
c.f. Radii of NS∼10km, the highest resolution of the previous work is $\Delta x \approx$180m (Liu et al. 08, Giacomazzo et al. 11, Anderson et al. 08)

Nested grid ⇒ Finest box=$70\text{km}^3$, Coarsest grid =$4480\text{km}^3$ ($N\sim 10^9$) , a long term simulation of about 100 ms

Magnetic field lines of NS

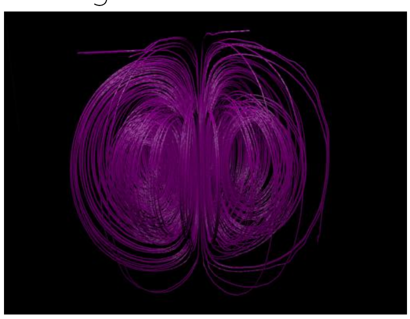

<u>Fiducial model</u>
EOS : H4 (Gledenning and Moszkoski 91) ($M_{max}\approx 2.03M_\odot$)
Mass : 1.4-1.4 $M_\odot$
B-field : $10^{15}$G

Evolution of the magnetic field energy

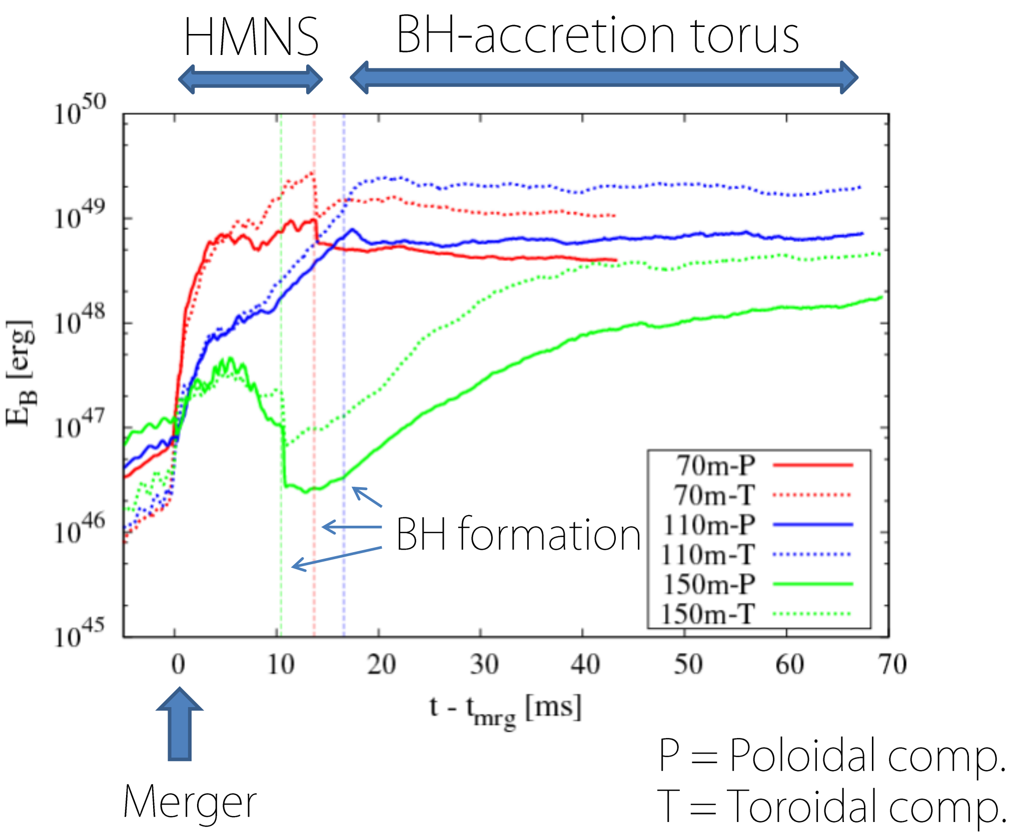

# Kelvin-Helmholtz instability (Rasio-Shapiro 99)

GRMHD by AEI (Giacomazzo et al. 11)

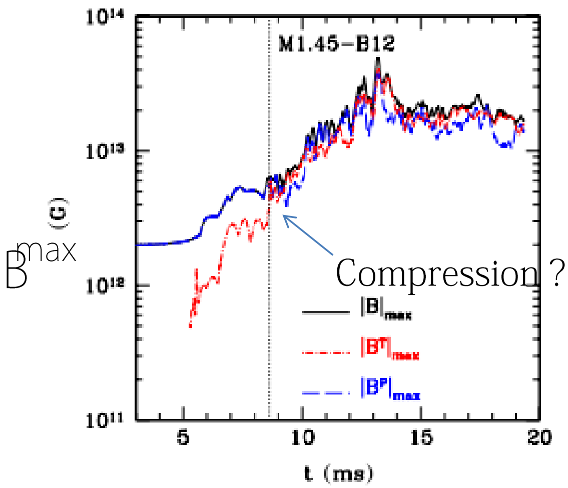


Can really the KH vortices amplify the B-fields ?

Yes !

Field lines and strength @ merger

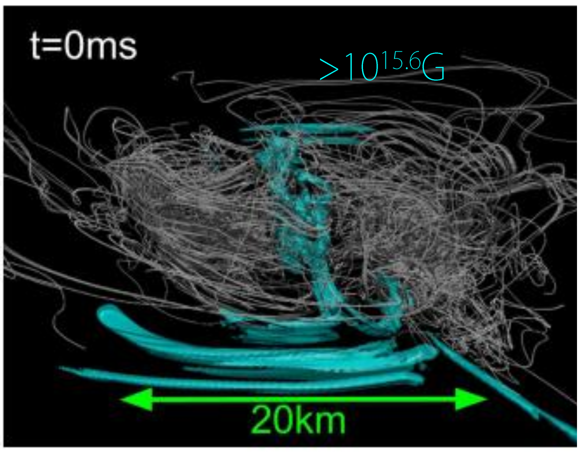


Amplification factor vs resolution

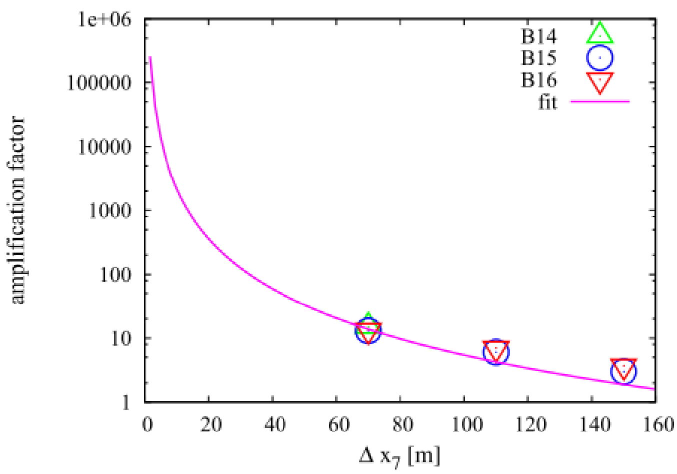


- The smaller $\Delta x$ is, the higher growth rate is.
- The amplification factor does not depend on the initial magnetic field strength
- It is consistent with the amplification mechanism due to the KH instability. (Obergaulinger et al. 10, Zrake and MacFadyen 13)

Field lines and density iso-contour inside HMNS

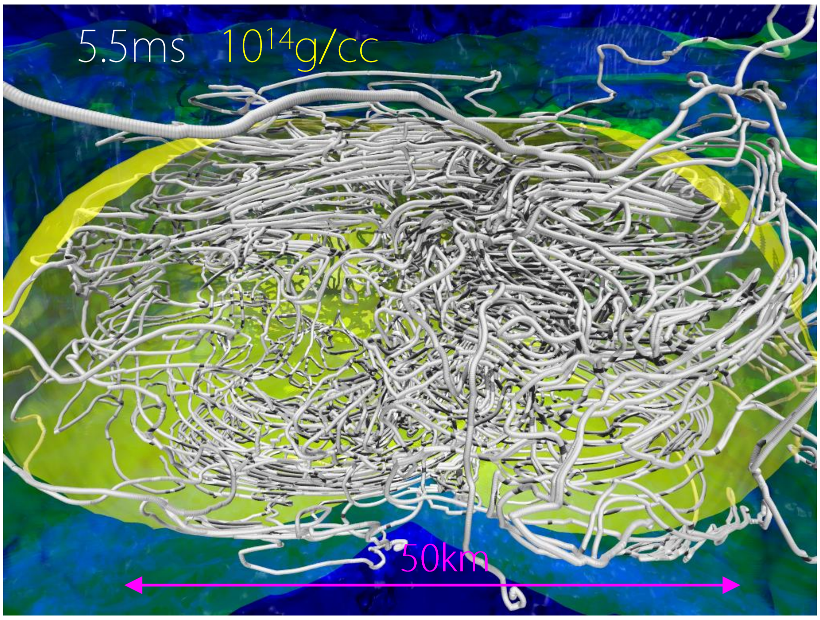


- Turbulent state inside HMNS
- HMNS is differentially rotating ⇒ Unstable against the Magneto Rotational Instability (Balbus-Hawley 92)
- Magnetic winding works as well

## B-field amplification inside HMNS

Density contour of HMNS (Meridional plane)

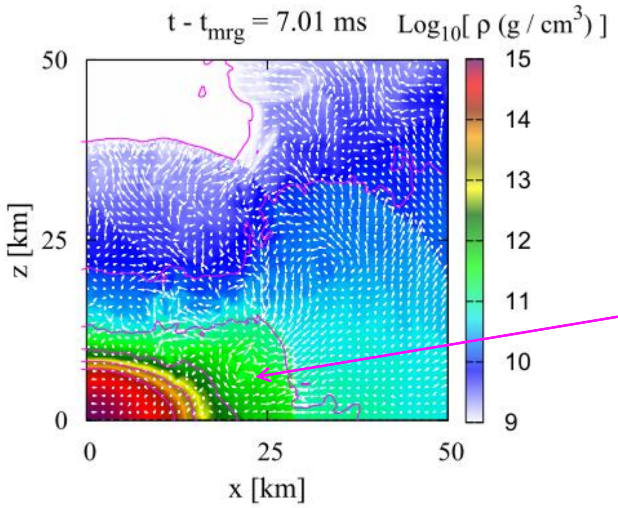


Magnetic field energy inside $10^{11}$g/cc ≤ $\rho$ ≤ $10^{12}$g/cc

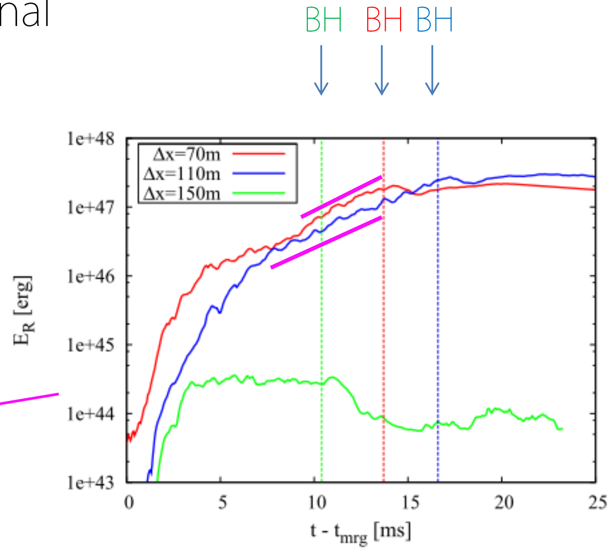


- $\lambda_{MRI} = B/(4\pi\rho)^{1/2}\, 2\pi/\Omega$
- The condition $\lambda_{MRI,\varphi}/\Delta x \gtrsim 10$ is satisfied for the high and medium run, but not in low run. B = Toroidal magnetic field
- Growth rate of B-fields for 8 - 14 ms ≈130-140Hz～O(0.01)Ω

# B-field amplification inside HMNS

B-fields energy in$10^a$g/cc ≤ $\rho$ ≤ $10^{a+1}$g/cc   a=10-14 for high-res. run

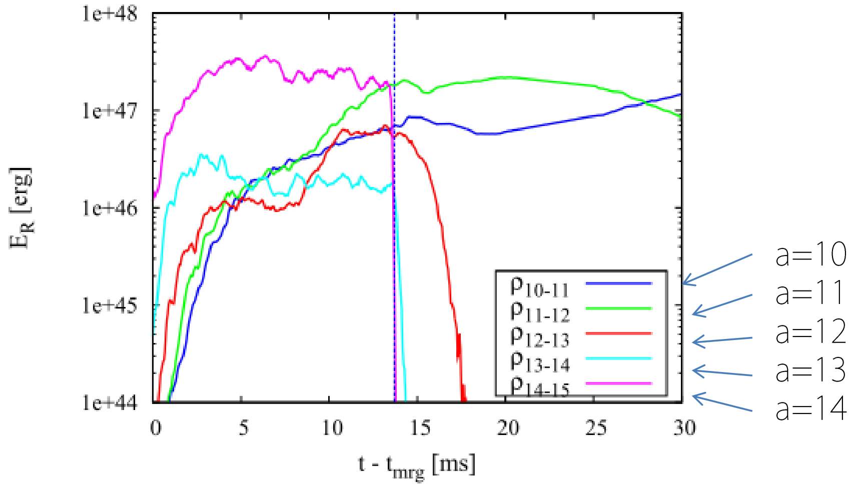


▶The high the density is, the high the growth rate is because of higher angular velocity

▶B-field amplification in relatively low density regions is cause by the non-axisymmetric MRI (Balbus – Hawley 92)

▶Magnetic winding works as well for the toroidal fields

$B_\varphi \sim B_R\,\Omega\,t \sim 10^{16}\mathrm{G}(B_R/10^{15}\mathrm{G})(\Omega/10^3\mathrm{rad/s})(t/10\mathrm{ms})$

## Black hole—accretion torus

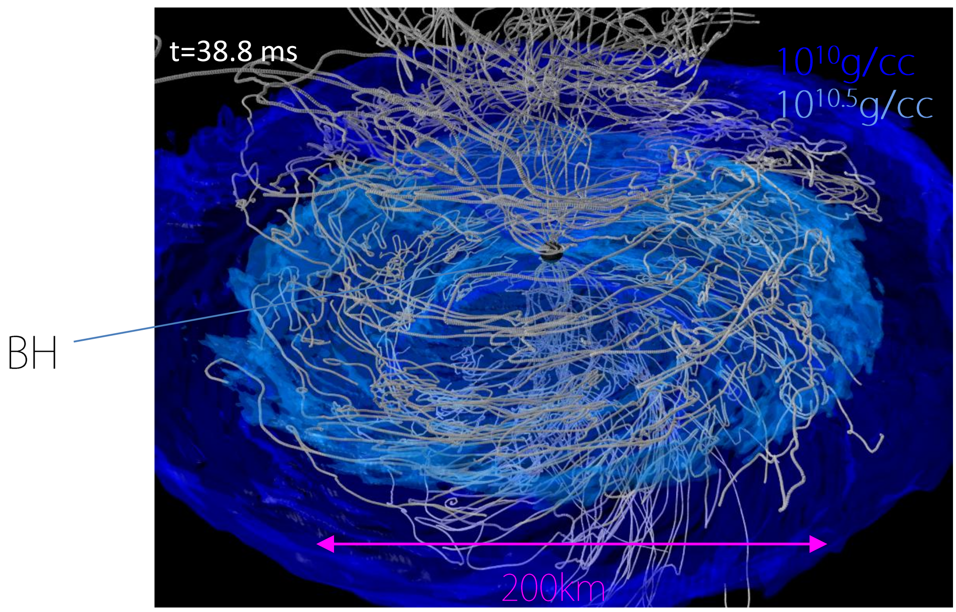


▶ We have not found a jet launch.

▶ Ram pressure due to the fall back motion~$10^{28}$ dyn/cm$^2$(Need $10^{14\text{-}15}$G in the vicinity of the torus surface)

▶Necessity of the poloidal motion to build a global poloidal field

# Summary of the magnetic field amplification during the BNS merger

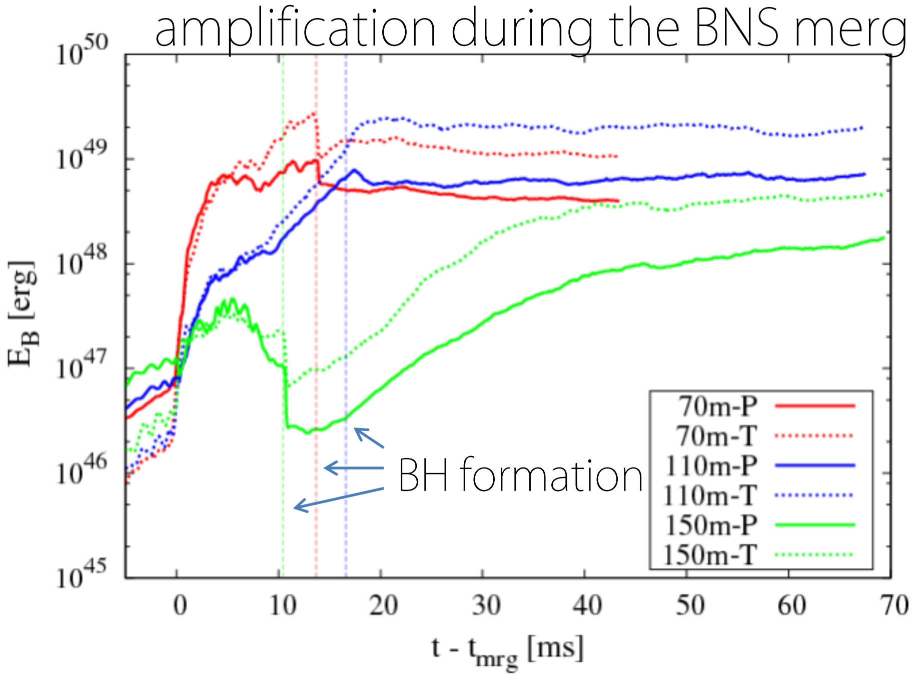


▶KH instability at the merger and MRI inside the HMNS ⇒ Significant amplification of B-fields

▶Low res. run cannot follow this picture ⇒ Amplification inside the BH-torus (picture drawn by the previous works)

## Summary

We have performed a highest resolution simulation of magnetized binary neutron star merger simulation in the framework of Numerical Relativity.

▶ Kelvin-Helmholtz instability at the merger
▶ Non-axisymmetric MRI inside the hyper massive neutron star

are key ingredients.

The accretion torus is strongly magnetized at its birth.
⇒ Qualitatively different picture of the previous works

If the NS magnetic field is weak, e.g., $10^{11}$ G, this picture is still valid, but more challenging numerically.

Necessity to launch an outflow to build a global poloidal magnetic field.

# B-fields amplification via Kelvin-Helmholtz

Magnetic field energy

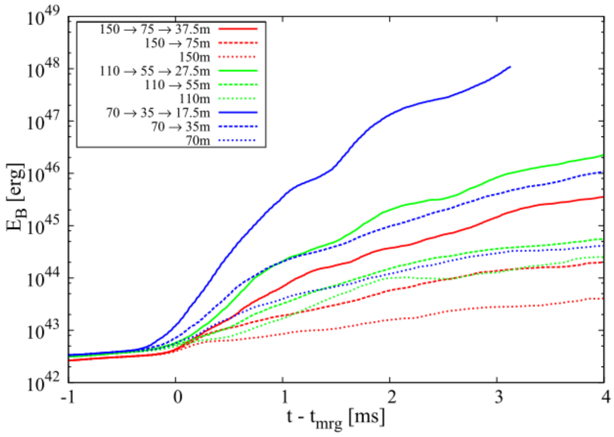


Maximum magnetic field strength

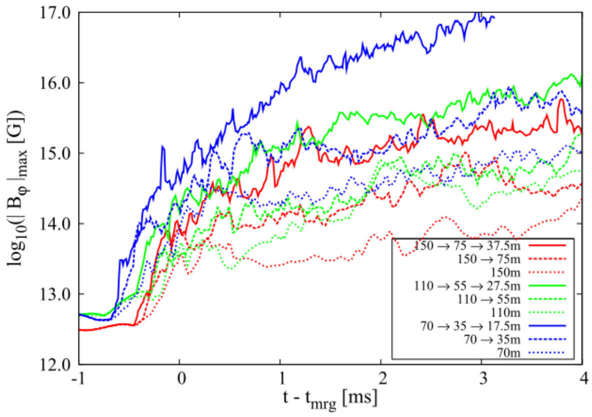


▶ The amplification is almost determined by the grid resolution.
▶ The maximum field strength almost reaches at the virial value, i.e., $\sim 10^{17}$G.
▶ The amplification of the magnetic-field energy is about $10^6$ times at lease in the highest res. run ; the root mean square value of the magnetic field strength is about $10^3$ times.

“Constraining the equation of state of neutron stars from binary mergers”

Kentaro Takami

[JGRG24(2014)111212]

# Constraining the Equation of State of Neutron Stars from Binary Mergers

GOETHE UNIVERSITÄT FRANKFURT AM MAIN

Kentaro Takami

Institute for Theoretical Physics, Goethe University Frankfurt

Collaborators : Luciano Rezzolla and Luca Baiotti

The 24th Workshop on General Relativity and Gravitation,
10-14 November 2014.



# Introduction

## What is a Binary Neutron Star?

$\rightarrow$ Flaminio's and Kiuchi's talk had nice introductions.

- observationally existence (as opposed to binary black holes)
- one of the strongest sources of gravitational waves
- central engine of short gamma ray bursts
  - the released energies $\sim 10^{48-50}$ erg, which is equivalent to what released by the whole galaxy over $\sim$ 1 year
- the GWs will be observed by advanced detectors (advanced LIGO, advanced VIRGO and KAGRA) within the next 5 years
  - realistic rate $\sim$ 40 BNSs inspirals a year, *i.e.* , $\sim$ 1 event a week (Abadie+2010)



## What is a Binary Neutron Star?

- For BBHs, we know what to expect:

  $$\mathrm{BH} + \mathrm{BH} \Longrightarrow \mathrm{BH} + \mathrm{GW}$$

- For BNSs, the question is more subtle: the merger leads to a hyper-massive neutron star (HMNS), *i.e.* , a metastable equilibrium:

  $$\mathrm{NS} + \mathrm{NS} \Longrightarrow \mathrm{HMNS} + ? \Longrightarrow \mathrm{BH} + \mathrm{torus} + ? \Longrightarrow \mathrm{BH}$$

  All complications are in the intermediate stages; the rewards:
  - studying the HMNS will show strong and precise imprint on the EOS
  - studying the BH+torus will tell us on the central engine of GRBs

## What is a Binary Neutron Star?

- For BBHs, we know what to expect:

  BH + BH $\Longrightarrow$ BH + GW

- For BNSs, the question is more subtle: the merger leads to a hyper-massive neutron star (HMNS), *i.e.* , a metastable equilibrium:

  NS + NS $\Longrightarrow$ HMNS + ? $\Longrightarrow$ BH + torus + ? $\Longrightarrow$ BH

  All complications are in the intermediate stages; the rewards:

  - studying the HMNS will show strong and precise imprint on the EOS
  - studying the BH+torus will tell us on the central engine of GRBs

Introduction Methodology Results Conclusions

## GW from a HMNS

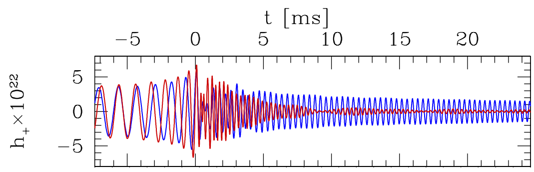


The GW potentially give us many information, such as the mass, EOS and so on.

## GW from a HMNS

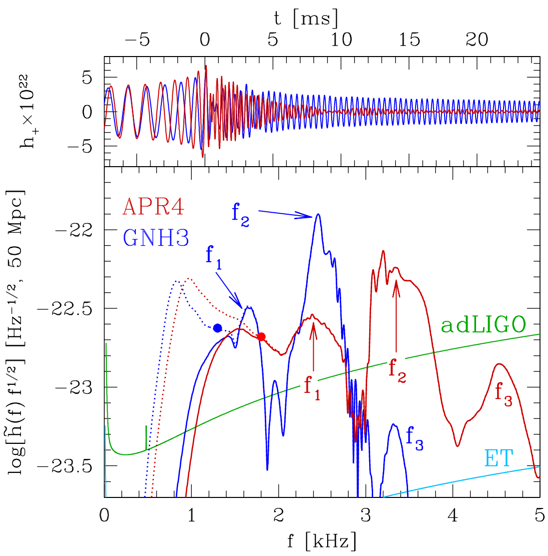


Three clear peaks, $f_1$, $f_2$ and $f_3$.

- $f_1 \cdots$ nonlinear interaction between quadrupole and quasiradial modes
- $f_2 \cdots$ fundamental quadrupolar fluid mode (Stergioulas+2011)
  $f_2 \cdots$ simple function of the average mass density, independent of the EOS considered (Bauswein+2012)
- $f_3 \cdots$ larger uncertainty in the physical interpretation
- using $f_1$ and $f_2$, we have constructed method to decide the redshift(Messenger+PRX2014).
- using $f_1$ and $f_2$, we have developed powerful tool to constrain EOS(Takami+PRL2014).

Introduction Methodology Results Conclusions

GW from a HMNS

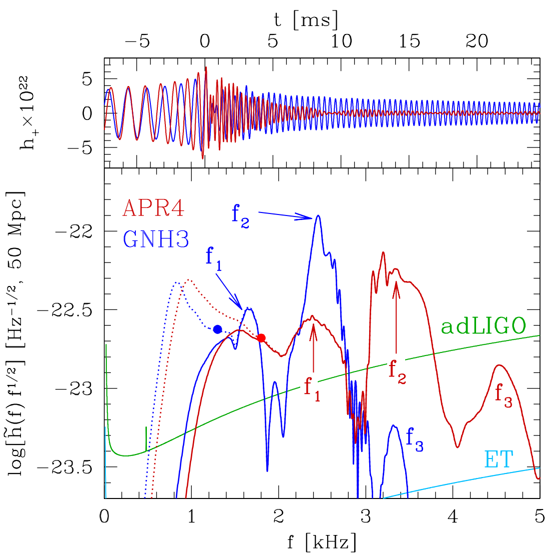

Three clear peaks, $f_1$, $f_2$ and $f_3$.

- $f_1 \cdots$ nonlinear interaction between quadrupole and quasiradial modes
- $f_2 \cdots$ fundamental quadrupolar fluid mode (Stergioulas+2011)
  $f_2 \cdots$ simple function of the average mass density, independent of the EOS considered (Bauswein+2012)
- $f_3 \cdots$ larger uncertainty in the physical interpretation
- using $f_1$ and $f_2$, we have constructed method to decide the redshift(Messenger+PRX2014).
- using $f_1$ and $f_2$, we have developed powerful tool to constrain EOS(Takami+PRL2014).

# Methodology



## Numerical Method

All of our calculations have been performed in full general relativity.

**< spacetime evolution >**


McLachlan code which is a part of publicly available Einstein Toolkit (Löffler+2012).

- BSSNOK formalism (Nakamura+1987, Shibata+1995, Baumgarte+1998)
- 4th-order finite differencing method

**< fluid evolution >**


Whisky code which is our privately developed code (Baiotti+ 2005).

- finite-volume method
- HLLE approximate Riemann solver
- PPM reconstruction
- 4th-order Runge-Kutta scheme

## Equation of State

### “hybrid” equation of state (EOS)

based on a piecewise polytropic (PP) EOS augmented by an ideal gas:

$$p = p_{\rm c} + p_{\rm th}\,, \qquad \varepsilon = \varepsilon_{\rm c} + \varepsilon_{\rm th}\,,$$

where

$$
\begin{aligned}
p_{\rm th} &= (\Gamma_{\rm th} - 1)\,\rho\,\varepsilon_{\rm th} && : \text{ideal gas}\,,\\
p_{\rm c} &= K_i\,\rho^{\Gamma_i} && : \text{piecewise polytropic EOS}\,,\\
K_{\ell+1} &= K_\ell\,\rho_\ell^{(\Gamma_\ell - \Gamma_{\ell+1})} && : \text{continuity of pressure}\,,\\
\varepsilon_{\rm c} &= \varepsilon_i + \frac{K_i}{\Gamma_i - 1}\,\rho^{(\Gamma_i - 1)} && : \text{first law of thermodynamics}\,.
\end{aligned}
$$



## Equation of State

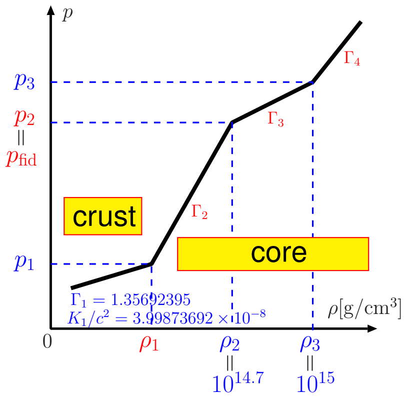


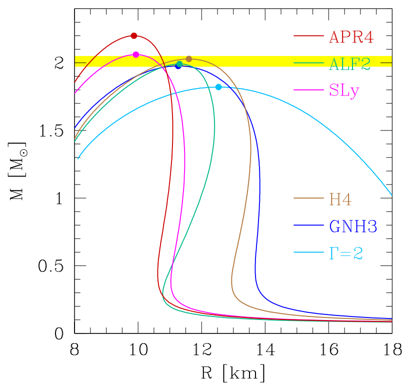


- we use PP EOSs with 4-piece regions which are good approximation of realistic EOS (Read+2009)
- Observed maximum mass is $2.01 \pm 0.04 M_\odot$ for PSR J0348+0432 (Antoniadis+2013).

# Results



## Dynamics

rest-mass density

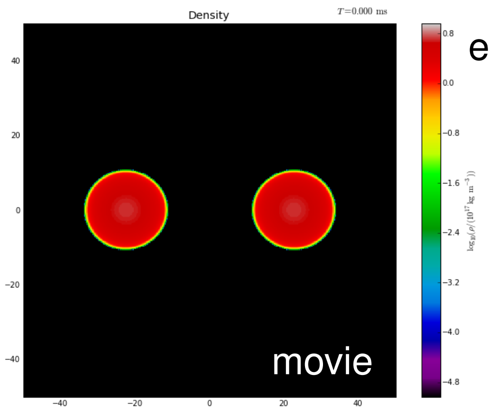


e.g.,

- H4 EOS (relativistic mean-field theory including effects of hyperons)
- $M_{\rm tot} = 2.600 M_{\odot}$
- $R \approx 9.173 M_{\odot} \approx 13.54[km]$
- tidal deformability $\lambda / M^5 \approx 1391$

## Dynamics and Waveforms

H4 EOS, $1.3M_{\odot}$.

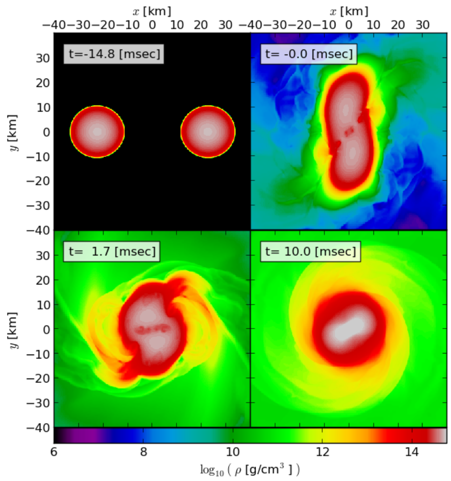


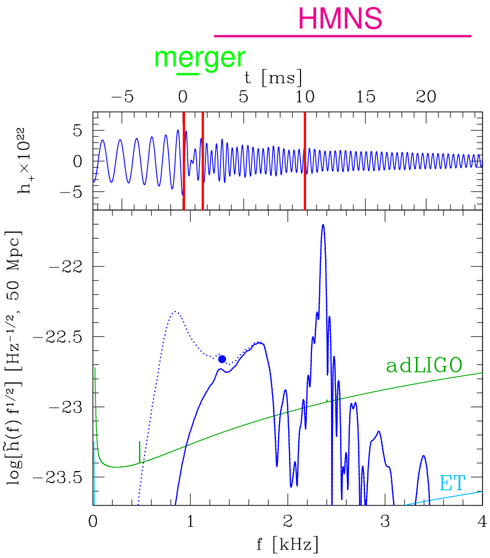


Introduction Methodology **Results** Conclusions

## Dynamics and Waveforms

H4 EOS, $1.3M_{\odot}$.

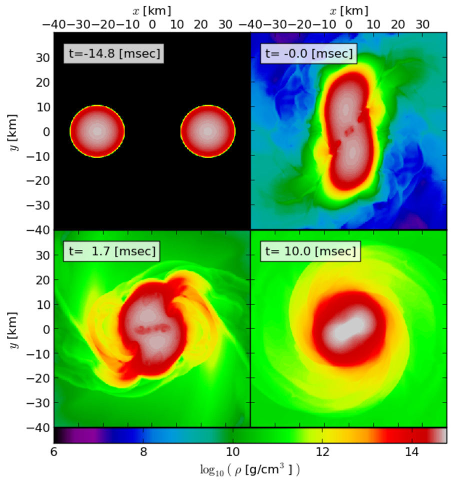


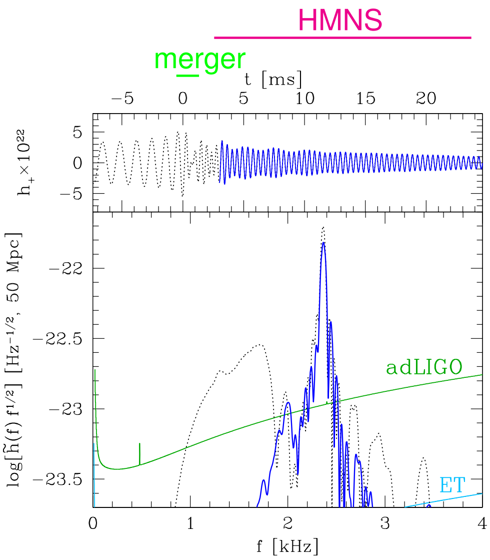

## Dynamics and Waveforms

H4 EOS, $1.3M_\odot$.

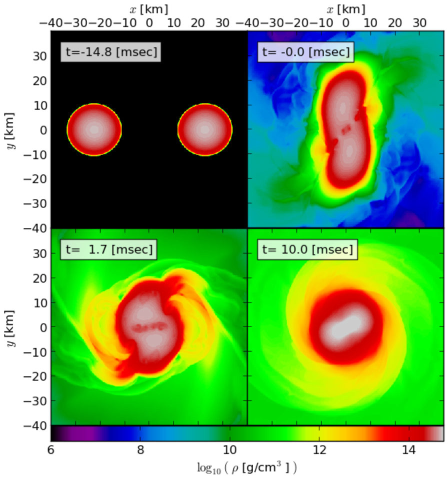


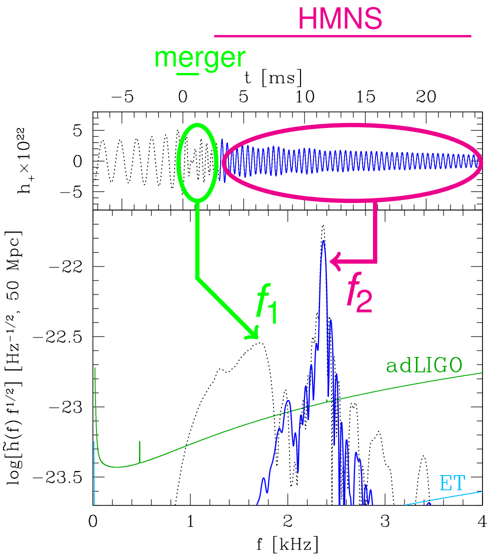




## Correlations of $f_1$ and $f_2$

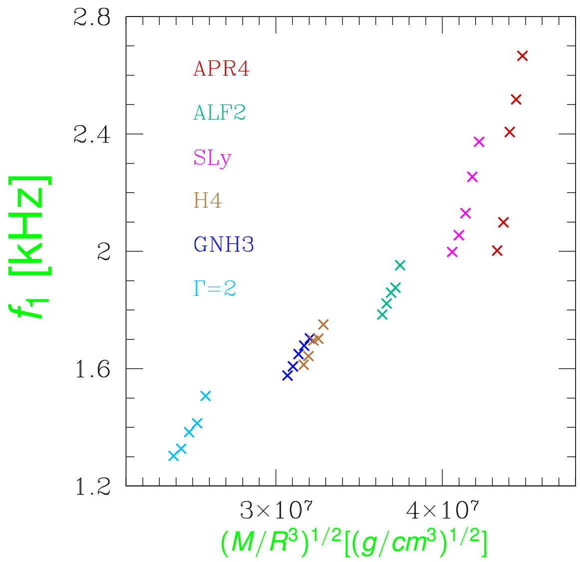


- 6 EOSs, and 5 different mass models for each EOS
  $\rightarrow$ 30 models
- $f_1$ and $f_2$ are characterized by the properties of BNS at infinite separation
- *e.g.* ,
  $f_1$ as a function of $(M/R^3)^{1/2}$
  $\rightarrow$ no good correlation

## Correlations of $f_1$ and $f_2$

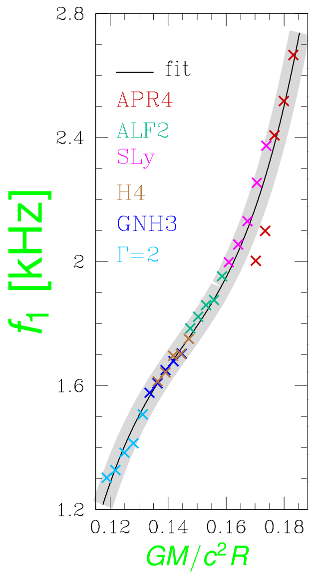


- $f_1$ (low-frequency peak)
  - all points can be fitted by a cubic polynomial function

Introduction Methodology Results Conclusions

## Correlations of $f_1$ and $f_2$

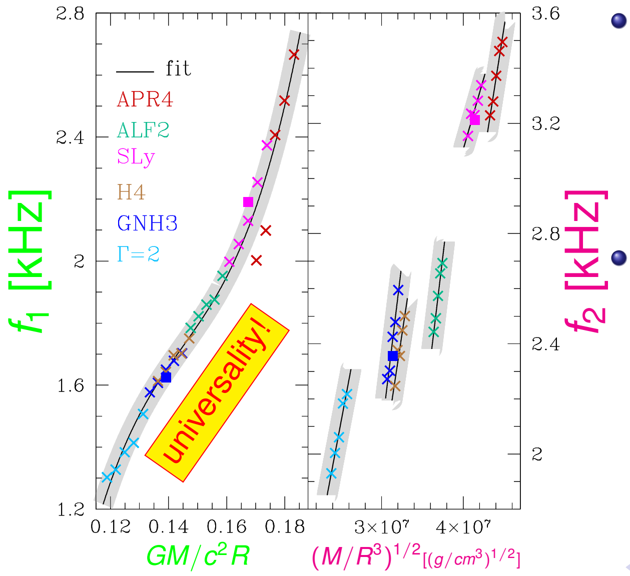


- $f_1$ (low-frequency peak)
  - all points can be fitted by a cubic polynomial function
  - universal behaviour independently of each EOS
- $f_2$ (high-frequency peak)
  - no universality
  - the points for each EOS can be fitted by a linear function
  - $f_{1,2}$ are not very sensitive to initial mass ratio (Bauswein+2011, Hotokezaka+2013)

## Constraining the EOS ( e.g., 1 )

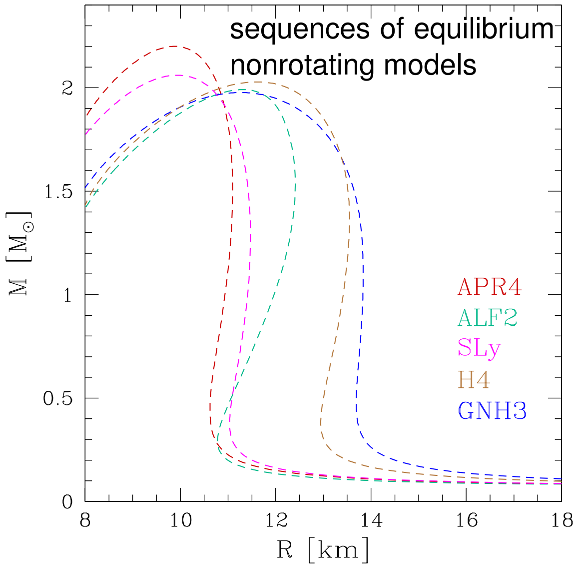


1. observe GW and extract $f_1$ and $f_2$

Introduction Methodology **Results** Conclusions

## Constraining the EOS ( e.g., 1 )

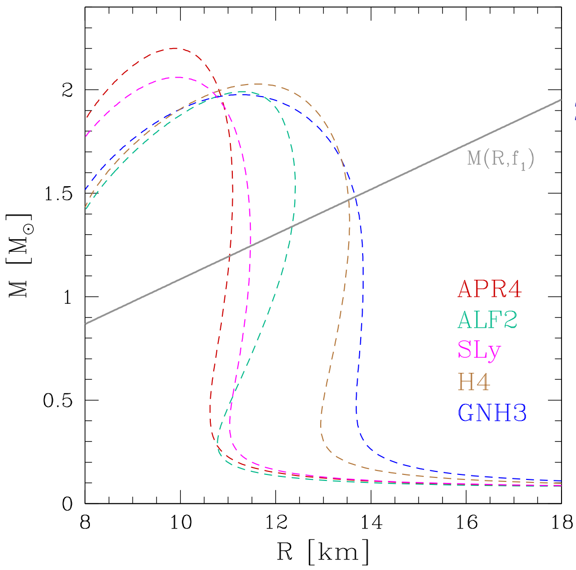


1. observe GW and extract $f_1$ and $f_2$
2. construct $M(R, f_1)$

## Constraining the EOS ( e.g., 1 )

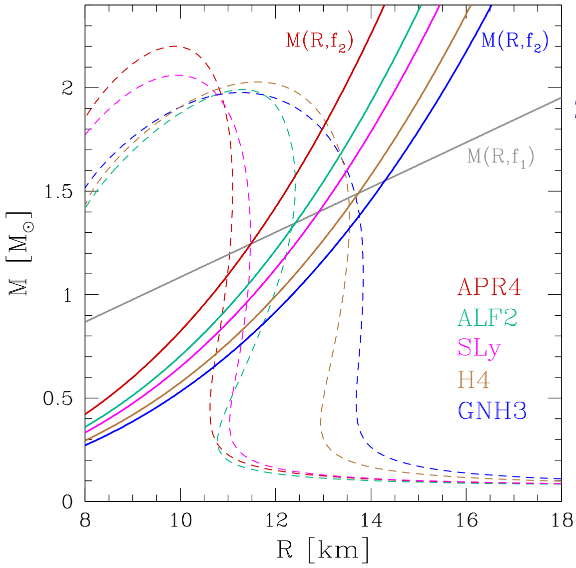


1. observe GW and extract $f_1$ and $f_2$
2. construct $M(R, f_1)$ and $M(R, f_2; \mathrm{EOS})$ curves

Introduction Methodology Results Conclusions

## Constraining the EOS ( e.g., 1 )

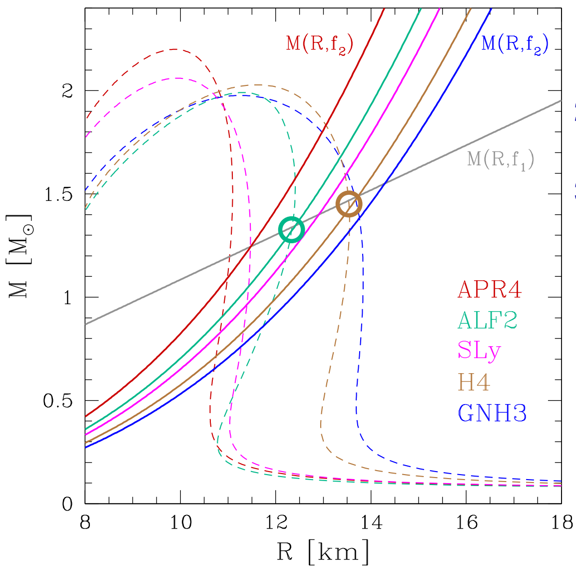


1. observe GW and extract $f_1$ and $f_2$
2. construct $M(R, f_1)$ and $M(R, f_2; \mathrm{EOS})$ curves
3. only the ALF2 and H4 EOSs have (near) crossings at one point

## Constraining the EOS ( e.g., 1 )

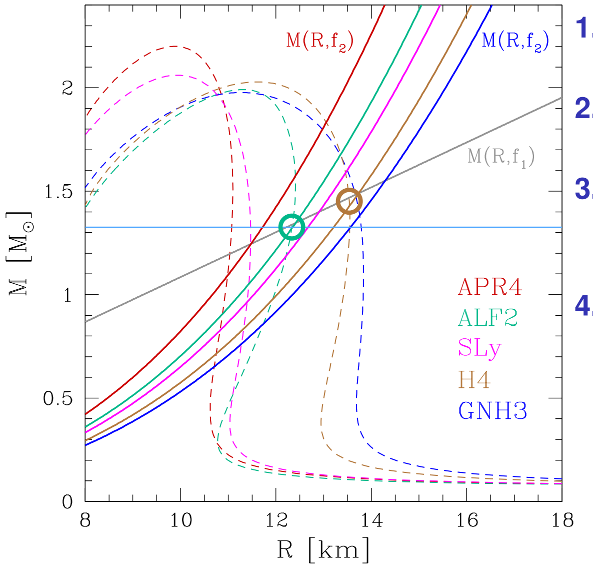


1. observe GW and extract $f_1$ and $f_2$
2. construct $M(R, f_1)$ and $M(R, f_2; \mathrm{EOS})$ curves
3. only the ALF2 and H4 EOSs have (near) crossings at one point
4. the uncertainty can be removed, if the mass of the binary is known from the inspiral signal

Introduction Methodology Results Conclusions

## Constraining the EOS ( e.g., 1 )

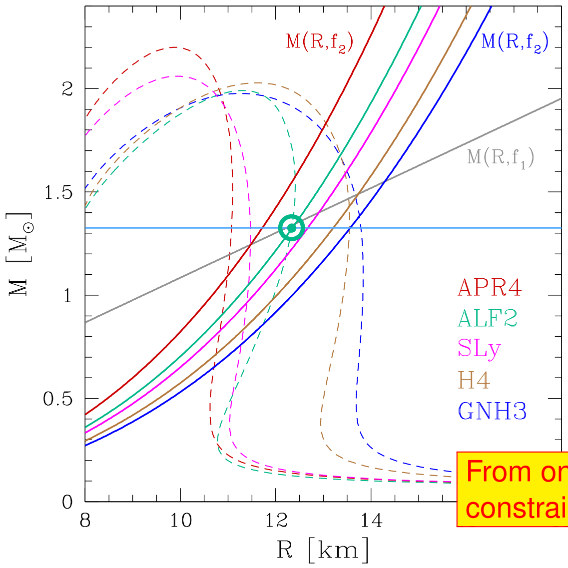


1. observe GW and extract $f_1$ and $f_2$
2. construct $M(R, f_1)$ and $M(R, f_2; \mathrm{EOS})$ curves
3. only the ALF2 and H4 EOSs have (near) crossings at one point
4. the uncertainty can be removed, if the mass of the binary is known from the inspiral signal

From only one observation, we can constrain to **ALF2** EOS in this case.

## Constraining the EOS ( e.g., 2 )

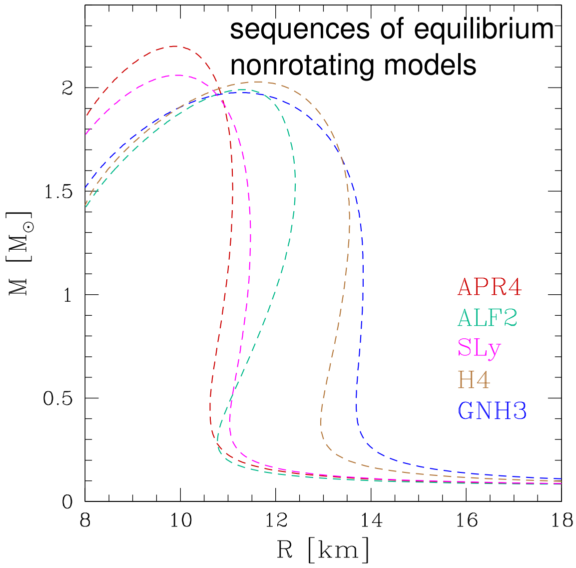


1. observe GW and extract $f_1$ and $f_2$



## Constraining the EOS ( e.g., 2 )

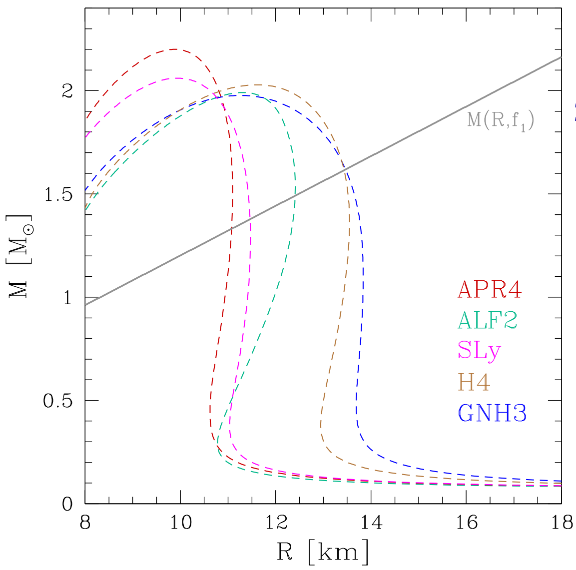


1. observe GW and extract $f_1$ and $f_2$
2. construct $M(R, f_1)$

## Constraining the EOS ( e.g., 2 )

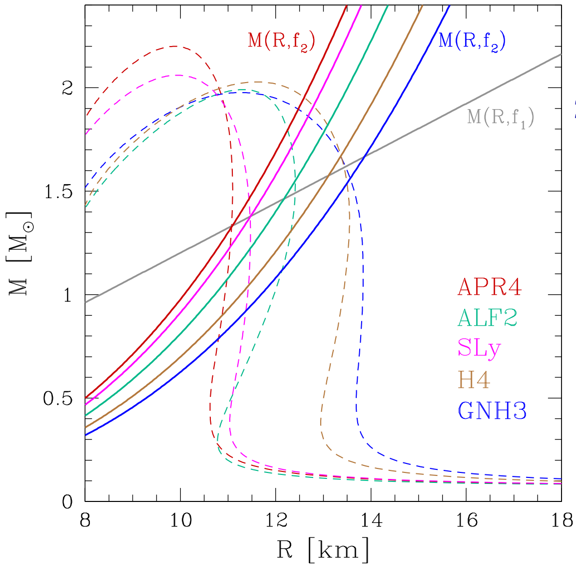


1. observe GW and extract $f_1$ and $f_2$
2. construct $M(R, f_1)$ and $M(R, f_2; \mathrm{EOS})$ curves



## Constraining the EOS ( e.g., 2 )

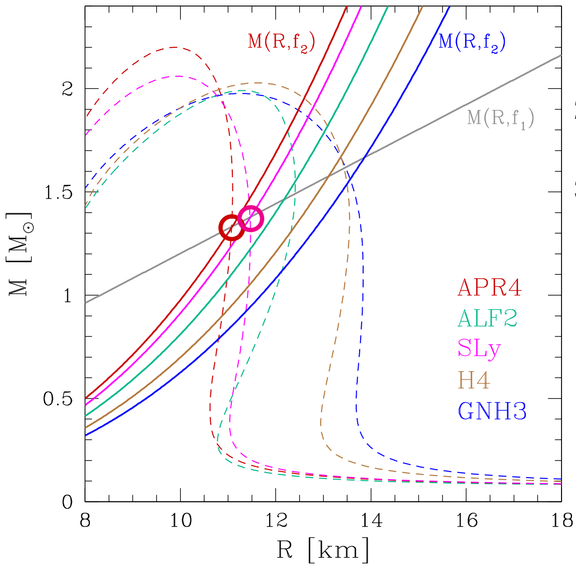


1. observe GW and extract $f_1$ and $f_2$
2. construct $M(R, f_1)$ and $M(R, f_2; \mathrm{EOS})$ curves
3. only the APR4 and SLy EOSs have (near) crossings at one point

## Constraining the EOS ( e.g., 2 )

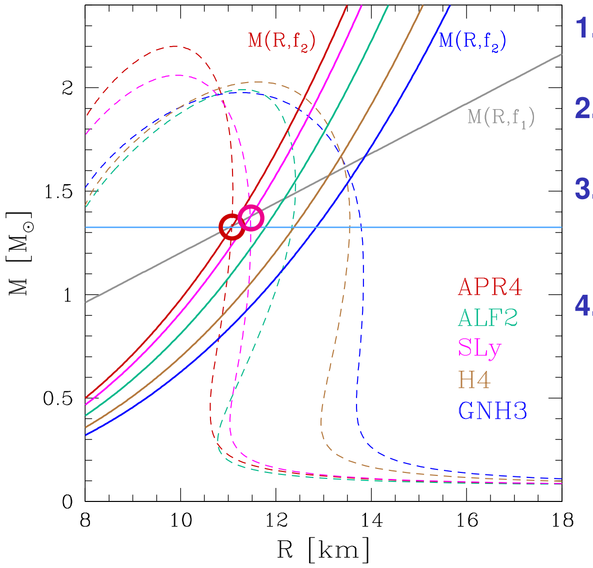


1. observe GW and extract $f_1$ and $f_2$
2. construct $M(R, f_1)$ and $M(R, f_2; \mathrm{EOS})$ curves
3. only the APR4 and SLy EOSs have (near) crossings at one point
4. the uncertainty can be removed, if the mass of the binary is known from the inspiral signal



## Constraining the EOS ( e.g., 2 )

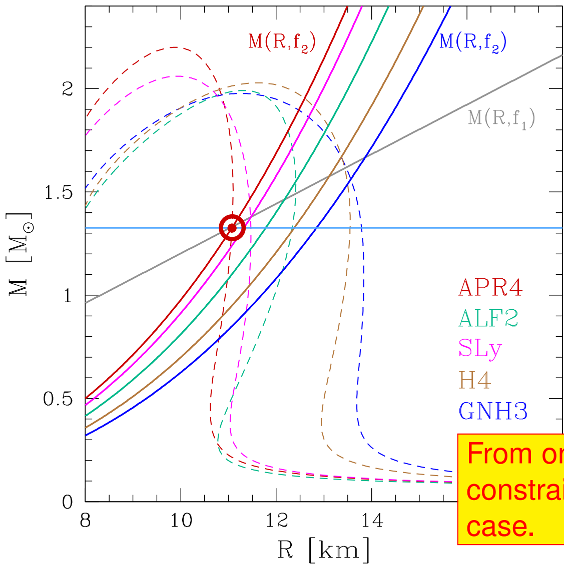


1. observe GW and extract $f_1$ and $f_2$
2. construct $M(R, f_1)$ and $M(R, f_2; \mathrm{EOS})$ curves
3. only the APR4 and SLy EOSs have (near) crossings at one point
4. the uncertainty can be removed, if the mass of the binary is known from the inspiral signal

From only one observation, we can constrain to **APR4** EOS in this case.

# Conclusions



## Conclusions

- we have carried out a large sample of accurate and fully general-relativistic simulations of the inspiral and postmerger of BNSs with nuclear EOSs
- we have confirmed that the GW spectral properties of HMNSs have clear and distinct two peaks, which are called $f_1$ and $f_2$
- we have found that $f_1$ peaks exhibit a tight correlation with the stellar compactness that is essentially EOS-independent, while a correlation of $f_2$ depend on EOSs
- we have developed and shown the powerful tool to constrain the EOS via GWs

“Fragmentation Effects in Rotating Relativistic Supermassive Stars”

Motoyuki Saijo

[JGRG24(2014)111213]

# Fragmentation Effects in Rotating Relativistic Supermassive Stars

Motoyuki Saijo (Waseda University)

CONTENTS





The 24th workshop on General Relativity and Gravitation
12th November 2014 @ Kavli IPMU, the University of Tokyo, Chiba, Japan

## 1. Introduction

### Supermassive Objects

dwarf Seyfert 1 (Barth et al. 04) NGC4839 (McConnel et al. 11)

$$(10^5 M_\odot - 10^{10} M_\odot)$$

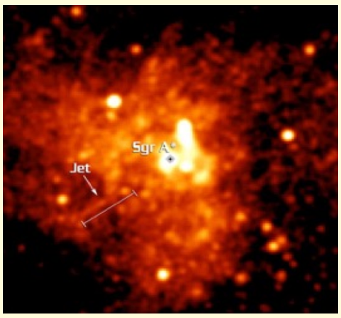


Our galaxy (Sgr A*) @Chandra

Exist in the center of most galaxies

Formation theory still uncertain

- Monolithic formation of supermassive object
- Mergers of smaller hole or mass
- Accretion of mass onto stars



1978 October *Quasars* 215

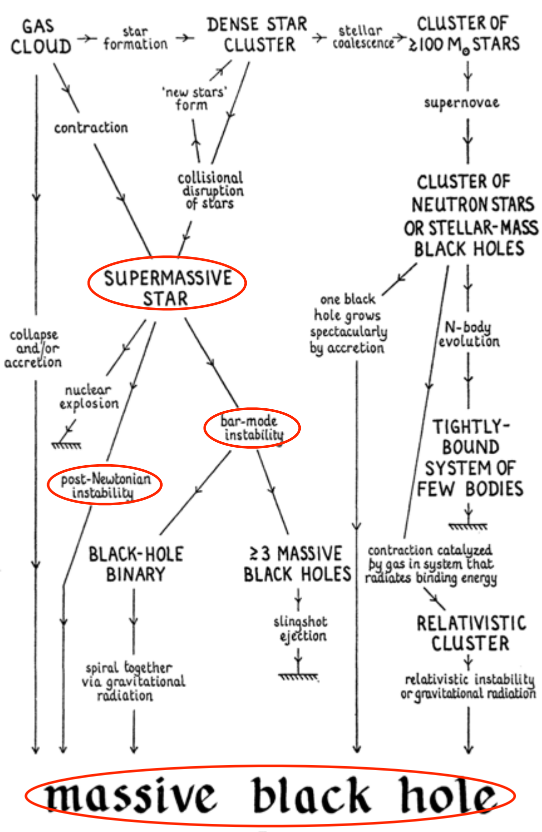


FIG. 2
Possible modes of formation of a massive black hole in a galactic nucleus.

## “Fragmentation” instability

(Zink et al. 06)

Fragmentation instability sets in

- n=3 polytropic EoS
- High degree of differential rotation
- Toroidal configuration
- (off-centered density maximum)
- Large compactness of the star

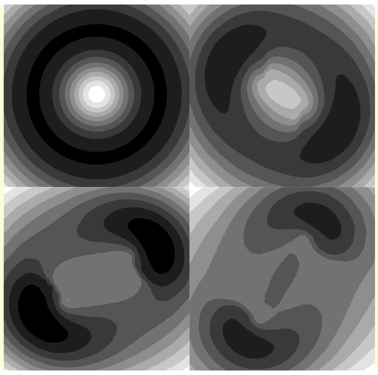

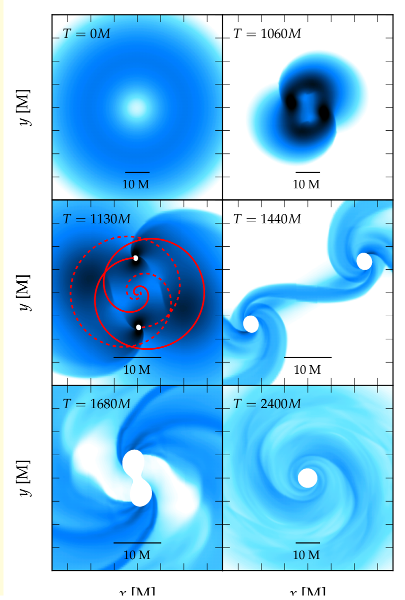


(Resswig et al. 13)

- Possibility of SMBH binary formation and merger in the early Universe
- Detectable in Decigo/BBO
- up to z>10



## Corotation resonance

(Watts, Andersson, Jones 05)

Sheer instability may occur when the degree of differential rotation exceeds some critical value

The flow and the turbulence of the fluid has a resonance interaction at the corotation radius → Turbulence excites and absorbs by the resonance interaction

$$\boxed{\Omega = \omega/m}$$

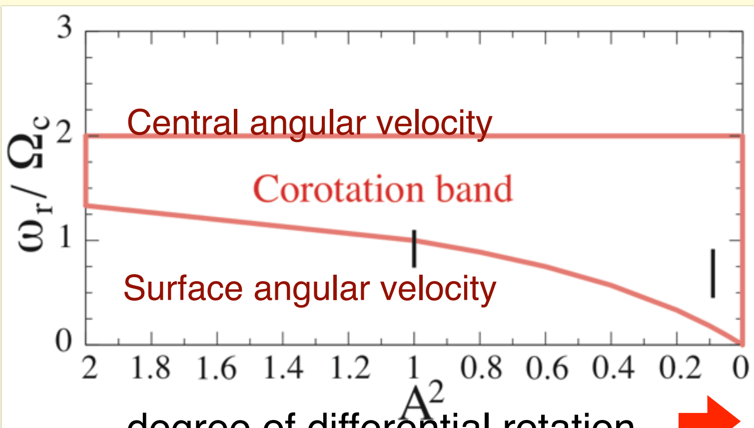


degree of differential rotation

(MS, Yoshida 06)

Corotation radius plays a key role to trigger low T/W instability (investigation of canonical angular momentum)

# 2. Relativistic Hydrodynamics in Conformally Flat Spacetime

## Conformally Flat Spacetime

$$ds^2 = (-\alpha^2 + \beta_k\beta^k)dt^2 + 2\beta_k dx^k dt + \psi^4 \delta_{ij} dx^i dx^j$$

$\alpha$ : lapse function $\beta^k$ : shift vector $\psi$ : conformal factor

- Conformally flat metric with fully relativistic hydrodynamical equations
- High resolution shock capturing scheme (HLLE) for shock treatment

➡ Elliptic equations to solve gravitational field equations (no need to solve evolution equations)

Advantages

- Satisfactory approximation when gravitation is not so strong (includes 1PN gravity)
- Stable for arbitrary long time, in principle
- Retains all the nonlinear terms necessary to maintain exact dynamics for a spherical star

Disadvantages

- Dangerous to treat strong gravitation regime
- Difficult to follow BH growth and formation (Although Kerr spacetime does not satisfy conformally flat condition, it is quite well approximated for few percent up to a/M~0.9 )



# 5. Fragmentation Effects in Supermassive Stars

## Requirements for equilibrium stars

- Radially unstable ➡ High compactness of the star
- Existence of coronation radius ➡ High degree of differential rotation

## Equilibrium stars

| Model | $r_p/r_e$ | T/W | $J/M^2$ | M/R |
|---|---|---|---|---|
| I | 0.25 | 0.214 | 1.65 | 0.0305 |
| II | 0.25 | 0.214 | 1.40 | 0.0428 |
| III | 0.25 | 0.215 | 1.25 | 0.0535 |
| IV | 0.25 | 0.215 | 1.16 | 0.0627 |
| V | 0.25 | 0.215 | 1.09 | 0.0705 |

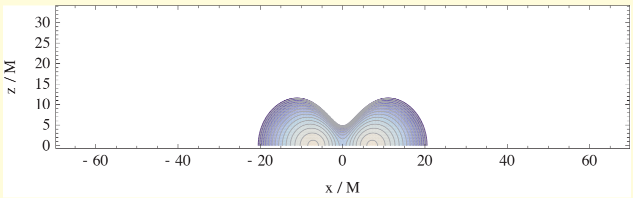


- n=3 polytropic equation of state (supermassive star sequence)
- High degree of differential rotation

$$\Omega_c/\Omega_{eq} \approx 10$$

## Evolution

### central density

- Analytical criterion of the radial instability in differentially rotating stars is unknown

➡ Evolution is necessary to determine the radial stability of the star
Perturbation: m=0 (pressure deplete), m=2 (rest mass density)

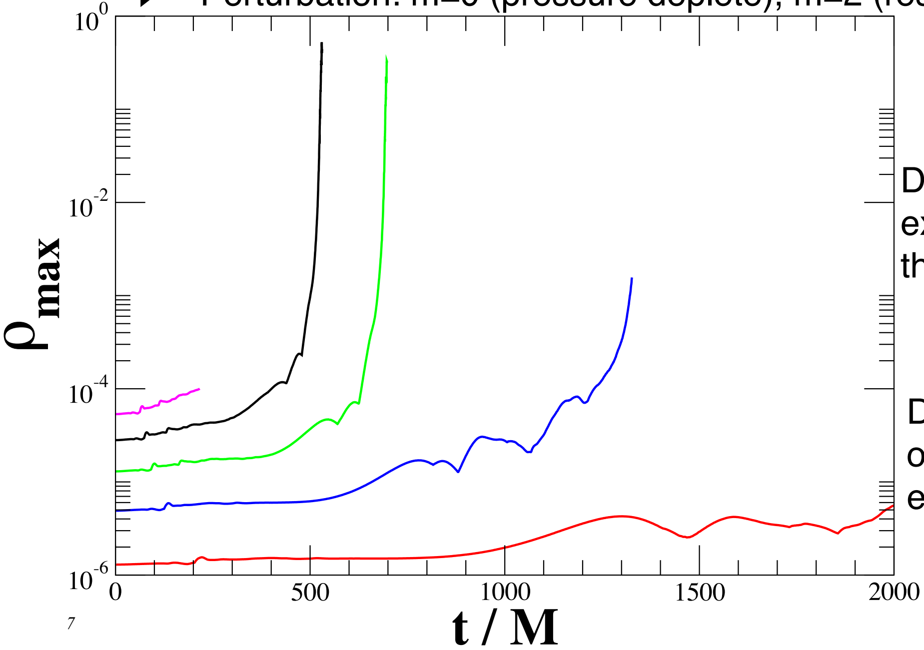


Unstable

Diagnostics has an exponential growth throughout the evolution

Stable

Diagnostics remains oscillation around the equilibrium



### density snapshots in the equatorial plane

Model II

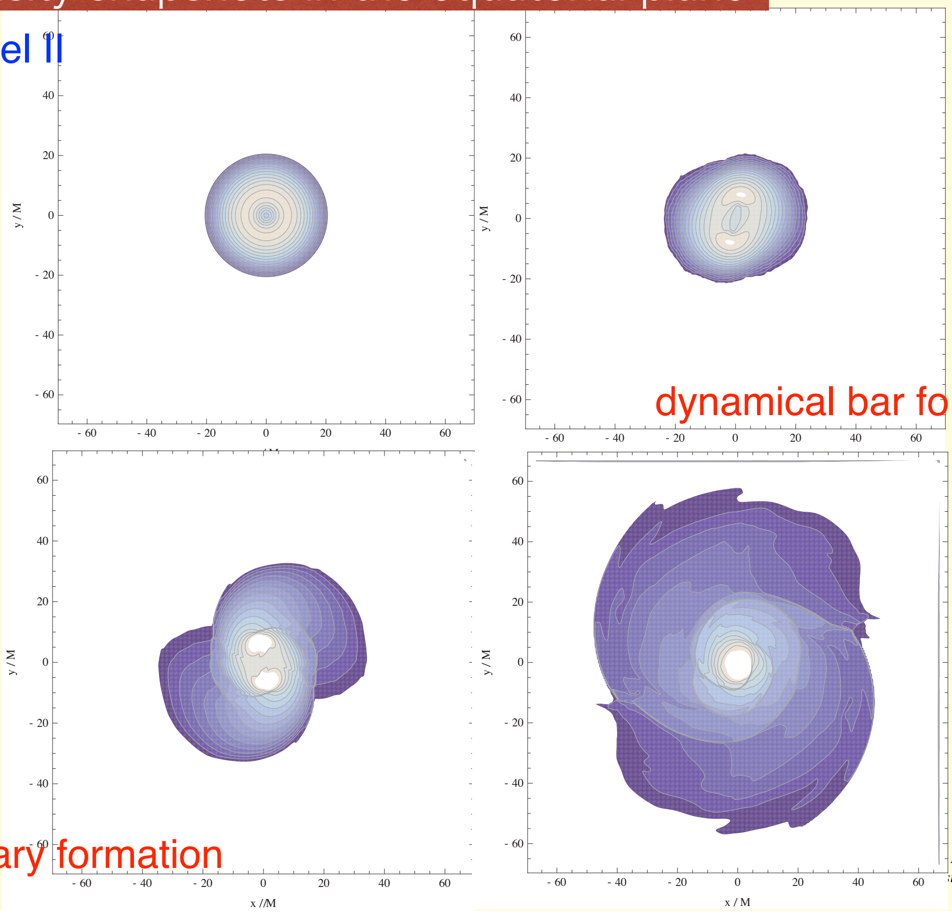


dynamical bar formation

binary formation

## Evolution

## Diagnostics for m=2

Diagnostics

$$Q = \langle e^{im\varphi} \rangle_{m=2}$$

density weighted average

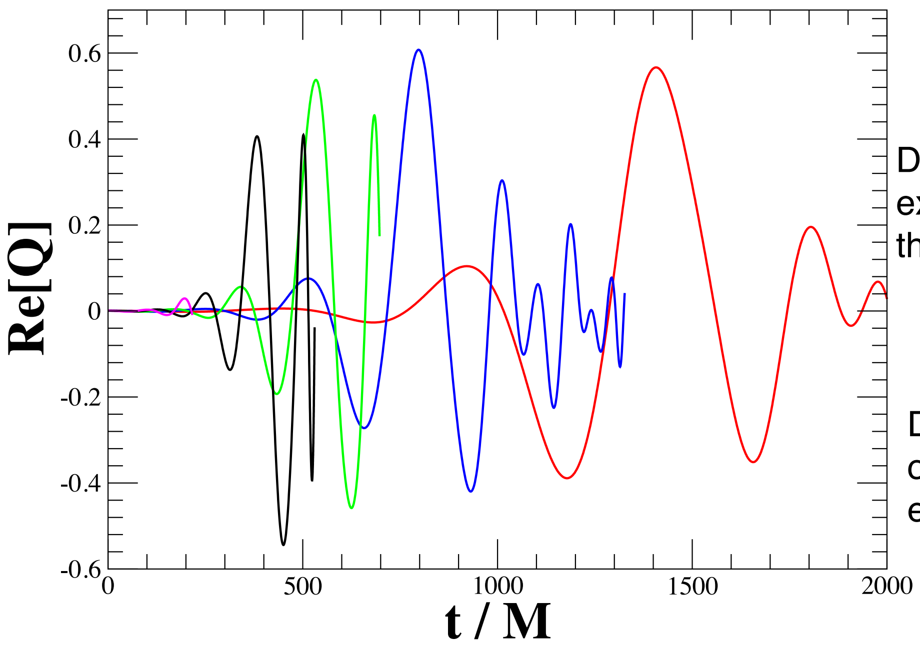


Unstable

Diagnostics has an exponential growth throughout the evolution

Stable

Diagnostics remains oscillation around the equilibrium





## Gravitational Waveform

Quadrupole formula (observer along the rotation axes)

$$\frac{rh_+}{M} = \frac{1}{2M}\frac{d}{dt}(\dot{I}_{xx} - \dot{I}_{yy})$$

$$\frac{rh_\times}{M} = \frac{1}{M}\frac{d}{dt}\dot{I}_{xy}$$

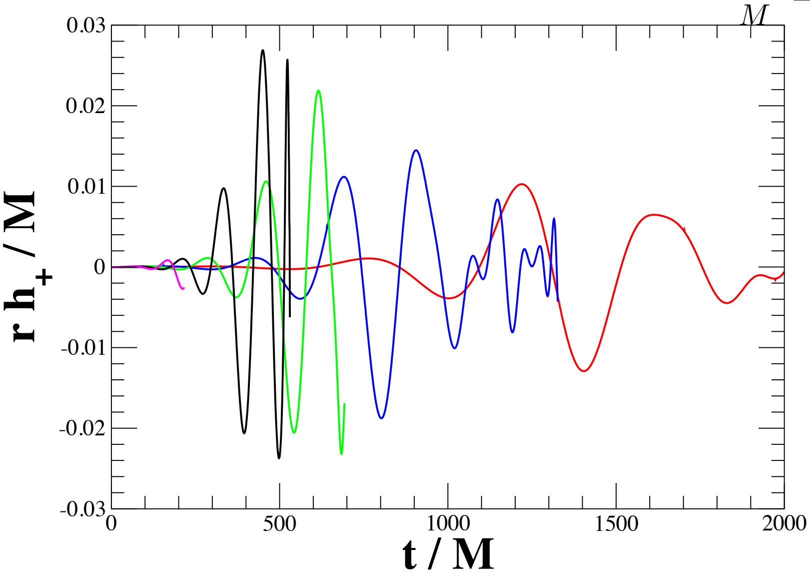


Characteristic frequency and amplitude

$$f_{\rm chr} \approx \frac{1}{2\pi t_{\rm dyn}} \approx 4\times10^{-4}\left(\frac{10^6 M_\odot}{M}\right)\left(\frac{20M}{R}\right)^{3/2} \qquad h_{\rm chr} \approx 5\times10^{-19}\left(\frac{M}{10^6 M_\odot}\right)\left(\frac{1\mathrm{Gpc}}{r}\right)\left(\frac{rh_+/M}{0.01}\right)$$

Promising source for eLISA!

## 5. Summary

We investigate the fragmentation effect of a rotating supermassive star by means of three dimensional hydrodynamical simulations in conformally flat, relativistic gravitation

- We recovered the fragmentation effect in supermassive star sequences
- We find an indication that coronation resonance plays a key role in fragmentation, in addition to bar formation
- Rotating supermassive star collapse is a promising source of burst and quasi-periodic gravitational waves
- Proper diagnostic such as canonical angular momentum is necessary for further investigation

“New views of gravitational magnification”

Marcus Werner

[JGRG24(2014)111214]

# New Views of Gravitational Magnification

Marcus C. Werner

KAVLI IPMU INSTITUTE FOR THE PHYSICS AND MATHEMATICS OF THE UNIVERSE

12 November 2014
JGRG 24

## Lensing magnification

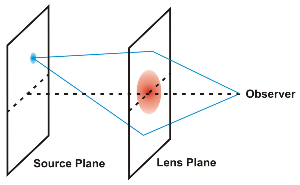


Lens plane: $\mathbf{x} \in L = \mathbb{R}^2$,
source plane: $\mathbf{y} \in S = \mathbb{R}^2$.
Lens model in $L$:
surface mass density $\kappa(\mathbf{x})$,
deflection potential $\Psi(\mathbf{x})$,
with $\Delta\Psi(\mathbf{x}) = 2\kappa(\mathbf{x})$.

Standard quasi-Newtonian impulse ('thin lens') approximation:

Lensing map: $\eta : L \to S$,
Lens equation: $\mathbf{y} = \mathbf{x} - \nabla\Psi(\mathbf{x})$.

Given the flux $F$ with and $F_0$ without the lens, the magnification of a lensed image at $\mathbf{x}_i$ is

$$\mu(\mathbf{x}_i) = \mu_i = \frac{F}{F_0} = \frac{1}{|\det \text{Jac}\,\eta(\mathbf{x}_i)|}.$$

## Lensing magnification

- $\mu$ has interesting geometrical properties, e.g. invariant sums

$$\sum_i p_i\mu_i = \text{const.}, \quad p_i = \pm 1 \text{ (image parity)},$$

  apparently related to topological invariants via Lefschetz fixed point theory. Cf. Werner, *Journal of Mathematical Physics* (2009).
- $\mu$ is **not** directly observable for resolved strong lensing systems in general: image positions, time delays, fluxes are observable.

## Strongly lensed supernova

Recent discovery at Kavli IPMU:

- first **direct** measurement of gravitational magnification,
- first strongly lensed supernova of type Ia

Transient PS1-10afx:

- at $z \simeq 1.39$ with $\mu \simeq 30$, i.e. $\Delta m(\lambda, t) = \text{const.} \simeq -3.7\text{mag}$,
- lensed images unresolved,
- foreground galaxy lens at $z \simeq 1.12$.

Quimby, Werner, Oguri, et al., *Astrophysical Journal Letters* (2013);
Quimby, Oguri, More, et al., *Science* (2014).

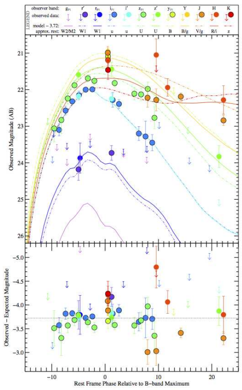

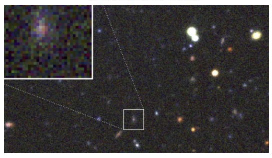

## Implications for cosmology

- More instances of strongly lensed type Ia supernovae to be found in upcoming surveys.
  $\Rightarrow$ direct measurements of $\mu$ become more common
- Powerful new constraints for modelling lenses, especially with resolved images.
  $\Rightarrow$ new tests of cosmology (even gravity?), since
  time delay between images $\Delta t(M, H)$, and
  magnification of images $\mu(M, H)$ depend **differently** on
  lens mass $M$ and Hubble parameter $H$.
- How can the standard definition of $\mu$ be extended to spacetime?

## Magnification in spacetime

Given a luminosity $L(\bar{x})$ at the emission event $\bar{x}$ and a flux $F(x)$ observed at the event $x$, the luminosity distance $D(\bar{x}, x)$ is

$$D(\bar{x}, x) = \sqrt{\frac{L(\bar{x})}{4\pi F(x)}}.$$

**If** the flux comparison with a lensless spacetime is meaningful, a possible extension of $\mu$ to spacetime is

$$\mu(\bar{x}, x) = \frac{F(x)}{F_0(x)} = \frac{D_0^2(\bar{x}, x)}{D^2(\bar{x}, x)}. \tag{1}$$

Cf. Schneider, Ehlers and Falco (1992), eq. 4.81.

How to evaluate this? What is its geometrical meaning?

## World function

In a spacetime $(M, g)$ with $\mathrm{d}s^2 = g_{\mu\nu}\mathrm{d}x^\mu \mathrm{d}x^\nu$, consider geodesics $\gamma$ from $\bar{x}$ to $x$, with geodesic length

$$\sigma_\gamma(\bar{x}, x) = \int_\gamma \mathrm{d}s.$$

In a normal convex neighbourhood of $M$, there is a unique geodesic from $\bar{x}$ to $x$, and the world function is the scalar defined as

$$\Omega(\bar{x}, x) = \frac{1}{2}\sigma_\gamma^2(\bar{x}, x).$$

Obviously, $\Omega(\bar{x}, x) = 0$ for null geodesics.

E.g. Poisson, Pound & Vega, *Living Reviews* (2011); Synge (1960).

## van Vleck determinant

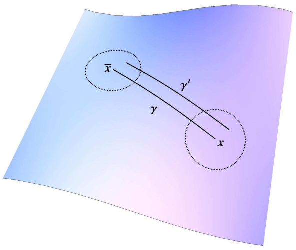


Comparing neighbouring $\gamma, \gamma'$,

$$H(\bar{x}, x) = \det \left[ \frac{\partial^2 \Omega(\bar{x}, x)}{\partial \bar{x}^\mu x^\nu} \right]$$

is **non-zero** for null geodesics.

Hence, construct a scalar measuring geodesic flow focusing,

$$\Delta(\bar{x}, x) = \frac{H(\bar{x}, x)}{\sqrt{\det g(\bar{x}) \det g(x)}},$$

called the van Vleck determinant.

E.g. Visser, *Physical Review D* (1993).

Evaluated in a **normal** chart (centered at $\bar{x}$),

$$\Delta(\bar{x}, x) = \sqrt{\frac{\det g(\bar{x})}{\det g(x)}}. \qquad (2)$$

## Application to lensing

In **any** normal convex neighbourhood of $M$, using a **normal** chart (centered at $\bar{x}$) and proper time $\bar{\tau}$ of the emitting source, the luminosity distance is

$$D(\bar{x}, x) = -\frac{\partial \Omega(\bar{x}, x)}{\partial \bar{\tau}} \left( \frac{g(x)}{g(\bar{x})} \right)^{\frac{1}{4}}. \qquad (3)$$

Cf. Etherington, *Philosophical Magazine* (1933), eq. 18.

Hence, using (1), (2) and (3), our spacetime lensing magnification becomes

$$\mu(\bar{x}, x) = \left( \frac{\frac{\partial \Omega_0}{\partial \bar{\tau}}}{\frac{\partial \Omega}{\partial \bar{\tau}}} \right)^2 \frac{\Delta}{\Delta_0}. \qquad (4)$$

This is again a scalar, applicable to **any** normal convex neighbourhood and **any** chart.

## Concluding remarks

- Eq. (4) extends the standard gravitational lensing magnification to a spacetime scalar depending on the van Vleck determinant.
- Can the comparison of fluxes with a hypothetical 'lensless spacetime' be made more precise mathematically?
- How can this definition be extended beyond convex normal neighbourhoods?
  $\Rightarrow$ important for the case of multiple lensed images
- Are there extensions of magnification invariants from the standard approximation to a spacetime setting?

This is ongoing work with Amir Babak Aazami, Kavli IPMU.

"Gravitational lensing in Tangherlini space-time"

Takao Kitamura

[JGRG24(2014)111215]

# Gravitational lensing in Tangherlini space-time

Takao Kitamura (Hirosaki)

with Naoki Tsukamoto (Fudan),
Koki Nakajima (Hirosaki), and Hideki Asada (Hirosaki)

**Phys. Rev. D 90, 064043 (2014)**

## Contents

- Introduction
- Tangherlini space-time
  - deflection angle
  - amplification
- Summary

# Gravitational lens

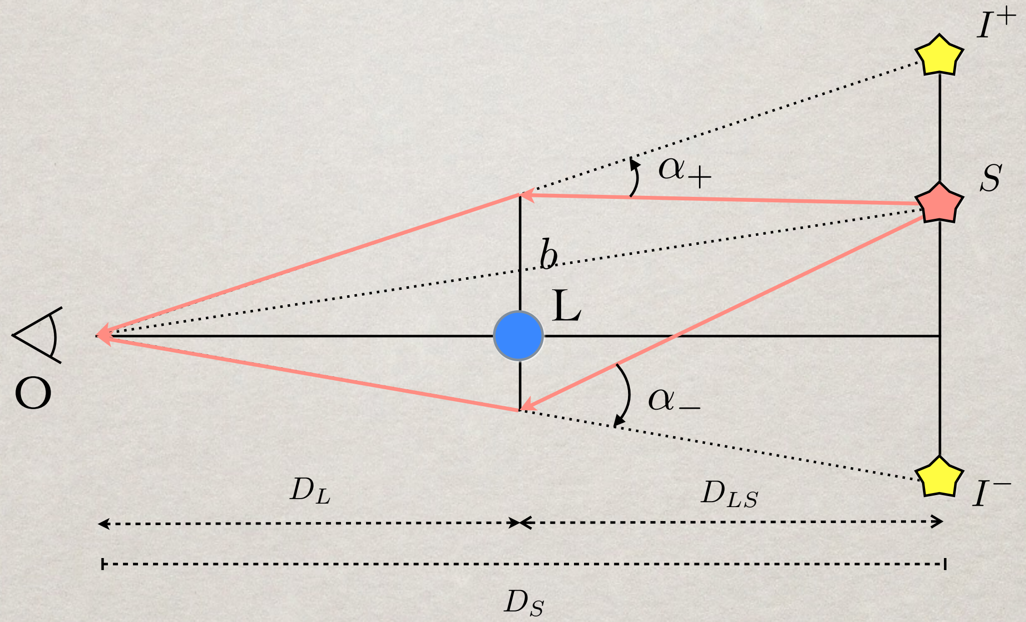


- Image magnification: Microlens

# References


[F. Abe, Astrophys. J. 725, 787 (2010).]

[Y. Toki, TK, H. Asada, and F. Abe, Astrophys. J. 740, 121 (2011).]

[N. Tsukamoto, and T. Harada, Phys. Rev. D 87, 024024 (2013).]

[N. Tsukamoto, T. Harada, K. Yajima, Phys. Rev. D 86, 104062 (2012).]

[K. Nakajima, and H. Asada, Phys. Rev. D 85, 107501 (2012).]

[K. Izumi, C. Hagiwara, K. Nakajima, TK, and H. Asada, to be published in Phys.Rev. D(2013)]

[TK, K. Nakajima, and H. Asada, Phys. Rev. D 87, 027501 (2013).]

[R. Takahashi, and H. Asada, Astrophys. J. 768, L16 (2013).]


# Modified space-time

$$\boxed{ds^2 = -\left(1 - \frac{\varepsilon_1}{r^n}\right) dt^2 + \left(1 + \frac{\varepsilon_2}{r^n}\right) dr^2 + r^2 \left(d\theta^2 + \sin^2\theta d\phi\right) + \mathrm{O}(\varepsilon_1^2, \varepsilon_2^2, \varepsilon_1\varepsilon_2)}$$

spherical symmetric
asymptotically flat
static

$$\left(\left|\frac{\varepsilon_1}{r^n}\right| \& \left|\frac{\varepsilon_2}{r^n}\right| \ll 1, \right)$$

$$\boxed{\alpha = \frac{\bar{\varepsilon}}{b^n}}$$

$$\bar{\varepsilon} = (\text{positive constant}) \cdot (n\varepsilon_1 + \varepsilon_2)$$

N.Tsukamoto, T. Harada (2013) PRD

TK et al. (2013) PRD

## Light Curve

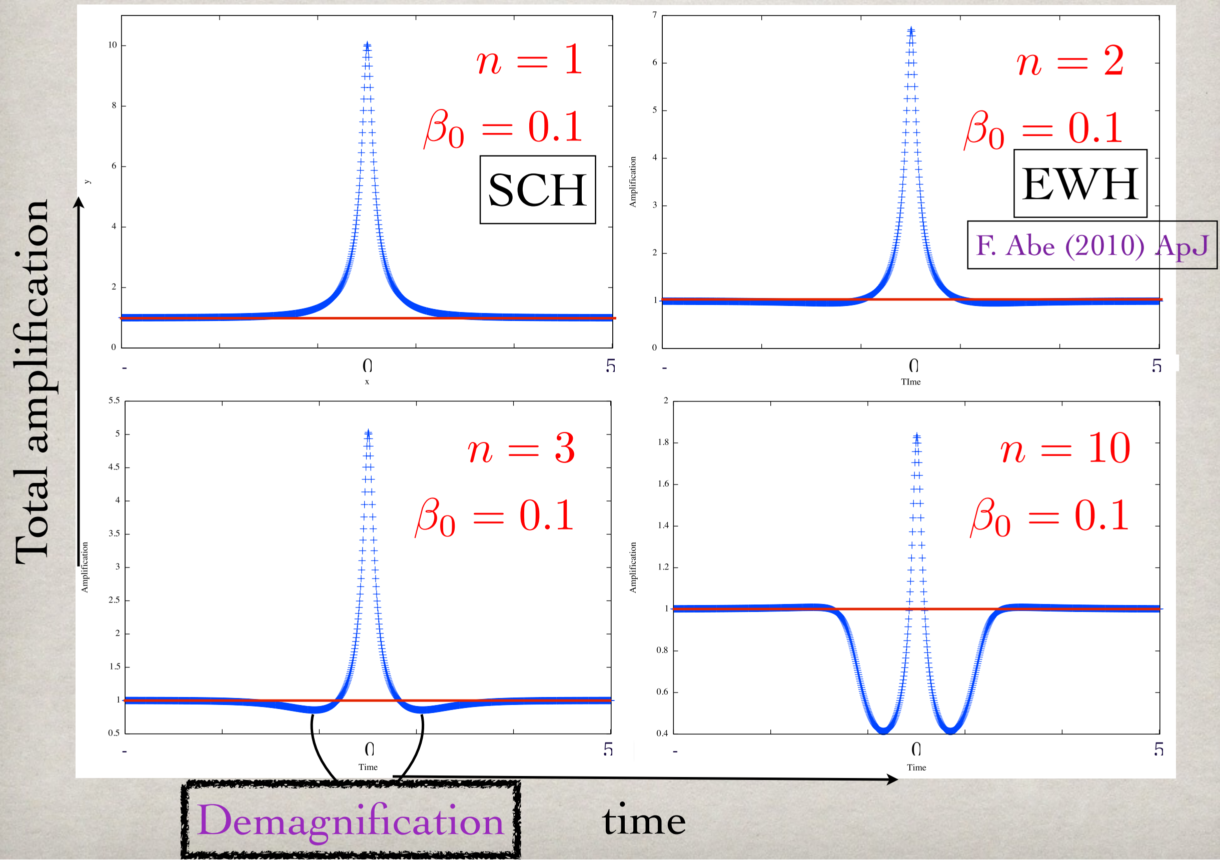


But...

This metric can only treat "weak field".

We must consider "strong field"

# Relativistic Image

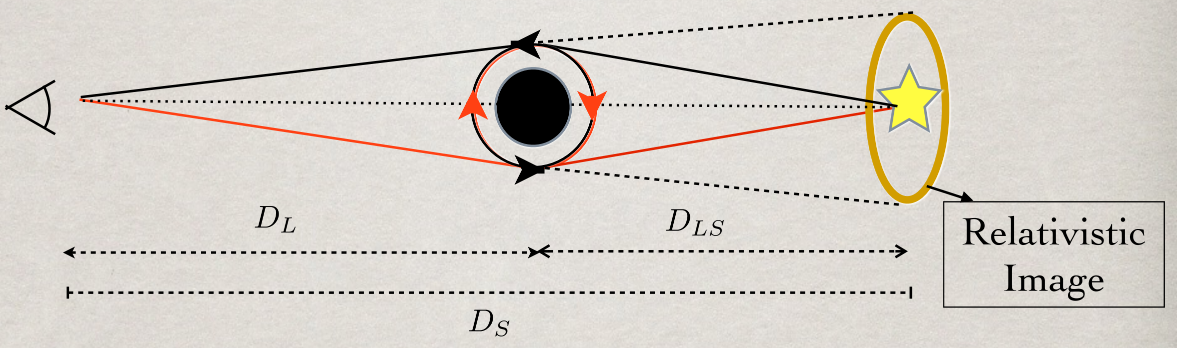


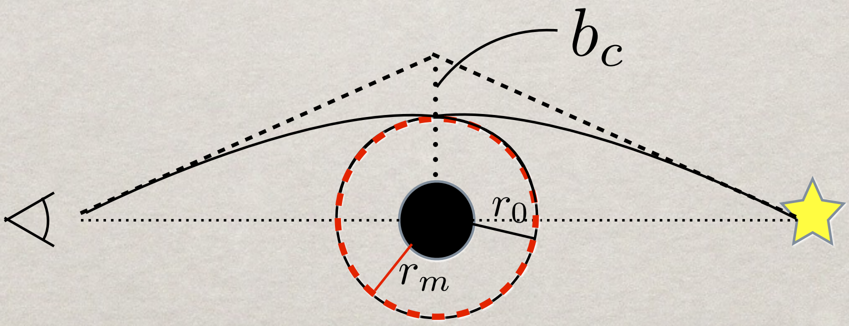


# Total Amplification

Amp(weak field) + Amp(relativ. Image)

Amp(relativ. Image) is always much smaller than Amp(weak field)

in the Schwarzschild space-time

## Our question

# Is it General ??

# Tangherlini space-time

$$ds^2 = -\left[1 - (\frac{r_g}{r})^n\right]dt^2 + \frac{dr^2}{1-(r_g/r)^n} + r^2 d\sigma^2$$

$$\left[d\sigma^2_{d-2} = d\theta_1^2 + \sum_{j=2}^{d-3}\prod_{i=1}^{j-1}\sin^2\theta_i d\theta_j^2 + \prod_{i=1}^{d-3}\sin^2\theta_i d\phi^2\right]$$

F. R. Tangherlini (1963)

n = number of dimension - 3

$r_g$ is event horizon in every dimension

n = 1 $\Rightarrow$ Schwarzschild space-time

# Tangherlini space-time

$$ds^2 = -\left[1 - (\frac{r_g}{r})^n\right]dt^2 + \frac{dr^2}{1-(r_g/r)^n} + r^2 d\sigma^2$$

$$\left[d\sigma^2_{d-2} = d\theta_1^2 + \sum_{j=2}^{d-3}\prod_{i=1}^{j-1}\sin^2\theta_i d\theta_j^2 + \prod_{i=1}^{d-3}\sin^2\theta_i d\phi^2\right]$$

$\sin\theta_i = 1$

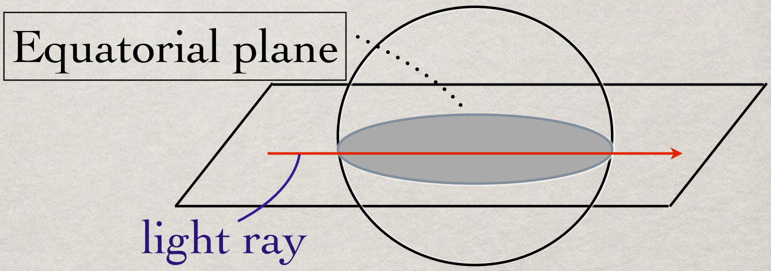


$$ds^2 = -\left[1 - (\frac{r_g}{r})^n\right]dt^2 + \frac{dr^2}{1-(r_g/r)^n} + r^2 d\phi^2$$

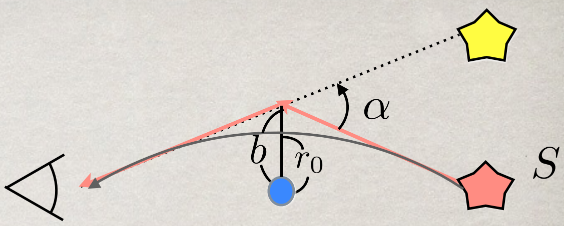


$$\left(\frac{dr}{d\phi}\right)^2 = r^4 G(r,b)$$

$$\boxed{G(r,b) \equiv \frac{1}{b^2} - \frac{1}{r^2} + \frac{r_g^n}{r^{n+2}}}$$

$$\frac{1}{b^2} = \frac{1}{r_0^2}\left(1 - \left(\frac{r_g}{r_0}\right)^n\right) \qquad (r_0 : \text{closest distance})$$

$$\alpha = I(b) - \pi$$

$$I(b) \equiv 2\int_{r_0}^{\infty} \frac{dr}{r^2\sqrt{G(r,b)}}.$$

- Introduction
- Tangherlini space-time
  - Weak field
  - Strong field
- Summary

# Weak field approximation

$\boxed{\text{for n = 1}}$ $\longrightarrow$ $\boxed{\text{C. R. Keeton, A. O. Petters (2006)}}$

$$h \equiv \left(\frac{r_g}{r_0}\right)^n \ll 1$$

$$\alpha = 2\int_0^1 \frac{dx}{\sqrt{1-x^2}\sqrt{1-hf(x)}} - \pi, \quad x \equiv \left(\frac{r_0}{r}\right)$$

$$f(x) \equiv \frac{1-x^{n+2}}{1-x^2} = \frac{1+x+x^2+\cdots+x^{n+1}}{1+x}$$

# Weak field approximation

n = Even

$$\alpha = \frac{\pi}{2}\left[1+\sum_{m=1}^{L}\frac{(2m-1)!!}{(2m)!!}\right]\left(\frac{r_g}{b}\right)^n + \mathcal{O}\left[\left(\frac{r_g}{b}\right)^{2n}\right] \quad (L=2n)$$

n = Odd

$$\alpha = \left[1+\sum_{m=1}^{L}\frac{(2m-2)!!}{(2m-1)!!}\right]\left(\frac{r_g}{b}\right)^n + \mathcal{O}\left[\left(\frac{r_g}{b}\right)^{2n}\right] \quad (L=2n-1)$$

$$A_w \simeq \left(\left(1+\sum_{m=1}^{L}\frac{(2m-1)!!}{(2m)!!}\right)\frac{D_{LS}}{D_S}\right)^{\frac{1}{n+1}}\left(\frac{r_g}{D_L}\right)^{\frac{n}{n+1}}\frac{2}{(n+1)\beta}$$

$\boxed{\text{TK et al. (2013) PRD}}$

- Introduction
- Tangherlini space-time
  - Weak field
  - Strong field
- Summary

# Strong field limit

$\boxed{\text{for n = 1}} \longrightarrow \boxed{\text{V. Bozza (2002)}}$

$$(r_0 - r_m) \ll 1$$

$$z \equiv 1 - \left(\frac{r_0}{r}\right)$$

$$G(z, r_0) = \frac{1}{r_0^2}\left\{1 - \left(\frac{r_g}{r_0}\right)^n + (1-z)^{\frac{2}{n}}\left[-1 + \left(\frac{r_g}{r_0}\right)^n (1-z)\right]\right\}$$

$$I(r_0) = I_D(r_0) + I_R(r_0)$$

$$\boxed{I_D(r_0) : \text{divergent part} \quad I_R(r_0) = I(r_0) - I_D(r_0)}$$

# Strong field limit

$$\alpha(b) = I_D(b) + I_R(b) - \pi$$

$$y \equiv (1-z)^{\frac{1}{n}}$$

$$I_D(b) = -\frac{1}{\sqrt{n}}\log\left(\frac{b}{b_c}-1\right) + \frac{1}{\sqrt{n}}\log\frac{2(n+2)}{n^2} + \mathrm{O}\big((b-b_c)^{\frac{1}{2}}\big)$$

$$I_R(b) = 2\sqrt{n+2}\int_0^1 \frac{dy}{\sqrt{n-(n+2)y^2+2y^{n+2}}} - \frac{2\sqrt{n}}{n}\int_0^1 \frac{dz}{z} + O\left((b-b_c)^{\frac{1}{2}}\right)$$

$b_c =$ critical impact parameter

$$A_R \simeq \frac{1}{\beta}\frac{b_c^2}{D_L^2}\frac{D_s}{D_{ls}}\exp\sqrt{n}(\bar{b}-2\pi)$$

$$\bar{b} = \frac{1}{\sqrt{n}}\log\frac{2(n+2)}{n^2} + I_R - \pi$$

# Amplification

$$\frac{A_w}{A_R} \sim \left(\frac{D_L}{b_c}\right)^{\frac{n+2}{n+1}} \frac{1}{\sqrt{n}(n+1)}\exp\sqrt{n}(2\pi-\bar{b})$$

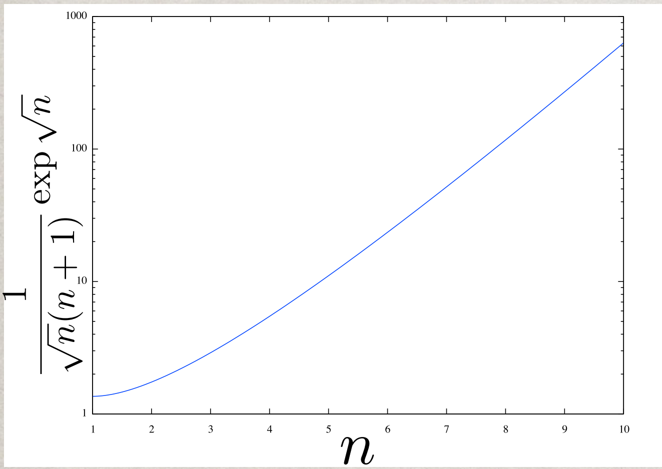


$$\frac{D_L}{b_c} \gg 1$$

$$\frac{1}{\sqrt{n}(n+1)}\exp\sqrt{n} \underset{n\to\infty}{=} \infty$$

# Summary

- Relativ. Images are fainter than Images
  in the weak field also in the Tangherlini space-time
- It would not be important Relativ. Images
  for total amplification in general n

# Future work

- Other models
- Tests of higher dimensions by the micro lensing
- Higher order of expansion


Thank you
for your
attention

“Linear stability of the post-newtonian triangular solution

to the general relativistic three-body problem”

Kei Yamada

[JGRG24(2014)111216]

# Linear Stability of Post-Newtonian Triangular Solution to General Relativistic Three-Body Problem

Kei Yamada
Hirosaki Univ.

with Tsuchiya-san (Waseda) & Asada-san (Hirosaki)

## Contents

- Introduction
- Post-Newtonian Triangular Solution
- Linear Stability
- Summary

# Contents

- Introduction
- Post-Newtonian Triangular Solution
- Linear Stability
- Summary

# Recent Works of Three-body Systems

- ``A millisecond pulsar in stellar triple system''
  [Ranson et al., Nature (2014)]
- GW & three-body interactions
  [Wen, ApJ (2003); Seto, PRL (2013)]
- PN triangular solution
  [KY & Asada, PRD (2012)]

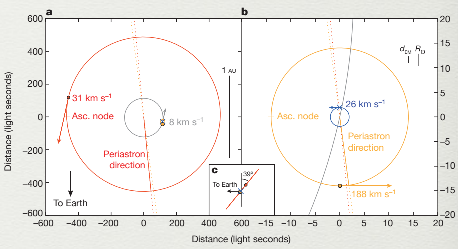


[Ranson et al., Nature (2014)]

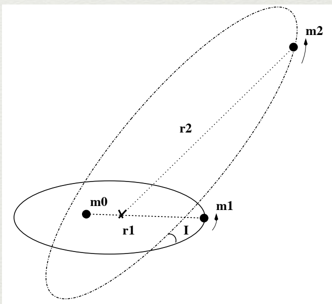


Fig. 1.—Geometry of a hierarchical triple system

[Wen, ApJ (2003)]

# Equilibrium Solutions in Newton

Lagrange's equilateral triangular solution (1772)

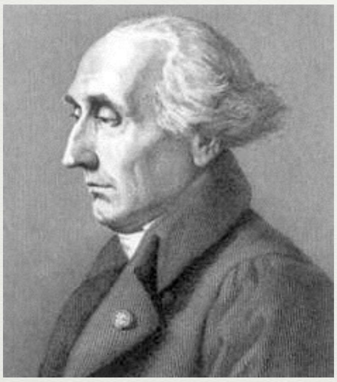

J. L. Lagrange

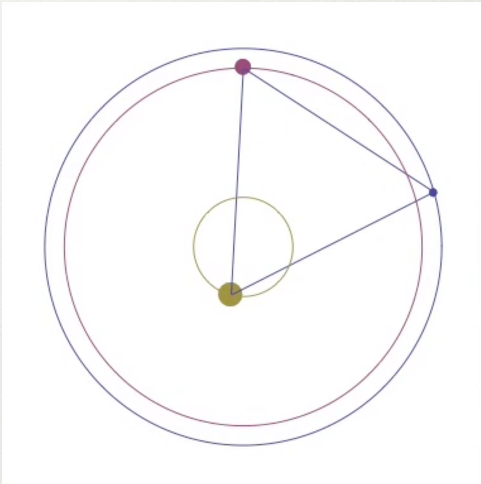

Is the solution Stable?

# Condition of Stability

Condition of stability for Lagrange solution in Newton

[Gascheau (1843); Routh (1875)]

$$\frac{m_1 m_2 + m_2 m_3 + m_3 m_1}{(m_1 + m_2 + m_3)^2} < \frac{1}{27}$$

For the restricted case ( $m_3 \to 0$ ) in GR

[Douskos & Perdios (2002); Singh & Bello (2014)]

$$\frac{m_1 m_2}{(m_1 + m_2)^2} < \frac{1}{27}\left(1 - \frac{391}{54}\varepsilon\right), \quad \varepsilon \equiv \frac{GM}{c^2 r} \ll 1$$

# Contents



# Equations of motion for N-bodies

Einstein-Infeld-Hoffman (EIH) equations of motion (@ 1PN)

Newtonian term

$$
\begin{aligned}
m_K \frac{d^2 \boldsymbol{r}_K}{dt^2} = \sum_{A \neq K} \boldsymbol{r}_{AK} \frac{G m_A m_K}{r_{AK}^3} \Bigg[ 1 &- 4 \sum_{B \neq K} \frac{G m_B}{c^2 r_{BK}} - \sum_{C \neq A} \frac{G m_C}{c^2 r_{CA}} \left( 1 - \frac{\boldsymbol{r}_{AK} \cdot \boldsymbol{r}_{CA}}{2 r_{CA}^2} \right) \\
&+ \left( \frac{\boldsymbol{v}_K}{c} \right)^2 + 2 \left( \frac{\boldsymbol{v}_A}{c} \right)^2 - 4 \left( \frac{\boldsymbol{v}_A}{c} \right) \cdot \left( \frac{\boldsymbol{v}_K}{c} \right) - \frac{3}{2} \left( \frac{\left( \frac{\boldsymbol{v}_A}{c} \right) \cdot \boldsymbol{r}_{AK}}{r_{AK}} \right)^2 \Bigg] \\
&- \sum_{A \neq K} \left[ \left( \frac{\boldsymbol{v}_A}{c} \right) - \left( \frac{\boldsymbol{v}_K}{c} \right) \right] \frac{G m_A m_K}{r_{AK}^3} \boldsymbol{r}_{AK} \cdot \left[ 3 \left( \frac{\boldsymbol{v}_A}{c} \right) - 4 \left( \frac{\boldsymbol{v}_K}{c} \right) \right] \\
&+ \frac{7}{2} \sum_{A \neq K} \sum_{C \neq A} \boldsymbol{r}_{CA} \boxed{\frac{G m_C m_K}{r_{CA}^3} \frac{G m_A}{c^2 r_{AK}}}
\end{aligned}
$$

Triple product

Employ the EIH equations of motion in a circular motion

# PN Corrections to Separation of Bodies

PN **inequilateral** triangle
$r_{IJ} = a(1+\varepsilon\rho_{IJ}),\ \varepsilon = \mathrm{O}(1\mathrm{PN})$

$\rho_{12} + \rho_{23} + \rho_{31} = 0$

scale fixing

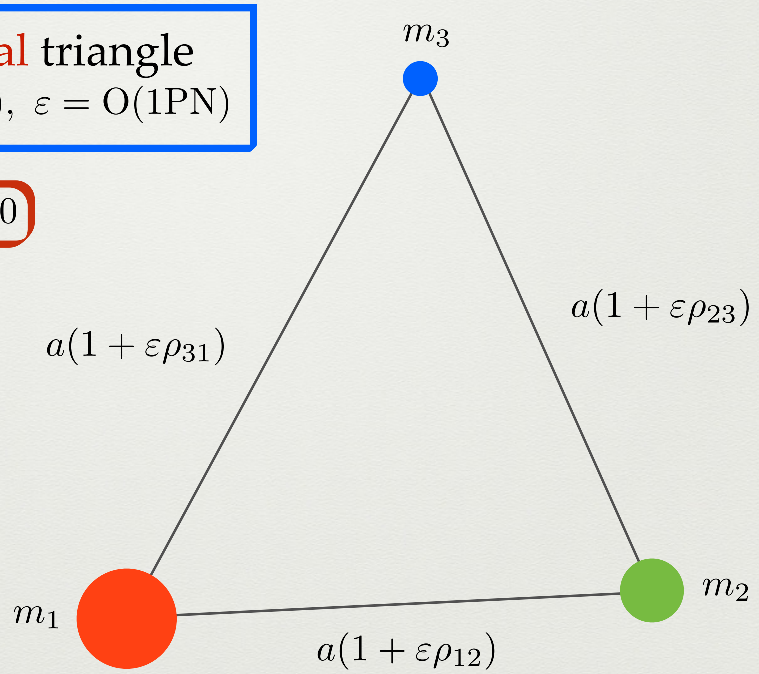


# Equilibrium Triangular Solution in GR

PN corrections for equilibrium solution are uniquely

$$
\begin{aligned}
\rho_{12} &= \frac{1}{24}[(\nu_2-\nu_3)(5-3\nu_1)-(\nu_3-\nu_1)(5-3\nu_2)],\\
\rho_{23} &= \frac{1}{24}[(\nu_3-\nu_1)(5-3\nu_2)-(\nu_1-\nu_2)(5-3\nu_3)],\\
\rho_{31} &= \frac{1}{24}[(\nu_1-\nu_2)(5-3\nu_3)-(\nu_2-\nu_3)(5-3\nu_1)],
\end{aligned}
$$

$\nu_I = m_I/(m_1+m_2+m_3)$

**PN Triangular solution** in for general masses
[KY & Asada (2012)]

# Contents



# Perturbations to PN Triangular Solution

4 perturbations in the orbital plane: $\chi_{12}, \sigma, X, \psi_{23}$

$\omega$ : angular velocity

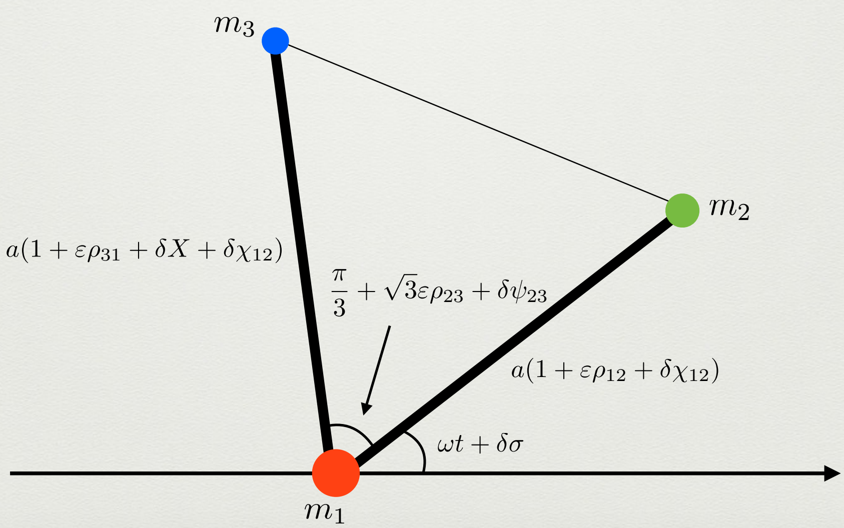

# Equations of Motion for Perturbations

$$
\begin{aligned}
&\biggl[(D^2-3)\chi_{12}-2D\sigma-\frac{9}{4}\nu_3X-\frac{3\sqrt{3}}{4}\nu_3\psi_{23}\biggr]+\varepsilon\biggl[-\frac{1}{32}\Bigl\{4\sqrt{3}(\nu_1-\nu_2)(7-9\nu_3)\nu_3D\\
&+(36\nu_2^3+234\nu_1\nu_2^2-146\nu_2^2+261\nu_1^2\nu_2-488\nu_1\nu_2+155\nu_2+63\nu_1^3-155\nu_1^2+137\nu_1\\
&-585)\Bigr\}\chi_{12}-\frac{1}{24}(27\nu_2^3+135\nu_1\nu_2^2-21\nu_2^2+135\nu_1^2\nu_2-210\nu_1\nu_2+24\nu_2+27\nu_1^3-21\nu_1^2\\
&+24\nu_1-155)D\sigma-\frac{1}{32}\nu_3\Bigl\{4\sqrt{3}(9\nu_1\nu_2+10\nu_2+9\nu_1^2-6\nu_1-4)D-(216\nu_2^2+288\nu_1\nu_2\\
&-154\nu_2+171\nu_1^2-38\nu_1+420)\Bigr\}X+\frac{1}{32}\nu_3\Bigl\{4(18\nu_2^2+27\nu_1\nu_2-2\nu_2+9\nu_1^2+14\nu_1\\
&-12)D+\sqrt{3}(51\nu_2^2+114\nu_1\nu_2+2\nu_2+87\nu_1^2-120\nu_1+155)\Bigr\}\psi_{23}\biggr]=0,
\end{aligned}
$$

$$
\begin{aligned}
&\biggl[(D^2-3)\chi_{12}-2D\sigma+\left(D^2-3+\frac{9}{4}\nu_2\right)X-\left(2D+\frac{3\sqrt{3}}{4}\nu_2\right)\psi_{23}\biggr]+\varepsilon\biggl[-\frac{1}{32}\Bigl\{4\sqrt{3}\\
&\times(\nu_3-\nu_1)(7-9\nu_2)\nu_2D+(36\nu_3^3+234\nu_1\nu_3^2-146\nu_3^2+261\nu_1^2\nu_3-488\nu_1\nu_3+155\nu_3\\
&+63\nu_1^3-155\nu_1^2+137\nu_1-585)\Bigr\}\chi_{12}-\frac{1}{24}(27\nu_3^3+135\nu_1\nu_3^2-21\nu_3^2+135\nu_1^2\nu_3-210\nu_1\nu_3\\
&+24\nu_3+27\nu_1^3-21\nu_1^2+24\nu_1-155)D\sigma-\frac{1}{32}\Bigl\{4\sqrt{3}\nu_2(9\nu_3^2+9\nu_1\nu_3+8\nu_3-4\nu_1-4)D\\
&-(180\nu_3^3+270\nu_1\nu_3^2-224\nu_3^2+198\nu_1^2\nu_3+8\nu_1\nu_3+419\nu_3+108\nu_1^3-54\nu_1^2+321\nu_1\\
&+165)\Bigr\}X+\frac{1}{96}\Bigl\{4(27\nu_3^3-39\nu_3^2-27\nu_1^2\nu_3+165\nu_1\nu_3-54\nu_3+36\nu_1^2-102\nu_1+191)D\\
&+3\sqrt{3}\nu_2(51\nu_3^2+114\nu_1\nu_3+2\nu_3+87\nu_1^2-120\nu_1+155)\Bigr\}\psi_{23}\biggr]=0,
\end{aligned}
$$

$$
\begin{aligned}
&\biggl[2D\chi_{12}+D^2\sigma-\frac{3\sqrt{3}}{4}\nu_3X+\frac{9}{4}\nu_3\psi_{23}\biggr]+\varepsilon\biggl[-\frac{1}{32}\Bigl\{4(9\nu_2^3+45\nu_1\nu_2^2+9\nu_2^2+45\nu_1^2\nu_2\\
&-30\nu_1\nu_2-18\nu_2+9\nu_1^3+9\nu_1^2-18\nu_1+61)D+3\sqrt{3}\nu_3(12\nu_2^2-6\nu_1\nu_2+14\nu_2-15\nu_1^2\\
&+4\nu_1-5)\Bigr\}\chi_{12}-\frac{1}{24}\Bigl\{(3\nu_2^2+12\nu_1\nu_2-18\nu_2+3\nu_1^2-18\nu_1+10)D^2-3\sqrt{3}(\nu_1-\nu_2)\\
&\times\nu_3(9\nu_2+9\nu_1+4)D\Bigr\}\sigma+\frac{1}{32}\nu_3\Bigl\{4(18\nu_2^2+27\nu_1\nu_2+8\nu_2+9\nu_1^2+16\nu_1-12)D\\
&+\sqrt{3}(36\nu_2^2+72\nu_1\nu_2-54\nu_2+81\nu_1^2-90\nu_1+160)\Bigr\}X+\frac{1}{32}\nu_3\Bigl\{4\sqrt{3}(9\nu_1\nu_2+8\nu_2\\
&+9\nu_1^2-4)D-9(21\nu_2^2+14\nu_1\nu_2-10\nu_2+13\nu_1^2-8\nu_1+45)\Bigr\}\psi_{23}\biggr]=0.
\end{aligned}
$$

$$
\begin{aligned}
&\biggl[2D\chi_{12}+D^2\sigma+\left(2D-\frac{3\sqrt{3}}{4}\nu_2\right)X+\left(D^2-\frac{9}{4}\nu_2\right)\psi_{23}\biggr]+\varepsilon\biggl[-\frac{1}{32}\Bigl\{4(9\nu_3^3+45\nu_1\nu_3^2\\
&+9\nu_3^2+45\nu_1^2\nu_3-30\nu_1\nu_3-18\nu_3+9\nu_1^3+9\nu_1^2-18\nu_1+61)D-3\sqrt{3}\nu_2(12\nu_3^2-6\nu_1\nu_3\\
&+14\nu_3-15\nu_1^2+4\nu_1-5)\Bigr\}\chi_{12}-\frac{1}{24}\Bigl\{(3\nu_3^2+12\nu_1\nu_3-18\nu_3+3\nu_1^2-18\nu_1+10)D^2\\
&-3\sqrt{3}(\nu_3-\nu_1)(13-9\nu_2)\nu_2D\Bigr\}\sigma+\frac{1}{32}\Bigl\{4(9\nu_3^3-19\nu_3^2-9\nu_1^2\nu_3+27\nu_1\nu_3-2\nu_3-2\nu_1^2\\
&-10\nu_1-49)D+\sqrt{3}(72\nu_3^2+54\nu_1\nu_3-12\nu_3+36\nu_1^2-78\nu_1+145)\nu_2\Bigr\}X-\frac{1}{96}\Bigl\{4(3\nu_3^2\\
&+12\nu_1\nu_3-18\nu_3+3\nu_1^2-18\nu_1+10)D^2-12\sqrt{3}(9\nu_3^2+9\nu_1\nu_3+12\nu_3-4\nu_1-4)\nu_2D\\
&-27(21\nu_3^2+14\nu_1\nu_3-10\nu_3+13\nu_1^2-8\nu_1+45)\nu_2\Bigr\}\psi_{23}\biggr]=0.
\end{aligned}
$$

# Matrix Form of Equations of Motion

Defining new variables

$$\dot{\chi}_{12}\equiv D\chi_{12},\ \ \dot{X}\equiv DX,\ \ \dot{\sigma}\equiv D\sigma,\ \ \dot{\psi}_{12}\equiv D\psi_{12},\quad D\equiv\frac{d}{dt}$$

Equations of motion for the perturbations are

$$D\boldsymbol{X}=M\boldsymbol{X},\qquad M\text{: } 8\times 8 \text{ matrix}$$

$$\boldsymbol{X}\equiv(\dot{X},\dot{\chi}_{12},\dot{\sigma},\dot{\psi}_{23},X,\chi_{12},\sigma,\psi_{23})$$

Roots can be formally expressed

$$\chi_{12}=C_1e^{\lambda_1t}+C_2e^{\lambda_2t}+\cdots$$

$$C_I\quad(I=1,2,\cdots)\text{ : constants, }\ \lambda_I\text{ : eigenvalues of }\ M$$

# Conditions of Stability in GR

Eigenvalue equation (secular equation) of the matrix $M$ is

$$\left[\lambda^6 + 2\left(1 - \frac{1}{8}\varepsilon\left[77 - 10(\nu_1\nu_2 + \nu_2\nu_3 + \nu_3\nu_1)\right]\right)\lambda^4 \right.$$
$$+ \left(\left[1 + \frac{27}{4}(\nu_1\nu_2 + \nu_2\nu_3 + \nu_3\nu_1)\right] - \frac{1}{16}\varepsilon\left[308 + 1265(\nu_1\nu_2 + \nu_2\nu_3 + \nu_3\nu_1) + 162\nu_1\nu_2\nu_3 - 378(\nu_1\nu_2 + \nu_2\nu_3 + \nu_3\nu_1)^2\right]\right)\lambda^2$$
$$\left. + \left(\frac{27}{4}(\nu_1\nu_2 + \nu_2\nu_3 + \nu_3\nu_1) - \frac{9}{32}\varepsilon\left[521(\nu_1\nu_2 + \nu_2\nu_3 + \nu_3\nu_1) - 72\nu_1\nu_2\nu_3 - 126(\nu_1\nu_2 + \nu_2\nu_3 + \nu_3\nu_1)^2\right]\right)\right] = 0,$$

linear stable $\Longleftrightarrow$ $\lambda =$ pure imaginary number

$$\Downarrow$$

$$\boxed{\frac{m_1m_2 + m_2m_3 + m_3m_1}{(m_1 + m_2 + m_3)^2} + \frac{15}{2}\frac{m_1m_2m_3}{(m_1 + m_2 + m_3)^3}\varepsilon < \frac{1}{27}\left(1 - \frac{391}{54}\varepsilon\right)}$$

# Stable Region of Mass Ratios

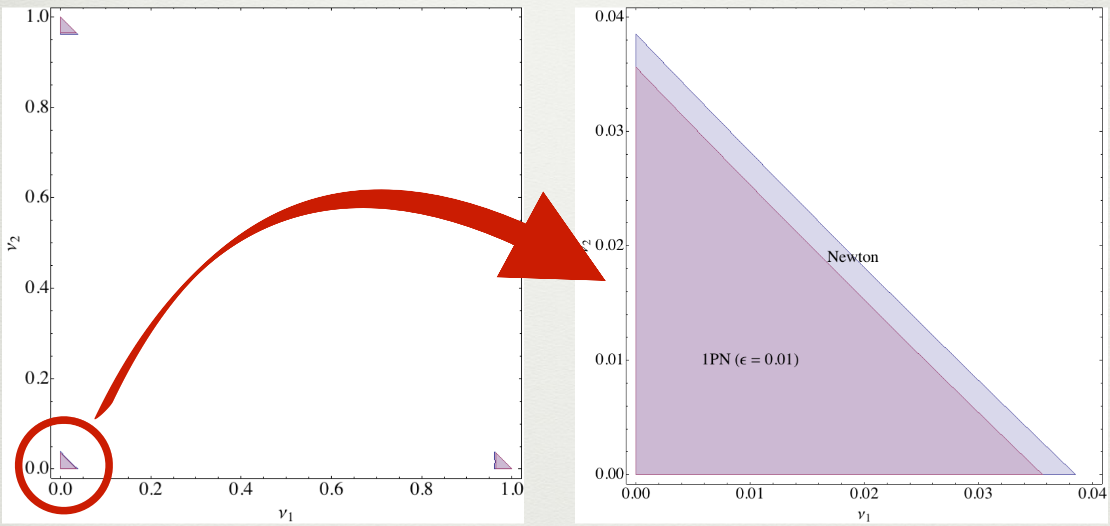


Stable region is more narrow by the PN effects

# Comparison with Restricted Case

For the restricted case ( $m_3 \to 0$ ) in GR
[Douskos & Perdios (2002); Singh & Bello (2014)]

$$\frac{m_1 m_2}{(m_1+m_2)^2} < \frac{1}{27}\left(1 - \frac{391}{54}\varepsilon\right), \quad \varepsilon \equiv \frac{GM}{c^2 r} \ll 1$$

Our work for general masses

$$\frac{m_1 m_2 + m_2 m_3 + m_3 m_1}{(m_1+m_2+m_3)^2} + \boxed{\frac{15}{2}\frac{m_1 m_2 m_3}{(m_1+m_2+m_3)^3}\varepsilon} < \frac{1}{27}\left(1 - \frac{391}{54}\varepsilon\right)$$

PN 3-body interaction!

# Contents

- Introduction
- Post-Newtonian Triangular Solution
- Linear Stability
- Summary

# Summary

- The condition of stability is more strict (PN 3-body interaction)
- Stable with one dominant mass
  → around SMBHs
- More unstable by PN effects
  → GW radiation may be affected

# On-going Works

- GW reaction to Triangular solution
  (Poster No. A01 by Iseki-san
  & No. A02 by Harada-san)

Iseki-san

Harada-san

- Marginally Stable Circular Orbit (MSCO)
  (Poster No. B01 by Suzuki-san
  & No. B02 by Ono-san)

Suzuki-san

Ono-san

THANK YOU FOR YOUR ATTENTION

“Slowly rotating gravastars with a thin shell”

Nami Uchikata

[JGRG24(2014)111217]

# SLOWLY ROTATING GRAVASTARS WITH A THIN SHELL

Nami Uchikata
(CENTRA, Universidade de Lisboa, Portugal)
and
Shijun Yoshida
(Astronomical Institute, Tohoku University, Japan)

## Gravastars

- Mazur & Mottola (2004)

Compact object model alternative to black holes without the event horizon.

During the gravitational collapse, a quantum phase transition occurs before the event horizon is formed.

Spherically symmetric, as compact as black holes.

de Sitter core + shell + Schwarzschild

Thin shell :

Stable against radial perturbations. (Visser & Wiltshire 2008)

- How to distinguish them from black holes by observations?
  - Oscillation modes (gravitational ⇨ O, electromagnetic ⇨ X?)

    (Chirenti & Rezzolla 2007, 2008, Pani *et* al. 2008, Cardoso *et* al. 2009)
  - Quadrupole deformation (rotating case)

    Exterior of rotating stars ≠ Kerr spacetime
- No general solution for rotating gravastars.

- We use the slow rotation approximation up to O( $\varepsilon^2$) and assume the shell is thin.

( $\varepsilon = \Omega / \Omega_{k,} \ll 1$, $\Omega$ : angular velocity of the shell, $\Omega_k$: Keplerian frequency)

# Metric

$$
\begin{aligned}
ds^2 = & -f(r)(1+2\epsilon^2 h(r,\theta))dt^2 \\
& + \frac{1}{f(r)}\left(1+\frac{2\epsilon^2 m(r,\theta)}{rf(r)}\right)dr^2 \\
& + r^2(1+2\epsilon^2 k(r,\theta))(d\theta^2+\sin^2\theta(d\phi-\epsilon\omega(r)dt)^2).
\end{aligned}
$$

$$
f^+(r) = 1-2M/r \qquad f^-(r) = 1-r^2/L^2,
$$

+ : outside the shell, - : inside the shell

M : mass of gravastar, L :de Sitter horizon radius

$$
\begin{aligned}
h(r,\theta) &= h_0(r) + h_2(r)P_2(\cos\theta), \\
m(r,\theta) &= m_0(r) + m_2(r)P_2(\cos\theta), \\
k(r,\theta) &= k_2(r)P_2(\cos\theta).
\end{aligned}
$$

# Outside the shell

- Hartle (1967), Hartle & Thorne (1968)

B = 0 for the Kerr metric

angular momentum

change of mass

quadrupole moment
Q = $J^2/M+8\ BM^3/5$

$$\omega^+ = \frac{2J}{r^3},$$

$$m_0^+ = \delta M - \frac{J^2}{r^3},$$

$$h_0^+ = -\frac{\delta M}{r-2M} + \frac{J^2}{r^3(r-2M)},$$

$$h_2^+ = J^2\left(\frac{1}{Mr^3}+\frac{1}{r^4}\right) + BQ_2^2\left(\frac{r}{M}-1\right),$$

$$k_2^+ = -\frac{J^2}{r^4} - B\frac{2M}{\sqrt{r(r-2M)}}Q_2^1\left(\frac{r}{M}-1\right) - h_2^+,$$

$$m_2^+ = (r-2M)\left(-h_2^+ + \frac{r^4}{6}\left(\frac{d\bar\omega}{dr}\right)^2\right).$$

# Inside the shell

Solving Einstein equations with a cosmological constant

$$\omega^- = C_1, \tag{2.13}$$

$$m_0^- = 0, \tag{2.14}$$

$$h_0^- = C_2, \tag{2.15}$$

$$h_2^- = \frac{C_3}{8r^2}\left(\frac{-3L^2+5r^2}{L^2 f^-(r)} + \frac{3Lf^-(r)\mathrm{Arctanh}(r/L)}{r}\right), \tag{2.16}$$

$$k_2^- = \frac{C_3}{8r^2 L}\left(\frac{3L^2+4r^2}{L} - \frac{3(L^2+r^2)\mathrm{Arctanh}(r/L)}{r}\right), \tag{2.17}$$

$$m_2^- = -rf^-(r)h_2^-. \tag{2.18}$$

Functions are regular at the origin.
$C_1$, $C_2$ and $C_3$ are given from the junction condition. (Israel 1966)

# Thin shell

the radius of the shell
in the zero-rotation limit

- Location of the shell $\left(x^{\pm}\right)^{\mu}=\left(A^{\pm}T,\boxed{R}+\varepsilon^{2}\xi^{\pm},\Theta,\Phi\right)$

(A$^+$=1, A$^-$ = const.)

- Stress energy tensor of the shell

$$S_{ab}=(\underbrace{[[K_{ab}]]}_{\text{Jump of the extrinsic curvature}}-h_{ab}[[K]]),$$

- Solutions stable against radial perturbations (Visser and Wiltshire 2004)

$$\begin{cases}\sigma_0=\dfrac{\sqrt{f^-}-\sqrt{f^+}}{4\pi R},\\ p_0=-\dfrac{1}{8\pi R^2}\left(\dfrac{M-R}{\sqrt{f^+}}+R\dfrac{1-2R^2/L^2}{\sqrt{f^-}}\right).\end{cases}\qquad(\varepsilon\to 0)$$

- The shell satisfies the dominant energy condition. $\sigma_0 \geq p_0$

---

- The shell is a perfect fluid. (isotropic pressure)

- Equation of state of the shell

In this talk, we assume the shell to be a polytropic fluid with n =1.

- Total particle number is conserved.

$$\delta M=-\frac{(2J-R^3\Omega_k)^2}{2R^3\sqrt{f^+}\sqrt{f^-}}-\frac{J(J-2MR^2\Omega_k)}{R^2f^+}+\frac{R^2(R-3M)\Omega_k^2}{2f^+}.$$

# Results (L = 1)

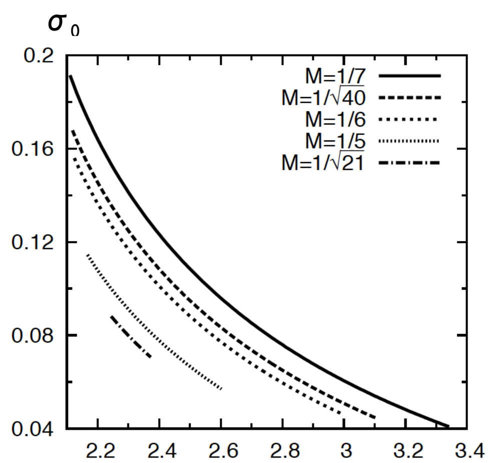


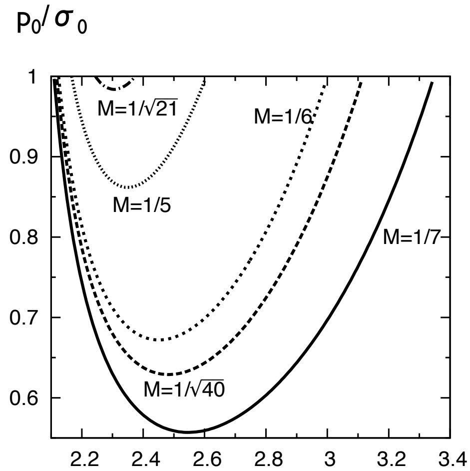


R/M

(Endpoints of R/M are determined from the dominant energy condition.)

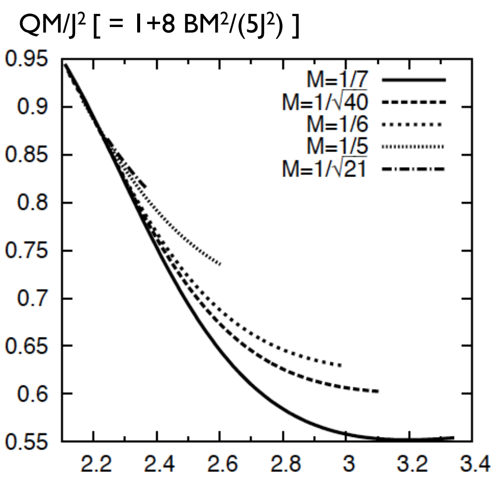


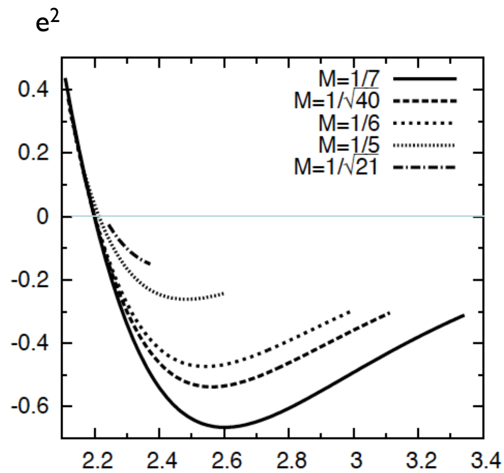


R/M

**Perturbed energy density and pressure**

$$\delta\sigma = \delta\sigma_0 + \delta\sigma_2 P_2(\cos\Theta)$$
$$\delta p = \delta p_0 + \delta p_2 P_2(\cos\Theta)$$

quadrupole perturbations

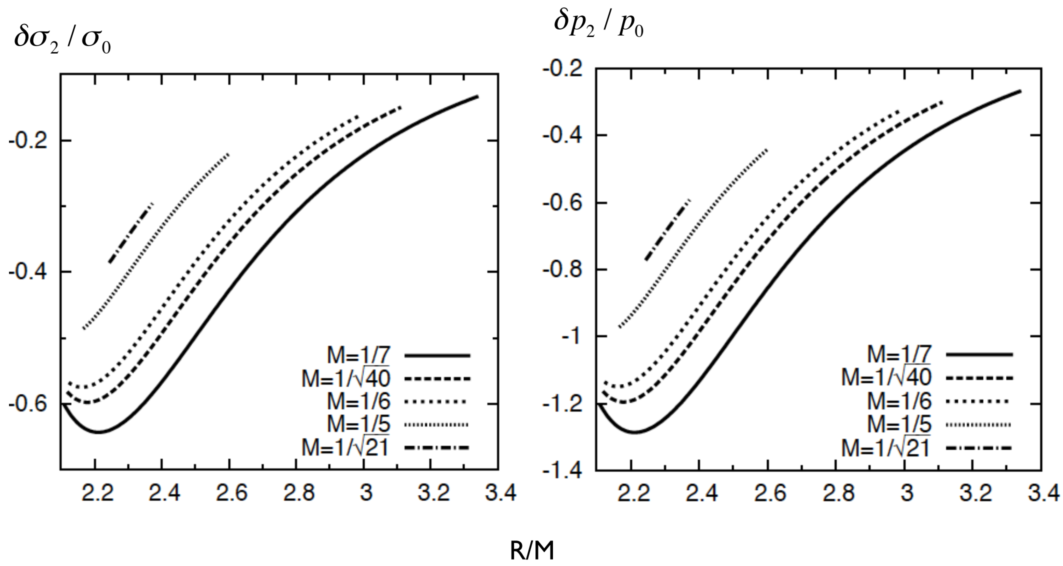


spherically symmetric perturbations

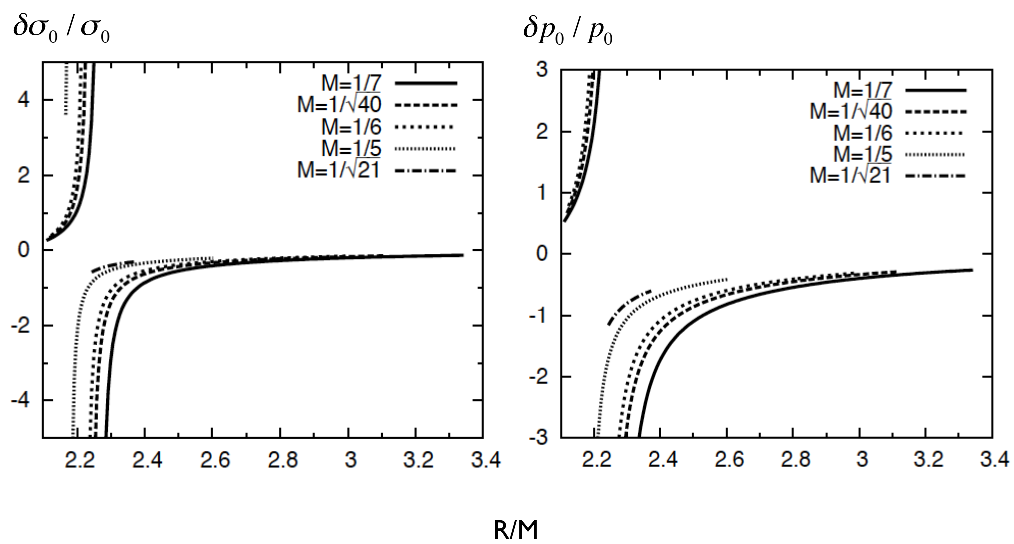

# Summary

- We have constructed solutions of slowly rotating gravastars with a thin shell up to $O(\varepsilon^2)$.

- We have found that most of the solutions have a prolate shell.

- We can not get solutions $2.2M \lesssim R \lesssim 2.3M$.

# “Particle Collision in Wormhole Spacetimes”

Naoki Tsukamoto

[JGRG24(2014)111218]

# Particle Collision in Wormhole Spacetimes

**Naoki Tsukamoto**

**(Fudan University in China)**

N. T. and C. Bambi, arXiv:1411.xxxx

November 10-14, 2014 JGRG24 @ Kavli IPMU, Tokyo University in Chiba



# Particle Collision near the Kerr black hole.

- In 1975, Piran, Shaham and Katz investigated a collisional Penrose process and pointed out that **the center-of-mass (CM) energy for the collision of two particles can be arbitrary high.**
- In 2009, Bañados, Silk and West (BSW) rediscovered it.

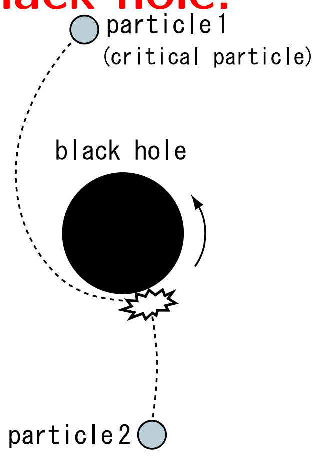


Figure in Harada and Kimura (2014).

## BSW effect. Bañados, Silk and West (2009)

- $E_{CM}$ of a collision of particles in the extremal Kerr spacetime in the near horizon limit $r \to r_+$ on the equatorial plane:

$$\lim_{r\to r_+} \frac{E_{CM}(r)}{2m} = \lim_{r\to r_+} \left(p^\mu_{(1)} + p^\mu_{(2)}\right)\left(p_{(1)\mu} + p_{(2)\mu}\right)$$
$$= \sqrt{\frac{1}{2}\left(\frac{2ME_{(1)} - L_{(1)}}{2ME_{(2)} - L_{(2)}} + \frac{2ME_{(2)} - L_{(2)}}{2ME_{(1)} - L_{(1)}}\right)},$$

$p^\mu$: four-momentum, $m$: particle mass, $M$: black hole mass, $E$: conserved energy, $L$: conserved angular momentum

- **Critical particle: $L = 2ME$.**
- $E_{CM}/2m$ **diverges if either of two particles is critical and the other is non-critical. (BSW effect.)**



## About a critical particle.

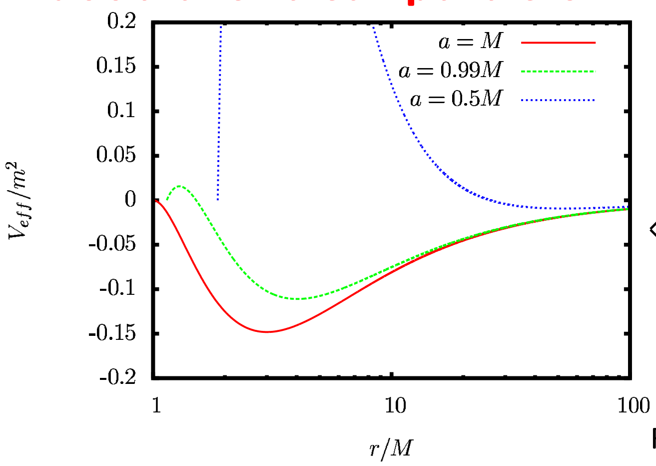


$a$: the spin parameter.

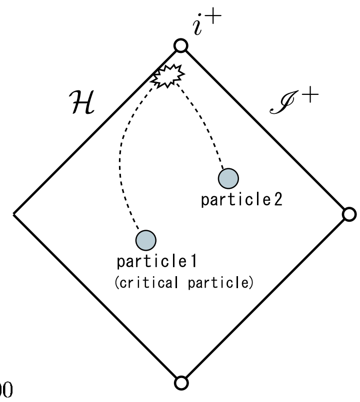


Figure in Harada and Kimura (2014).

- **Critical particles can directly reach the horizon only in the extremal case $a = M$.**
- It needs infinite proper time to reach the horizon.

# BSW effect of extremal charged BH.

Zaslavskii (2010)

- **If either of two particles is critical, $E_{CM}$ diverges.**
- Critical particle has $q = \sqrt{4\pi}E$.
- It needs infinite proper time for the critical particle to reach the event horizon.
  (The force balance of "gravitational force" and Coulomb force.)
- **There are a clear correspondence to the Kerr BH case.**

- **BSW effect is an essential feature of extremal BHs.**



# Criticisms for BSW mechanism.

- It needs infinite proper time for the critical particle to reach the event horizon in the extremal Kerr spacetime.
- The back reaction effects will suppress $E_{CM}$.
  $\longrightarrow$ **In realistic situations, $E_{CM}$ would be a finite and large value.**
- There is an upper bound on the black hole spin parameter $a < 0.998M$ for an astrophysical situation. (Thorne 1974)
  $\longrightarrow$ **The bound depends on the models of accretion disks and it can be violated.**
- The observer at infinity will observe highly red-shifted phenomena after high energy collision.
  $\longrightarrow$ **This is not a criticism but an aspect of the BSW effect. We can observe red-shifted phenomena after particle collisions in principle.**

# Harada san will give us a better review than mine.

**Tomorrow 17:15-17:30 Tomohiro Harada (Rikkyo)**
**"Black holes as particle accelerators: a brief review"**
I guess that he **will** talk on

- the BSW effect on non-equatorial planes
- a collisional Penrose process
- the collision of ISCO particles
- gravitational radiation reaction,

he **may** talk on

- effects of magnetic field

and he **will not** talk on

- higher dimensional case (N.T., M. Kimura and T. Harada, 2014).



# Instability and BSW effect.

- The gravity induced by particles after the collision is so strong that a new black hole can be born near an extremal black hole. (M. Kimura, K. Nakao and H. Tagoshi, 2011.)

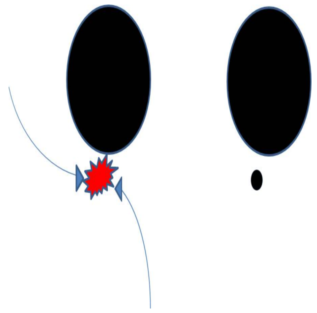

- From this point of view, BSW effect suggests a tight relation to instability of background spacetime by the process of a particle collision. (cf. a test field instability of the extremal BHs.)

In this talk, I will consider particle collision in a highly rotating wormhole spacetime and discuss instability of the wormhole against particle collisions following this idea.

## A Rotating Wormhole (Teo, 1998)

Teo considered a rotating wormhole metric in spherical polar coordinates which is given by

$$ds^2 = -N^2dt^2 + \frac{1}{1-\frac{b}{r}}dr^2 + r^2K^2\left[d\theta^2 + \sin^2\theta(d\phi - \omega dt)^2\right],$$

$$N = K = 1 + \frac{16a^2 d\cos^2\theta}{r}, \quad \omega = \frac{2a}{r^3}.$$

$b$, $d$: positive constants

$a \geqq 0$: angular momentum

The radial coordinate $r \geq b$.

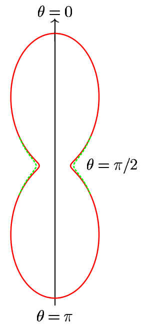


The throat has a peanut-shell-like shape.

- The wormhole throat exists at $r = b$.
- If $a > b^2/2$, the ergoregion exists in the range $2a|\sin\theta| > r^2 > b^2$.
- Null energy condition $T_{\mu\nu}k^\mu k^\nu \geq 0$ is violated at the throat in some regions of $\theta$.



## Simplification and Configuration of Particle Collision.

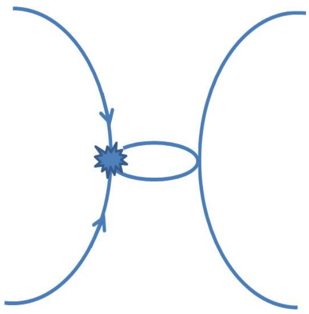

- We concentrate on $\theta = \pi/2$.

$$ds^2 = -dt^2 + d\rho^2 + r^2(\rho)\left(d\phi - 2a/r^3(\rho)dt\right)^2,$$

- a new radial coordinate $-\infty < \rho < \infty$

$$\rho \equiv \pm\left[\sqrt{r(r-b)} + b\log\left(\sqrt{\frac{r}{b}} + \sqrt{\frac{r}{b} - 1}\right)\right].$$

- Wormhole throat is at $\rho = 0$
- For simplicity, we concentrate on $L < 0$ and $E > 0$.
- Particles moving along the geodesic satisfy the forward-in-time condition everywhere:

$$\frac{dt}{d\lambda} = \mathcal{E}(\rho) \equiv E - \frac{2aL}{r^3(\rho)} \geq 0,$$

where $\lambda$ is an affine parameter.

## $E_{CM}$ of particle collision at $\rho = 0$ is given by

$$E_{CM}^2 = m_{(1)}^2 + m_{(2)}^2 + 2\mathcal{E}_{(1)}\mathcal{E}_{(2)} - \frac{2L_{(1)}L_{(2)}}{b^2} + 2\sqrt{R_{(1)}}\sqrt{R_{(2)}}.$$

$$R_{(1)} \equiv -m_{(1)}^2 + \mathcal{E}_{(1)}^2 - \frac{L_{(1)}^2}{b^2}, \quad \mathcal{E}_{(1)} \equiv E_{(1)} - \frac{2aL_{(1)}}{b^3}.$$

- In the static case $(a = 0)$, the wormhole **cannot** be a particle accelerator since $E^2 (> m^2 + L^2/b^2)$ should be large for $b \ll |L_I|$.

$$\begin{aligned} E_{CM}^2 &= m_{(1)}^2 + m_{(2)}^2 + 2E_{(1)}E_{(2)} - \frac{2L_{(1)}L_{(2)}}{b^2} \\ &\quad + 2\sqrt{-m_{(1)}^2 + E_{(1)}^2 - \frac{L_{(1)}^2}{b^2}}\sqrt{-m_{(2)}^2 + E_{(2)}^2 - \frac{L_{(2)}^2}{b^2}}. \end{aligned}$$

- In highly rotating and small $b$ case ( $b \ll a^{\frac{1}{2}}$, $|L_I/E_I|$ and $|L_I/m_I|$), high energy collisions **can** occur **without** critical particles.

$$E_{CM}^2 \sim 16a^2 L_{(1)}L_{(2)}/b^6.$$



## Potential for particle which can reach $\rho = 0$.

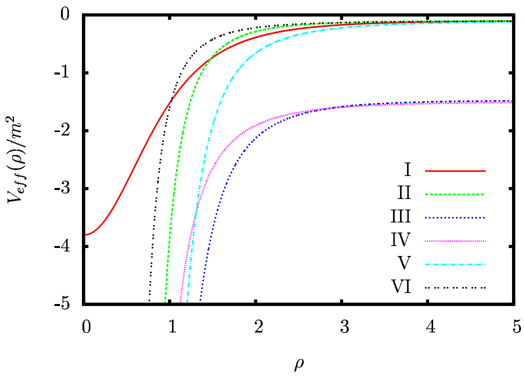


I ($a = 1$, $m = 1$, $E = 1.1$, $L = -1$, $b = 1$)
II ($a = 1$, $m = 1$, $E = 1.1$, $L = -1$, $b = 0.001$)
III ($a = 1$, $m = 1$, $E = 2$, $L = -2$, $b = 0.001$)
IV ($a = 1$, $m = 1$, $E = 2$, $L = -1$, $b = 0.001$),
V ($a = 2$, $m = 1$, $E = 2.2$, $L = -1$, $b = 0.001$)
VI ($a = 1$, $m = 2$, $E = 2.2$, $L = -1$, $b = 0.001$)

- The allowed region is given by $V_{eff}(\rho) \leq 0$.

$$V_{eff}(\rho) \equiv \frac{1}{2}\left[m^2 - \left(E - \frac{2aL}{r^3(\rho)}\right)^2 + \frac{L^2}{r^2(\rho)}\right].$$

- $V_{eff}(-\rho) = V_{eff}(\rho)$. $\qquad \frac{dV_{eff}(0)}{d\rho} = 0$.
- **We can see that proper time is finite.**

# Particle collision and instability of wormhole.

- $E_{CM}$ **only depends on the metric.**
- **On the other hand, stability of wormholes should depend on the matter as gravitational source.**
- **Does the high** $E_{CM}$ **suggest instability of the wormhole under the process of the particle collision?**

An example of stability of wormholes: Simplest wormhole metric case.

- The Ellis wormhole (filled with a phantom scalar field)is unstable under linear perturbations.
$ds^2 = -dt^2 + d\rho^2 + (\rho^2 + b^2)(d\theta^2 + \sin^2\theta d\phi^2)$.
- A wormhole with **the same metric but different matters** is linearly stable under both spherically symmetric perturbations and axial perturbations. (Bronnikov et al. 2013)
- (The later seems to be the first example of stable wormhole without thin shells in GR.)



# Conclusion and Discussion.

- In highly rotating and small $b$ wormhole case ( $b \ll a^{\frac{1}{2}}$, $|L_I/E_I|$ and $|L_I/m_I|$), high CM energy collisions can occur near the wormhole throat.
- We do not need particles with a fine-tuned angular momentum.
- Particles can reach the throat in finite proper time.
- The wormhole spacetime is not extremal at all in any sense.
- **Does high** $E_{CM}$ **imply instability of a background spacetime under the process of particle collisions?**

# Conclusion and Discussion.

- In highly rotating and small $b$ wormhole case ( $b \ll a^{\frac{1}{2}}$, $|L_I/E_I|$ and $|L_I/m_I|$), high CM energy collisions can occur near the wormhole throat.
- We do not need particles with a fine-tuned angular momentum.
- Particles can reach the throat in finite proper time.
- The wormhole spacetime is not extremal at all in any sense.
- **Does high $E_{CM}$ imply instability of a background spacetime under the process of particle collisions?**

## Thank you.

“Negative tension branes as stable thin shell wormholes”

Takafumi Kokubu

[JGRG24(2014)111219]

# NEGATIVE TENSION BRANES AS STABLE THIN-SHELL WORMHOLES

Takafumi Kokubu (D1) and Tomohiro Harada
@ Rikkyo University
In preparation.

## 0.MOTIVATION

- criterion of existence of wormholes
- Negative tension branes have no internal dynamical degrees of freedom.

# 1. WORMHOLES

What is wormhole?

Naively,
"wormholes are space-time structures which connect two different universes
or
two different points of our universe"

Theoretical prophecy from GR

Some exact solutions to Einstein Eqs.

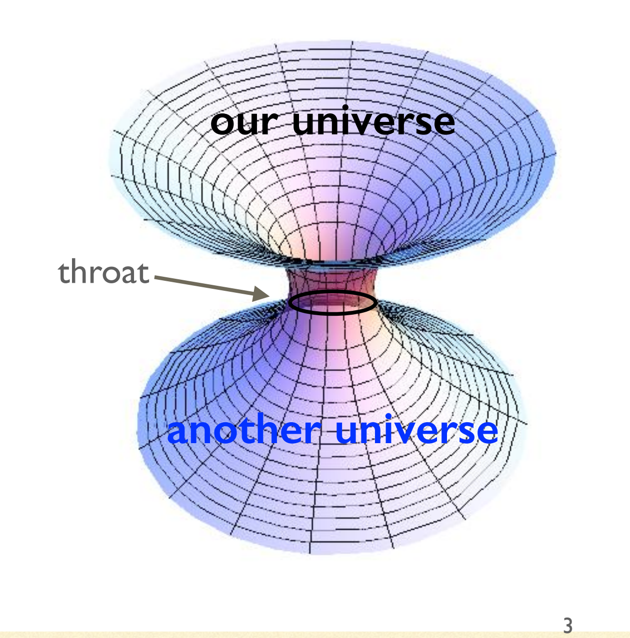




# 2. CONSTRUCTION

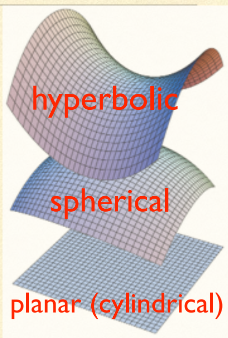


Higher dimensional Einstein eqs.

$$G_{\mu\nu\pm} + \frac{(d-1)(d-2)}{6}\Lambda g_{\mu\nu\pm} = 8\pi T_{\mu\nu\pm} \qquad (d \geq 4)$$

Static space-times

$$ds^2 = -f(r)dt^2 + f(r)^{-1}dr^2 + r^2(d\Omega^k_{d-2})^2,$$

$$f(r) = k - \frac{\Lambda r^2}{3} - \frac{M}{r^{d-3}} + \frac{Q^2}{r^{2(d-3)}}$$

$$(d\Omega^k_{d-2})^2 = \begin{cases} k=1 : (d\Omega^1_{d-2})^2 = d\theta_1^2 + \sin^2\theta_1 d\theta_2^2 + \ldots + \prod_{i=2}^{d-3}\sin^2\theta_i d\theta_{d-2}^2 \\ k=0 : (d\Omega^0_{d-2})^2 = d\theta_1^2 + d\theta_2^2 + \ldots + d\theta_{d-2}^2 \\ k=-1 : (d\Omega^{-1}_{d-2})^2 = d\theta_1^2 + \sinh^2\theta_1 d\theta_2^2 + \ldots + \sinh^2\theta_1 \prod_{i=2}^{d-3}\sin^2\theta_i d\theta_{d-2}^2 \end{cases}$$

sphere

plane (cylinder) ← **RNdS is a specific solution**

hyperboloid

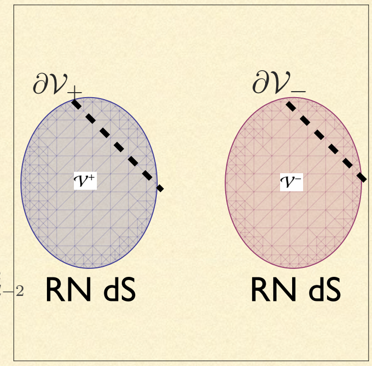


The junction conditions:

$$S^i_j = -\frac{1}{8\pi}(\kappa^i_j - \delta^i_j \kappa^l_l), \qquad n_{\alpha\pm} \equiv \pm\frac{F_{,\alpha}}{|g^{\mu\nu}F_{,\mu}F_{,\nu}|^{\frac{1}{2}}} \qquad F = r - a(\tau) = 0$$

$$\kappa^i_j = (K^{i+}_j - K^{i-}_j)\big|_{\partial\mathcal{V}} \qquad K^{\pm}_{ij} \equiv (\nabla_\mu n^{\pm}_\nu)e^\mu_{(i)\pm}e^\nu_{(j)\pm}$$

EoS : negative tension brane $$p = -\sigma$$

(No internal dynamical degrees of freedom)

$\sigma$ : the surface energy density
$p$ : the surface pressure

$$S^{ij}{}_{|j} + [T^{\alpha}_{\beta} e^{i}_{\alpha} n^{\beta}] = 0 \quad \Rightarrow \sigma = -|\alpha|, p = +|\alpha|$$

$([X] := (X_+ - X_-)|_{\partial\mathcal{V}})$

$\alpha$ : negative const.

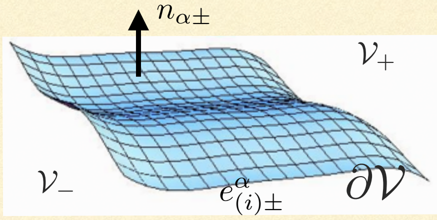


the conservation law of mechanical energy for the shell
$$\dot{a}^2 + V(a) = 0 \qquad V(a) = f(a) - \left(\frac{4\pi\alpha}{d-2}\right)^2 a^2$$

E.O.M for the shell
$$\ddot{a} = -\frac{1}{2}V'(a)$$

the stability condition : $V''(a_0) > 0$

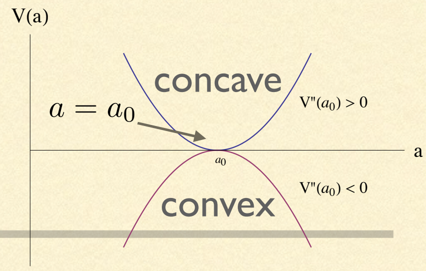


# Stabilities of wormholes with a negative tension brane

stabilities consist of…

$\boxed{\text{Static solution, Stability condition, Horizon avoidance}}$

Static solution: $\frac{a_0}{2} f'(a_0) - f(a_0) = 0$

Stability condition: $V''(a_0) > 0$

Horizon avoidance: $f(a_0) > 0$

$$f(a) = k - \frac{\Lambda a^2}{3} - \frac{M}{a^{d-3}} + \frac{Q^2}{a^{2(d-3)}}$$

$$V(a) = f(a) - \left(\frac{4\pi\alpha}{d-2}\right)^2 a^2$$

$\Lambda$ only contributes to horizon avoidance

k=+1 : spherical symmetry
k=-1 : hyperbolic symmetry
k=0 : plane (cylindrical) symmetry

## M>0 $\quad k = +1$ : spherical symmetry

$$\dot{a}^2 + V(a) = 0 \Leftrightarrow \left(\frac{\ln a}{d\tau}\right)^2 + \tilde{V}(a) = \Lambda_{\text{eff}}$$

$$\tilde{V}(a) \equiv \frac{k}{a^2} - \frac{M}{a^{d-1}} + \frac{Q^2}{a^{2(d-2)}}, \; \Lambda_{\text{eff}} \equiv \frac{\Lambda}{3} + \left(\frac{4\pi\alpha}{d-2}\right)^2$$

$\boxed{Q \neq 0}$ :

Horizon avoidance: Figure I

$$f(a_0) > 0 \Leftrightarrow \lambda < H(d,q)$$

$$\left(\lambda := \frac{\Lambda}{3} M^{\frac{2}{d-3}}, q := \frac{|Q|}{M}\right)$$

Wormhole without $\Lambda$

$$1 < 4\left(\frac{|Q|}{M}\right)^2 < \frac{(d-1)^2}{4(d-2)}$$

$d$=4, $M \to 2m$: Barcelo-Visser :

$$1 < \left(\frac{|Q|}{m}\right)^2 < \frac{9}{8}$$

$\boxed{Q = 0}$ : None

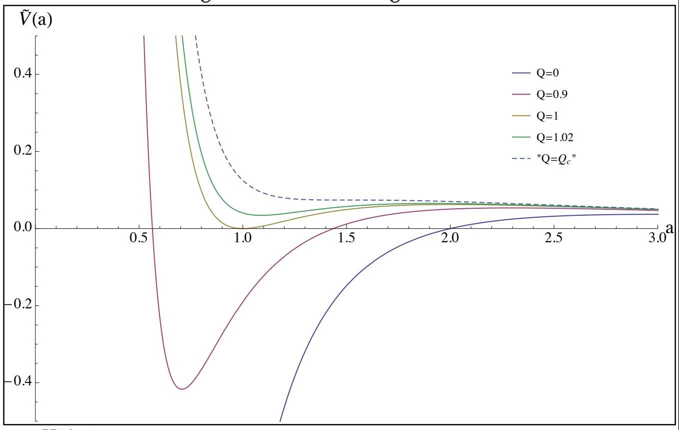


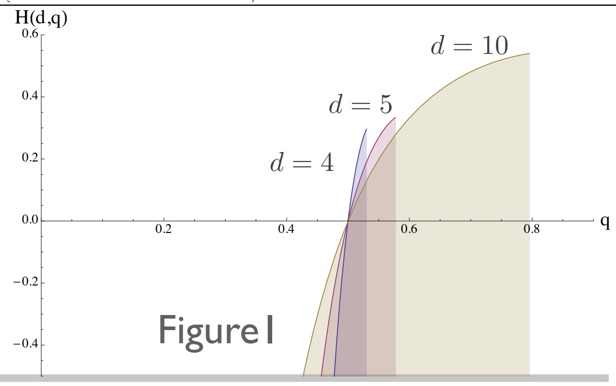


Figure I

## $k = +1$ : spherical symmetry

### M<0

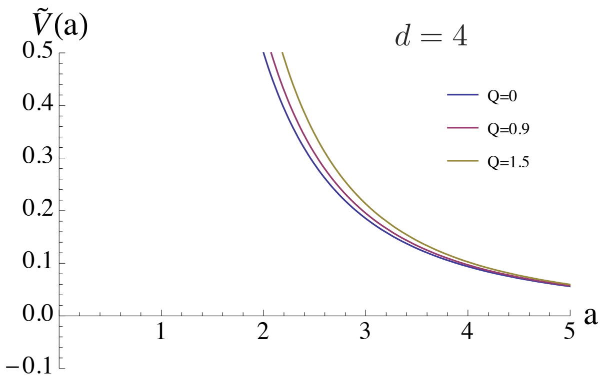


None

### M=0

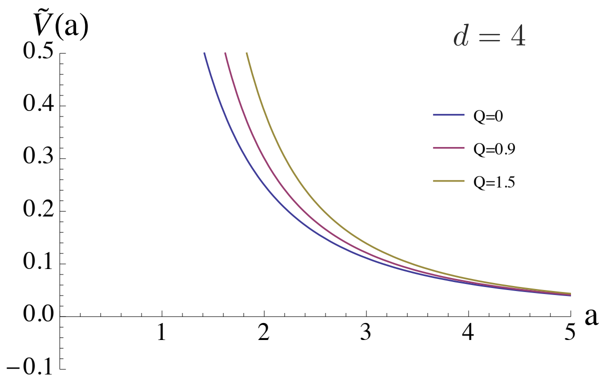


None

# $k = -1$ : hyperbolic symmetry

## M>0

$\boxed{Q \neq 0:}$

Horizon avoidance: Figure2

$$f(a_0) > 0 \Leftrightarrow \lambda < I(d,q)$$

$$\left(\lambda := \frac{\Lambda}{3} M^{\frac{2}{d-3}}, q := \frac{|Q|}{M}\right)$$

$\boxed{Q = 0:}$ None

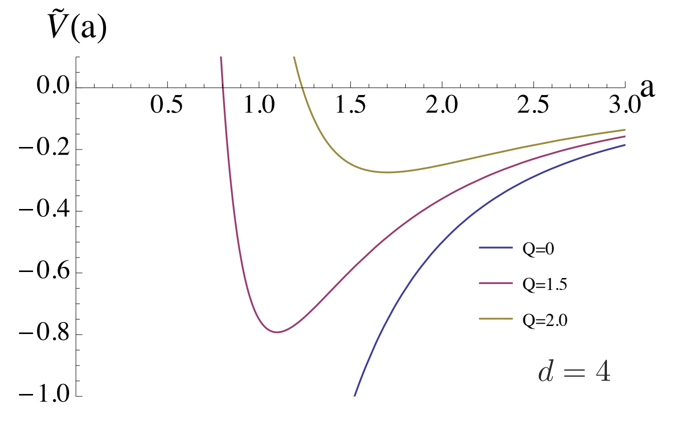


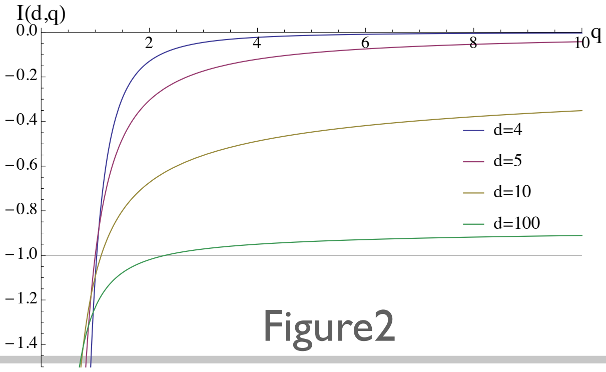


Figure2

# $k = -1$ : hyperbolic symmetry

## M<0

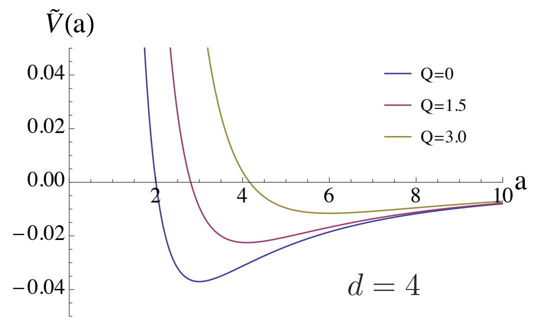


Horizon avoidance:

$\boxed{Q \neq 0:}$

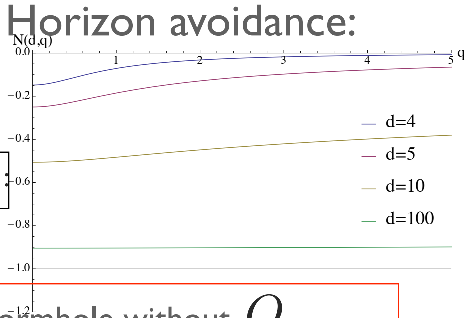


Wormhole without $Q$

$\boxed{Q = 0:}$ $\lambda < -\left(\frac{2}{d-1}\right)^{\frac{2}{d-3}} \frac{d-3}{d-1}$

## M=0

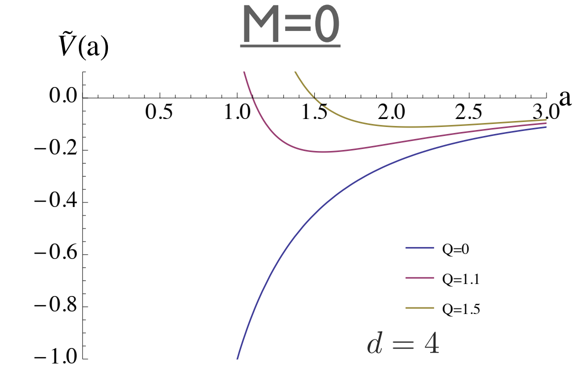


Horizon avoidance:

$\boxed{Q \neq 0:}$

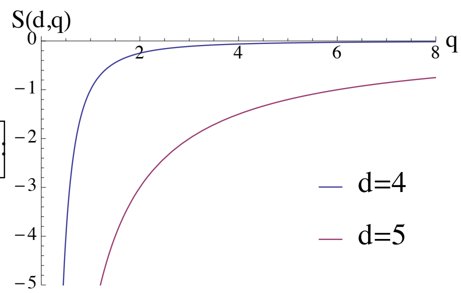


$\boxed{Q = 0:}$ None

## $k = 0$ : plane or cylindrical symmetry

**M>0**

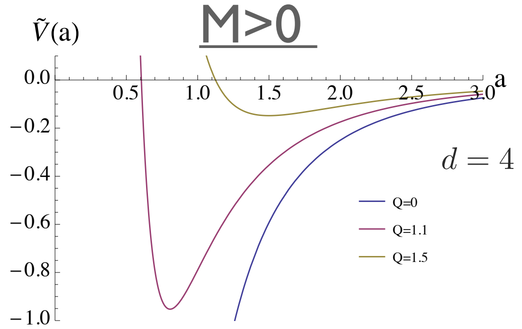


$\boxed{Q \neq 0}$: Horizon avoidance:Figure3

$\lambda < J(d, q)$

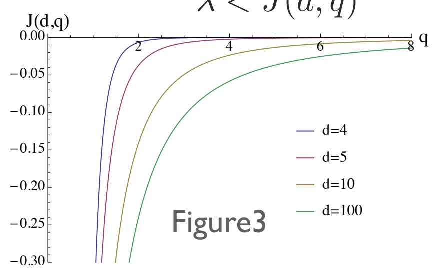


$\boxed{Q = 0}$: None

**M<0** None

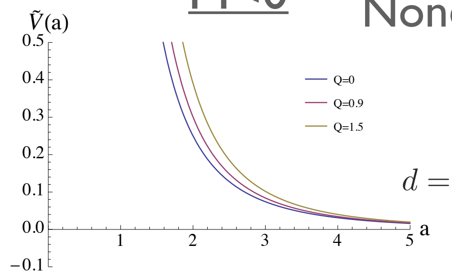


**M=0**

$\boxed{Q = 0}$: Marginally stable (AdS)

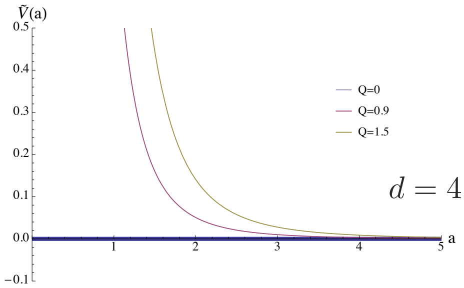


$\boxed{Q \neq 0}$: None

# SUMMARY

- We used a negative tension brane as an exotic matter.
- We found stable thin shell wormholes in several geometries and higher dimension.
- In general, charge and a cosmological constant are needed to sustain wormholes.
- However there are stable wormholes without a cosmological constant or charge in certain situations.
- There is no qualitative difference for stabilities when the number of dimensions *d* increases.